LEACHING OF NICKEL LATERITE WITH A SOLUTION OF AMMONIA AND AMMONIUM CARBONATE UTILIZING SOLIDS LIQUID SEPARATION UNDER PRESSURE

by

Mothobi Erasmus

Thesis presented in partial fulfillment
of the requirements for the degree
of

MASTERS OF SCIENCE IN ENGINEERING

(EXTRACTIVE METALLURGICAL ENGINEERING)

in the Faculty of Engineering
at the Stellenbosch University

Supervisor
Dr Raymond Els

March 2012

DECLARATION

By submitting this thesis electronically, I declare that the entirety of the work contained therein is my own, original work, that I am the sole author thereof (save to the extent explicitly otherwise stated), that reproduction and publication thereof by Stellenbosch University will not infringe any third party rights and that I have not previously in its entirety or in part submitted it for obtaining any qualification.

…… …….

Signature Date

SYNOPSIS

Leaching of nickel laterite was conducted with a solution of ammonia and ammonium carbonate in a closed vessel. The vessel used in this study was designed to leach and perform solid-liquid separation at the same time. For solid-liquid separation, stainless steel sintered metal filter media were used. The sintered metal filter medium was selected for its high strength to withstand pressure, chemical resistance to caustic solution and back flushing properties.

Optimum leaching conditions were determined by varying temperature, ammonia concentration, ammonium carbonate concentration and oxygen pressure. After leaching and filtration, the pH of the leach liquor was measured and samples were analyzed for dissolved metals (Ni, Fe and Co) using atomic absorption spectrophotometry.

The most significant variable effect on leaching of nickel was the ammonia concentration. The maximum dissolution of nickel from the unroasted ore was 11.90% at 4 M NH_3, 100^oC, 2 M $(NH_4)_2CO_3$ and 2 bar O_2 pressure. Optimization from the leaching data was done using response profiling and desirability in Statistica software. Optimum leaching conditions were determined to be 3 M NH_3, 2 M $(NH_4)_2CO_2$, 100^oC and 2 bar O_2 pressure.

The mineralogy of the ore before and after leaching was studied to understand why nickel extraction from unroasted ore was poor. XRF analysis of solids after leaching showed that iron, silicon, and magnesium remained the same. The only metal which showed significant decrease from solids was nickel. XRD analysis of solids after and before leaching showed that most mineral phases present in the ore are not affected by the leaching solution. SEM with EDS detection was used to determine nickel distribution within the ore. The results showed that nickel is mostly associated with iron. The iron is surrounded by magnesium and silicon. Silicate minerals do not react with ammonia and ammonium carbonate solution.

From filtration experiments, the filtration differential pressure had no significant effect on the filtration rate. An average filtration rate of 0.29±0.07 ml/min.cm^2 was obtained. The filtration rate from these experiments was very low. The main reason was due to quick pore clogging of sintered metals. Pore clogging was found to be mainly on the surface of the filter medium. Laterites have been found to have low permeability due a lot of clay present in the ore.

Rheological studies on this ore showed that the ore has shear thickening behavior. However, a very clear filtrate was obtained. After each leach and filtration experiment, the sintered metals was unblocked by back flushing with water and air. Back flushing was successful because all 18 experiments were carried out using the same sintered filter medium.

The effect of roasting the ore prior to leaching was investigated using optimum conditions obtained when leaching the unroasted ore. There was a slight improvement in nickel extraction when the ore was roasted. The average percentage extraction of nickel from 3 experimental runs was 19.25%±0.19 at 100^{o}C, 3M NH_3, 2M $(NH_4)_2CO_3$, and 5 bar oxygen pressure. Some part of nickel in the ore was unextractable due to association of nickel with recrystallized silicate minerals in the reduced ore. Roasting improved permeability of the ore. The filtration rate improved significantly after roasting the ore. The average filtration rate was 2.60±0.05 ml/min.cm^2.

Dissolution kinetics of the unroasted and roasted saprolitic laterite were investigated with regard to the effects of temperature, ammonia concentration, ammonium carbonate concentration, and oxygen pressure. For the unroasted ore, it was found that dissolution rate and degree of nickel extraction increases with increasing temperature. Increase in ammonia concentration improves the degree of nickel extraction. Nevertheless, nickel extraction does not depend entirely on ammonia concentration because even when ammonia concentration is high and ammonium carbonate concentration is zero nickel extraction is low. An increase in ammonium carbonate concentration also increases the degree of nickel extraction. Ammonium carbonate is critical for the extraction, since ammonium ions in the solution prevent hydrolysis of the nickel ammine complex. Oxygen did not have a significant effect on the degree of nickel extraction.

The leaching of nickel laterite was found to be a two stage leaching process. In the first stage, the dissolution of nickel is faster but after 15 minutes, the reaction rate is reduced. The reaction rate is reduced by inert minerals which host nickel. These minerals contain iron magnesium and silicon. The fast dissolution of nickel in the first stage represents leaching of free nickel in the ore. The data for the second stage of leaching was analyzed by the shrinking core model, and the results suggested that the dissolution rate is controlled by mixture kinetics (ash layer diffusion and surface reaction control). The activation energy for the dissolution reaction was calculated as 56.5 KJ/mol. The reaction order with respect to ammonia and ammonium carbonate were determined to be 0.3 and 0.26 respectively.

For the roasted ore, the highest degree of nickel extraction was obtained at 60^{o}C, 3M NH_3, 2M $(NH_4)_2CO_3$, and 5 bar oxygen pressure. The percentage extraction under these conditions was 28.7%. Temperature did not have a significant effect on the leaching rate. An increase in NH_3 and $(NH_4)_2CO_3$ increased the final extraction of nickel but did not have any effect on leaching rate in the first stage of leaching. In the absence of ammonium carbonate, nickel extraction is almost zero. The experimental data did not give linear fit to the shrinking core models investigated for the unroasted ore. The reason for this could be due to the sampling time interval which was too far apart, or the leaching behavior of roasted nickel is complicated and cannot explained by shrinking core model alone.

Leaching experiments demonstrate that for a high degree metal extraction and improved reaction kinetics with ammonia and ammonium carbonate, the solution temperature should be high (>100^{o}C) for the unroasted ore. In order to leach at high temperature with ammonia and ammonium carbonate a closed vessel is required to prevent reagent loses. The reaction kinetics showed that the reaction is controlled mostly by ash layer diffusion; this indicates that a low degree of nickel extraction in the unroasted saprolitic laterite is due to inert minerals (ash layer) which host nickel within the ore.

In order to obtain a high degree of nickel extraction, the ore needs to be roasted under reducing conditions. Roasting conditions need to be carefully controlled to ensure high dissolution of nickel. In fact optimum roasting conditions which will give maximum dissolution of nickel, must be determined before working with the bulk of the ore.

OPSOMMING

Logingstoetse van saprolitiese lateriet met ‘n oplossing van ammonia en ammonium karbonaat is gedoen in ‘n druk houer. Die logingsvat vir hierdie studie is ontwikkel om die loging sowel as die vloeistof – vastestof skeiding te doen. Gesinterde metaal filter medium was gebruik vir die vloeistof – vastestof skeiding aangesien dit die volgende eienskappe vertoon; die vermoë om druk te weerstaan, die chemiese weerstand teen bytsoda oplossing, asook voordelige terugspoel eienskappe.

Optimum loogkondisies is bepaal deur die temperatuur, ammoniak konsentrasie, ammonium karbonaat konsentrasie, en suurstof druk te varieer. Na loging en filtrasie is die pH van die loogvloeistof gemeet en monsters is deur atoom absorpsie spektrofotometrie geanaliseer vir opgeloste metale (Ni, Fe en Co).

Die veranderlike wat die grootste effek op die loging van nikkel gehad het was die ammoniak konsentrasie. Die maksimum herwinning van nikkel van uit ongeroosterde erts was 11.9 % by 4 M NH_3, 100 ^oC, 2 M $(NH_4)_2CO_3$ en 2 bar O_2 druk. Optimisering van die loogdata is gedoen deur die respons profiel te analiseer met Statistica sagteware. Optimum loogkondisies was bepaal as 3 M NH_3, 2 M $(NH_4)_2CO_2$, 100 ^oC en 2 bar O_2 druk.

Die mineralogie van die erts voor en na loging is bestudeer om te bepaal waarom die nikel opbrengs van ongeroosterde erts so laag was. XRF analise van die vastestof na loging het gewys dat yster, silikon en magnesium nie deur loging affekteer is nie. Slegs nikkel het ‘n merkwaardige afname getoon. XRD analsiese van die vastestof voor en na loging wys dat die meeste mineraal fases teenwoordig in die erts nie deur die loogoplossing affekteer is nie. SEM met EDS deteksie is gebruik om die nikkel verspreiding in die erts te bepaal. Die resultate wys dat nikkel meestal met yster assosieer. Die yster is omring deur magnesium en silikon. Silikaat minerale reageer nie met ammoniak en ammonium karbonaat oplossing nie.

In filtrasie eksperimente is daar gevind dat die filtrasie differensiële druk geen noemenswaardige effek op die filtrasie tempo gehad het nie. Die gemiddelde filtrasietempo was 0.29 ± 0.07 ml/min.cm^2. Die filtrasie tempo van hierdie eksperimente was baie laag, hoofsaaklik as gevolg van blokkasie van porieë van die sinter metaal filter medium. Dit is gevind dat blokkasie van porieë hoofsaaklik op die oppervlak van die filter medium

plaasvind. Lateriedes toon ‘n lae deurlaatbaarheid as gevolg van die erts se hoë klei inhoud. Rheologiese studies op hierdie erts wys dat die erts skuif verdikking (“shear thickening”) gedrag vertoon. ‘n Baie helder filtraat is egter verkry. Die gesinterde metale is na elke loog en filtrasie eksperiment skoongemaak deur terugspoeling met water en lug. Hierdie procedure was suksesvol, aangesien al 18 eksperimente met dieselfde filter medium uitgevoer is.

Die effek van erts roostering voor loging is ondersoek by die optimum kondisies wat verkry was vir die loging van ongeroosterde erts. Nikkel ekstraksie het effens verbeter met geroosterde erts. Die gemiddelde persentasie ekstraksie van nikkel van drie eksperimentele lopies was 19.25 % $\pm$ 0.19 by 100 ^{o}C, 3 M NH_3, 2 M $(NH_4)_2CO_3$, en 5 bar suurstofdruk. ‘n Gedeelte van die nikkel in die erts was onherwinbaar as gevolg van die assosiasie van nikkel met her-gekristaliseerde sillikaat-minerale in die gereduseerde erts. Die porositeit van die erts is verbeter deur dit te rooster. Die filtrasie tempo het merkwaardig verbeter nadat die erts gerooster is. Die gemiddelde filtrasie tempo was 2.6$\pm$0.05 ml/min.cm^2.

Kinetika vir die oplossing van ongeroosterde en geroosterde saprolitiese lateriet is ondersoek, met in ag geneem die effekte van temperatuur, ammonia konsentrasie, ammonium karbonaat konsentrasie en suurstofdruk. Vir ongeroosterde erts is gevind dat die oplossingstempo en graad van nikkel ekstraksie toeneem met toenemende temperatuur. Toename in ammoniak konsentrasie lei tot ‘n toename in nikkel ekstraksie, maar nikkel ekstraksie is nie alleenlik afhanklik van ammoniak nie. ‘n Toename in ammonium karbonaat konsentrasie lei ook tot ’n toename in nikkel ekstraksie. Ammonium karbonaat is krities vir die ekstraksie, aangesien ammonium ione in die oplossing die hidrolise van die nikkel-amien kompleks verhoed. Suurstof het nie ‘n merkwaardige effek op die totale nikkel ekstraksie gehad nie. Vir die bepaling van reaksie kinetika is 100˚C gebruik as die logingstemperatuur.

Die loging van saprolitiese nikkel lateriet vind in twee stadia plaas. In die eerste fase is die oplossing van nikkel vinnig, maar na 15 minute neem die reaksietempo af. Die reaksietempo word verlaag deur inerte minerale wat teenwoordig is in die nikkel erts. Hierdie minerale bevat yster, magnesium en silikon. Die vinnige oplossing van nikkel in die eerste fase verteenwoordig die loging van vry nikkel in die erts. Die data vir die tweede stadium is geanaliseer deur die krimpende kern model, en die resultate dui aan dat die oplossingstempo deur ‘n gemengde meganisme beheer word (as laag diffusie en oppervlak reaksie beheer). Die aktiveringsengergie vir die oplossingsreaksie was bereken as 56.5 kJ/mol. Die

reaksieorde ten opsigte van ammoniak en ammonium karbonaat is onderskeidelik bepaal as 0.3 en 0.26.

Die hoogste graad van nikkel ekstraksie vir die geroosterde erts is verkry by 60^{o}C, 3 M NH_3, 2 M $(NH_4)_2CO_3$, en 5 bar O_2 druk. Die persentasie ekstraksie by hierdie kondisies was 28.7 %. Temperatuur het nie ‘n merkwaardige effek op loogtempo gehad nie. ‘n Toename in NH_3 en $(NH_4)_2CO_3$ het die graad van nikkel ekstraksie laat toeneem, maar het nie enige effek op die loogtempo gehad nie. In die afwesigheid van ammonium karbonaat het byna geen nikkel ekstraksie plaasgevind nie. Die eksperimentele data het nie ‘n lineêre passing vir die krimpende kern model soos vir die ongeroosterde erts ondersoek gegee nie. Die rede hiervoor is dat die monsternemings interval te groot was, of dat die logings karakteristiek van geroosterde nikel gekompliseerd is en nie alleen deur die krimpende kern model voorspel kan word nie.

Logings eksperimente wys dat die temperatuur hoog moet wees (> 100 ^{o}C) om ‘n hoë graad van nikkel ekstraksie te verkry met die ongeroosterde erts. ‘n Geslote reaktor word benodig om by ‘n hoë temperatuur met ammoniak en ammonium karbonaat te loog om reagens verliese te verhoed. Die reaksie kinetika word grootliks deur aslaag diffusie beheer. Hieruit kan gesien word dat ‘n lae graad van nikkel ekstraksie uit die ongeroosterde saprolitiese lateriet die gevolg is van nie-reaktiewe minerale (aslaag) waarin die nikkel binne die erts bevat word.

Om ‘n hoë graad van nikkel ekstraksie te verkry moet die erts onder reduserende kondisies gerooster word. Rooster kondisies moet versigtig beheer word om hoë oplossing van nikkel te verseker. Optimum rooster kondisies om maksimum nikkel oplossing te verkry, moet bepaal word voordat daar met groter hoeveelhede erts gewerk kan word.

ACKNOWLEDGEMENTS

The work in this thesis was carried out at Stellenbosch University in the Department of Process Engineering. I would like thank the department of Process Engineering's staff for providing knowledge, friendly environment, and support to carry out this work. Many people had significant contributions into this project and I am grateful for their support. A great thank goes to the following people for their supports.

First, I would like to thank God almighty for giving wisdom and strength to work under a stressful condition.

My study leader, Dr. Raymond Els for his undying support, guidance, and encouragement throughout the course of the study

My sponsors, Letseng Diamond (Pty) Ltd, for granting scholarship, and the financial support in the project.

Anglo platinum South Africa for their financial support and kind supply of nickel oxide ore.

Max Pelser of Anglo Platinum for his guidance and making sure that we get nickel oxide ore.

Mintek for freely roasting the ore using their equipment and chemicals.

The work personnel of the Department of Process Engineering in particular Mr. J.M Barnard, Anton for their help, and technical support from Mrs. J.E Botha.

My friend Mr. Phiri Mohau for his support.

My family especially my younger brother for his support

List of Abbreviations

AAS	Atomic Absorption Spectroscopy
CAF	Central Analytical Facility
CCD	Counter Current Decantation
EDX	Energy Dispersive X-ray
ICP	Inductively Coupled Plasma
PAL	Pressure Acid Leaching
PDE	Post Graduate Diploma
SEM	Scanning Electron Microscope
RSM	Response Surface Methodology
XRD	X-ray Diffraction
XRF	X-ray Fluorescence

List of Symbols

A	Cross sectional area (m^2)
b	Stoichiometric coefficient of species
C_{Ag}	Bulk concentration of reactants (M)
c_m	Weight percent of metal in the ore
C_{mi}	Concentration of metal (g/L)
d	Impeller diameter (m)
De	Effective diffusivity (m^2/s)
D_i	Internal diameter of the vessel (mm)
η	Dynamic viscosity (Pa.s)
e	Minimum thickness (mm)
Ea	Activation energy (kJ/mol)
F	Design stress (N/mm^2)
f	Stoichiometric coefficient of species
g	Stoichiometric coefficient of species
k, k_s, k_d, k_f	Apparent rate constant (s^{-1})
k”	Intrinsic rate constant ($mol/(m^2$ Pa s))

m	Stirring speed (s^{-1})
m_l	Mass of water (g)
m_o	Mass of empty flask (g)
m_s	Mass of solids (g)
m_{sl}	Mass of solids and water
H	Height of solids (mm)
M	Initial mass of ore added to the reactor (g)
n	Reaction order
N	Stirrer speed (m/s)
N_f	Critical agitator speed (rpm)
$[NH_3]$	Concentration of ammonia (M)
$[(NH_4)_2CO_3]$	Concentration of ammonium carbonate (M)
p_i	Internal pressure (N/mm^2)
ΔP	Pressure change (Pa)
Q	Volumetric flow rate (m^3/s)
r	Filter medium radius (m)
R	Gas constant (kJ/mol.K)
Re	Reynolds number
R_o	Initial particle radius (m)
ρ_B	Density of reacted particle (g/cm^3)
ρ_d	Particle density (g/cm^3)
ρ_f	Density of water (g/cm^3)
ρ_l	Density of water (g/cm^3)
ρ_p	Pulp density (%w/w)
ρ_{SL}	Solid to liquid ratio (g/g)
t	Time (min)
U	Superficial velocity (m/s)
U_a	Actual flow rate (m/s)
μ	Viscosity of water at 25^{o}C (cP)
V	Initial volume (L)
v_i	Volume of solution sample (L)
v_L	Volume of water (ml)
V_p	True volume of particles (ml)
V'_p	Bulk volume of particles (ml)

v_s	Volume of solids (ml)
X_B	Fraction reacted
x	Fraction extracted

Table of Contents

List of figures

List of tables

1 Introduction

1.1 Pyro-metallurgy and hydrometallurgy

Historically, most processes for recovering metals from their ores have been based on pyro-metallurgy in which the ore is roasted and smelted to extract metal content (Shurtz, 1984). In pyro-metallurgy, metal containing material such as ore, slag and scarp are heated with appropriate agents such as reducing and or oxidizing agents to the melting fusion point mixture. At such high temperatures, there is generally a separation of metallic values from gangue or waste materials. The separation procedure involves heating of metals at a temperature at which both metals and gangue are molten (Shurtz, 1984).

High temperatures involved in this technique are achieved via electric furnaces, blast furnaces, reverberatory furnaces etc. Temperature required for metals such as copper, iron and nickel would generally range from 1000^{o}C to 2000^{o}C. This separation is a high energy consuming process and should be close to the energy source. An advantage in this method is that recoveries of the metal values are typically high (Tolley and Rademaker, 1982). However, these processes tend to produce noxious fumes, which require the installation of a scrubber, bag houses and other equipment to eliminate dust and fumes. Because of compliances with air pollution regulations, this has led to increased capital and operating costs. As a result, considerable research has been devoted to developing alternative processes that inherently limit the dust and fumes problems (Shurtz, 1984).

Hydrometallurgical processes provide a viable alternative to environmental challenges, while offering more efficient and cheaper means for recovery of metals from low-grade ores. These processes involve aqueous solutions of the common mineral acids such as hydrochloric acid (HCl), sulfuric acid (H_2SO_4) and nitric acid (HNO_3) and alkaline solutions such as sodium carbonate or sodium bicarbonate (Na_2CO_3/$NaHCO_3$), ammonium hydroxide (NH_4OH), ammonium carbonate ($(NH_4)_2CO_3$) and other alkaline reagents to leach metal values from their ores. Acid or alkaline leach at low or high pressure have been developed for extracting copper, uranium, nickel, zinc, molybdenum, gold and other metals.

These hydrometallurgical processes offer several advantages over traditional pyrometallurgical operations in the following areas:

- A greater volume of ore can be processed in a given period.
- By closing the process loop or recycling process streams, effluents and emissions can be eliminated to comply with environmental regulations.
- The process units are smaller in most instances and can be placed at smaller or more remote ore-body sites.
- These process units, if designed properly, can minimize operating personnel as well as cut maintenance and downtime cost.
- Ore dressing operations for enriching ores, such as flotation, can be bypassed. These operations are more cost-effective and efficient for leaching low grade, even complex ores (Shurtz, 1984).

However, hydrometallurgical processes have not yet met the peak of their goal. Late studies show that energy costs for hydrometallurgical process are about 3 times higher than for pyro-metallurgical processes (Li *et al.*, 2009). Furthermore, recoveries are relatively low. Therefore, in the long term it is still necessary to study and improve on existing techniques. Many industries are now undertaking research aimed at improving this process. Of the recent developments is the use of alkaline solutions for leaching of high acid consuming ores for extracting metals such as nickel laterites economically from their ores.

Previously, many industries have used only two common leaching processes which are; sulfuric acid and sodium carbonate/bicarbonate leaching. The reagents used in each are; sulfuric acid (H_2SO_4) and sodium carbonate /bicarbonate (Na_2CO_3/$NaHCO_3$) respectively. None of the above mentioned reagents is recoverable or recyclable after the leaching process (Goldwyer, 2007).

Ammonium carbonate $(NH_4)_2CO_3$ being the least exploited reagent, seems to be promising in the future development of hydrometallurgical processes in comparison with the sulfuric acid and sodium carbonate /bicarbonate leaching. Its advantages over these leaching processes include:

- Ammonium carbonate filters five times faster than sodium carbonate or sodium bicarbonate because sodium carbonate or bicarbonate forms sticky substances after reaction with the ore, especially in the presence silica in the ore. On the other hand, ammonium carbonate does not react with silica (Goldwyer, 2007).

- Ammonium carbonate is recoverable and recyclable. Furthermore, after leaching the reagent can be supplemented from cheap reagents such as hydrolyzed urea (Goldwyer, 2007).
- The reagent is applicable to a variety of complex ores.
- Precipitation of the metal values after extraction from the purified leach is by steam heating. During this process, the ammonium carbonate leachant thermally decomposes to NH_3 and CO_2, which are then channeled to absorption towers for recycling.
- It does not require expensive construction materials such as in acid leaching whereby the leaching vessel is sometimes lined with titanium.
- With proper conditions, the reagent can be used to extract metal economically from low-grade ores.
- It is compatible with strict environmental controls (non-zero effluent) (Harvey, 2006).

Ammonium carbonate has been used as leaching solution for several metals such as uranium, nickel, copper, gold and zinc but many problems have been experienced when using this reagent for many ores.

- The reagent cannot be used directly to leach sulfide ores, spinel and ferrite. Roasting or fuming is usually required prior to leaching thus making the process pyro-hydrometallurgical and very expensive.
- The ultimate recovery of metal values from their ores is often lower than equivalent acid leaching.(Harvey, 2006).

The motive of the project is to continue and improve on the work, which has already been done by other researchers on leaching with ammonium carbonate and to come up with cheap processes. But the main focus of this study looking at the leaching of nickel oxide ore (saprolitic laterite) with a solution of ammonia and ammonium carbonate. In most commercial processes, leaching nickel laterites with ammonium carbonate solution is carried out at temperatures below 60^oC. In open systems above 60^oC, ammonium carbonate decomposes into ammonia and carbon dioxide. Therefore, even at milder conditions in an open reactor, the reagent would be lost. Furthermore operating at low temperatures implies a slow reaction rate. It is important to be able to operate at high temperatures in order to

improve reaction kinetics. In addition, pressure creates an equilibrium condition that prevents decomposition of ammonium carbonate (Goldwyer, 2007).

$$(NH_4)_2CO_3 \xrightarrow{heat} CO_2(g) + 2NH_3(g) + H_2O(l) \qquad \text{Equation 1-1}$$

This is valid according to Le chatetlier's principle. An increase in pressure on a system at equilibrium will cause the reaction to shift to the side of with fewer moles of gas.

Recovery of metal values after leaching with ammonium carbonate solution involves precipitation. Precipitation of metal values from the pregnant liquor involves removal of ammonia from the pregnant liquor. When ammonia is removed from the leach liquor, the pH drops, and metal values precipitate out of the solution. The pH at which precipitation starts, is different for each metal (Langston *et al*., 1957). Operating in open reactors, increases chances of ammonia loses before leaching is completed. This implies that some metal values will be lost before solid-liquid separation due to precipitation (Meng and Han, 1996). It is essential that when working with ammonium carbonate solution, leaching and solid-liquid separation be carried out under pressure to prevent loses of ammonia.

Filtration in a pressurized vessel will prevent ammonia losses thus preventing precipitation of metals before solid-liquid separation is completed. For example in solid liquid separation processes such as counter- current decantation, it takes about one day to separate solids from liquids and normally metal loses occur as result of their coprecipitation and re-adsorption on iron hydroxide (Suarez and Villanueva, 2003). In most hydrometallurgical processes, the ore is leached in multiple stages and then the slurry is pumped from the leaching vessel to the separating unit. Energy cost required for pumping slurries from one point to another can be reduced if leaching and solid separation can be done in one vessel.

Filtration is carried out using sintered metal medium, which has the following advantages over other filtration media.

- Shape stability i.e. Self-supporting structural elements suitable for high differential pressure and pressure swings
- High heat resistance and thermal stability up to 950^{o}C
- High permeability with low-pressure drop
- Precise filtration because of homogeneous pore size distribution
- Chemical resistance against acids and caustic solution in various pH range

- Back-flushing and easy cleaning with supersaturated, superheated steam, chemical solvent, thermal processes and ultrasonically (GKN, 2009)

The possibility of filtering with sintered metal was established in a project carried out for a Post Graduate Diploma study at Stellenbosch University. In the project, the effect of pressure, particle size of the ore, and pore size of filter medium were investigated for filtration rate and clarity of filtrate. The aim was to obtain to optimum conditions on clarity of filtrate at a reasonable filtration rate. Filtration experiments were carried out using water and a sphalerite ore. Optimum filtration rate and clarity of filtrate were obtained when using a 20µm filter medium at pressure of 1 bar (Erasmus, 2008). From the filtration experiments, it was further established that porous sintered metals could be unblocked easily by back-flushing with water.

1.2 Objectives of the project

1. Determine the effect of operating conditions on the extraction of nickel from the ore (saprolitic laterite) with a solution of ammonia and ammonium carbonate.
2. Separate the pregnant liquor from the solids and obtain a clear filtrate by using leaching vessel designed for this project and equipped sintered metal filter medium.
3. Determine the limiting factor in the leaching mechanism of nickel laterite with solution of ammonia and ammonium carbonate.

1.3 Project plan

Nickel laterite will be leached with a solution of ammonium carbonate and the mother liquor will be separated from the solids by the filtration process. The mother liquor will then be analyzed using atomic absorption spectrophotometry (AAS) to determine the amount of metals extracted from the ore. The information obtained from leaching experiments will be used to determine the following:

- Optimum leaching conditions for unroasted laterite ore by varying the following variables using central composite design:

a. Temperature
b. Ammonium carbonate concentration
c. ammonia concentration
d. Oxygen pressure

- Leaching experiments were also carried out with roasted ore at optimum conditions. These optimum conditions were also used to design experiments for kinetic reactions.
- The kinetics of leaching roasted and unroasted nickel oxide ore with the vessel using ammonia and ammonium carbonate were studied.

1.4 Outline of the dissertation

The first part of this study is a review of literature on the leaching behavior of nickel laterite with a solution of ammonia and ammonium carbonate.

In Chapter 3 gave a detailed description of the design considerations for the leaching vessel. Chapter 4 focused on leaching and filtration experiments with roasted and an unroasted nickel laterite ore. The first part of leaching involved optimization while the second part involved a kinetic study of the leaching of unroasted and roasted laterite ore. Optimization experiments were done, using face centered central composite design with four factors. The four factors studied were temperature, ammonia concentration, ammonium carbonate concentration, and oxygen pressure.

Chapter 5 focuses on analyzing and discussing results of leaching and filtration experiments. Leaching experiments discussed are optimization reactions with an unroasted ore, leaching of roasted ore and kinetic reaction. Filtration results for the roasted and unroasted are also discussed.

2 Literature Review

This section deals with a literature review on leaching of nickel laterite with ammonia and ammonium carbonate solution.

Leaching of nickel laterite with ammonia and ammonium carbonate solution in this study incorporates solid-liquid separation under pressure. Solid-liquid separation is achieved with filtration using sintered metal filter medium. The next section discusses the application of sintered metal filter medium in filtration.

The possibility of using porous sintered metal for filtration under pressure was investigated by Erasmus (2008) in a Post Graduate Diploma project. The main objective of that study was to investigate the possibility of using porous sintered metal filter media in a pressurized vessel for solid-liquid separation. From that study, a pressurized filtration vessel was developed. The slurry of sphalerite ore was filtered under pressure (see Figure (A-1) in Appendix A for the picture of the vessel). Factors studied were the effect of pore size of the filter medium (20, 60 and 80µm), particle size of the ore (P < 53, P< 106 and P<150µm) and air pressure (0.5, 1 and 1.5 bar). The primary aim was to obtain a clear filtrate, which signifies leach liquor free from contaminants.

The results showed that the clarity of the filtrate and filtration rate were affected by pore size of the filter medium and air pressure. The filtration rate was found to increase with both an increase in air pressure and in pore size of the filter medium. On the other hand, the clarity of the filtrate decreased with an increase in air pressure and in pore size of the filter medium. Optimum conditions for clarity of filtrate and filtration rate were determined simultaneously using response profiling and desirability using Statistica Software. The optimum conditions for filtration rate and clarity of filtrate were determined to be 20µm filter medium, particle size smaller than 106 µm and air pressure of 1 bar (Erasmus, 2008). The results of the study are presented in Tables (A-1) and (A-2) in Appendix A. The possibility of unblocking the pores of the filter medium after filtration by back-washing was also investigated. In this case, eight experimental runs were carried out under the same conditions and after each run, the filter medium was back washed with water. The results indicate that filtration rate remained constant for the eight runs. There was no indication of residual pore clogging after back washing. The results are presented in Figure (A-2) in Appendix A.

2.1 **Hydrometallurgy**

There has been a tendency to place hydrometallurgy on a competitive basis with smelting for treatment of base metals sulfide. In fact, smelting processes have improved a lot. Modern smelting plants meet SO_2 emission standards by installation of double contact acid plants. Arguments that hydrometallurgical processes are less capital intensive than smelting processes are not entirely true, as some hydrometallurgical processes have multiple steps and others are coupled with pyro-metallurgical process like the Caron process. Another argument is that hydrometallurgical processes are non-polluting, but effluent may carry heavy metals and therefore must be treated (Rousseau, 1987).

Hydrometallurgical processes still need to be thoroughly developed if they are to be compatible with smelting processes. However, hydrometallurgy is unique in its application to the processing of low grade ores which cannot be beneficiated economically. It has distinct potential for in situ extraction of complex sulfide ores and concentrates.

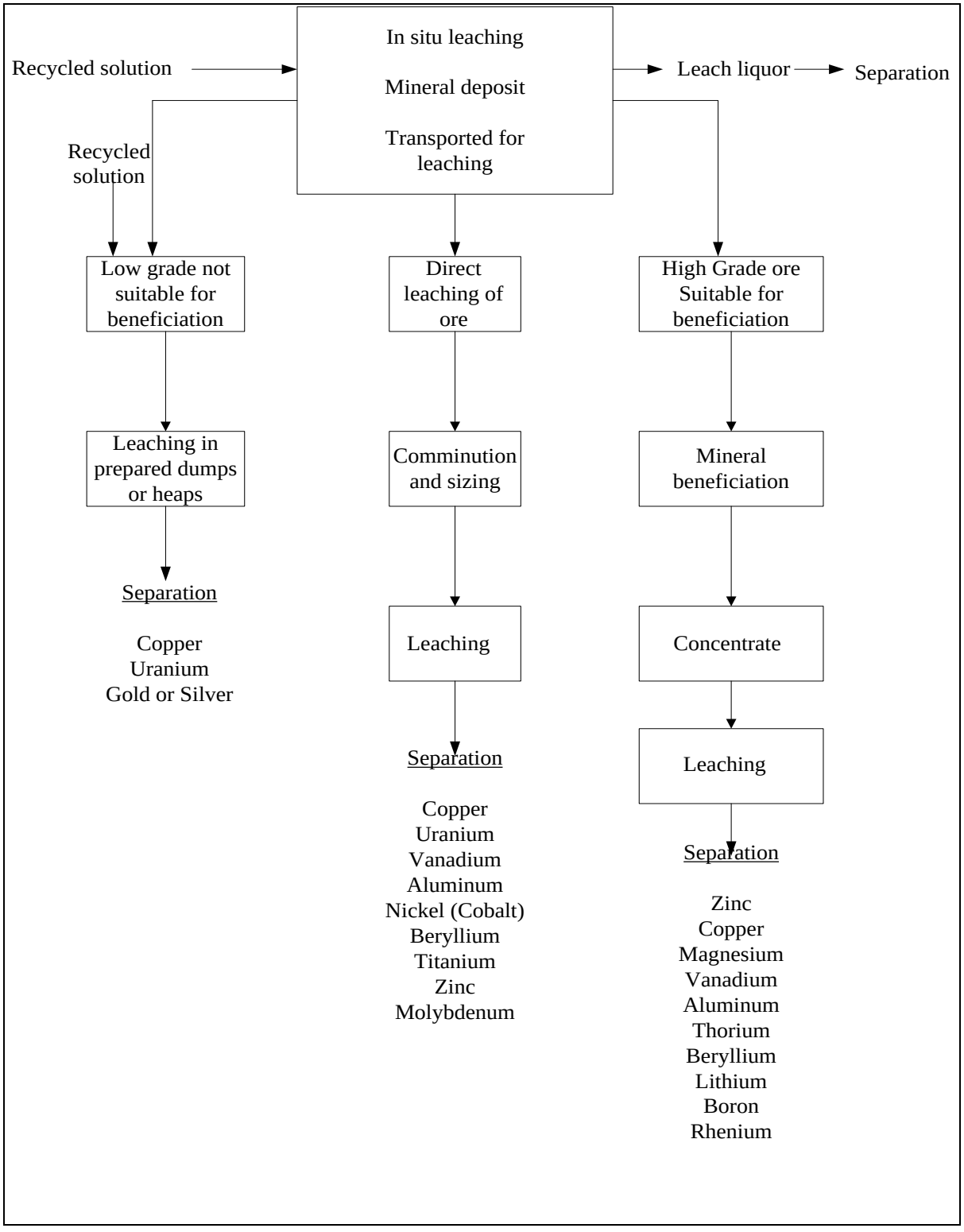

Figure 2-1: Various paths for handling ore in leaching practice (Redrawn from (Rousseau, 1987))

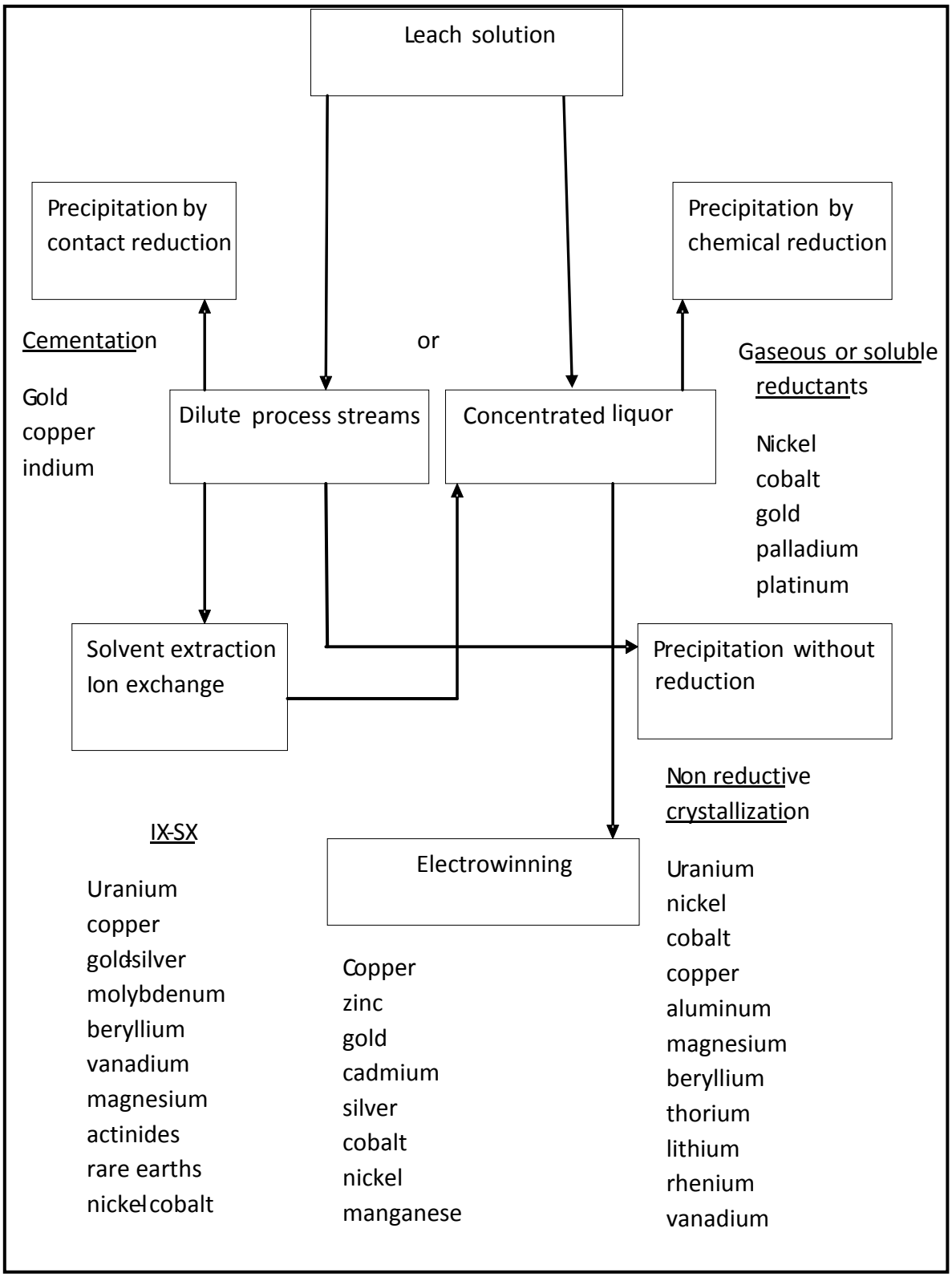

Figure 2-2: Methods for separating metals from dilute and concentrated process streams (redrawn from (Rousseau, 1987))

Figures (2-1) and (2-2) illustrate the general flow of ore in leaching practice and separation respectively. The ore is usually transported from the mineral deposit for leaching. In some

cases, leaching occurs in situ but examples of in situ leaching are few. Normally, the ore transportation and treatment depend on its type. These types are, direct leaching of low-grade ore and high-grade ore. Each of these ore types has their own leaching process. Each process produces leach liquor, which must be treated by separation for the recovery of metal values as metal or salts requiring further treatment (Rousseau, 1987).

2.2 Comparison of ammonium carbonate with other leaching solutions

Ammonia, ammonium carbonate, and sodium carbonate are important examples of alkaline leaching process. These reagents have been proven by many researchers to be more effective than acid leaching process (Harvey, 2006). For example in the treatment of uranium bearing ores containing limestone (CaO), sodium carbonate leaching has proven more attractive than the acid process. It avoids the high reagents consumption (Langston *et al*., 1957). In addition, the corrosion problems associated with acid that require expensive vessels (titanium lined) are negligible with sodium carbonate. However, carbonate leach process does not yield as high an extraction of uranium as the acid process (Langston *et al*., 1957).

Table 2-1: Series of tests for uranium leaching (redrawn from (Stapp, 1983)).

lixiviant	additives	catalyst
A. 2.0%NH_4HCO_3	0.5%$NaClO_3$	0.1% $CuSO_4.2H_2O$
B. 2.0%NH_4HCO_3	0.5% NH_4NO_3	-
C. 2.0%$(NH_4)_2CO_3$	0.5% NH_4NO_3	0.1% $CuSO_4.2H_2O$
D. 2.0%NH_4HCO_3	0.5% NH_4NO_3	0.1% $CuSO_4.2H_2O$
E. 2.0%$(NH_4)_2CO_3$	1.0% $NaNO_3$	0.1% $CuSO_4.2H_2O$
F. 2.0%Na_2CO_3	1.0% $NaNO_3$	0.1% $CuSO_4.2H_2O$

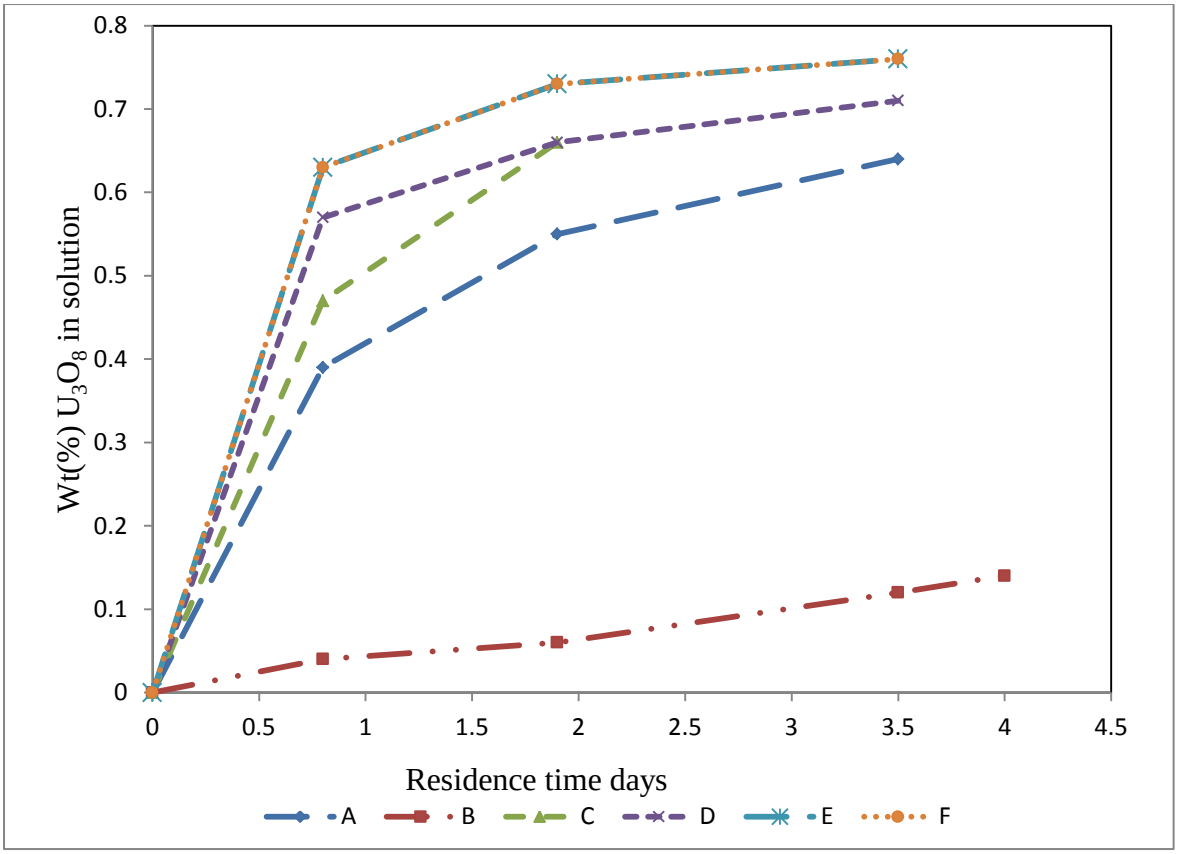

Figure 2-3: Results for series of test in uranium leaching (redrawn from (Stapp, 1983)).

Many researchers (Harvey, 2006; Rousseau, 1987) seem to arrive at a general conclusion that acid processes have higher yields than carbonate processes in treating the same ore under same leaching condition. Even though, it is believed that the ammonium carbonate leaching process yield is low, recent researches reveals that the ammonium carbonate process can overcome most problems associated with sodium carbonate or sodium bicarbonate (Goldwyer, 2007).

Ammonium carbonate decomposes to ammonia (NH_3) and carbon dioxide (CO_2) at temperatures above 60^{o}C. NH_3 and CO_2 can be recovered and reused again in the leaching process. This makes ammonium carbonate leaching more economic and environmentally safe than the sodium carbonate process (Goldwyer, 2007). Stapp (1983) showed that when uranium ore is leached with sodium carbonate or sodium bicarbonate and ammonium carbonate under same conditions (shown in Table (2-2)), ammonium carbonate produces the same extraction yield and rate. The results of this are shown in Figure (2-3). About 75% dissolution of uranium is achieved with ammonium carbonate. Ammonium carbonate process

has been used for leaching many ores such as nickel, zinc, and uranium (Langston *et al*., 1957; Harvey, 2006; Vosahlova and Weir, 1972).

2.3 Ammonium carbonate leaching of nickel ores

In leaching, it is important to consider three types of ores: low grade ores, direct leaching and high grade. An example of direct leaching is nickel oxide ore. This type of ore has sufficient value that it can be crushed and ground to appropriate size for agitation leaching. Pre-treatment by oxidative or reductive roasting may be necessary to render them suitable for leaching. High-grade ores have sufficient value that they may be beneficiated to reduce particle size and concentrate. The concentrate produced may be pre-treated by roasting prior to leaching (Rousseau, 1987). Nickel oxide and nickel sulfide are treated more or less in the similar manner except for the recovery process step. Both processes for the low grade and high grade ores originate from the same process, which was developed in the 1920s, called the Caron process.

In 1924, Caron obtained a US patent for a hydrometallurgical process for treating nickel laterites (Rousseau, 1987). The process involves the use of ammoniacal ammonium carbonate leach solution for the dissolution of an iron nickel alloy produced in the reductive roast pre-treatment (Rousseau, 1987; Bare, 1960; Vosahlova and Weir, 1972). The Caron method became known as the Nicaro process and was first used in Cuba in 1944 (Rousseau, 1987).

The process was developed because it was realized that certain types of ores are not suitable for sulfuric acid leaching. The silicate type of nickel ($H_2(Mg)SiO_4.H_2O$) associated with large quantities magnesium oxide (MgO) is entirely unsuitable for sulfuric acid leaching (Gupta, 2003).

According to Baghalha (1998), magnesium silicates rich in nickel dissolve rapidly releasing Ni and Mg in acid solution. Extra amounts of acid are required for the dissolution of magnesium. Dissolution of magnesium from serpentine proceeds according to the following equation;

$$2Mg_3Si_2O_5(OH)_{4(s)} + 12H^+ \rightarrow 6Mg^{2+} + 4SiO_2 + 10H_2O \qquad \text{Equation 2-1}$$

Sulfuric acid consumption for pressure acid leaching of limonite is 18 to 26 weight percent of dry ore, and, for saprolite is 40 to 60 weight percent. Evidently, extra amounts of acids are required due to higher Mg content in the saprolite (Papangelakis, 1998). Therefore, these types of ores are well suited for ammoniacal ammonium carbonate leaching. In broad terms, the Nicaro process involves the following; Laterite ore is ground, dried and reduction roasted in a multiple hearth furnace to convert the nickel and cobalt values to a leachable crude metal state (Vosahlova and Weir, 1972). A reduction step can be conducted with one or more reducing agents such as C, CO and H_2 at suitable temperature, according to the following reactions;

$$NiO + H_2 \rightarrow Ni + H_2O \qquad \text{Equation 2-2}$$

$$3Fe_2O_3 + H_2 \rightarrow 2Fe_3O_4 + H_2O \qquad \text{Equation 2-3}$$

The hot calcine is then quenched in recycled ammoniacal ammonium carbonate leach solution. Quenching is conducted to produce slurry having a temperature of about 50^{o}C. This is the temperature at which leaching is done. The slurry from the quenched step is pumped to a leaching tank. Air or oxygen is blown into the slurry to provide oxidizing conditions. Leaching of the nickel values take place according to the following reactions:

$$Ni + \frac{1}{2}O_2 + nNH_3 + H_2O \rightarrow Ni(NH_3)_n^{2+} + 2OH^- \qquad \text{Equation 2-4}$$

$$(NiFe) + O_2 + 6NH_3 + 4H^+ \rightarrow Ni(NH_3)_6^{2+} + Fe^{2+} + 2H_2O \qquad \text{Equation 2-5}$$

During leaching, iron is also oxidized, however iron oxidation takes several steps during the oxidation process. First metallic iron goes in solution as ferrous ammonium complex. The ferrous iron complex is oxidized and eventually iron precipitates out of the solution as hydrated oxides (Dutrizac and Monhemius, 1986). Iron precipitates according to the following reactions in ammonia ammonium carbonate solution in the presence of oxygen;

$$Fe + 2NH_4^+ + xNH_3 + 1/2O_2 \rightarrow Fe(NH_3)_{2+x}^{2+} + CO_3^{2-} + H_2O \qquad \text{Equation 2-6}$$

$$4Fe(NH_3)_{2+x}^{2+} + 10H_2O + O_2 \rightarrow 4Fe(OH)_3 + 8NH_4^+ + 4xNH_3 \qquad \text{Equation 2-7}$$

The leach reactions are exothermic; the temperature of the slurry will increase, while nickel dissolves into solution to form an ammonia complex. Beside nickel, other minerals such as copper and cobalt dissolve in the leach solution. Cobalt contamination is minimized by terminating the leaching process before a large portion of cobalt dissolves in the solution. Following leaching, the leach liquor is separated from solids through counter current

decantation (CCD). During solid liquid separation, some portion of the product liquor is recycled to build up the concentration to higher values (Nikoloski and Nicol, 2004).

After solid-liquid separation, nickel is recovered by boiling the solution or steam stripping to recover ammonia and carbon dioxide. In the process, dissolved nickel and cobalt precipitate in the form of carbonate compounds. Nickel precipitation proceeds as follows;

$$Ni(NH_3)_6^{2+} + 2CO_2 + 2OH^- \xrightarrow{\text{steam strip}} Ni(HCO_3)_2 + 6NH_3 \qquad \text{Equation 2-8}$$

The precipitate obtained from the above process is then heated to convert nickel carbonate to the nickel oxide product as shown in the following reaction;

$$Ni(HCO_3)_2 \xrightarrow{\text{Heat}} NiO + 2CO_2 + H_2O \qquad \text{Equation 2-9}$$

The product, nickel oxide, can then be reduced using carbon dioxide/hydrogen to obtain pure nickel (Zubryckyj, 1972).

$$NiO + C\ (coke) \rightarrow Ni + CO \qquad \text{Equation 2-10}$$

The standard reduction roast ammoniacal ammonium carbonate leach process explained above (Caron process) has been satisfactorily applied to the processing of low grade nickel oxide. The extraction process explained here is outlined in the flow sheet shown in Figure (2-4).

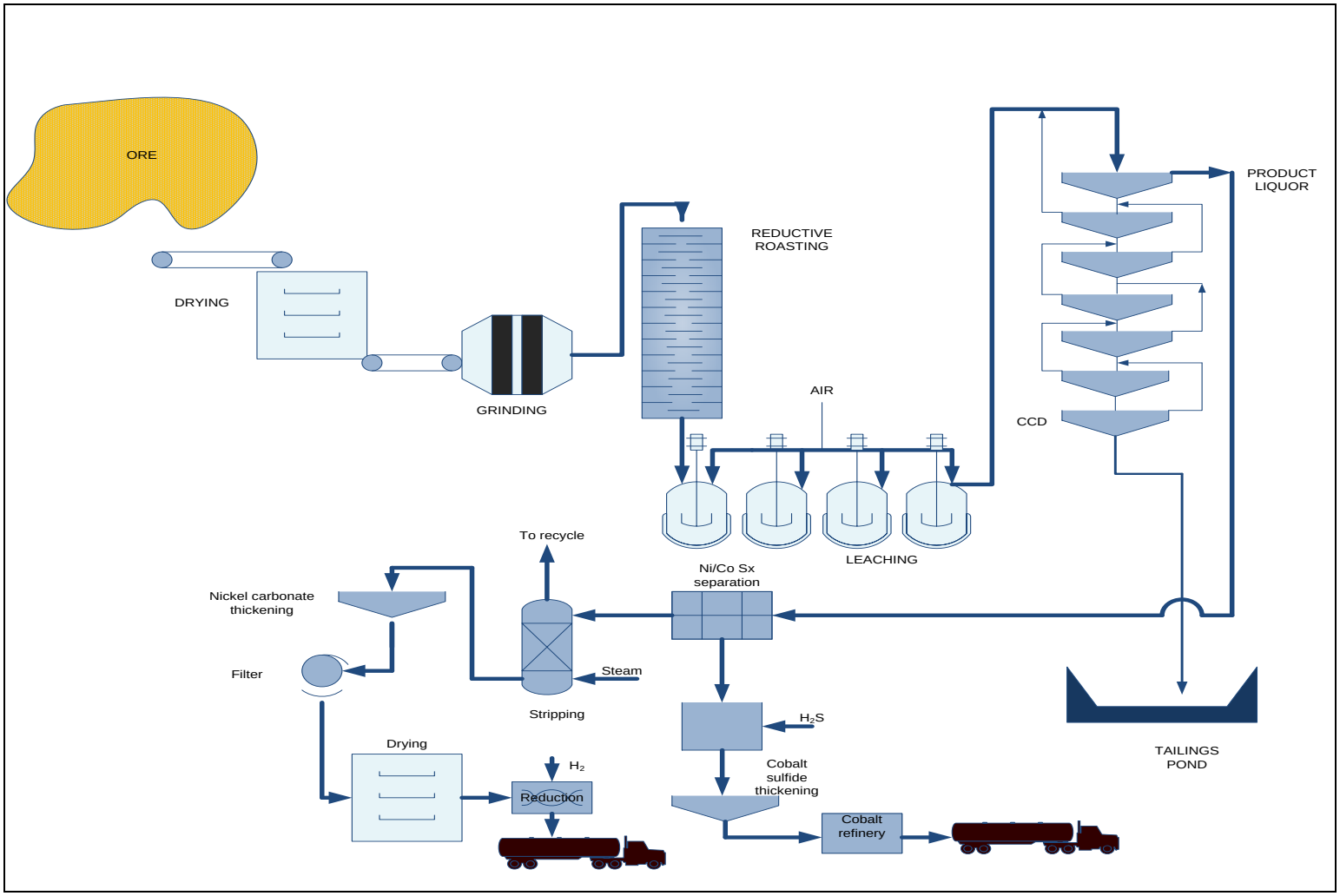

Figure 2-4 : flow sheet for the processing of nickel laterites (modified Caron process) (redrawn from Nikoloski and Nicol, 2004)

2.4 Developments in the Caron process for nickel leaching

2.4.1 Leaching

In a typical Caron process, the reduced ore that is cooled to about 85^{o}C is quenched in ammoniacal ammonium carbonate solution containing about 6.5% ammonia and 3.5% carbon dioxide. The slurry at 20% pulp density is delivered into compartmental impeller- equipped leaching tanks made of concrete to carry out leaching in the presence of oxygen. The function of oxygen is to oxidize nickel to ionic form before it can form an ammonia complex (Gupta, 2003). During oxidation, nickel and copper are oxidized to their +2 valence state and cobalt to its +3 valence state. These oxidized metals go into solution as their ammonia complexes and excess ammonia must be present in the leach solution at all times to prevent precipitation of metals as their hydroxide (Siemens, 1976).

Studies carried out on leaching of nickel show that low recoveries of nickel are obtained from leaching with ammonical ammonium carbonate solution (Gupta, 2003). There are several factors, which affect the recovery metal values in leaching, and some of these factors are discussed in the following sections.

2.4.2 Roasting

Roasting conditions for laterite ores vary according to their origin. Ore of different origin require specific roasting conditions, which must be predetermined for maximum conversion of nickel and cobalt oxide to their respective metallic state. For example in a study on the effect of roasting on leaching of laterite ores with ammonia solution by Valix and Cheng (2002), only 4% nickel recovery was obtained during leaching when the ore was calcined at 500 ^{o}C prior to roasting and 90% for uncalcined ore. In another study of Siemens, (1976), for maximum recovery of nickel during leaching, the ore must be calcined at 350^{o}C to 400^{o}C prior to roasting.

Saprolitic laterites consist mainly of a serpentine (magnesium hyrosilicate) phase, quartz (SiO_2), and goethite (FeOOH), which is the host mineral for nickel. Goethite is inert to ammonia solution. For nickel to be extractable, the goethite phase should be transformed to hematite Fe_2O_3. This phase transformation occurs as a result of high temperature during the

roasting process. However at high roasting temperature Ni-Fe (fayalite) is formed. This implies that during oxidative leaching with ammonia solution, iron will also be dissolved. Iron eventually precipitates out the solution as ferric hydroxide, which is a gelatinous substance. If the precipitate forms before dissolution of other metals, it forms a coating around the ore preventing further dissolution of other metals (Siemens, 1976).

2.4.3 **Concentration of ammonia and ammonium carbonate**

In the ammoniacal leaching process of nickel, the reagents used are ammonia and ammonium carbonate. In some cases, ammonium sulfate is used instead of ammonium carbonate. Carbonate solution can be introduced into the leaching system in the form of carbon dioxide gas or carbonate salt. Ammonium carbonate in solution decomposes in the presence of heat according to Equation (1-1).

Ammonia can be introduced as ammonia gas or as ammonia dissolved in water. When ammonia is dissolved in water, it forms ammonium hydroxide according to the following equation;

$$NH_3 + H_2O \rightarrow [NH_4OH] \qquad \text{Equation 2-11}$$

It is quite difficult to find the concentration which gives optimum extraction of nickel and cobalt from the literature because several reports give different concentrations of ammonia and ammonium carbonate. Most of the times leaching techniques are different and in some cases nickel powder instead of nickel ore is used during leaching process (Morioka and Shimakage, 1971). No study was found which uses ammonium carbonate only in leaching of nickel laterites.

Im and Johnson (1976) studied the leaching of nickel using a combined process of grinding and aqueous ammoniacal solution. From their results, they found that the maximum extraction of nickel is obtained when leaching is carried out using ammonia in its gaseous state, which is equal to 100 g/L NH_3 and 50g /L CO_2 gas over a period of 6 hours (Im and Johnston, 1975). Suarez and Villanueva (2003) claim that when nickel ore is leached over a period of 3 hours using 60 g/L NH_3 and 30 g/L of CO_2 in solution, maximum extraction is

obtained. The leaching process in this case was carried out in a tubular reactor under oxygen pressures.

According to Morioka and Shimakage (1971), both ammonia and ammonium ions are important in stabilizing the nickel ammonia complex. In their experiments whereby 10 g of nickel powder was leached in an autoclave in the presence of oxygen, they found that ammonia and ammonium ions are important in increasing the dissolution of nickel powder, furthermore when ammonium ions are present in excess (above 0.5M) in the leach solution, nickel powder dissolves despite the absence of ammonia. In addition, nickel powder dissolves in the leach solution without ammonium ions when concentration of ammonia exceeds 2.5 mol/L. Their results also show that nickel dissolution does not increase in solution containing more than 6.0 mol/L of ammonia or more than 0.5 mol/L of ammonium sulfate.

When the ammonium sulfate concentration is less than 0.5 mol/L, hydrolysis of the $Ni(NH_3)_6^{2+}$ occurs due to the concentration of OH^- being sufficiently high and nickel precipitate as basic salts ($NiSO_4.8Ni(OH)_2.8H_2O$). OH^- ions in the solution are easily removed in the solution when there are sufficient $NH4^+$ ions according to the following equation.

$$OH^- + NH_4^+ \leftrightarrows NH_4OH \leftrightarrows NH_3 + H_2O \qquad \text{Equation 2-12}$$

On the other hand, when the concentration of ammonium sulfate is more than 0.5 mol/L, the amount of nickel powder dissolved becomes less because of the decrease in the solubility of oxygen in the solution. The amount of sulfate required for maximum dissolution of nickel powder is at least about 1.5 times the theoretical value calculated from the following equation.

$$Ni + 1/2O_2 + 6NH_4^+ \rightarrow Ni(NH_3)_6^{2+} + H_2O + 4H^+ \qquad \text{Equation 2-13}$$

On the other hand, Siemens (1976) argues that in order to obtain maximum extraction of nickel at rapid leach rates, the concentration of ammonium sulfate must be equal or greater than the concentration of ammonia. To be exact, he claims that the leach solution must contain 50 to 400 g/L ammonium sulfate and 25 to 400 g/L ammonia Furthermore, he adds that, when cobalt is present in the ore a more concentrated leach containing about 50g/L ammonia, and 300g/L ammonium sulfate gives optimum extraction.

Based on the above discussions it is quite difficult to conclude the ratio of ammonia to ammonium salt for optimum extraction. It is also difficult to compare the ratios because in some cases nickel powder is used and in others nickel ore which has a more complex composition. It can be concluded that the amount of reagent required depends on the composition of the ore.

2.4.4 **Temperature and pressure**

In most commercial ammoniacal ammonium carbonate processes, leaching is carried out in closed or open vessels with agitation at atmospheric pressure (Siemens, 1976). According to most researchers, the leaching temperature ranges between of 10^{o}C to 50^{o}C (Vosahlova and Weir, 1972; Francis, 2004). In the study of recovery of non-ferrous metals from oxide ores, Siemens (1976) argues that there is no advantage gained when leaching is carried at higher temperatures than 50^{o}C. Furthermore, when operating at temperatures above 80^{o}C there is no further improvement in extraction but there is an increase in operating cost. Higher temperatures increase pressure within the leaching vessel thus requiring expensive equipment that will withstand such higher pressure. On the other hand, in open vessels operating at higher temperatures results in losses of ammonia.

In another study on high pressure leaching of nickel powders in ammonia ammonium sulfate solution, the leaching rate was found to be directly proportional to oxygen partial pressure. In that study, it was further revealed that in the absence of oxygen extraction of nickel does not occur. It was found that the action of oxygen in leaching was accelerated by increasing temperature. This is assumed be due to the fact that, the dissolution of oxygen in water increases with temperatures above 80^{o}C. Therefore enhanced solubility of oxygen in ammonium solution results in increased dissolution of nickel (Morioka and Shimakage, 1971).

2.4.5 **Magnesium effect**

Laterite ores that contain substantial amounts of magnesium pose problems in ammoniacal ammonium carbonate leaching. During leaching, substantial amounts of magnesium in the

ore goes into solution if not treated in the reduction roasting process (Vosahlova and Weir, 1972; Siemens, 1976). Part of this dissolved magnesium precipitates out of solution during the recycling operation in the Caron process. This precipitate forms scales in the piping. Therefore, the process requires double piping between thickeners. Although this solves the problem, operating costs are increased unless precipitation of magnesium is prevented.

According to Vosahlova and Weir (1972), the magnesium problem can be reduced by prolonging the leaching operation beyond that required for complete dissolution of nickel. This enables the greatest part of magnesium in the solution to precipitate onto the slurry solids and in addition to permit the major portion of cobalt values in the ore to be solubilized. Eva *et al.*, (1972) studied the relationship between magnesium leaching time and removal from the solution. The relationship is shown in the Figure (2-5).

Figure (2-5) shows that magnesium dissolution is high at the beginning of leaching but eventually most of it precipitates out of the solution. Leaching is terminated when the greatest part of the dissolved magnesium which is solubilized during early stages of leach has precipitated from the solution on the slurry solids. The strategy discussed only solves the problem of magnesium precipitating in pipes; however, allowing magnesium to precipitate in the vessel poses another problem. When magnesium precipitates in the leaching vessel, the precipitate will cover some of the undissolved nickel ore thus preventing further dissolution of essential metals. There is a very short period to guarantee that at that all essential metals will be dissolved before magnesium precipitates out of the solution.

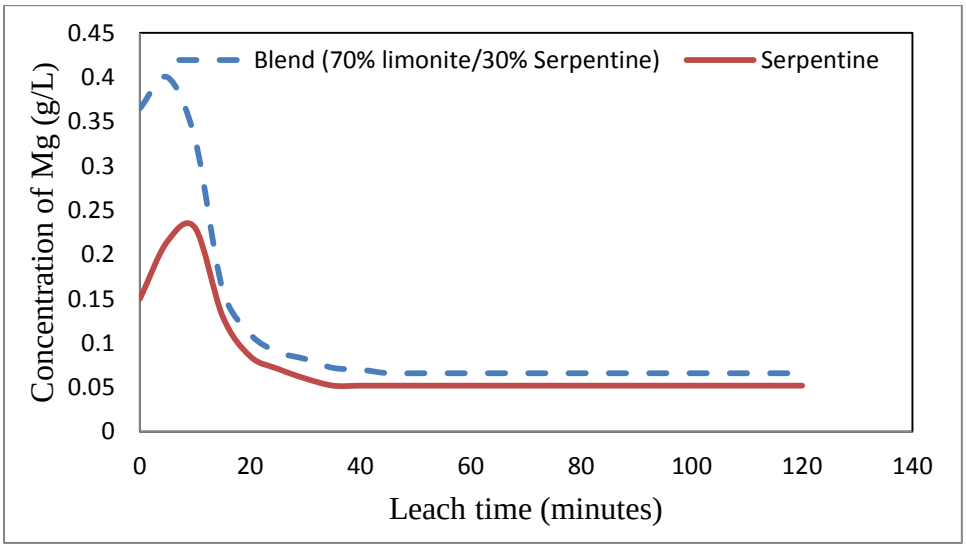

Figure 2-5: Concentration profile of magnesium with time during ammoniacal ammonium carbonate leaching (redrawn from (Vosahlova and Weir, 1972)).

2.4.6 **Iron effect.**

One of the major problems in the Caron Process is precipitation of iron oxide during leaching. Iron oxide precipitation is believed to be one of the reasons why nickel recovery in the Caron process is poor (Anand and Das, 1994; Bell, *et al*., 1995; Matson, 1971). Laterite ores contain a high content of iron, about 40 %. Most of the iron is reduced together with nickel to the metal state during reduction roasting process. Iron needs to be controlled carefully as it is associated with low extraction of nickel during leaching. During leaching all iron that was reduced to its elemental state is oxidized. Iron oxidation proceeds in a stepwise fashion, first to ferrous state (Fe^{2+}) and later to ferric state (Fe^{3+}). Ferrous ion is soluble, while ferric iron is insoluble in leach solution and precipitates as gelatinous hydrated oxide [$Fe(OH)_3$] (Suarez and Villanueva; 2003; Matson, 1971) .

A study of iron oxide precipitation from ammonia-ammonium sulfate solutions show that during oxidation process ferric hydroxide precipitate is not the only precipitate which is formed. The chemistry of iron oxide precipitation shows that several reactions are involved in iron oxide precipitation to form various forms Fe(II) and Fe(III) precipitates (Anand and Das, 1994). Equations showing iron oxide precipitation in ammoniacal ammonium carbonate solution are given in Equations (2-21) and (2-22). The following reactions are involved.

$$FeSO_4 + 4NH_3 \rightarrow Fe\,(NH_3)_4SO_4 \qquad \text{Equation 2-14}$$

The ferrous ammine complex formed in this reaction is very stably buffered in solution. The ferrous ammine is hydrolyzed as follows;

$$Fe\,(NH_3)_4SO_4 + 2H_2O \leftrightarrows Fe(OH)_2 + (NH_4)_2SO_4 + 2NH_3 \qquad \text{Equation 2-15}$$

In the presence of oxygen, $Fe(OH)_3$, $Fe_2O_3.3H_2O$ or Fe_2O_3 are formed. In addition to this oxides of amorphous ferric hydroxide known as ferrihydrites ($5Fe_2O_3.9H_2O$), or $Fe_5HO_8.4H_2O$, $Fe_6(O_4H_3)_3$) will also be formed (Anand and Das, 1994).

$$2Fe\,(NH_3)_4SO_4 + 5H_2O + O_2 \rightarrow 2Fe(OH)_3 + 2(NH_4)_2SO_4 + 4\,NH_3 \qquad \text{Equation 2-16}$$

The amorphous ferric hydroxide may give either goethite or magnetite (Anand and Das, 1994)

$$Fe(OH)_3 + 2\ Fe(NH_3)_4SO_4 + O_2 + 2H_2O \rightarrow 3FeOOH + 2(NH_4)_2SO_4 + 4NH_3$$

Equation 2-17

$$2Fe(OH)_3 + 4\ Fe(NH_3)_4SO_4 + H_2O + O_2 \rightarrow 2Fe_3O_4 + 4\ (NH_4)_2SO_4 + 8NH_3$$

Equation 2-18

If oxidation of ferrous iron to ferric is allowed to occur before the non-ferrous metals are oxidized and stabilized in solution as their ammonia complexes, the hydrated ferric or ferric hydroxide is precipitated out and forms a coating or film on the ore particles. This precludes further extraction of metals from its ore (Siemens, 1976; Dutrizac and Monhemius; 1986). The precipitated iron oxide adsorbs nickel and cobalt in ammonia ammonium carbonate solution according to the following reactions (Dutrizac and Monhemius, 1986):

$$_XFe(OH)_3 + Ni(NH_3)_6^{2+} + 2H_2O \rightarrow [Fe(OH)_3]_x[Ni(OH)_2] + 2NH_4^+ + 4NH_3$$

Equation 2-19

$$_XFe(OH)_3 + Co(NH_3)_5^{2+} + 2H_2O \rightarrow [Fe(OH)_3]_x[Co(OH)_2] + 2NH_4^+ + 3NH_3$$

Equation 2-20

According to Suarez and Villanueva (2003), the formation of $Fe(OH)_3$ during leaching causes 1-5% losses in nickel and 20-40% losses in cobalt, because of their readsorption on the ferric hydroxide precipitate.

It has been found that the leach process maybe controlled in such a fashion that complete oxidation of nickel, cobalt, and copper may be accomplished and metal ions stabilized in solution as their ammonia complexes before oxidation of ferrous iron. Iron hydroxide formation can be delayed during the leaching process by supplying oxygen at a lower level than required for reduced iron to react with oxygen. This can be achieved if an oxygen deficiency is maintained in the leaching vessel until 90% of the reduced non-ferrous metals are oxidized and iron oxidation is limited to the formation of ferrous oxide. After this, the rate of oxidation can be increased (Siemens, 1976).

In another study it is claimed that during ammoniacal leaching of nickel, control of oxygen supply also limits the amount of copper dissolved in the leach solution. In that study, copper dissolution is minimized by limiting the oxygen supply in such way that the redox potential is kept at -200mV (Matson, 1971). The Fe-S-CO_3-H_2O Eh-pH at 25^{o}C diagram also shows that at higher oxygen partial pressures iron (III) oxide is the more stable species over the entire pH range of the solution. At 100^{o}C, the diagram shows that iron (III) oxide is stable at even

low oxygen partial pressure (Ciminelli and Osseo-Asare, 1987). Dutrizac and Monhemius (1986) also confirm the fact that controlling oxidation potential during leaching does not only limits dissolution of iron but also of copper.

Iron absorption on metals can be decreased not only by limiting oxygen supply to the leach solution, but also by using a high concentration of CO_2 in the leach solution. This way the absorption of nickel and cobalt is greatly reduced. Higher concentration of CO_2 implies high concentration of ammonium ions in the solution. It is believed high ammonium ion concentrations decrease the coprecipitation of divalent cations with ferric hydroxide (Dutrizac and Monhemius, 1986). However, according to Morioka and Shimakage (1971), high concentration of salts in the leach solution results in low extraction of metals. High salt concentration causes low solubility of oxygen in the leaching solution.

Even though the above technique minimizes dissolution of iron, nickel extraction becomes very poor. While minimizing of oxygen supply seems to be the best solution for preventing formation of ferric oxide and minimizing of copper dissolution in the leach solution this however causes a slow leaching process. According to Mirioka and Shimakage (1971), the leaching rate in ammonia ammonium sulfate leaching of nickel in the presence of oxygen is directly proportional to the oxygen partial pressure. Therefore, if the oxygen supply is limited, the rate of nickel dissolution will be low. So far, the methods of limiting iron oxidation involve controlling the leaching process by changing leaching conditions. However, in all process approaches taken so far, there is a problem of a slow leaching rate.

Only one study (Bell *et al*., 1995) that uses a different approach was found. In that study, iron oxidation to ferric hydroxide is prevented by addition of saccharides or related organic compounds. It is believed that OH groups in this organic compound will act as sequestering agents which will prevent further oxidation of iron, thus keeping iron in solution. In this study, manitol and dextrose were added to the leaching solution. Hydrogen peroxide was added as an oxidant. Results from the experiments showed that there was an improvement in the iron dissolution. However, copper extraction was low. Low extraction of copper was associated with use of hydrogen peroxide as an oxidant and the reductive nature of the organic compounds used.

2.4.7 **Recovery**

In the Caron process, after the separation of the trace amounts of ferrous iron present in the leach liquor by oxidation and precipitation as hydroxide, the ammoniacal liquor goes to stills for steam heating to remove ammonia. In this process precipitation starts when the concentration of ammonia, comes down to about 2%. When ammonia is further removed, insoluble basic nickel carbonate [$Ni(HCO_3)_2$] separates out according to Equation (2-14).

The nickel carbonate slurry is filtered, washed, and calcined to yield nickel oxide. The calcined nickel oxide powder is pelletized along with anthracite coal and sintered to yield a product containing 88% of nickel in metallic form. Besides nickel, the product contains 0.7 % Co, 0.3 % Fe, 1.7 % SiO_2 and 7.5 % O_2. The overall recovery of nickel from the sinter is around 76 % (Gupta, 2003). The original Caron process described above is handicapped by the fact that the sintered oxide contains considerable amounts of cobalt, recovery of which is rather difficult. In order to improve the recovery of both nickel and cobalt, many researchers have modified the Caron process.

Bare (1960) found out that temperature and retention time have adverse effects on extraction of cobalt. This is believed to be caused by the presence of sulfidic sulfur in the reduced ore and can be overcome when a sufficient amount of a sulfur component which will produce sulfite ions [$(SO_3)^{2-}$] is added to the leach solution. Bare (1960) conducted experiments using Mayari ore varying addition of sulfur dioxide (SO_2) in the ammoniacal ammonium carbonate solution.

From the results, when 4.72kg/ton SO_2 ore is added, there is an increase of 20% recovery for cobalt compared to when sulfur was not added to the leach solution. It is believed that, the sulfite ions react with sulfide sulfur (S^{2-}), which is present in the reduced ore to form soluble sulfur compounds. These compounds are predominantly thiosulfates and they do not interfere with extraction and recovery of cobalt. Addition of sulfur in the form of SO_2 can be added at any stage in the multiple stages leaching (Bare, 1960).

In another modification, recovery of nickel is improved by addition of H_2S to the product leach liquor after ammoniacal ammonium carbonate leaching. H_2S gas is brought into contact with the leach liquor to precipitate all cobalt and some of nickel as sulfides. The sulfide product after washing, drying, and calcinations will contain 3.9 % Ni, and 93 % Co. The

cobalt free mother liquor is treated in the usual way to yield an oxide containing 90 % nickel (Gupta, 2003).

According to Zubryckyj *et al*. (1972), cobalt and copper can be removed from the leach solution after thickening and filtration by reacting them with sulfudizing agents such as H_2S, $(NH_4)_2S$, Na_2S or sodium salt of sulfur to precipitate copper and cobalt with small amounts of nickel. The leach liquor product will contain nickel which is free from cobalt and copper but which still contains sulfur and other impurities such as magnesium, aluminum, silica, and small amounts of iron and manganese. Nickel is recovered from the leach liquor by the usual distillation. In this process sulfur and other impurities also precipitate with basic nickel carbonate. Sulfur present in the leach liquor is usually in the form of sulfates and partly in the form of unsaturated sulfur compounds such as thiosulfates ($S_2O_3^{2-}$) and polythionates ($S_3O_6^{2-}$).

If sulfur in basic nickel carbonate is in excess of 1% by weight, it is removed. If it is not removed, some nickel will be lost in solution during boiling to precipitate as basic nickel carbonate. In this modification, excess sulfur removal is accomplished by providing sodium compounds e.g. sodium hydroxide (NaOH), Na_2CO_3 in order of 2-20 g/l, capable of combining with sulfate to form sodium sulfate in the leach solution prior to the first boiling step. The sodium compounds tie up available sulfate ions in the solution, thus preventing formation of basic nickel, iron and manganese sulfates (Zubryckyj *et al*., 1972).

The basic nickel from the first boiling step is redissolved in pure concentrated ammoniacal ammonium carbonate solution to produce a concentrated ammoniacal nickel carbonate solution containing about 50 to 150 g/L of dissolved nickel. It is claimed that this step provides a concentrated nickel ammonium carbonate system suitable for subsequent treatment in the reduction step. In addition, maximum dissolution of nickel with minimum dissolution of impurities such as magnesium, silica, aluminum, iron, manganese is obtained.

In the case where nickel and cobalt are recovered by solvent extraction, presence of sulfur should be minimized. In such case, sulfur is reduced from the reduction stage by using CO as sole reductant and with use of sulfur containing fuel oils. Presence of sulfur prevents oxidation of cobalt to +3 state. This increases the amount of hydrogen peroxide, which is required to ensure that all cobalt is oxidized +3 state. In solvent extraction, cobalt should be oxidized +3 in order to obtain maximum recovery. Solvent extraction is carried out using a counter-current bank of mixer-settler units. The extracting agent consists of α-hydroxy

oxime, commonly known as LIX_64N dissolved in a kerosene type hydrocarbon solvent. It is claimed that this process can achieve up to 98% nickel recovery (Siemens, 1976).

2.5 Chemistry of leaching nickel oxides and gangue minerals

The chemistry of ammoniacal leaching for transition metals and their compounds involves not only oxidation-reduction, but also complexation equilibria. Generally, phase relationships of various state of transition metals in aqueous systems can be best identified using stability diagrams. A number of researchers have reported stability for Cu-NH_3-H_2O, Co-NH_3-H_2O and Ni-NH_3-H_2 (Meng and Nan, 1996). Nickel, cobalt, and copper are included in this discussion because they are present in nickel ores and furthermore, copper and cobalt affect the final recovery of nickel if they are present in sufficient amount in the ore.

2.5.1 Cu-NH_3-H_20 Systems

In the Cu-NH_3-H_2O systems there are species such as NH_3, NH_4^+, H^+, C^{2+}, $Cu(OH)_3$, $Cu(OH)^{2-}$, $Cu_2(OH)_2^{2+}$, $CuNH_3^+$, $Cu(NH_3)_2^+$, $Cu(NH_3)_3^{2+}$, $Cu(NH_3)_4^{2+}$, and $Cu(NH_3)_2^{2+}$, coexisting together in the solution. The Eh-pH diagram of copper in ammonia solution at 25°C can be found in literature (Meng and Nan, 1996). According to the Eh-pH diagram, at pH around 9 the dominant species in ammonia solution are $Cu(NH_3)_4^{2+}$ and $Cu(NH_3)_2^+$.The ratio of $Cu(NH_3)_4^{2+}$ to $Cu(NH_3)_2^+$ depends on the oxidation potential in the system. The redox reaction for the system is given in equation 2-27. The relationship between the potential and this can be written as:

$$Cu(NH_3)_4^{2+} + e^- \rightarrow Cu(NH_3)_2^+ + 2NH_3 \qquad \text{Equation 2-21}$$

$$Eh = 0.074 - 0.01182\log[NH3] + 0.05911 log \frac{[Cu(NH3)_2^+]}{[Cu(NH3)_4^{2+}]} \qquad \text{Equation 2-22}$$

It can be noted that, the higher oxidation state of the two namely complex; $Cu(NH_3)_4^{2+}$ and $Cu(NH_3)_2^+$ can serve as an oxidant and a reductant, respectively. If $Cu(NH_3)_4^{2+}$ is used as an oxidant in a hydrometallurgical process, the pH should be kept in the range of 9-11 so as to obtain maximum activity of $Cu(NH_3)_4^{2+}$.

2.5.2 **Co-NH_3-H_2O System**

The Co-NH_3-H_2O Eh-pH diagram at 25°C and total pressure of 1 atm in ammonia solution is given in the literature (Meng and Nan, 1996). According to the Co-NH_3-H_2O system, $Co(NH_3)_6^{3+}$, $Co(NH_3)_5^{2+}$ and $Co(NH_3)_4^{2+}$ are the major soluble species over the pH range 9 to 11. The redox reactions for the system are given in Equation 2-29 and 2-30 respectively. The ratio of $Co(NH_3)_6^{3+}$ to $Co(NH_3)_4^{2+}$ or $Co(NH_3)_5^{2+}$ are determined by the potential of the system and the relationship can be expressed as:

$$Co(NH_3)_6^{3+} + e^- \rightarrow Co(NH_3)_4^{2+} + 2NH_3 \qquad \text{Equation 2-23}$$

$$Co(NH_3)_6^{3+} + e^- \rightarrow Co(NH_3)_5^{2+} + NH_3 \qquad \text{Equation 2-24}$$

$$Eh = 0.871 - 0.1182log[NH_3] + 0.0591\log\frac{[Co(NH_3)_4^{2+}]}{[Co(NH_3)_6^{3+}]} \qquad \text{Equation 2-25}$$

$$Eh = 0.871 - 0.0591\log[NH_3] + 0.0591\log\frac{[Co(NH_3)_5^{2+}]}{[Co(NH_3)_6^{3+}]} \qquad \text{Equation 2-26}$$

Under practical conditions, $Co(NH_3)_6^{3+}$ is dominant. Its stability region on the Eh scale is at pH 9.5. Therefore, $Co(NH_3)_6^{3+}$ can be used as an oxidant in ammonia solutions and when it does, the conditions of the solution should be maintained within the stability region as indicated by the Eh-pH diagram (Meng and Nan, 1996).

2.5.3 **Fe-NH_3-H_2O System**

The Eh-pH diagram for Fe-NH_3-H_2O system at various concentrations of NH_3 and Fe(II) is given by Dutrizac and Monhemius (1986). At 0.01 M Fe(II) and 5 M NH_3 solution at 25°C dominant species are Fe, Fe^{2+}, $Fe(NH_3)^{4+}$ and $Fe(OH)_2$ at low oxidation potential and Fe^{3+} and $Fe(OH)_3$ at higher oxidation potentials (Dutrizac and Monhemius, 1986). At pH below 10.8, ferrous hydroxide begins to precipitate at oxidation potential as low as -0.5V. In another Eh-pH diagram for Fe-NH_3-H_2O at Fe(II) total concentration 0.2 M and 5 M NH_3 and at 25°C, ferrous hydroxide exists at pH below 8.4 and at above 10.8. At pH 8.4 most NH_3 in the solution is bound as ammonium ions and therefore there is low quantity of free NH_3 to complex ferrous ion as $Fe(NH_3)^{4+}$. From the Eh-pH diagrams discussed here, it can be seen

that in ammonium carbonate systems no ferrous hydroxide should form if the dissolved iron in the solution is low (Dutrizac and Monhemius, 1986).

2.5.4 **Ni-NH_3-H_20 Systems**

The Eh-pH diagram for Ni-NH_3-H_2O system at 25^oC, total pressure of 1 atm and ammonia solution is given in literature (Meng and Nan, 1996). According to the Eh-pH diagram, there is no mono or tri-valent nickel ion species thermodynamically stable under conditions considered in the Eh-pH diagrams. The predominant species is $Ni(NH_3)_5^{2+}$ in the pH range of 8.5 to 10.5. The other predominant specie is $Ni(NH_3)_6^{2+}$ which is stable around pH of 11 at low activity of soluble species. According to Eh-pH diagrams discussed so far, it is clear that, unlike copper and cobalt, nickel ammine complex ions cannot serve as an oxidant in aqueous solutions, because no lower or higher oxidation state of nickel can be paired under these conditions (Meng and Nan, 1996). From this discussion, it clear that nickel is stable over a wide pH range in ammonia solution at ambient temperatures, this indicates that ammonia is a suitable solution for dissolution of nickel. However, dissolution of nickel in ammonia solution should be carried out in an oxidizing environment.

2.6 **Dissolution kinetics**

In general leaching involves the transfer of metals from the solid phase to the liquid phase by the dissolution process. Dissolution of metals is represented stoichiometrically as follows;

$$<M> + a(A)_{(gas)} + b(B)_{(liquid)} \rightarrow c(C) + d(D) \qquad \text{Equation 2-27}$$

M stands for metal, A and B stands for reactants, C and D stands for products and a, b, c and d stands for stoichiometric coefficients. The overall dissolution process of transferring metals from solid phase to the liquid phase involves several processes.

- Dissolution of gaseous reactant in liquid,
- diffusion of gaseous reactant A through the film surrounding the particle to the surface of the solids,
- diffusion of reactants through the pores of the particle to the mineral of interest,

- Chemical reaction between reactants and the mineral of interest and diffusion of reactant products from solid particle through the liquid and gas film to the leaching solution (levenspiel, 1999).

In all these processes, the slowest step will determine the leaching rate. The rate-controlling step is influenced by reaction conditions. Besides the above mentioned steps, there are other two processes that can affect the overall rate; heat transfer and changes in the structure of solids during the reaction. Solid-liquid reactions either consume or generate heat. Heat transfer involves convection/radiation between solid and surrounding, and conduction in solids.

Several models have been developed and more are still being developed, that are used to describe the dissolution behavior of metals in leaching solutions. The most commonly used model is the shrinking core model. The model can be applied to varying spherical particle sizes and single spherical particle sizes of unchanging or changing particle size.

2.6.1 **Copper**

According to a literature survey conducted by Xia and Hu (1980), the dissolution of copper in ammoniacal solution in the presence of oxygen is an electrochemical process. Dissolution is followed by formation of copper oxide and then dissolution of the oxide. Under low oxygen pressure conditions, the dissolution process is controlled by the oxygen diffusion through a mass transfer boundary layer at the cathodic site. Under high oxygen pressure, the dissolution process is controlled by surface reaction. The rate expression established from the literature survey, the dissolution rate depend on both ammonia and oxygen concentration.

Ekmekyapar *et al.,* (2003) studied dissolution kinetics of copper oxide ore in ammonium chloride solution over a temperature range of 10 to 50^{o}C in the absence of oxygen. According to this study, the dissolution rate is controlled by ash layer diffusion and chemical reaction. The following equation was found to be suitable for explaining dissolution kinetics of copper in ammonium chloride solution;

$$1 - 2(1 - X)^{1/3} + (1 - X)^{2/3} = kt \qquad \text{Equation 2-28}$$

When experimental variables such as temperature, particle size, ammonium chloride concentration stirring speed and solid to liquid ratio are incorporated into the above equation, the following kinetic model was finally derived. (Ekmekyapar *et al.*, 2003)

$$1 - 2(1 - X)^{1/3} + (1 - X)^{2/3} = k_o c^a d_p^b \rho_{\frac{S}{L}}^f m^g e^{-Ea/RT} t \qquad \text{Equation 2-29}$$

Where k_o, a, b,f and g are constant, m is the stirring speed (s^{-1}) and $\rho_{S/L}$ is the solid to liquid ratio (g/g). The activation energy was determined to be 71 kJ/mol.

In another study of Bingol *et al*, (2005), the dissolution kinetics of copper oxide ore was studied in ammoniacal ammonium carbonate solution at temperatures of 15 to 60^{o}C in the absence of oxygen. Copper dissolution was found to be controlled by mixed kinetics. From experimental results, it was found that the leaching rate is fast at the beginning of the reaction and slows down as the reaction proceeds. It was established that interface transfer and diffusion of copper dissolution across the product layer limit the reaction. The leaching model was determined as follows;

$$1/3\ln(1 - X) - [(1 - (1 - X)^{1/3}] = kt \qquad \text{Equation 2-30}$$

The activation energy was found to be 15 kJ/mol.

Based on the information given above, copper oxide dissolves in ammonia solutions in the absence of oxygen. In the presence of oxygen, the dissolution is electrochemical. The dissolution process follows the unreacted shrinking core model, whereby the ash forms around the unreacted core. As the reaction proceeds and the ash layer builds and the reaction rate slows down.

2.6.2 **Nickel**

Dissolution of nickel powder (under oxygen pressure) in ammoniacal solution is electrochemical in nature and can be expressed as follows:

Anodic reactions

$$Ni \rightarrow Ni^{2+} + 2e^- \qquad \text{Equation 2-31}$$

$$Ni^{2+} + 6NH_3 \rightarrow Ni(NH_3)_6^{2+} \qquad \text{Equation 2-32}$$

Cathodic reactions

$1/2O_2 + H_2O + 2e^- \rightarrow 2OH^-$ Equation 2-33

$2OH^- + 2NH_4^+ \leftrightarrows 2NH_4OH \leftrightarrows 2NH_3 + 2H_2O$ Equation 2-34

The dissolution of oxygen through the leach solution to the nickel surface is the rate-determining step. The apparent activation energy was measured to be 8.9 kJ/mol (Bhuntumkomol *et al*,. (1982)

In another study on the high pressure leaching of metallic nickel powder in ammonium carbonate carried out by Mizoguchi *et al*, (1978), similar behavior was observed on the nickel dissolution. The dissolution of nickel powder was described in terms of a shrinking particle model with first order reaction kinetics at the solid-liquid interface. The initial rate of dissolution was a function of oxygen concentration, mass transfer coefficient, particle density, and radius. The apparent activation energy was found to be 6.28 kJ/mol at temperatures of 30-110^{o}C.

2.6.3 **Cobalt**

In a rotating disk system, the dissolution of cobalt metal at ambient conditions (25^{o}C and 1atm) and high ammonia concentration (0.8 M) exhibited a linear relationship between the dissolution rate and leaching time. At high ammonia concentration, the apparent activation energy of the dissolution was found to be 12.4 kJ/mol.

An empirical rate expression at pH 9.3 has been developed to be

$$rate = K(NH_3)_{Tot}^{0.5}(P_{O_2})^{0.75}$$ Equation 2-35

Where K is a parameter, which is proportional to the rate constant; NH_{3Tot} is the total concentration of ammonia including ammonium; P_{O2} is partial pressure of oxygen (Bhuntumkomol *et al.*, 1982).

2.7 Summary

This section has reviewed some challenges encountered in leaching of metals when using other leaching solutions. When ammonium carbonate was compared with these leaching solutions, it yields the same extraction of metals from the ore. Furthermore, Ammonium carbonate can be recovered after leaching and used again.

The largest part of this section has reviewed conditions for leaching nickel oxide ore with ammonium carbonate solution. In the extraction of nickel, roasting is very important. Roasting conditions must be controlled in such a way that extraction of iron is minimized. If iron is leached it will precipitate and adsorb on the ore preventing further dissolution of nickel.

The possibility of pressure filtration using porous sintered metal filter medium was established in a previous study (Erasmus, 2008) which has shown that solid-liquid separation using porous sintered metal under pressure is possible.

For high recovery of this nickel from their nickel ores, temperature should be high. In order to avoid reagent loss when leaching with ammonia and ammonium carbonate at high temperatures, a closed system is required. In all cases, air or oxygen is required for oxidizing nickel to the more soluble states during leaching. Besides providing an oxidizing atmosphere during leaching, oxygen is essential for creating a high pressure within the leaching vessel. Pressure provides equilibrium conditions which prevent decomposition of ammonium carbonate at high temperatures during leaching.

Leaching at high temperature improved reaction kinetics and metal recovery. For metals ore, which contain a lot of silica, leaching at temperatures greater than 120 ^{o}C resulted in excessive consumption of the reagent. Agitation during leaching had been found to improve reaction kinetics and metal recovery.

Based on the findings from the literature survey, the leaching vessel used to carry out the leaching experiments was designed to operate in chemical environment of ammonia at temperatures of up to 100 ^{o}C, pressurized with oxygen and with an agitation system.

3 Design of the leaching vessel and testing

This section deals with the materials used in the construction of the vessel, design considerations, components of the vessel, operation and testing of the vessel.

3.1 Materials of construction

Materials used in the construction of the vessel were chosen based on the chemical environment of the leaching solution. Leaching solutions used were ammonia and ammonium carbonate in the presence of oxygen. Appropriate materials for constructing a leaching vessel under these chemical environments were chosen based on the guide by Dillion (1992). For the metallic parts of the vessel, the appropriate materials of construction were found to be ferrous alloys of Austenitic grade. These are 304, 316 and 317 stainless steel. For non-metallic parts, suitable materials were found to be teflon and neoprene rubber (Dillion, 1992). The pump materials were chosen based on the same criterion. The pump head was made of stainless steel and o-rings were made of teflon. The pump valves were made of hastelloy and the pump diaphragm was made of Teflon.

3.2 Design considerations

3.2.1 Design pressure.

The vessel was designed to with stand maximum operating pressure of 10 bar. For the vessel under high internal pressure, the design pressure is normally taken as the pressure at which the relieve valve is set (Coulson and Richardson, 1983). In this study, the vessel was pressurized using oxygen and maximum oxygen supply was 5 bar. At high temperatures, ammonium hydroxide and ammonium carbonate vaporize and therefore contribute another pressure inside the vessel. The maximum operating pressure was considered as 10 bar. Selection of the pump was based on the maximum internal pressure of the vessel. The pump used here had a maximum inlet pressure of 17 bar and maximum flow rate of 29 L/min.

However due to connection of the pump to the motor through pulleys, when the pump was calibrated it was found that maximum flow rate that could be achieved was 25 L/min. Calibration data and the graph are given in Appendix B.2.

3.2.2 **Design temperature**

Strength of materials decrease with an increase in temperature, therefore the maximum allowable stress will depend on the material temperature. The design temperature at which the design stress is evaluated should be taken as the maximum working temperature of the material (Coulson and Richardson, 1983). The maximum working temperature in this vessel was taken as 120^{o}C. The vessel was heated using external heating bands, this implies that the temperature on the walls of the vessel was much higher than 120^{o}C. Since the temperature on the walls of the vessel was not calculated, the temperature of 120^{o}C was used in determining design stress. Appropriate materials and thickness of the vessel must be chosen based on this temperature. Stress on the vessel walls is a function of temperature and pressure. The thickness of the vessel was determined using the design temperature and pressure according to the following equation.

$$e = \frac{(p_i - D_i)}{(2F - p_i)} \qquad \text{Equation 3-1}$$

Where p_i is the internal pressure, D_i is the internal diameter, F is the design stress, and e is minimum thickness. For maximum operating pressure, temperature of 120^{o}C and internal pressure of 10 bar, design stress is 135 N/mm^2 (Coulson and Richardson, 1983). Substituting all parameters into equation, minimum thickness can be calculated as follows;

$$e = \frac{1\,{}^{N}/_{mm^2} \times 150mm}{\left(\left(2 \times 135\,{}^{N}/_{mm^2}\right) - 1.0\,{}^{N}/_{mm^2}\right)} = 0.56mm$$

If corrosion allowance is added which is 2.00 mm (Coulson and Richardson, 1983), minimum thickness required equals;

$$0.56 + 2.00 = 2.56 \sim 3mm$$

The thickness of the vessel in this design was 3mm, which is the thickness required for the vessel to withstand stress on the walls due operating temperature and pressure within the

vessel. Figure (3-4) shows the photograph of the vessel and Figure (3-5) shows the photograph of the pump for the recirculation of water.

3.2.3 **Stirrer design**

The vessel developed in this study is a stirred reactor. The mixing system for the vessel was designed to ensure that the solids are suspended and to maintain proper hydrodynamic and gas-liquid mass transfer. It is important that solids are always suspended to prevent cake formation on the filter medium. Cake formation on the filter medium can result in pore clogging of the filter medium before filtration is achieved. The mixing system was designed without baffles in the vessel. The fact that there were no baffles within the vessel, a dual impeller system was decided to be the best selection for the vessel to prevent swirling motion of the liquid. Swirling mass of the liquid generates an oscillating surge in the tank, which coupled with the deep vortex may create a large fluctuating force acting on the mixer shaft (Perry, 2007). The bottom impeller will ensure proper mixing solids and liquid while the top will ensure proper mixing of gas and liquid. Some guidelines were sourced from the literature of Gogate *et al*. (2000).

Impellers are classified according to the mixing regimes, either laminar or turbulent. For laminar mixing impeller diameters approach the diameter of the vessel. Therefore, the transportation of momentum is poor in laminar mixing impeller. On the other hand, turbulent mixing impellers are typically one quarter to one-half of the vessel diameter and therefore transportation of momentum is good. For turbulent flow the Reynolds number (Re)= ($ND^2\rho/\mu > 10^4$). For the solids to be suspended, a good transportation of momentum is required. Therefore, an impeller which produces turbulent flow is required. Turbulent flow impellers are classified into radial flow and axial flow. Typical radial flow impellers are flat and curved blade. The pitched blade turbines and propellers are axial flow or mixed flow impellers (Gogate *et al*., 2000). The mixing system for the vessel selected was two pitched blade turbines in order to provide turbulent mixing regime within the vessel.

For solid-liquid mixing agitation is important to promote chemical reaction between solids and liquids, to obtain a relatively uniform concentration of particulate solids in liquids and to keep solids particle suspended in the liquid. Performance of particle suspension is often

measured in terms of the fraction of the particles resting at the bottom of the vessel for a specified time interval. Suspension of particles at the bottom of a stirred tank is due to turbulence fluctuations near the bottom. This depend on the impeller speed, defined as critical impeller speed at which no particle will settle at the bottom for a period varying from one second to three seconds. For a dual impeller system, the bottom impeller plays an important role in solids suspension. However, the actual energy for requirements dual impeller can be high compared to single impeller due to energy requirement to maintain the same critical impeller speed as for single impeller. Energy required can be reduced if impeller spacing is less than the impeller diameter (Gogate *et al*., 2000). Multiple impellers have been recorded to provide high mass transfer coefficient as well as for gas-liquid mass transfer coefficient (Gogate *et al*., 2000).

For the vessel used in this study, the bottom will be an upward pumping four-blade impeller and 20mm above the sintered metal. The upper impeller will be a down pumping four-blade impeller. The impeller diameters will be 75mm which is about half of the vessel diameter and the spacing between the two impellers will be 50mm which is less the impeller diameter to reduce energy requirements.

The critical agitation speed in unbaffled vessel was determined following the guidelines given by Nagata (1975). According to Nagata (1975), the following equation maybe used to calculate critical agitation speed.

$$N_f = KD_i^{-2/3} d_p^{1/3} \left(\frac{\rho_d - \rho_l}{\rho_l}\right) \left(\frac{\mu}{\rho_l}\right)^{-1/9} \left(\frac{V_p'}{V_p}\right)^{-0.7} \qquad \text{Equation 3-2}$$

K is the constant of proportionality. The constant K for a flat bottom vessel with impeller diameter of $0.5D_i$ and four blades of 45°C is 191 according the values of proportional constants given by Nagata (1975). D_i is the vessel diameter, ρ_d is the particle density, ρ_l is the density of liquid, μ is viscosity of liquid, V_p is the true volume of particles and V_p' is the bulk volume of particles. The viscosity of water was given as 0.89 Cp which is viscosity of water at 25°C and density was assumed to be density of water at 25°C. V_p and V_p' were calculated from the data which was used in the calculation of particle density and bulk density given in Table B-11.The value of critical agitator speed is 120 rpm and calculations are given in Appendix B in Table B-2. The agitation used during leaching was 320 rpm. The agitation speed increased by a factor of three to ensure that solids are suspended.

3.3 Components of the vessel

Pressure leaching and filtration experiments were conducted at Stellenbosch University in a 5.3L stainless steel vessel. The vessel was constructed from a stainless (314) steel pipe with an outside diameter of 158 mm and an internal diameter of 152 mm. The top and bottom of the vessel were cut from 3 mm thick sheet of stainless steel metal. The two pieces were wielded to their respective position at Stellenbosch University workshop. The vessel was divided into two sections. The top and bottom sections were joined by stainless flat face flanges with a neoprene-rubber gasket material for sealing the vessel (see Figure (3-1)). Flanges sizes were selected following the standard pipe flanges given by Coulson and Richardson (1993). The top section was 100mm and the bottom was 200mm in height. The bottom section was further divided by stainless steel porous filter medium supplied by GKN Sintered Metals (SIKA-R 20AX).

The vessel was equipped with a variable speed stirrer, a vent valve, a sample port, an oxygen inlet valve, wash water outlet valve, sampling valve, leach solution recycling valves, a positive displacement stainless steel head pump, heating bands of 200W, 230V with temperature sensor and thermocouple for regulating the temperature and pressure gauges for indication of pressure inside the vessel. The recycle outlet of the vessel was connected to 12mm rubber hose which was connected to the pump inlet. The pump outlet was connected to the bottom of the vessel through the rubber hose. The stirrer was equipped with two impellers and the speed was varied with a variable speed drive connected to a motor. The motor was connected to the vessel stirrer through two pulleys whose diameters were predetermined to deliver the required maximum speed of 320 rpm to the stirrer (see Figure (3-2) for the arrangement of pulleys). The calculations for determining pulley diameter are given in Appendix B. The stirrer shaft was sealed with 10mm mechanical seal with maximum working pressure of 15bar supplied by John Crane (Pty) Ltd. The pump used in this study is G-10X hydracell gear shaft pump supplied by Autrex Industrial (Pty) Ltd. The pump was connected to the motor by fan belt through two pulleys. Heating bands fitted around the tank with controllers were supplied by Unitemp. Figure (3-3) shows the arrangement of each component to the vessel.

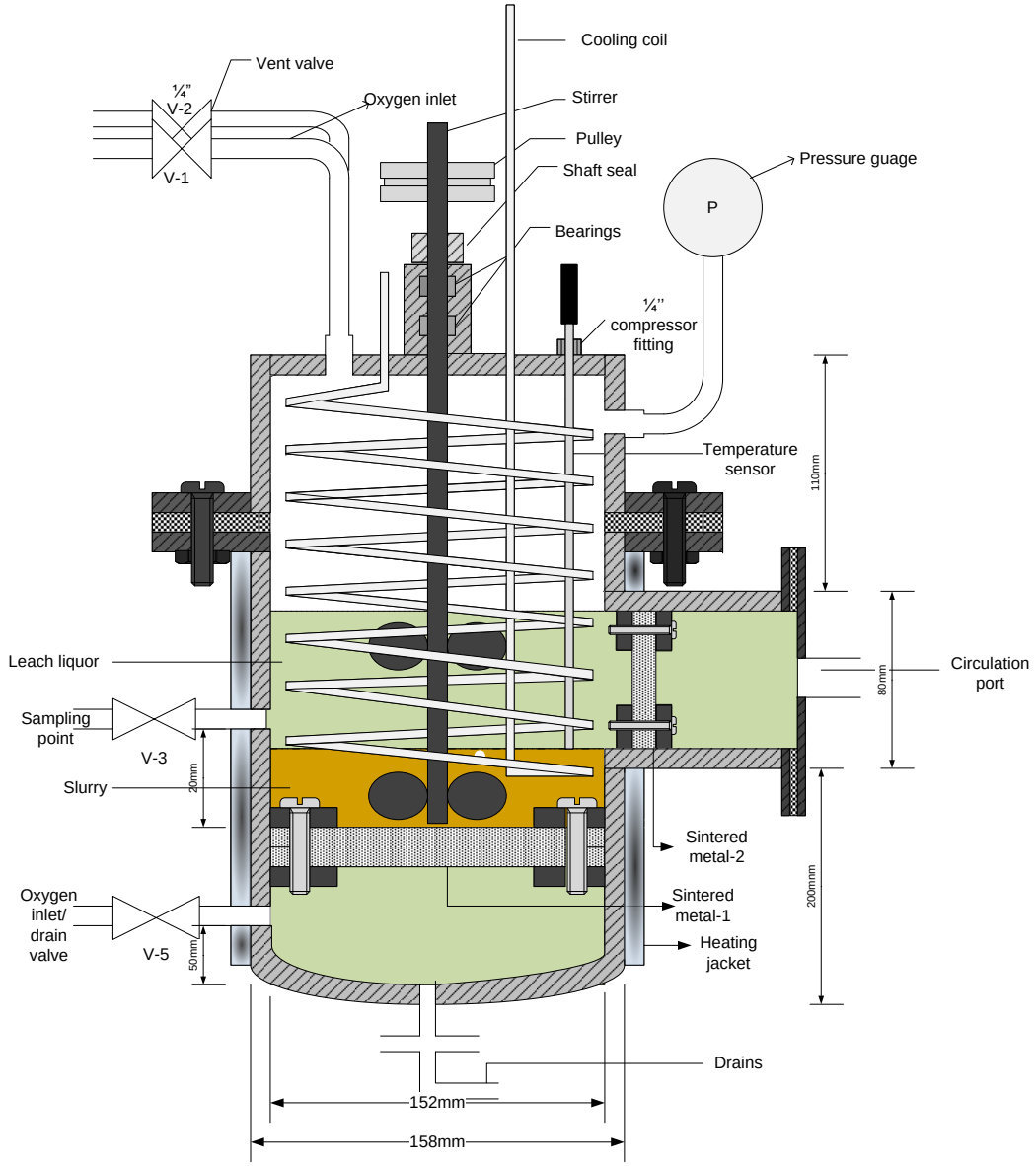

Figure 3-1: Cross sectional view of the leaching vessel

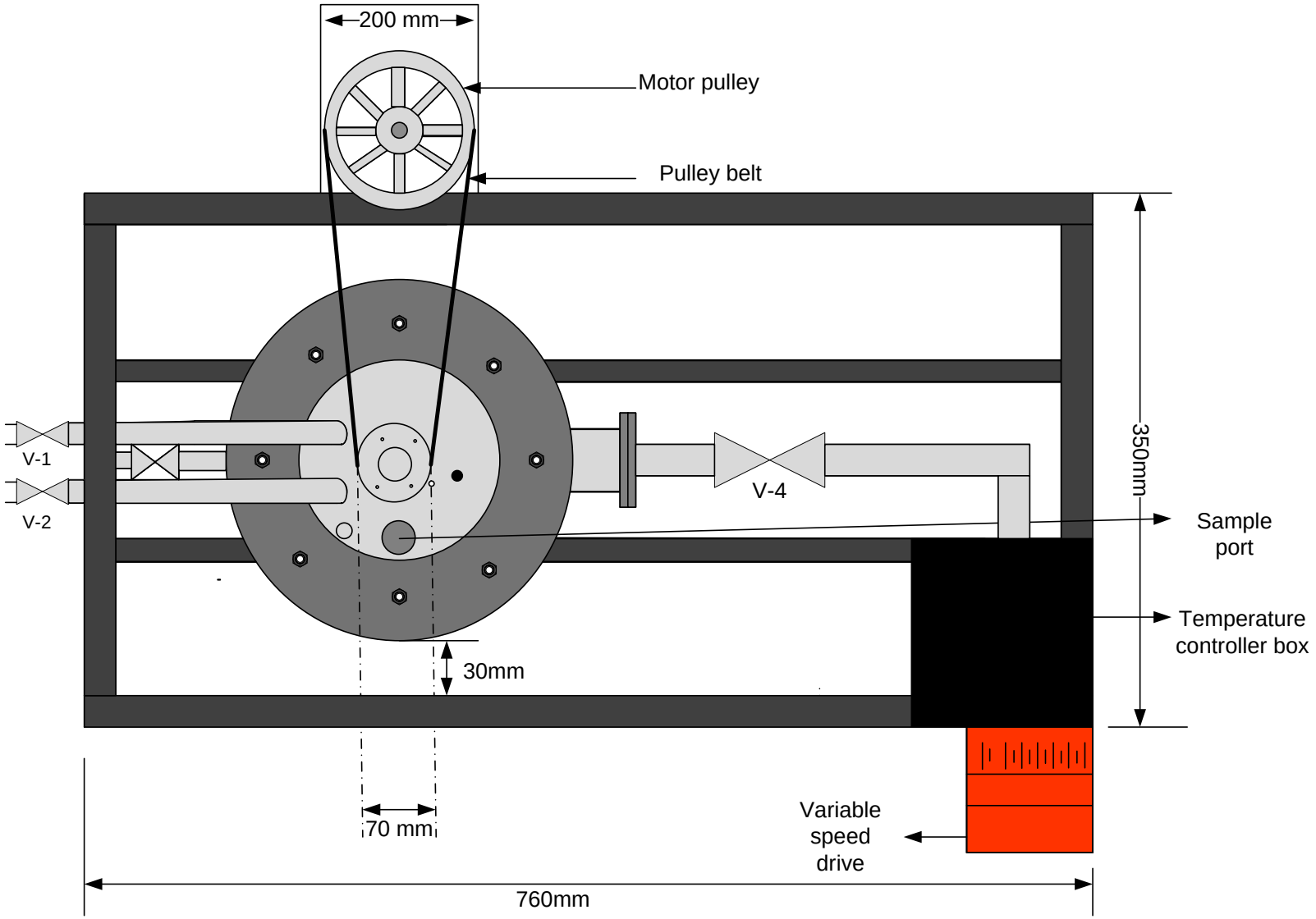

Figure 3-2: Top view of the vessel on the frame

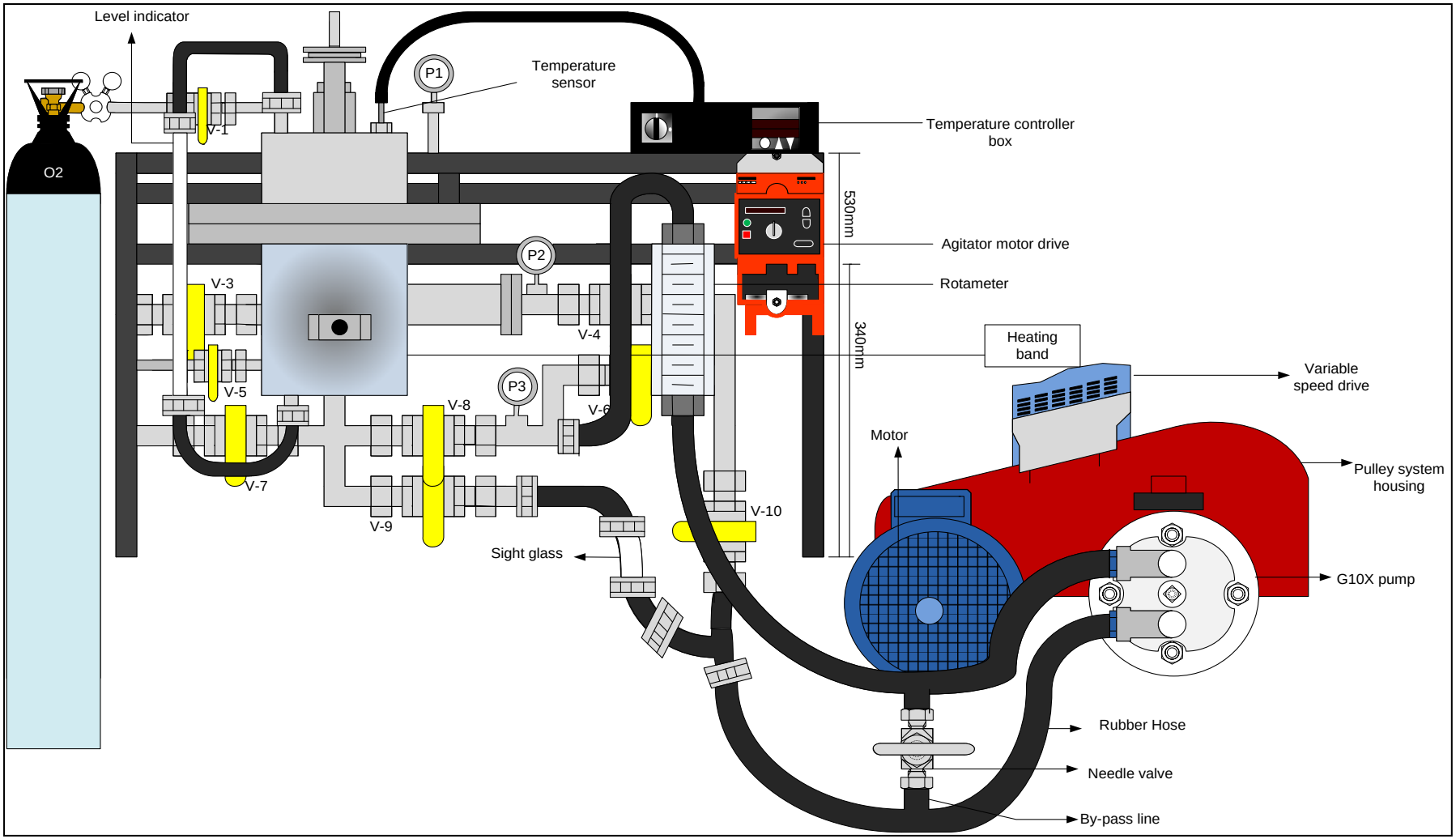

Figure 3-3: Schematic representation of the vessel on the frame

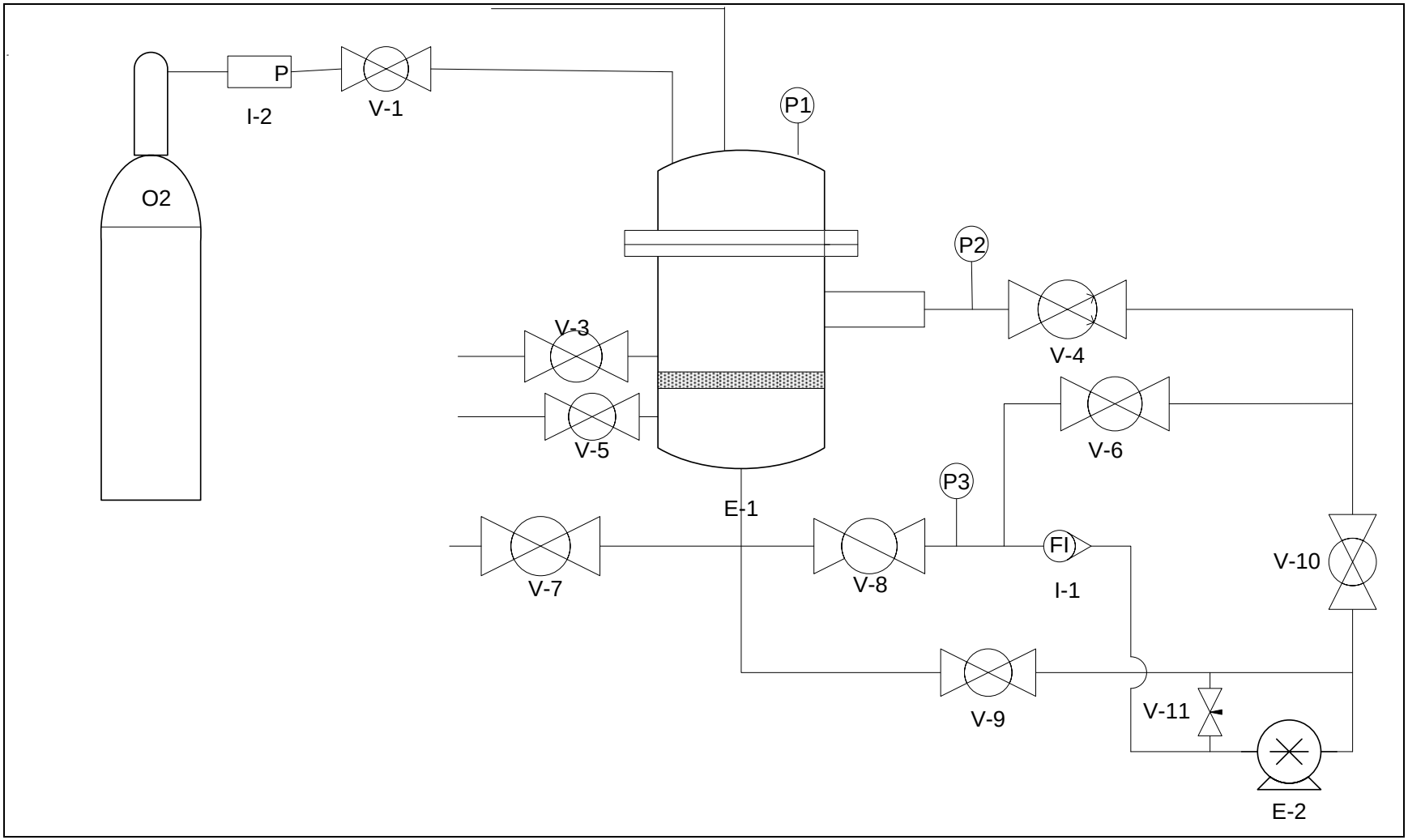

Figure 3-4: Flow diagram for leaching and filtration process with recirculation pump

Table 3-1: Description of list of the valves shown in the flow diagram

Valve List		
Displayed Text	Description	Line Size
V-1	Oxygen inlet	1/4"
V-10	Recirculating inlet to the pump	1/2"
V-11	Bypass	1/2"
V-2	Vent valve	1/4"
V-3	Sampling point / wash water outlet	1/2"
V-4	Recirculating inlet to the pump/ backflushing outlet	1/2"
V-5	Sampling point	1/4"
V-6	Back flushing outlet	1/2"
V-7	Wash water inlet/drain valve	1/2"
V-8	Recirculating outlet from the pump	1/2"
V-9	Back flushing inlet to the pump	1/2"

Table 3-2: Description of list of the equipment shown in the flow diagram

Instrument List		
Displayed Text	Description	Connection Size
I-1	Rotameter	1/2"
I-2	Oxygen regulator	1/4"

Table 3-3: Description of the list of equipment shown in the flow diagram

Equipment List			
Displayed Text	Description	Material	Model
E-1	Leaching and Filtration vessel	Stainless steel	
E-2	Positive displacement pump	Stainless steel	G-10X

Figure 3-5: Photograph showing the pressurized leach and filtration vessel

Figure 3-6: Photograph showing the pump for circulating leaching solution

3.4 Operation of the vessel with the recirculation pump

3.4.1 Recirculation the leach liquor

The leaching and filtration was placed in a fume cupboard. The leach solution (ammonia and ammonium carbonate) was prepared in fume cupboard. Before preparation of the leach solution, the fume extractor fan was started.

The calculated amount of solids and liquid were loaded into the vessel through the sample port shown in Figure (3-2). The sample port was then closed and the agitator was started on the agitator motor drive shown in Figure (3-3). At the beginning, all valves were closed. Valve (V-4) was opened to allow some leach solution to pass through filter medium-2, while keeping solids in the vessel. The valves that followed to be opened were V-10 and V-8. These valves can be seen clearly on Figure (3-4). The pump (E-2) was started on the pump variable speed drive. The leach solution enters the pump on the side of V-10 and comes through V-8. The pump discharge rate to the vessel was measured through the rotameter (I-1) and the inlet pressure was measured through pressure gauge (P-2) while the outlet through (P-3). (P-3) also served the purpose of monitoring the discharge pressure of the pump. If the pressure increased above 10 bar that would imply that the sintered metal filter medium-1 is blocked and this can result in rupturing of the pump diaphragms. The external heating bands were turned on and the temperature inside the vessel was adjusted to the desired temperature on the temperature control box shown in Figure (3-3). The temperature inside the vessel was measured with a thermocouple sensor and controlled with PID controller. Upon reaching the desired temperature, the pressure inside the vessel was noted through (P-1). Oxygen was admitted into the vessel through (V-1). The amount of oxygen to be admitted into the vessel was added to the internal pressure after heating. The oxygen regulator was set to deliver total pressure (Required oxygen + internal pressure after heating). This was done so that when subtracting the internal pressure after heating from the total pressure, the required oxygen pressure is admitted into the vessel.

3.4.2 Reversing the flow during leaching

The purpose of reversing the flow was to unblock the filter media during leaching process. The pump was first stopped before the flow was reversed. (V-10) was closed and (V-9) was opened so that it opens the feed to the pump. (V-8) was closed and (V-6) was opened. The pump was then started again. The duration of leaching with a reversed flow was 5min.

3.4.3 Back washing

After a leaching duration of 3hours, the pump was stopped and all valves were closed. The contents of the vessel were cooled and a sample was obtained through (V-5). After obtaining the sample, the vessel was drained through (V-7) and (V-3) while agitating. During unblocking of filter medium-1, the wash water enters through (V-7) and comes out through (V-3). When cleaning filter medium-2, (V-8) and (V-6) were opened and the wash water comes out through (V-3) and (V-7). Finally, the pump was started to drain all the water in the pipes.

3.5 Testing for possibility of circulating the leaching solution through the vessel

The vessel was equipped with two stainless steel sintered metal filter media, named sintered metal 1 and 2 as shown in Figure (3-1). Filter medium 1 and 2 have 149.6 cm^2 and 12.6 cm^2 surface area available for filtration with an average pore diameter of 20 µm. Other properties of the filter media were determined from permeability data given in the GKN Sintered Metals brochure (2009). The data is given in Appendix B in Table B-4.

Before leaching experiments were carried out, the vessel was tested by circulating water (without solids) within the vessel through sintered metal filter media using a positive displacement pump. Water was circulated at various flow rates. At a high flow rate above 15 L/min air locks developed in the pipes, indicating that the flow was not continuous. This indicated that the water flow rate delivered by the pump was more than the filter medium 2 can allow to pass through. However when the vessel was pressurized to 5 bar, water was circulating through the vessel continuously at 15 L/min. This indicates that permeability of

water through sintered metal filter medium increases with an increase in pressure as indicated in GKN Sintered Metal brochure (2009).

However according to the brochure, permeability increases linearly with pressure up to certain point. At high pressures an asymptotic value of flow rate is reached. This behavior indicates that the relation between pressure drop and flow rate can divided into linear (laminar flow) and non-linear (turbulent flow). Calculations for water flow through the filter medium at high pressure were done using the Ergun equation, which includes a laminar and turbulence term. The flow rate of water was calculated for different values of pressure drop (5000, 10000, 50000, and 100000 Pa). The Sintered metal disk was taken as a fixed bed assuming that the solids are suspended due to agitation. The data and sample calculation are given in section B.3 in appendix B.

A second test was performed by circulating water with unroasted nickel laterite ore inside the vessel. The amount of ore used, was the same as to be used during the leaching experiments. The vessel was charged with water and the ore required to make a 20% (w/w) suspension which is solid concentration used by many authors in the studies involving leaching ammoniacal solution (Rousseau, 1987; Bare, 1960; Vosahlova and Weir, 1972). After charging the vessel with ore and water, the agitator was turned on. The purpose of the agitator was to ensure that solid particles are always suspended to prevent cake formation on the sintered metal filter medium during pressurization. The vessel was then pressurized with compressed air to 1, 2, and 5 bar. In all tests, it was impossible to get continuous flow of recirculation water. This is because the sintered metal filter medium-2 was clogged. When the flow was reversed to unblock the pores of the sintered metal-2, the pressure gauge showed an increase in pressure (over 10 bar). The pump was shut down and filter medium was inspected.

The filter medium was deformed and cracked because of the pressure build up. Furthermore, the surface of sintered metal had very sticky clay attached on it. Figure (3-7) shows the picture of the deformed filter medium. The sintered metal was send to GKN Sintered Metals for analysis. According to the results obtained with a Scanning Electron Microscope (SEM) and metallographic investigation by GKN Sintered Metals, there is complete clogging on the surface of the filter disk, but there is an insignificant amount of solids within the pores of the filter medium. The only particles that were stuck deep within the pores of the filter medium were particles that were less than the pore size of the filter medium (20 µm). As shown in the

particle size analysis (Figures (4-1 and 4-2)) of the ore, there is significant amounts of particles in the ore, which are less than 20 µm. SEM images showing the particles of the ore on the surface and within the pores of the sintered metal are given in Figures (B-2, B-4, and B-5) in Appendix B.

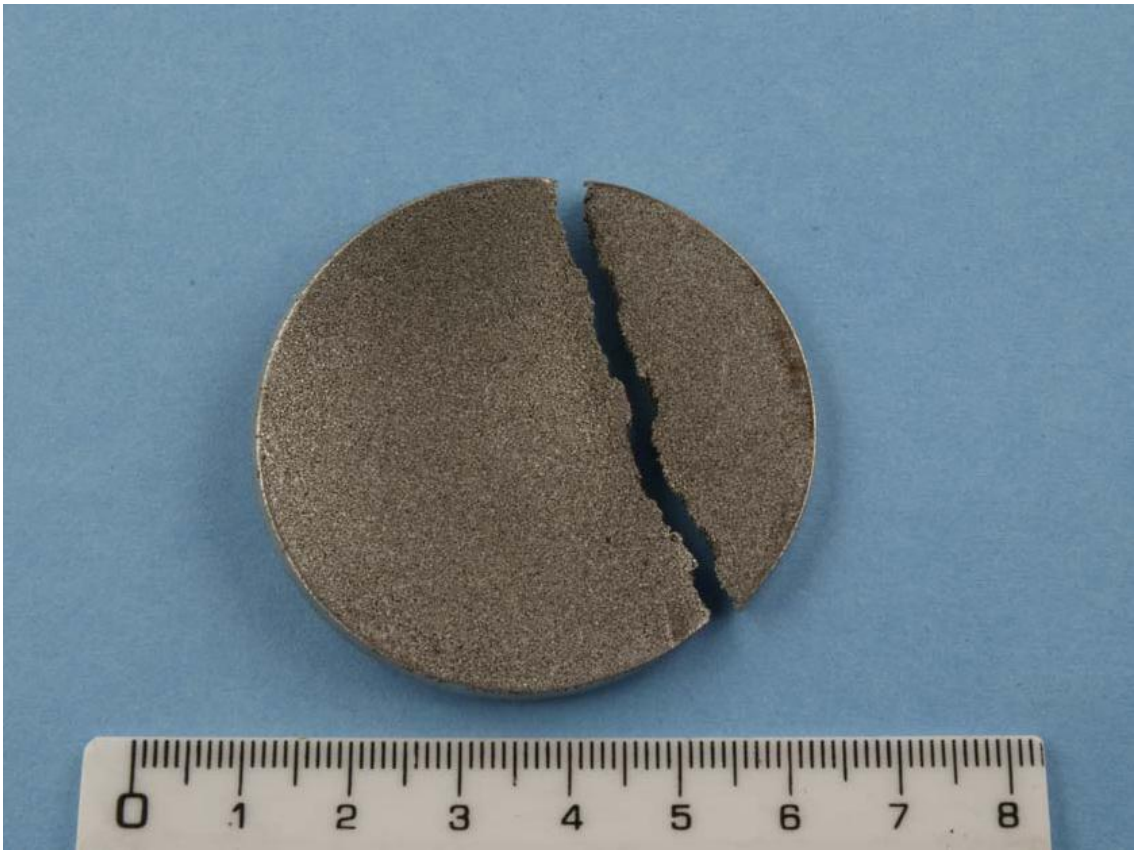

Figure 3-7: Picture showing a deformed and cracked sintered metal

Tests were also conducted using sintered metal filter medium with larger pores, 60, 80 and 150µm. For 60 µm, a similar behavior was observed to that of using the 20µm filter medium. In addition, the recirculating water contained some solid particles. For 80 and 150µm, although continuous flow of water was observed, significant amounts of solids passed through the filter medium. The solids accumulated in the pipes and eventually blocked the pipes completely.

From these tests, it was concluded that the ore properties does not allow good permeability of water through the filter medium. Studies on the rheological properties agree with the conclusion made. According to these studies (Bhattacharya *et al*., 1998), laterite suspensions exhibit non-Newtonian rheological properties that complicate slurry transportation and solid-

liquid separation processes such as filtration and sedimentation. The permeability of the laterite ore is controlled by type of mineral occurrence, morphology, and particle size. Although mineralogy of these ores is different, there is some similarity of mineral morphology in lateritic deposits throughout the world. Clay present in these ores causes laterite suspension to have high yield stress and viscosity. (Duyvesteyn, Liu and Davis, 2001; Bhattacharya *et al*., 1998); Klein & Hallbom, 2002).

After studying the behavior of laterite suspension, some experiments were conducted to study rheological properties of the ore used in this study. These experiments were conducted to confirm that, the problem of pore clogging of filter medium and low permeability is associated with rheological properties of the ore. Rheological measurements were conducted using a Rheoplus/32 V2.81. Rheological measurements were conducted at different solid concentrations of 15%, 20%, 30%, and 40%.The effect of temperature on rheological properties was also investigated at different solid concentrations. Viscosity measurements were conducted at 25^{o}C, 50^{o}C, and 70^{o}C. The results of this study are given in the following Figures (3-8) to (3-9). The results of the effect of temperature represented here are for 15% solids concentration. The results for other solids concentration (20%, 30%, and 40%) are presented in Figure (B-8) to (B-13) in appendix B.

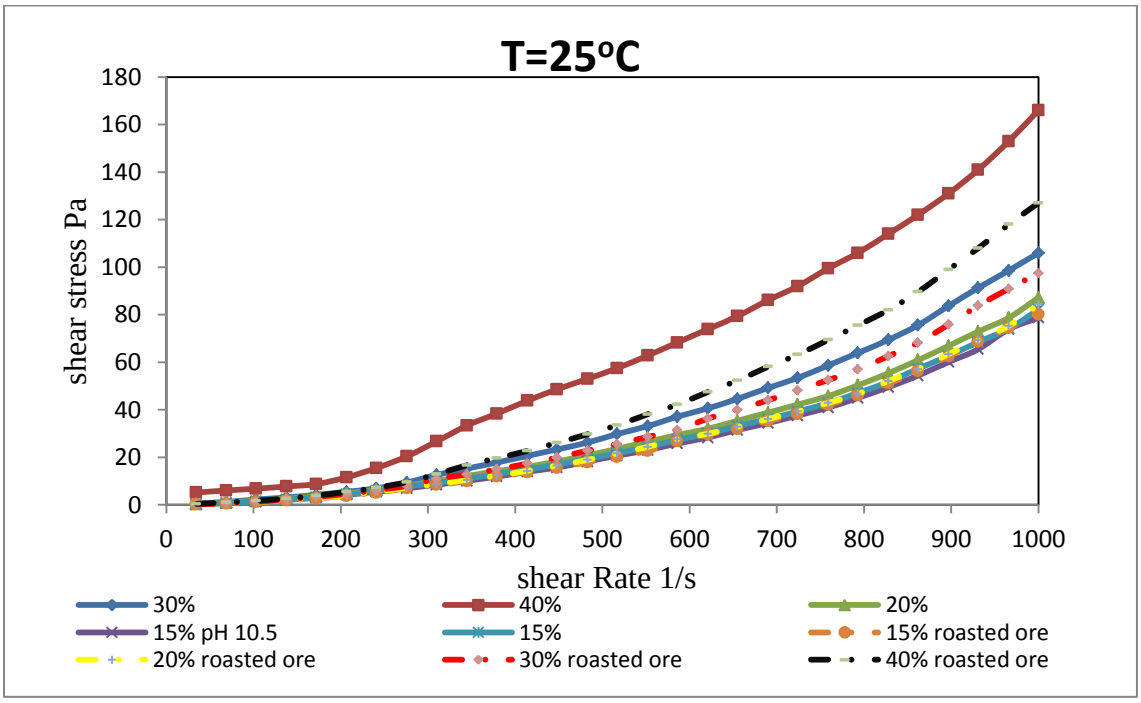

Figure 3-8: Variation of shear stress with shear rate at different solid concentration and pH

Figure (3-8) gives a plot of variation of shear stress with shear rate at different solid concentrations at 25°C for the roasted and unroasted ore. It can be observed from this figure that slurry shows non-Newtonian behavior at all solid concentrations. The effect of pH on the unroasted ore was also investigated by approximating the slurry pH to the leaching solution. However, pH did not have any effect of on shear stress at 15% solid concentration. The results indicate that shear stress values for the roasted are slightly lower than for the unroasted at low solid concentration. When the solid increases the difference between shear stress values for roasted and unroasted ore become greater. The data for the unroasted ore is fitted to a power law model. The mathematical model is given in the equation below. The model is described by the following equation.

$$\tau = k\gamma^n \qquad \text{Equation 3-3}$$

Where τ is shear stress, γ is the shear rate, and k and n are constant. K is the consistence index and n is the behavior index. The value of n indicates deviation from Newtonian behavior. For Newtonian fluids n=1. To determine the value of n, the above equation was linearized.

$$log\tau = logk + nlog\gamma \qquad \text{Equation 3-4}$$

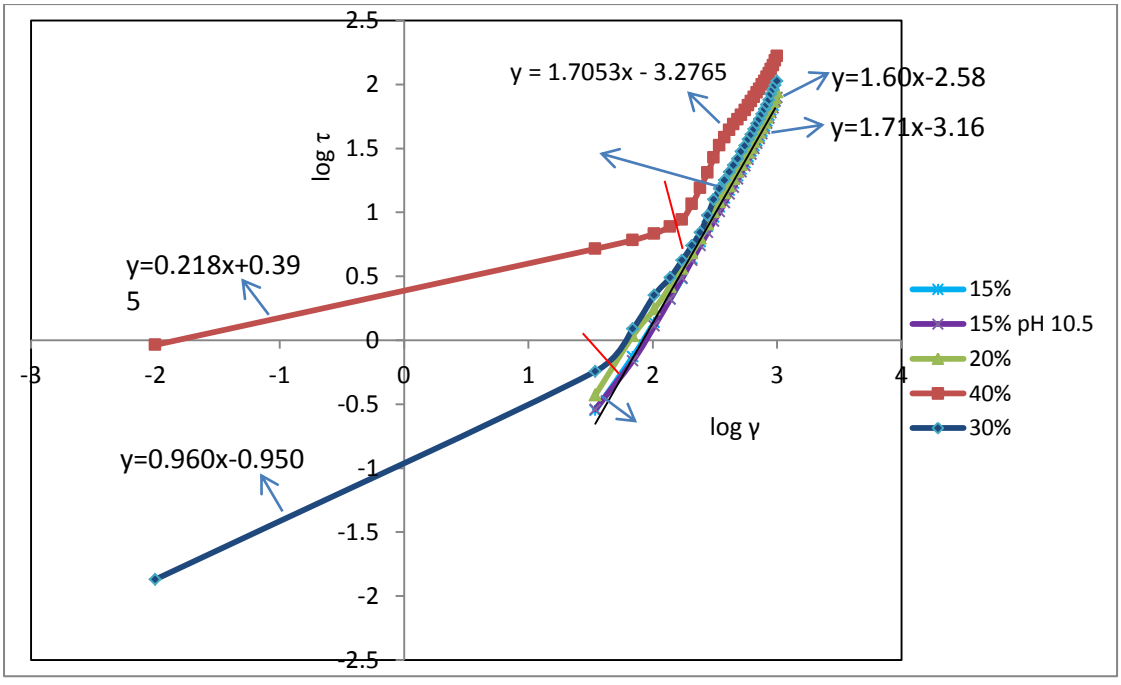

Figure 3-9: Plot of log shear stress against log shear rate

Figure (3-9) shows the plots of logτ against logγ. In these plots, the slopes of the lines indicate the value of n and intercept logk. For solids, concentration of 15%, and 20% n is greater 1 which indicates shear thickening behavior (increase in viscosity with shear rate). As the concentration of the slurries increases, viscosity increases. In this case, pH does not have significant effect on viscosity of the slurry at 15% solid concentration. For 30 and 40% solid concentration, the slurries have both shear thinning and thickening properties. The plots of these concentrations can be divided into two sections. In the first section of the plots, the slopes are less than 1 indicating shear thinning and as shear rate increases the slopes become greater than 1 indicating shear thickening. This behavior can be seen clearly in the plot of apparent viscosity against shear rate, which is given in Figure (3-10).

For slurry concentration of 15%, 20%, and 30% the apparent viscosity increases with an increase in shear rate for both the roasted and unroasted ore. For the roasted ore at 40% solid concentration, the apparent viscosity increases with an increase in shear rate whereas for the unroasted ore at 40% solid concentration, at low shear rate the apparent viscosity decreases but as the shear rate increases the apparent viscosity decreases. This shows that the unroasted ore at high solid concentration has shear thinning properties at low shear rate and shear thickening properties at high shear rate. For a high solid concentration particle-particle hydrodynamic interactions become significant and these influence the viscosity of the slurry. At low shear rate, particles arrange themselves into sheets and strings. At low shearing rate, slurries have shear thinning properties. Therefore as shearing rate increases particles change to a randomized structure and the hydrodynamic interaction becomes greater. The large magnitude of hydrodynamic interaction pushes particles into clusters.

These clusters jam the entire suspension flow and result in an increase in viscosity (Klein and Hallbom, 2002). This particle agglomeration is associated with goethite, which is present in laterite ores. Besides increasing the viscosity, particle agglomeration have a negative effect on leaching. The agglomerates limit diffusion of the leaching solution to the surface nickel (Klein and Hallbom, 2002). From the results above it can also be seen that roasting improves the rheological properties of the ore by lowering slurry viscosity.

Figure (3-11) shows the variation of shear stress with shear rate at different temperatures. It can be observed that, as temperature increases viscosity decreases. Battaccharya *et al*. (1998) found similar results on the study of rheological properties of laterite ores.

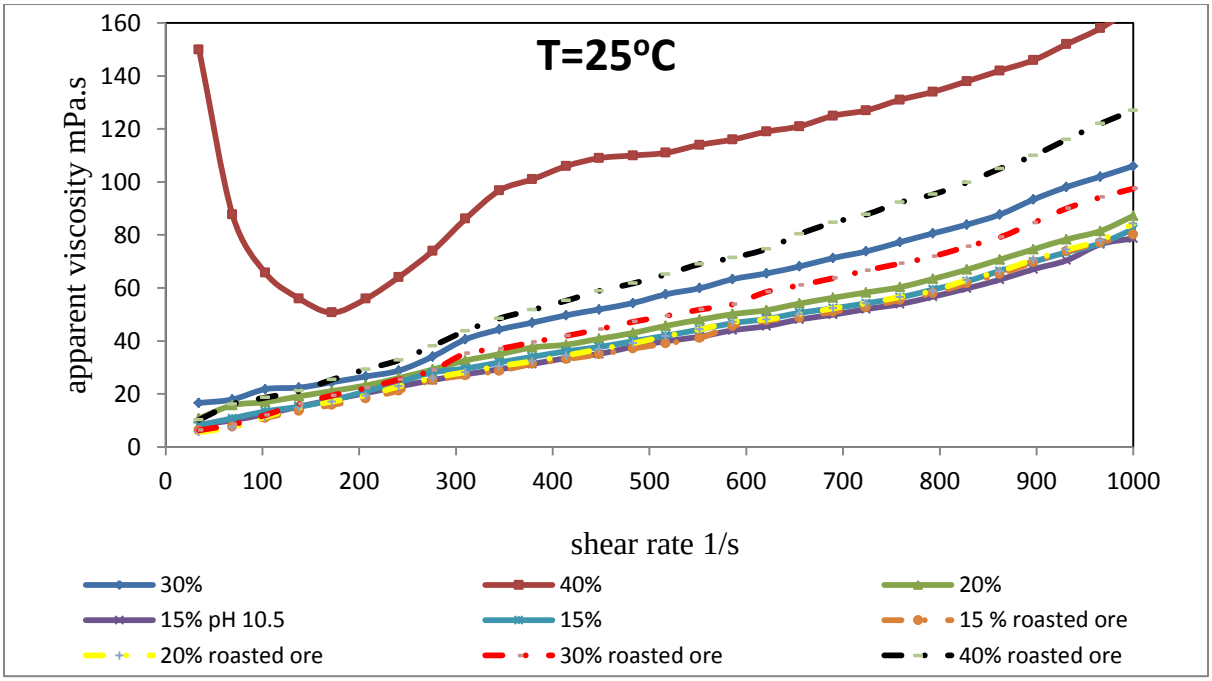

Figure 3-10: Variation of apparent viscosity with shear rate for different solid concentration

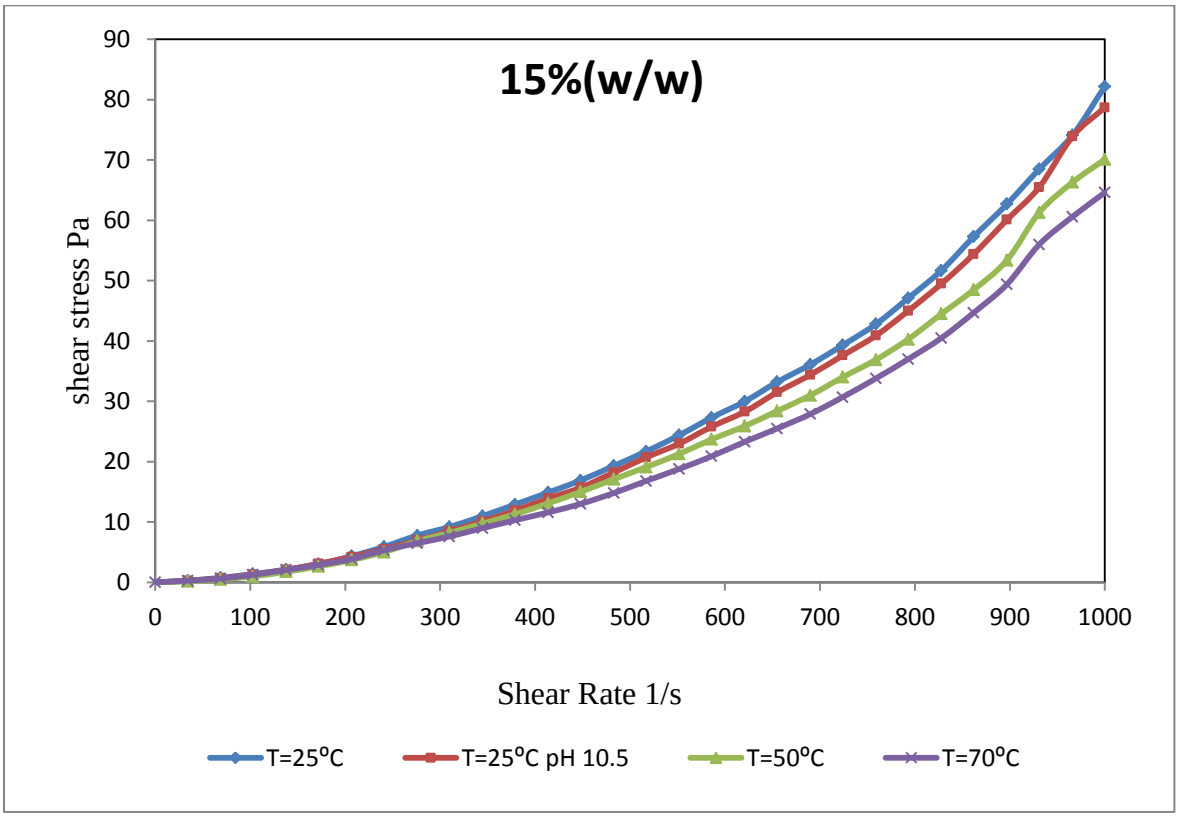

Figure 3-11: Variation of shear stress with shear rate at different temperatures

In light of the above discussion, new methods were tried to improve filtration of the ore and improve circulation of water through the vessel. The first was to lower concentration of the solids to 15 % w/w in order to reduce viscosity of the slurry. However, no improvement was observed. The next method involved putting a by-pass valve (needle valve) on the line between the inlet and outlet of the pump. A rotameter was also installed on the pump outlet just after the by-pass valve to monitor the flow rate water to the sintered metal. The by-pass valve would regulate the flow of water to the filter medium and ensure that the pump has a constant supply of water. In this case, the water circulated through the vessel for a short period and stopped due pore clogging of sintered metal. The by-pass also ensured that the pressure build was reduced during back flushing. When the water flow was reversed, the pressure build was not high enough to bend the sintered metal filter medium. The set-up with the by-pass is demonstrated in the diagram showing the side view of the leaching vessel in Figure (3-3).

3.6 **Summary**

In this chapter, the design considerations for the building of the vessel and nature of the experimental work done have been described. The vessel was constructed using stainless steel grade (314). For non-metallic components, like gasket material and hoses, neoprene rubber was used. The vessel was constructed to withstand an operating temperature of 100 ^{o}C and pressure of up to 10 bar. Filter medium used was stainless sintered metal disk with an average pore diameter of 20 µm.

Initially the set-up of the vessel was in such a way that the leach solution could be circulated within the vessel while keeping solids inside the vessel. This was to ensure that most of the leach solution is exposed to solids during leaching. Severe pore clogging of the sintered metal filter medium occurred. The pore clogging was mainly due to the rheological properties of the ore. The rheological properties of the ore were studied at Stellenbosch University using the Rheoplus/32. The sintered metal disk was sent for pore clogging analysis at GKN. According to the GKN analysis, only the upper surface of the disk was blocked. This further confirmed the initial speculation that the pore clogging was caused by the rheological properties of the ore.

4 Experimental procedure

4.1 Chemical reagents

Nickel oxide ore, saprolitic laterite from Brazil, was supplied by Anglo Platinum South Africa. About 60Kg of nickel ore was supplied. Chemicals used for leaching were ammonium hydroxide 28-30% NH_3 and ammonium carbonate extra pure supplied by Sigma Aldrich. Leaching solution was prepared by dissolving the reagents in distilled water. Pure nitrogen gas was used to purge the vessel before leaching in order remove air. Pure oxygen was used to pressurize the vessel during leaching. The two gases were supplied by Afrox.

4.2 Sample preparation

Nickel laterite ore bodies consist of two types of ores. These are the limonitic ore types which are high in iron and low in magnesium and silica content, and the saprolitic type, which are high in silica and magnesium and low in iron content. The saprolitic types are rich in serpentine ($Mg_3Si_2O_5(OH)_4$) but also contain goethite (FeOOH), quartz (SiO_2), magnetite (Fe_3O_4) and clinochlore-ferroan $(Fe, Mg, AL)_6(SiAL)_4O_{10}(OH)_8$. Most of the sample preparation and chemical analysis of the ore was done by Anglo Platinum. The ore was first crushed and then milled. After the ore samples were milled, they were not screened. According to Pelser (2009), when saprolite ore is milled and screened, different elements deport to different size fractions. Nickel reports to the fines and silica to the coarse fraction due to the varying hardness of each mineral in the ore. This makes chemical analysis of the ore difficult, because each size fraction would have to be analyzed individually, as different minerals are not evenly distributed throughout different size fractions.

4.2.1 **Particle size analysis and sampling**

Particle size analysis of the roasted and unroasted ore was performed at Stellenbosch University to analyze for size distribution using Micrometrics Saturn Digisizer 5200 Light Scattering Particle Size Analyzer. Particle size analysis was done using the Fraunhofer theory. In this theory particle sizing is related to bending of light around the edges of opaque objects (Webb, 2000). Figures (4-1 and 4-2) show cumulative volume percent and volume frequency distribution curves for the milled saprolitic laterite (unroasted and roasted) ore respectively. The volume frequency distribution curve shows that, there is a wide distribution of particle size within the unroasted ore. The distribution shows that the unroasted ore contains a significant amount of fine particles. According to the size analysis of the sample, the average particle diameter was found to be d_{50}=17 µm and an average mode was 38 µm for the unroasted ore. From the particle size analysis, it can be seen that after roasting the size ore has increased. Looking at Figure (4-1 and4-2) an average d_{50} =23.7 µm and average mode of 38 µm. The increase in particle can be explained from the work of Li *et al*. (2010). Roasting causes an increase in surface area and porosity of the ore (Li e*t al*., 2010). An increase in surface area and porosity would imply that the particle size would also increase. From the curves of unroasted and roasted ore, it can be seen that for unroasted ore frequency for particle size smaller than 10 µm is higher relative to that of roasted ore. Furthermore, the frequency distribution curve for the roasted ore is narrower than for unroasted ore, indicating that most particles size fall within the range of 38 µm. The results indicate that roasting has an influence on particle size distribution of the ore.

Since the sample had wide size distribution, 25 kg sample of d_{50}=17 and d_{50} =23.7 µm had to be divided into smaller portions using a sectorial splitter. This was done to ensure that representative samples were obtained for each of the leaching experiments. A sectorial splitter consists of a rotating metal cone with ridges and valleys. Samples are placed in a vibrating hopper with the adjustable vibration level set such that the sample particles slowly emerge and fall onto side of the rotating cone. Particles then fall into containers placed under each valley. Sectorial splitters minimize errors associated with segregation.

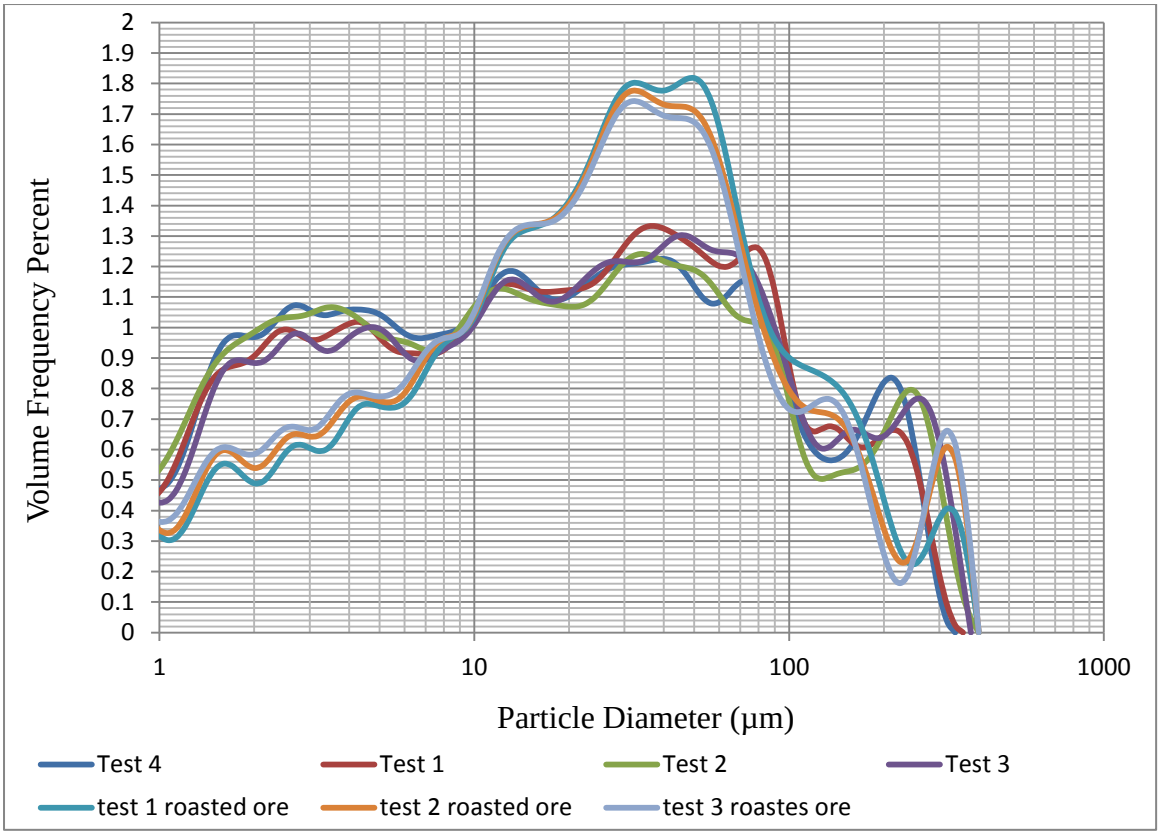

Figure 4-1: Volume frequency distribution curve for milled ore

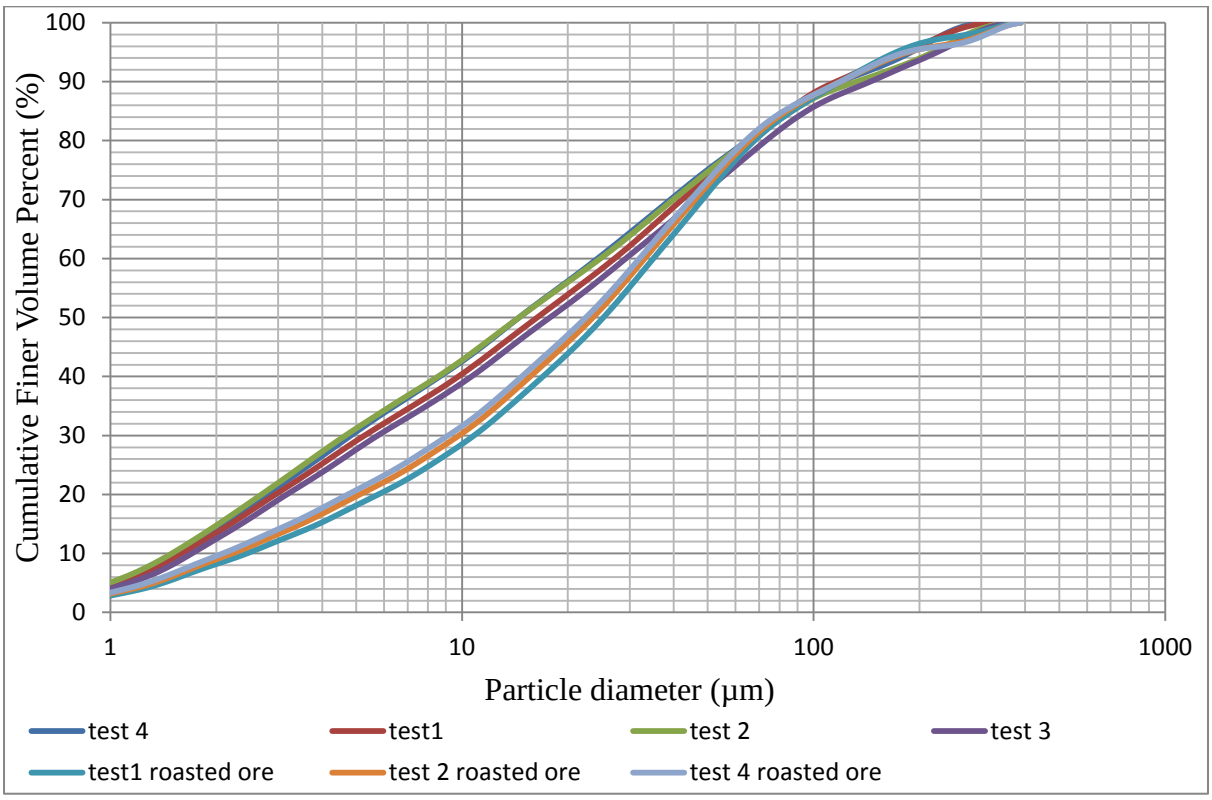

Figure 4-2: Cumulative volume percent distribution curve for milled ore

4.2.2 **Sample analysis**

The ore sample was analyzed by fusion ICP at Anglo Platinum. This technique involves fusion of the sample with lithium metaborate and followed by analysis with inductively coupled plasma (ICP). The analysis of the ore was confirmed at Stellenbosch University in the Central Analytical Facility (CAF) using X-ray Fluorescence (XRF). Table (4-1) shows elemental analysis of the ore from Anglo Platinum. Analysis from CAF is given in Table (B-14) in Appendix B. Analysis shows percentage content of selected elements present in the ore. Full analysis of the elements by Fusion ICP is given in Figure (B-14) in Appendix B. This shows that magnesium, silicon, and iron are present in large quantities. Copper and cobalt are present in trace amounts. The nickel content in the samples is 1.76%. Magnesium is associated with silicate in most laterite ores. From elemental analysis given in the table, it is clear that the ore is saprolite, which is rich in magnesium and silicate content (Valix and Cheung, 2002).

Table 4-1: Elemental analysis of milled saprolitic laterite

Constituents	Al	Co	Cr	Cu	Fe	Mg	Mn	Ni	Si
Content (wt%)	0.58	< 0.05	1.01	< 0.05	9.08	17.5	0.13	1.76	16.6

4.2.3 **Reduction roasting**

A portion of the ore was sent to Mintek for roasting under reducing conditions. Roasting was carried out in a rotating kiln. The sample was loaded into the rotary kiln furnace. Free flowing Ar gas was introduced into the furnace at a flow rate of approximately 1.5 L/min while the furnace was ramping up to the desired test temperature of 700°C. When the test temperature was reached, Ar gas was substituted by CO gas at the same flow rate. The sample was maintained at 700°C for a period of 3 hours and allowed to cool down with CO gas.

The initial mass of the sample was approximately 9 kg and mass after was 7.99 kg. The mass loss was about 11.24%, This loss includes moisture content, volatiles and decomposition of material

4.3 Nickel ore physical properties

Nickel laterite ore (saprolite) physical properties determined were particle density, bulk density, particle porosity of the ore and specific surface area. These properties are important in testing filtration and calculating the flow rate required for leaching solution to flow from the bottom of vessel against pressure inside the vessel and resistance of the filter medium. In addition, these properties are important in determining leaching kinetics especially if models such as shrinking core model are to be used in modeling leaching rate.

4.3.1 Particle density, bulk density and porosity

Most minerals have particle density ranging from 2.60 to 2.75 g/ml. However, particle density can be as high as 3.0 g/ml and as low as 0.9 g/ml depending on the composition of the mineral.

Particle density, bulk density, and porosity of the milled saprolitic laterite were determined following the procedure for soil particle density determination given by Globe (2005) and the details about this method can be found there.

The data for this procedure is given in Appendix B in Table (B-11). Using the data particle density was calculated using the equation given in Appendix B. Particle density was determined to be 2.58 g/cm^3

4.3.2 Specific surface area

The specific surface area of the unroasted and roasted saprolitic laterite was measured using gas adsorption according to Brunauer, Emmet, and Teller (BET) method. The BET method involves the determination of the amount of the adsorbate or adsorptive gas required to cover

the external and accessible internal pores of a solid surface with a complete monolayer of adsorbate (Wikipedia, 2010). This monolayer capacity can be calculated from the adsorption isotherm by means of the BET equation given in Appendix B.

The specific surface area of the unroasted and roasted saprolitic laterite was determined to be 76.6 m^2/g and 29.8 m^2/g, respectively. According to Li *et al.* (2009), roasting can either increase or decrease specific surface area of the ore. On their study on the effect roasting on laterite ore they found out that when the ore was roasted, increasing the roasting temperature above 300^oC does increase surface area. When roasting at 300^oC, the specific surface area increased from 16.23 m^2/g (raw ore) to 21.04 m^2/g. At 400, 500 and 700^oC specific surface area decreased to 19.21, 19.13 and 18.61 m^2/g respectively. At 800^oC, the specific surface area decreased to 13.23 m^2/g becoming even less than for the raw ore. The cause of this was explained to be due to some fine particles which reunite together. This might explain why the particle size of the ore increased after roasting as shown in Figure (4-1 and 4-2).

4.4 Experimental design

The vessel was to be operated at high temperatures to ensure that ammonia is lost through evaporation, which if lost before solid separation can result in precipitation of metal values in solution. The vessel was pressurized with oxygen during leaching. After leaching,solid-liquid separation would be achieved by high-pressure filtration. The leaching conditions were varied using an optimization procedure. Optimization was carried out using the response surface methodology (RSM) with an unroasted saprolitic laterite. After finding optimum conditions, three experimental runs were carried out at optimum conditions with roasted saprolitic laterite.

In the present work Central Composite Design, which is widely used form of RSM was employed for the optimization reaction. Four factors at three levels were used for designing the experiments. Factors investigated were; temperature, oxygen pressure, ammonia concentration and ammonium carbonate concentration. The factor levels were chosen based on the findings on leaching nickel oxides ores with ammonia and ammonium carbonate discussed in section 2.5 of literature review. The experimental conditions are shown in Table (4-2).

Table 4-2: Experimental leaching conditions for optimization.

	Factor levels		
Factor names	Low	Medium	High
Temperature (^{o}C)	50	70	100
Oxygen pressure (bar)	2	3	5
Ammonia (M)	0	2	4
Ammonium carbonate (M)	0.5	1	2

After a leaching duration of three hours, the pregnant solution was cooled to room temperature using cooling coils installed in the vessel. The cooled leach liquor was separated from the solids by filtration. Filtration was carried out at different pressures. Pressure was applied above the sintered metal filter medium using compressed air. The pressure settings were 2, 3 and 5 bar.

4.5 **Leaching experiments**

Because of the difficulties encountered in circulating water during filtration tests, the design of the leaching vessel was modified facilitate leaching and solid-liquid separation without circulating the leaching solution.

1. The pump was disconnected from the vessel
2. Oxygen was introduced above and below sintered metal medium-2. This was done to decrease the pressure drop across the filter medium during leaching so that a minimum amount of leaching solution can pass through the filter medium during leaching. The cross sectional view of the set-up is shown in Figure (4-3).
3. Sintered metal medium-2 was removed and in place of the sintered metal, a sheet of metal was placed in order to seal the hole.
4. During the supply of oxygen V-12 was opened first followed by V-13. Next V-1 and V-5 were opened simultaneously to supply oxygen above and below filter medium-1

5. During filtration process, V-13 and V-5 were closed. Then air was supplied from the top of the vessel through V-12 and V-1. The filtrates was then by opening V-9 into a 1000ml beaker.

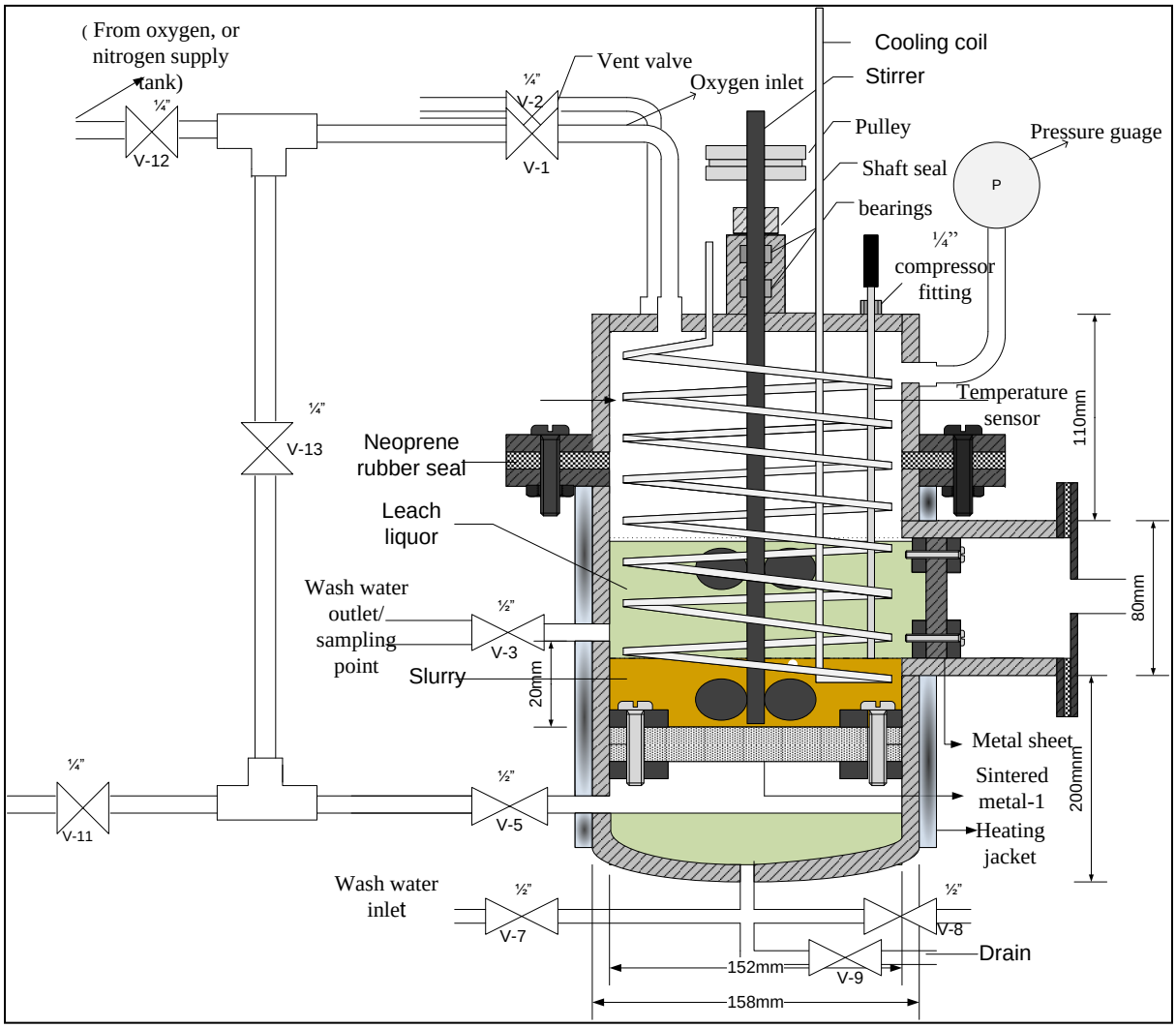

Figure 4-3: Pressurized leach and filtration vessel.

4.5.1 **Preparation of leaching solution**

The leaching solution was prepared in a 5 L beaker with distilled water at room temperature to minimize vaporization of ammonia. Before determining the amount of reagents required to prepare the leaching solution, the amount of solids and water required for making a pulp of 15%w/w density were determined using the following equation. Derivation of the equation is given in Appendix B section B.5

$$V_s = \frac{V_T \rho_d \rho_f}{(1-\varepsilon)\rho_p - (1-\varepsilon)\rho_p \rho_d + \rho_d \rho_f}$$ Equation 4-1

Where V_T is the total volume of the pulp, V_L is the fluid volume, ρ_f is the fluid density (assuming density of water), ε is the porosity of solids, ρ_p is the particle density of solids, (Vs) volume occupied by solids and ρ_d is the pulp density

After determining the amount of solids and liquid required for making a pulp of 3.5 L, the amount of ammonium hydroxide and ammonium carbonate required for making different solution concentration as shown in Table (4-2) were determined. Ammonium hydroxide solution had 28% NH_3 w/w, molecular weight of 17 g/mol and density of 0.9 g/cm^3. Derivation of equations used to prepare different concentrations of ammonia solution are given in Appendix B section B.5

Lastly, the amount of ammonium hydroxide required to give the required NH_3 concentration of 2 M and 4 M was determined according to the following relationship.

$$C_{m1}V_1 = C_{m2}V_2$$ Equation 4-2

The amount of ammonium carbonate required to prepare leaching solution of 0.5, 1 and 2 M was determined using the following equation.

$$C_M = \frac{n_{(NH4)2CO3}}{V_{solution}}$$ Equation 4-3

$$n_{(NH4)2CO3} = \frac{m_{(NH4)2CO3}}{m_M}$$ Equation 4-4

The mass of ammonium carbonate was calculated and dissolved in solution of water and ammonium hydroxide at room temperature. The calculations for determining the amount of ammonia and ammonium carbonate were done in a excel spreadsheet and are given in the Appendix Section B.5.

4.5.2 **Optimization reactions**

The pre-calculated amount of ammonium hydroxide, ammonium carbonate, and distilled water were mixed to get to make a solution of desired concentration. Before adding reagents, nitrogen gas was purged into the vessel to remove air. The calculated amount of leaching (3.2

L) and solids (572 g) were poured into the vessel through the sample port. The vessel was closed and heated to the desired temperature, while stirring the contents of the vessel at 150 rpm. Upon reaching the required temperature, the vapor pressure of the solution was noted. Oxygen was then admitted into the vessel below and above the filter medium (through V-5 and V-1) (see Figure (4-3))and stirrer speed was increased to 320 rpm. The residence time of all leaching experiments was 3 hours and timing was started when oxygen was admitted into the vessel. At the end of leaching, the contents of the vessel were cooled to room temperature and the leach solution below the filter was drained into a beaker. The volume collected and pH were measured and 25 ml of the sample was kept for analysis. The solution above the filter was filtered for about 20 minutes. The volume and pH of the filtered solution were measured and 25 ml of sample was kept for analysis.

4.5.3 **Leaching of roasted ore**

Optimum conditions for leaching saprolitic laterite with ammonia and ammonium carbonate solution were determined with an unroasted ore. For determination of optimum leaching conditions, 18 experiments were carried out requiring approximately 10 kg of ore. After obtaining optimum conditions, the results were used to design the experiments for kinetic reactions for the roasted and unroasted ore. For these experiments, about 8 kg of roasted ore was used. After optimization with unroasted saprolitic laterite, three experimental runs were conducted with roasted ore at the optimum conditions. Solid liquid separation after leaching was done in the same way as for the unroasted ore.

4.5.4 **Kinetics study reactions**

A leaching solution of the desired concentration of NH_3 and $(NH_4)_2CO_3$ was prepared. Quantities of leaching solution and saprolite ore required to make 15% pulp density were charged into the vessel. The calculated volume of leaching solution (2.02L) was first poured into the vessel and the calculated amount of saprolite ore (360g) was added into the vessel. The vessel was then closed and heated slowly to the desired temperature, while slowly stirring the contents. Upon reaching the required temperature, the vapor pressure of the solution was noted. Oxygen was then admitted into the vessel below and above the filter

medium (through V-1) and stirrer speed was increased to 320 rpm. Samples were taken 30 minutes time interval. The first sample was taken after 15 minutes after admitting oxygen into the vessel. The metals in samples were determined using various analytical techniques which are mentioned in the next section. The results were analyzed using the shrinking core model. For a changing single spherical particle size, the leaching process can be expressed according to the following equations.

For a film diffusion controlled reaction;

Small particles;

$$k_f t = 1 - (1 - X_B)^{2/3} \qquad \text{Equation 4-5}$$

$$k_f = \frac{2bDC_{Ag}}{\rho_B R_o^2} \qquad \text{Equation 4-6}$$

Large particles

$$k_f t = 1 - (1 - X_B)^{1/2} \qquad \text{Equation 4-7}$$

$$k_f = (const)\frac{C_{Ag}}{R_o^{3/2}} \qquad \text{Equation 4-8}$$

Surface reaction control

$$k_s t = 1 - (1 - X_B)^{1/3} \qquad \text{Equation 4-9}$$

$$k_s = \frac{bk''(C_{Ag})^n}{\rho_B R_o^2} \qquad \text{Equation 4-10}$$

Product layer diffusion

$$k_d t = 1 + 2(1 - X_B) - 3(1 - X_B)^{2/3} \qquad \text{Equation 4-11}$$

$$k_d = \frac{2bDMC_{Ag}}{\rho_B R_o^2} \qquad \text{Equation 4-12}$$

X_B is the fraction of reacted particle at time t; k_f, k_s and k_d are apparent rate constants; b is the stoichiometric coefficient; D is effective diffusivity; C_{Ag} is the bulk concentration of reactant; ρ_B is density of reacted particle; R_o is initial particle radius; k'' is the intrinsic rate constant and n is the reaction order.

4.5.5 Chemical and mineralogical analysis

Chemical and mineralogical analyses of solution samples and from the leaching experiments were done at University of Stellenbosch at the Department of Process Engineering. However some of the samples were taken to the Central Analytical Facility to verify the chemical analysis. The analysis of the solids before and after leaching was done for mass balance purposes. Solution samples were analyzed for nickel, cobalt, and iron using atomic absorption spectrophotometry (AAS). Solids samples were analyzed by X-ray fluorescence (XRF) and X-ray diffraction (XRD) for chemical and mineralogical analysis respectively. The fraction of Ni extracted was calculated from the experimental data using the following equation;

$$x_{mi} = \frac{\left(V - \sum_{j=1}^{i-1} v_j\right) C_{mi} + \sum_{=j}^{i-1} v_j C_{mj}}{M\left({}^{c_m}/_{100}\right)} \qquad \text{Equation 4-13}$$

Where x is the fraction extracted, m represent metal, V is the initial volume (L) of the solution; v_i is the volume (L) withdrawn each time, C_{mi} is the concentration of m (Ni) in the samples (mg/L), M is the initial mass of laterite (mg) added into the vessel and c_m is the concentration of Ni in the laterite ore.

4.6 Summary

Pore clogging prevented continuous circulation of the leach solution and therefore the set up of the vessel was slightly modified. All experiments were carried out without recirculation of the leach solution. Leaching experiments were carried out by pressurizing below and above the filter medium in order to equalize the pressure over the filter medium. After leaching, the leach liquor was separated from solids by filtration from the same vessel.

Two sets of leaching experiments were carried out, namely optimization and kinetics. In the optimization of the leaching experiments, a four-factor face centered central composite design was used. The four factors studied were temperature, oxygen pressure, ammonia concentration, and ammonium carbonate concentration. The leaching duration was 3 hours. After leaching, the leach liquor was filtered and the time taken to collect a certain amount of volume was recorded in order to calculate the filtration rate. The same procedure was

followed for the determination of reaction kinetics reactions. In this case, samples were taken at time intervals of 30 minutes.

Chemical and mineralogical analysis of liquids and solids were done at Stellenbosch University. Liquid samples were analyzed for nickel, cobalt, and iron, using AAS in the Central Analytical Facility (CAF). The mineralogy of the ore before and after leaching was determined in CAF using x-ray diffraction (XRD). Scanning Electron Microscope (SEM) was also used to determine the distribution of nickel within the ore.

5 Results and Discussions

Saprolitic laterite was leached with a solution of ammonia and ammonium carbonate. After the specified leaching period, the liquid was separated from the solids by pressure filtration. Extra experiments were carried out to study the leaching kinetics of nickel from the ore under varying experimental conditions. This section discusses the results obtained from leaching and filtration experiments.

5.1 Optimization reactions

Optimization reactions were carried in the vessel configuration as explained in chapter 3. After leaching, the leach liquor was analyzed for nickel, and iron. The concentrations of respective metals in the solution were converted to percentage metal extracted. A table showing the experimental concentrations, conversion to percentage extraction and experimental conditions is given in Appendix C in Table (C-1). Data from these experiments was statistically analyzed using Statistica software to identify the significant factors affecting the leaching. The complete experimental design matrix and responses based on experimental runs for percentage extraction of nickel, cobalt, and iron are given in Table (5-1).

From Table (5-1) it can be seen that there is no iron in the leach liquor, therefore the factor effects analysis and optimization were done based on the response of nickel only. The maximum extraction of nickel is 11.90% at a temperature of 100^{o}C, 4M [NH_3], 2M [$(NH_4)_2CO_3$] and O_2 pressure of 2 bar. Before admitting O_2 into the vessel, the vessel was heated to 100^{o}C and the pressure due NH_3 and H_2O vapor was 5bar. In order to add 2bar of O_2, the oxygen regulator was set to 7.0 bar. At these conditions, the total pressure in the vessel was 7 bar and pH of the solution after leaching was 11.24 for the solution below the filter medium and 11.53 above the filter medium. At this pH, Ni $(NH_3)_6^{2+}$ is the most stable species, according to the Eh-pH diagram for Ni-NH_3-H_2O system given by Meng and Han (1996).

Table 5-1: Experimental design matrix and response based on experimental runs

Runs	Temp ^{o}C	$[NH_3]$ (M)	$[(NH_4)_2CO_3]$(M)	O_2 (bar)	% extracted Ni	% extracted Fe
7	50.00	4.00	2.00	5.00	3.86	0
15	70.00	2.00	1.00	2.00	6.08	0
4	50.00	4.00	0.50	5.00	3.97	0
12	70.00	4.00	1.00	3.00	6.12	0
5	100.00	0.00	0.50	5.00	1.06	0
10	100.00	2.00	1.00	3.00	9.41	0
9	50.00	2.00	1.00	3.00	6.17	0
13	70.00	2.00	0.50	3.00	7.43	0
3	100.00	0.00	2.00	5.00	6.20	0
18	70.00	2.00	1.00	3.00	6.74	0
11	70.00	0.00	1.00	3.00	2.44	0
8	50.00	0.00	0.50	2.00	1.08	0
6	50.00	0.00	2.00	2.00	3.81	0
1	100.00	4.00	2.00	2.00	11.90	0
2	100.00	4.00	0.50	2.00	8.93	0
14	70.00	2.00	2.00	3.00	7.17	0
16	70.00	2.00	1.00	5.00	6.24	0
17	70.00	2.00	1.00	3.00	6.74	0

The percentage extraction of nickel is relatively low compared to the maximum extraction reported when the ore is roasted prior to leaching (Vosahlova and Weir, 1972; Siemens, 1976; Li *et al*., 2009). In this study, a small amount of nickel is extracted from the ore without roasting prior to leaching experiments. This implies that within the raw ore there is some amount of nickel, which is not associated with iron, which is leachable..

Analysis of variance (ANOVA) of experimental results was carried out to identify the significant factors, which effect the extraction of nickel. First, the model that best fit the data was selected. The model that was first selected was linear effect and 2-way interaction. ANOVA results for this model are given in Appendix C in Table (C-2). According to this model, there are no significant factor effects on extraction of nickel. Furthermore, the model accounts for 79% of the response variable (as indicated by R-square value in the table header) and thus this model was considered inadequate and yield poor description of the data.

The next model chosen was linear and quadratic effects. The ANOVA results for this model are given in Table (5-2). This model accounts for approximately 90% of the variation in the response variable (as indicated by R-square value in the table header). According to this model, temperature, NH_3, $(NH_4)_2CO_3$ and O_2 pressure have significant main effects. In

addition to the main effects, NH_3 concentration has significant quadratic effects. Significant factor effects on the ANOVA results have probability values (p-value) less than 0.05 (i.e. at 95% level of confidence).

Table 5-2: ANOVA table for extraction nickel

ANOVA; Var.:% extracted Ni; R-sqr=.8969					
factors	Sum of Squares	degrees of freedom	Mean Squares	F	p
(1)Temperature ^{o}C(L)	34.69	1.00	34.69	22.60	0.00
Temperature ^{o}C(Q)	0.94	1.00	0.94	0.61	0.45
(2) [NH_3] M(L)	40.75	1.00	40.75	26.55	0.00
[NH_3]M(Q)	16.05	1.00	16.05	10.46	0.01
(3) [$(N_{H4})_2CO_3$]M(L)	10.94	1.00	10.94	7.13	0.03
[$(NH_4)_2CO_3$] M(Q)	0.06	1.00	0.06	0.04	0.85
(4)O_2 pressure bar(L)	10.97	1.00	10.97	7.14	0.03
O_2 pressure bar(Q)	0.21	1.00	0.21	0.14	0.72
Error	13.82	9.00	1.54		
Total SS	134.05	17.00			

The Pareto chart in Figure (5-1) makes it easier to visualize significant factor effects. The chart shows the absolute values of the (standardized) individual effect and ranks them in order of magnitude. A vertical line on the chart indicates the P-level for significance (in this case 0.05). The most significant effect is NH_3 concentration and is positive which implies that in order to increase the extraction of nickel the concentration of ammonia should be increased. The next effect is temperature followed by the quadratic effect of NH_3, then the effect of O_2 and lastly the effect of $(NH_4)_2CO_3$. The effect of oxygen is negative which implies that oxygen pressure should be decreased for good recovery of nickel. The does not agree with literature especially when leaching roasted ore. However, there was no literature found on leaching of unroasted to compare the results. The negative effect of oxygen can be explained by the oxidized nature of an unroasted ore and therefore, the need for oxygen is not high. However, pressure is still required to preserve ammonium ions in solution as shown in Equation (1-1).

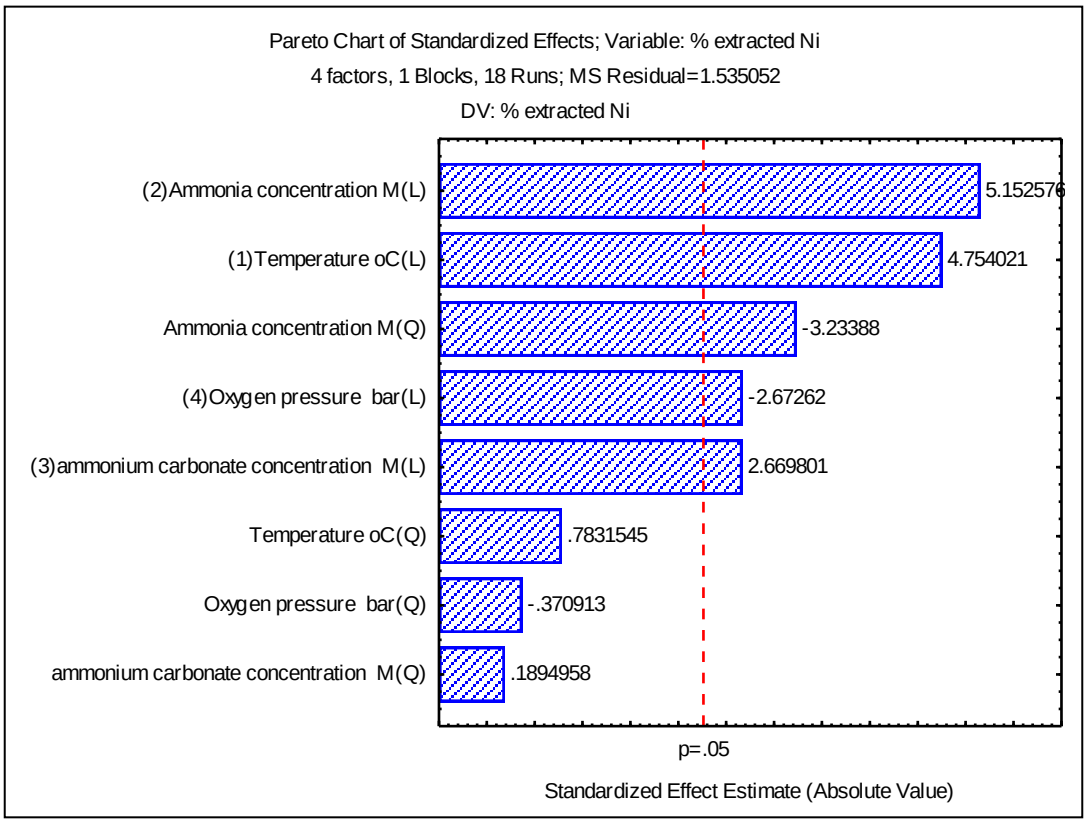

Figure 5-1: Pareto chart of standardized effect on nickel extraction

Three dimensional (3D) response surface contours were utilized to predict response by varying two factors while the other two were kept constant. The figures are given in the Appendix. Figure (C-1) shows the effect NH_3 concentration and temperature on the percentage extraction of nickel.

The maximum extraction is obtained when the concentration of NH_3 is 3M at a temperature of 110^{o}C. Figure (C-2) shows the effect of $(NH_4)_2CO_3$ and temperature on percentage extraction of nickel (see Appendix C). There seem to be a linear relationship between $(NH_4)_2CO_3$ concentration and percentage extraction. The maximum extraction is obtained when $(NH_4)_2CO_3$ is 2.2M at temperature of 110^{o}C. Figure (C-3) shows the effect of O_2 pressure and temperature on percentage extraction of nickel. According the figure maximum extraction is obtained at O_2 pressure of 3 bar at temperature of 110^{o}C. According to the analysis on response surface plots, some factor setting should be outside experimental conditions in order to get maximum extraction.

To find optimum conditions within experimental conditions, response profiling and desirability function was used in Statistica software. Table (5-3) shows the factor setting for

optimum extraction of nickel within experimental conditions. The desirability value of 1.00 indicates the factor settings were selected to give highest value of extraction of nickel. The predicted value for the percentage extraction of nickel under these factor settings is 11.96%. The profiles for predicted values and desirability are given in Appendix C in Figure (C-4).

Table 5-3: Predicted response for % extraction of nickel at optimum conditions

Level of Temperature ^{o}C	Level of NH_3 (M)	Level of $(NH_4)_2CO_3$ (M)	Level of O_2 pressure bar	Predicted % extracted Ni	Desirability Value
100.	3.	2.	2.	11.96	1.00

5.2 **Effect of leaching duration**

Using optimum leaching conditions of 2M $(NH_4)_2CO_3$, 3MNH_3, 100^{o}C and 2 bar O_2 pressure, additional leaching experiments were carried out at different leaching durations of 3, 6 and 12 hours. The experiments were carried to find the effect of leaching duration on percentage extraction of nickel. The results are given in table (5-4).

Table 5-4: Effect of leaching duration at optimum conditions

Time Hours	T ^{o}C	NH_3 (M)	$(NH_4)_2CO_3$ (M)	O_2 (bar)	% Ni extraction
Optimized 3 hours	100.00	3.00	2.00	2.00	12.56
Optimized 6 hours	100.00	3.00	2.00	2.00	12.69
Optimized 12 hours	100.00	3.00	2.00	2.00	15.14

The results show that for leaching durations of three and six hours, the extraction of nickel is almost the same. There is a slight increase in percentage of nickel for a leaching duration of 12 hours. The solids before and after leaching for the leaching duration of 12 hours at optimum leaching conditions were analyzed for elements and mineral present in the ore. For mineralogical analysis, XRD was used and XRF was used for elemental analysis. Some of samples were analyzed using SEM with an EDS detector to find nickel distribution in an unroasted of saprolitic laterite and the results will be discussed in the following section.

Elemental analysis on raw and leached ore is given in Table (5-5). The analysis shows that Fe, Si, and Mg were not affected by the leaching solution. In both raw and leached ore, the

amount of these elements remained the same after leaching for 12 hours. These elements are the major constituents of the ore within which most nickel is distributed. Analysis reveals that the only element significantly depleted from raw ore is nickel. The analysis shows about 14% depletion of nickel from the raw ore. These results are agreement with analysis made on liquid samples. The fact that other minerals such as Si, Mg and Fe were not affected by the solutions, suggest the reason why the extraction is low. The mineral phases of these elements are believed to be the major host for nickel in the saprolitic laterite (Chander and Sharmer, 1981). If these elements were not affected by leaching, then their mineral phases are inert to a solution of ammonia and ammonium carbonate.

Table 5-5: Elemental analysis of raw and leached laterite ore

elements	Fe	Mg	Mn	Si	Ti	Cr	Co	Ni	Cu
Raw ore (wt %)	11.65	17.82	0.15	16.58	0.03	0.46	0.02	2.29	0.00
Leached ore (wt %)	11.65	17.70	0.14	16.68	0.01	0.52	0.02	1.95	0.00

Mineralogical analysis of raw and leached ore was done using XRD. The XRD patterns of raw and leached ore are given in Figures (5-2) and (5-3) respectively. According to the XRD pattern in Figure (5-2), the main mineral present in the raw ore are lazardite $(Mg_{2.70}Fe_{0.18}Al_{0.11})(Si_{1.8}1Al_{0.19}O_5)(OH)_4$, quartz SiO_2, magnesium nickel iron(III) oxide $(Fe_{0.92}Mg_{0.08})(Fe_{1.08}Ni_{0.2}Mg_{0.72})O_4$ and Clinochlore-ferroan, $(Mg,Fe,Al)_6(Si,Al)_4O_{10}(OH)_8$. The main minerals, which are evident in XRD pattern in Figure (5-3), are clinochrysotile or lazardite Mg_3 $(Si_{2-x}O_5)$ $(OH)_{4-4x}$, quartz SiO_2 and magnesium diiron(III) oxide $MgFe_2O_4$. From the XRD pattern of raw and leached ore, there is seems to be the same minerals in both ores.

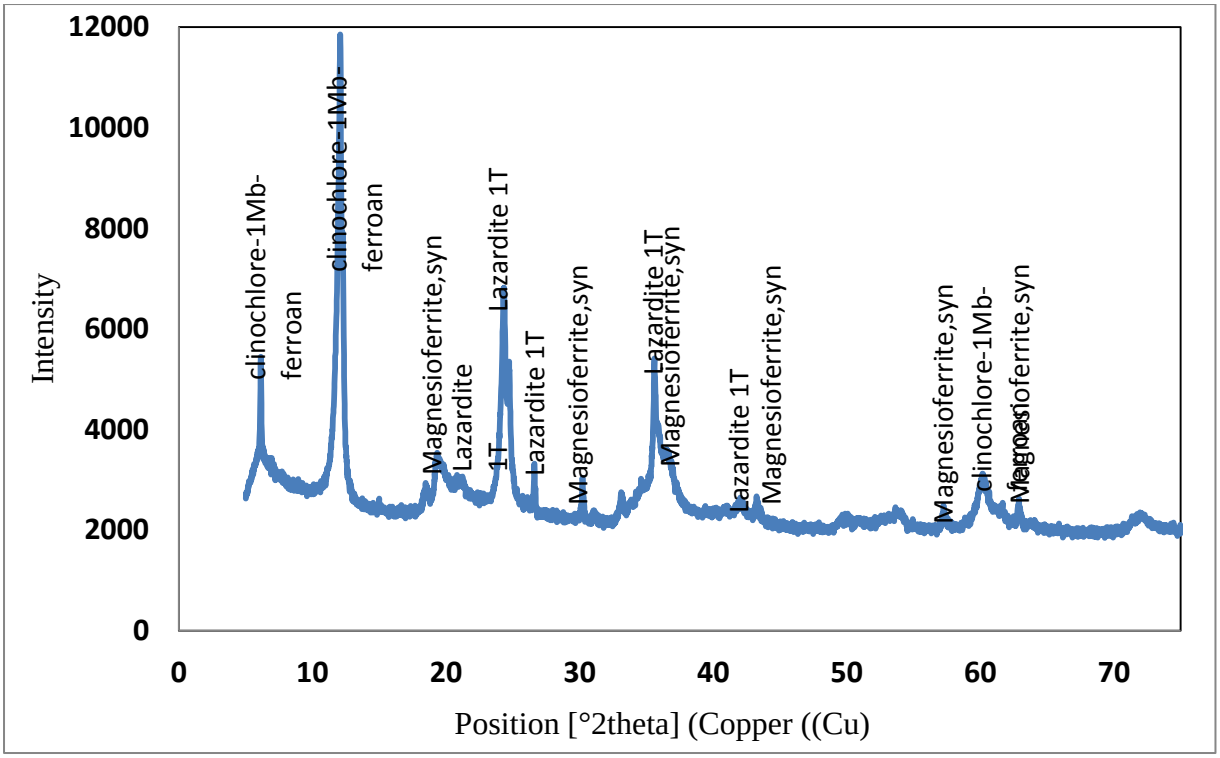

Figure 5-2: XRD pattern of raw ore (unroasted)

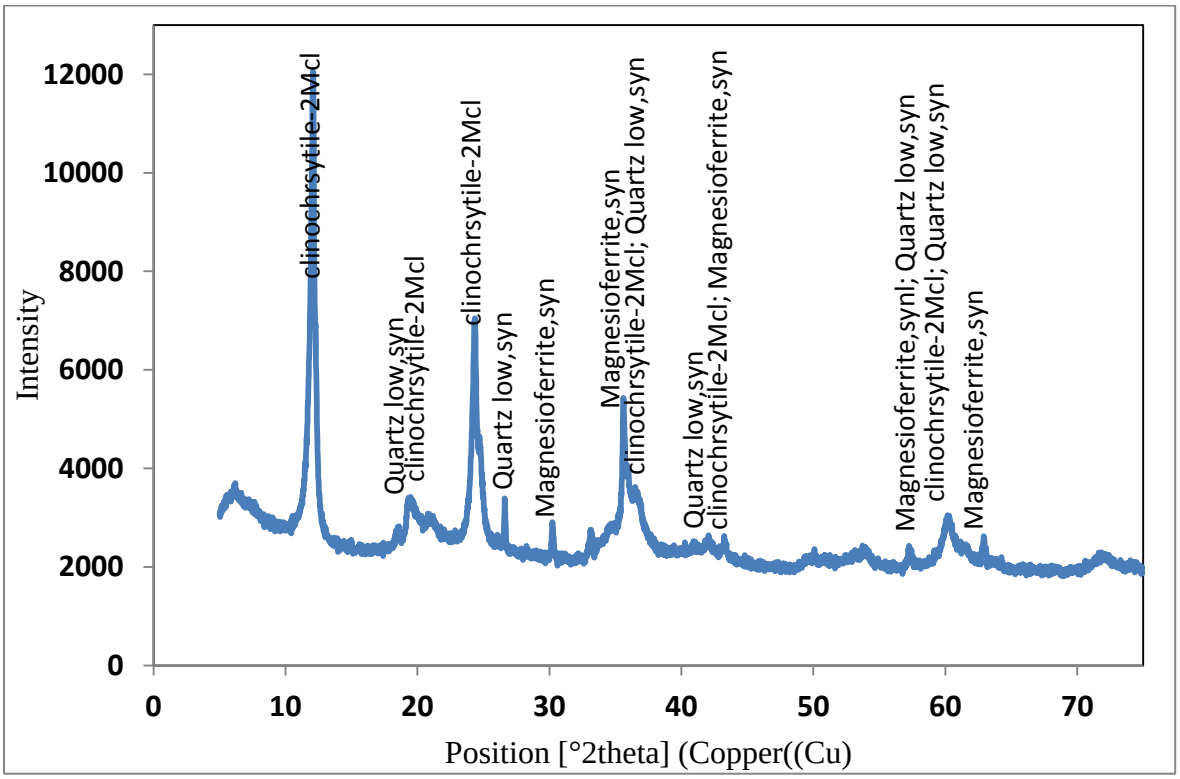

Figure 5-3: XRD pattern of leached ore at optimum leaching conditions

After leaching, the mineral phases present in raw ore are still present in leached ore. This indicates that these minerals are inert to a solution of ammonia and ammonium carbonate. On the other hand, there is no indication of free nickel or which is not associated with magnesium and iron. This could be that the amount of free nickel is too small to be detected by the instrument used. However, the results from other studies suggest that there is nickel in the ore, which is leachable (Mizoguchi *et al*., 1978). This was further confirmed by a study on the distribution of nickel in saprolitic laterite by Luo *et al*. (2010). In saprolitic laterite 0.38% is nickel sulfide, 10.14% is nickel oxide 15.22% is nickel in magnetite and 72.46% is nickel in silicate laterite. The nickel oxide in this ore as indicated here is probably the leachable nickel in unroasted saprolitic laterite.

SEM analysis was done on raw and leached ore at the optimum conditions. Dried ore was first pressed using a hydraulic press and coated with gold. Data on the general elements distribution was collected by elemental mapping with an energy dispersive spectrometer. Two maps were done on each solid for Ni, Si, Mg, and Fe. The data reveals the distribution of nickel in these elements. From selected point on the maps, areas with high content of nickel were targeted for quantitative analysis to document the compositional variability.

Figure (5-4) shows elemental mapping of Ni, Si, Mg, and Fe in raw ore. The maps show that the main constituents of the ore are magnesium and silicon. Within magnesium and silicon, there is iron, which is associated with nickel. The bright green, red, grey, and bright blue areas indicate Fe, Si, Mg, and Ni, respectively. According to the elemental maps, Ni is associated with areas with high Fe content. Figure (5-5) shows a mixed map of Si, Mg, Fe, and Ni. The mixed map is the combination of elemental maps of individual elements. On the map, the position of each element in relation to other elements is clearly visible. The red area indicates Si is dominant and inside the red area there are patches of grey indicating Mg. The green area indicating Fe is surrounded by red and grey and close to green area is blue area indicating Ni. The mixed map clearly show that Si and Mg are major constituents of the ore and that iron is associated with nickel within the ore.

From elemental maps, selected points were targeted for qualitative analysis. The analysis spectrum of selected points on the SEM image is given in Figure (5-6). The analyzed area was selected because of the high concentration of nickel as shown in Figure (5-4) on Ni map. The spectrum indicates that, there is significant amount of Si, Mg, and Fe in the selected area. The bulk of the nickel in the ore is associated with iron and a small amount is free nickel.

SEM analysis on the other areas of the ore is given in Appendix C in Section C.2. The results also show that wherever there is Ni, there is significant quantities of Fe, Mg, and Si, and that only a small portion of nickel is free from iron.

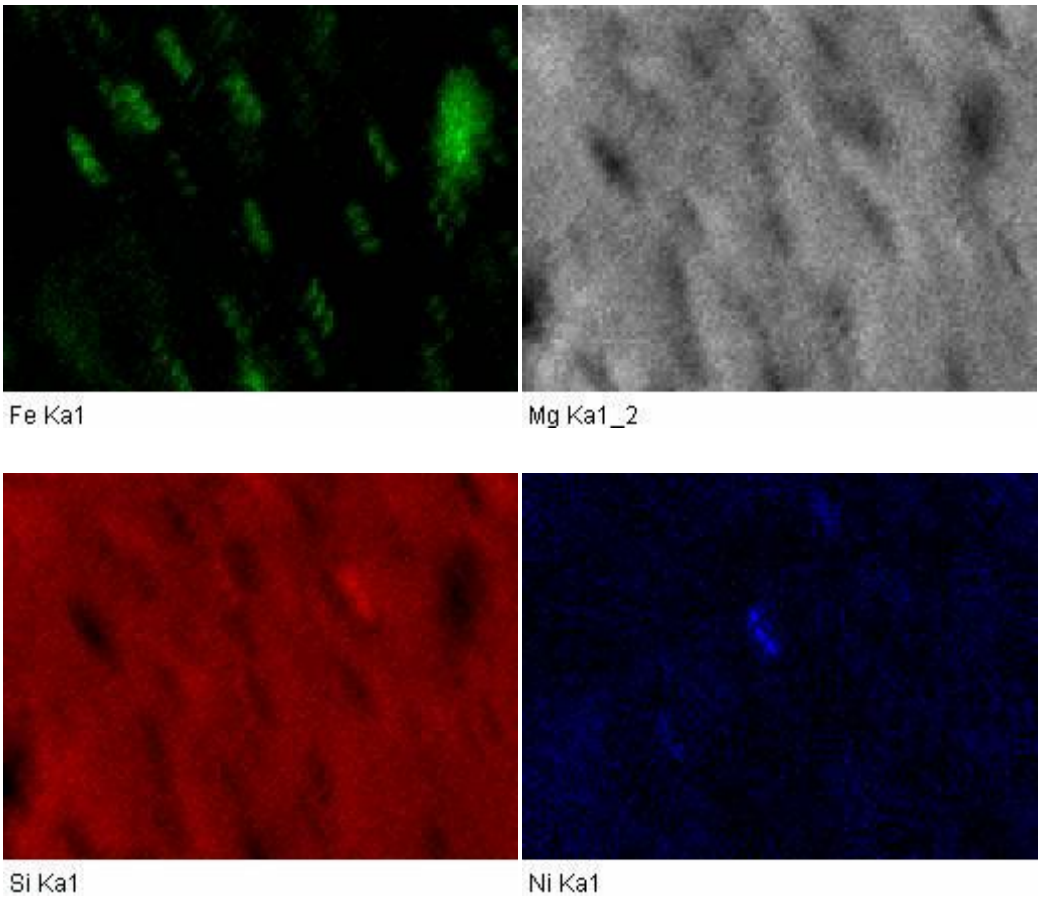

Figure 5-4: Distribution of Si, Mg, Fe, and Ni in raw Saprolitic laterite (Bright green=Fe, Red Si, Grey=Mg and Bright blue=Ni)

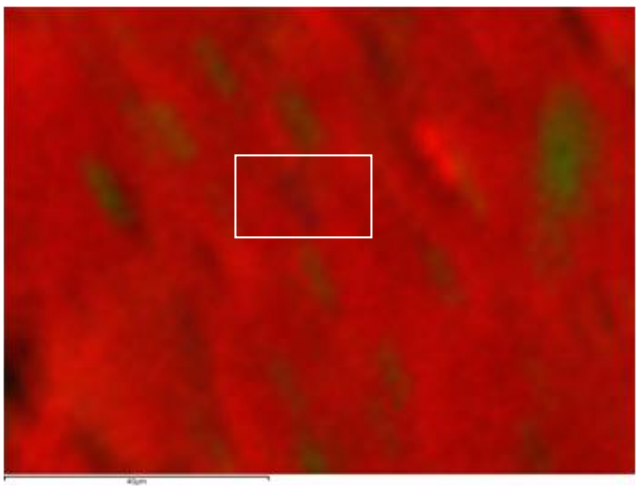

Figure 5-5: Mixed map of Ni, Si,Fe and Mg (red =Si, green=Fe, Grey=Mg, and blue Ni)

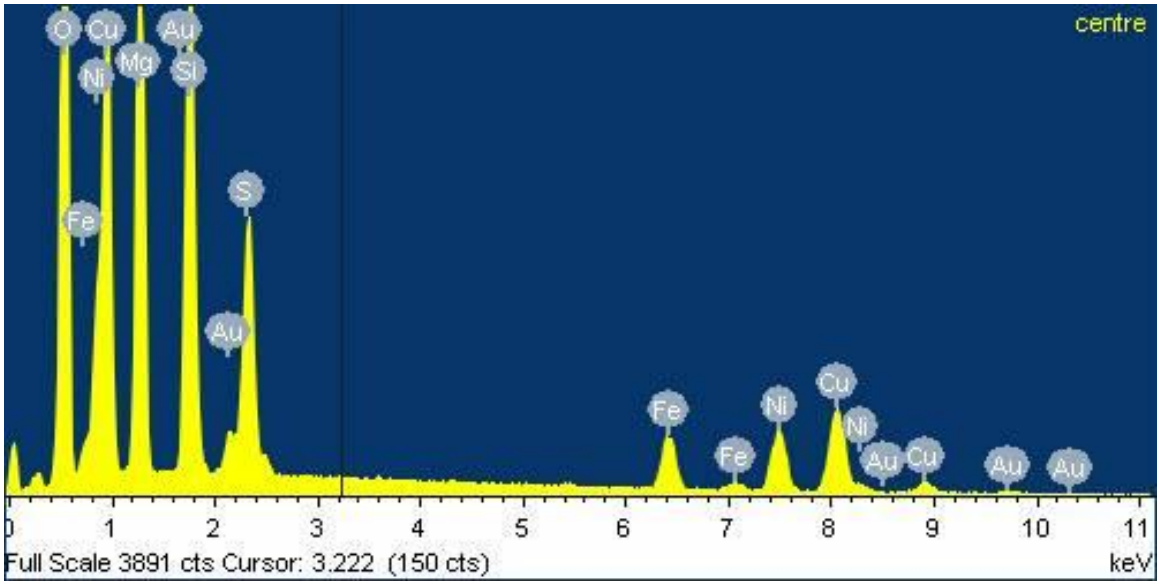

Figure 5-6: Analysis spectrum of the selected area on raw ore in Figure 4-5

The same analysis was done on the leached ore. The elemental maps of Si, Mg, Fe, and Ni in leached are given in Figure (5-7). In this case, the maps of the different elements are not distinguished by colors. The bright areas on the Fe map indicate Fe and likewise for Ni map. Similar to the maps of the raw ore Mg, Si, and Fe are the major constituents of the ore. Iron is surrounded by Mg, Si and Ni. The mixed map is given Figure (5-8). The distribution of Fe and Ni within Mg and Si is clearly visible. On the mixed map, Si is distinguished by red, Mg by grey, Fe by bright green, and Ni by Bright blue. The high concentration of nickel within the ore is associated with iron. The analysis spectrum of the elements in the leached ore is given in Figure (5-9). The spectrum indicates the presence of Mg, Si and Fe in high concentrations on the selected area. However, there is a decrease in the Ni not associated with iron which is in the leached ore. The decrease in peaks indicating Ni is due to depletion of free nickel during leaching.

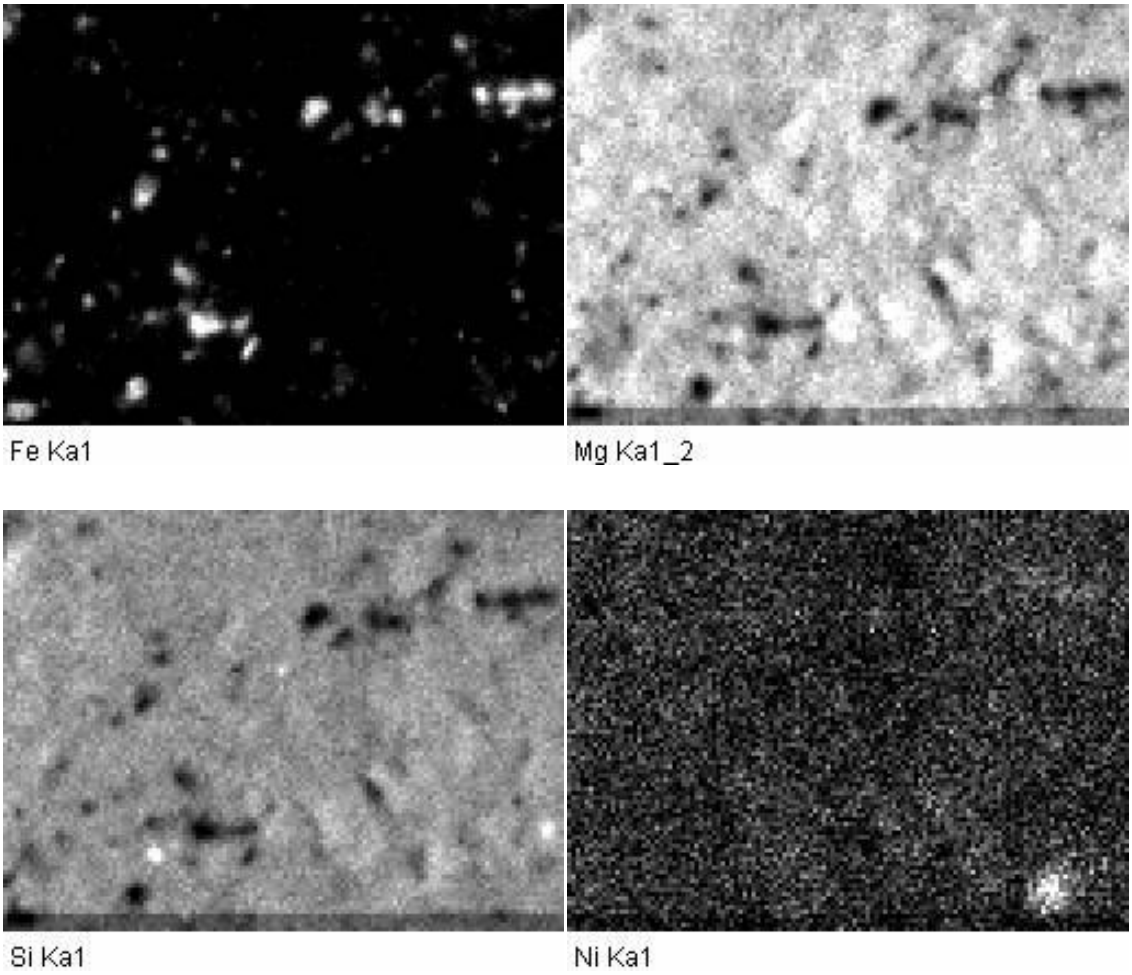

Figure 5-7: Distribution of Si, Mg, Fe, and Ni in leached Saprolitic laterite

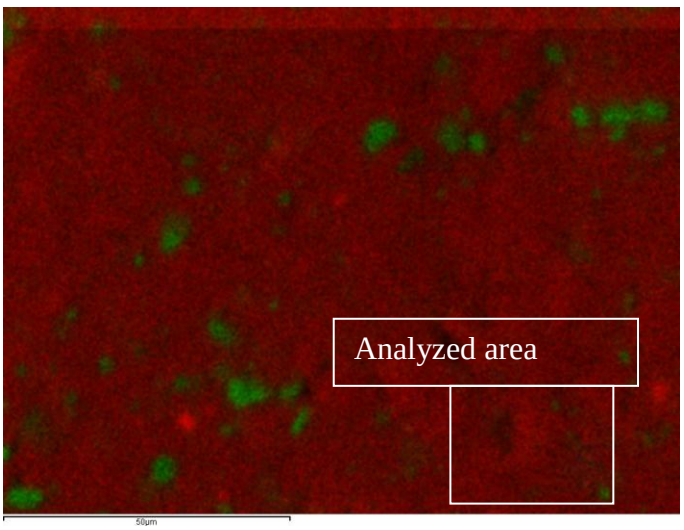

Figure 5-8: Mixed map of Ni, Si, Fe and Mg in leached ore (red =Si, green=Fe, Grey=Mg, and blue Ni)

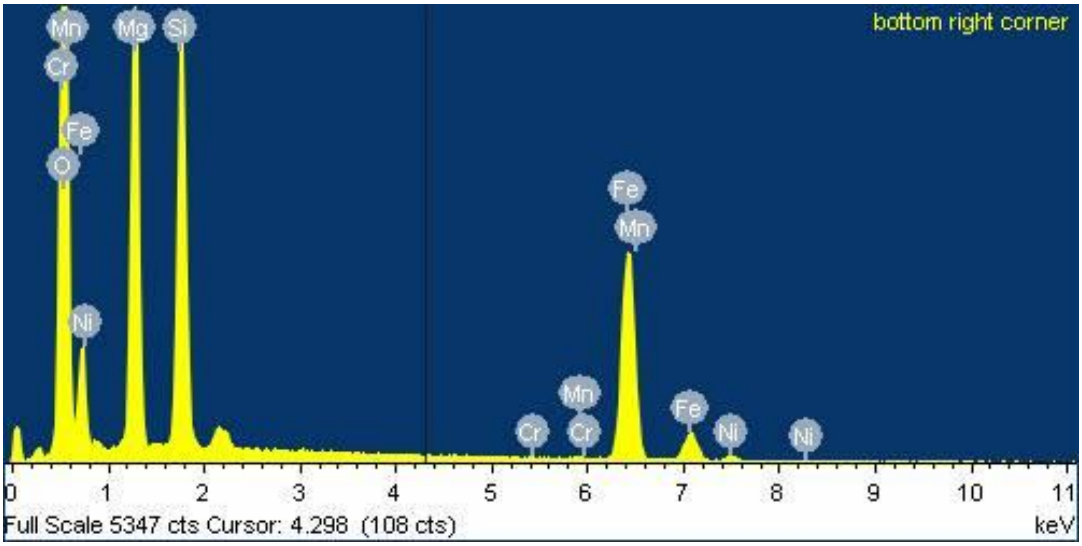

Figure 5-9: Analysis spectrum of the selected area on leached ore in Figure 5-8

Chemical and mineralogical analyses confirm that in the unroasted saprolitic laterite ore the main minerals present are inert to ammoniacal ammonium carbonate solution. The elements which make up the minerals were not depleted after leaching. In addition, the XRD patterns of leached ore show that these minerals were still intact. SEM analyses show that nickel is distributed within Mg and Si and that it is associated with iron in the form of either goethite or magnetite. There is an indication of free nickel, which is not associated with iron. Before concluding that the low recovery of nickel from unroasted ore was due to the nature of the ore, some experiments on the leaching kinetics were carried out. The experiments were carried out to establish whether diffusion of reagents to the nickel particle is the limiting factor due to inertness of minerals hosting nickel.

5.3 **Solid-liquid separation**

Leaching experiments were according to the CCD shown in Table (3-2). After leaching at different conditions, the contents of the vessel were cooled to room temperature using the cooling coil inserted into the vessel see Figure (4-3). The cooling process reduced the vapor pressure of ammonia and ensured that the leach liquor does not splash during draining. At the end of each leaching experiment, the leach solution below the filter medium was drained through V-9 and some was kept for analysis. The remaining mixture of solids and leaching solution above the filter medium was then filtered for about 20 minutes under pressure. The

volumes of solutions drained below the filter medium and the remaining volumes above the filter are given in Table (C-1) in Appendix C. Table (5-6) shows the filtered volume after 20 minutes. The pressure was varied according to the oxygen pressure setting in the design of leaching experiments (2, 3, and 5 bar). Because the filtration was varied according to the design given in Table (4-2), the filtration rate was analyzed in the similar manner to the leaching experiments.

Table 5-6: Filtration rate at different pressures

Runs	Temp (^oC)	[NH_3] (M)	[$(NH_4)_2CO_3$] (M)	Total Pressure (bar)	Volume (ml)	Time (min)	Filtration rate (ml/min.cm^2
7	50.00	4.00	2.00	5.00	1100.00	20.36	0.36
15	70.00	2.00	1.00	2.00	840.00	21.08	0.27
4	50.00	4.00	0.50	5.00	1040.00	21.20	0.33
12	70.00	4.00	1.00	3.00	1000.00	20.30	0.33
5	100.00	0.00	0.50	5.00	660.00	23.36	0.19
10	100.00	2.00	1.00	3.00	920.00	21.52	0.29
9	50.00	2.00	1.00	3.00	820.00	21.82	0.25
13	70.00	2.00	0.50	3.00	1160.00	21.44	0.36
3	100.00	0.00	2.00	5.00	1380.00	20.02	0.46
18	70.00	2.00	1.00	3.00	820.00	20.02	0.27
11	70.00	0.00	1.00	3.00	760.00	21.00	0.24
8	50.00	0.00	0.50	2.00	700.00	20.46	0.23
6	50.00	0.00	2.00	2.00	740.00	20.56	0.24
1	100.00	4.00	2.00	2.00	820.00	20.66	0.27
2	100.00	4.00	0.50	2.00	930.00	21.26	0.29
14	70.00	2.00	2.00	3.00	760.00	20.96	0.24
16	70.00	2.00	1.00	5.00	780.00	21.06	0.25
17	70.00	2.00	1.00	3.00	1200.00	21.06	0.38
						Average	0.29
						Std deviation	0.07
						Filter area	149.60cm^2

The main factor considered in this study was pressure (O_2 pressure). The complete design matrix of experimental runs with response variables is given in Table (5-6). The results from

Table (5-6) were analyzed using Statistica software to investigate the effect of pressure on filtration rate. The analysis of variance (ANOVA) was carried out investigate the effect of pressure on filtration rate. The model used for filtration rate included linear and quadratic effects. The ANOVA results for this model are given in Table (5-7). According to this model, both linear and quadratic effects of pressure are insignificant as indicated by p-value which is greater than 0.05. It might be expected that NH_3 and $(NH_4)_2CO_3$ concentration might have an effect on filtration rate because they affect pH of the solution, which in turn affects permeability of the slurry however; they did not have significant effect on filtration rate. Both linear and quadratic effects of NH_3 and $(NH_4)_2CO_3$ concentration did not have a significant effect on filtration rate. No factors under investigation had significant effect on filtration rate.

The average filtration rate was determined to be 0.29 ml/min.cm^2 ± 0.07. The filtration rate was slow. When filtering sphalerite ore with water using a 20µm sintered metal filter medium, a very clear filtrate and filtration rate of 1.99 ml/min.cm^2 was obtained at 1.5 bar (Erasmus, 2008). The results are given Table (A-1) in Appendix A. Filtration rate was slow in this case because of quick pore clogging of sintered metals. In Chapter 3, it was established that the ore has a non- Newtonian behavior. According to Battaccharya *et al*. (1998) slurry rheology plays a very important role in filtration. Viscosity of slurry increases with the decrease in particle size and the effect of increased viscosity can hinder slurry transportation and filtration. According (Battaccharya *et al*. 1998) high viscosity in laterites is mainly due goethite. Midigan *et al.* (2009) also support this. In his study, rheological behavior of slurries with varying amount of goethite at the same solid to liquid ratio was investigated. Viscosity was high in slurries with high goethite concentration. However, when the amount of goethite was kept constant and solid to liquid ratio was varied, viscosity was low in slurries with low solid to liquid ratio. When looking at filtration results for the roasted in section 5.4.2 filtration rate is relatively high. Furthermore looking at the results in Figure (3-10), viscosity of roasted ore is lower than for unroasted ore at all solid to liquid concentration. Low viscosity could be associated with the transformation of goethite during roasting. This indicates that rheological properties of unroasted ore play a role in slow filtration rate in an unroasted ore.

Table 5-7: ANOVA table for filtration rate at different pressures

	SS	df	MS	F	p
(1)Temperature ^{o}C(L)	0.0007	1	0.000698	0.109941	0.747802
Temperature ^{o}C(Q)	0.00029	1	0.000292	0.046032	0.834900
(2)NH_3 M(L)	0.00463	1	0.004633	0.729494	0.415202
NH_3 M(Q)	0.00016	1	0.000160	0.025234	0.877293
(3)$(NH_4)_2CO_3$ M(L)	0.00291	1	0.002912	0.458556	0.515327
$(NH_4)_2CO_3$ M(Q)	0.00086	1	0.000858	0.135165	0.721633
(4)O_2 bar(L)	0.00858	1	0.008579	1.350924	0.275010
O_2 bar(Q)	0.00227	1	0.002273	0.357866	0.564443
Error	0.05715	9	0.006350		
Total SS	0.07633	17			

Figure 5-10: A photograph showing pregnant liquor after filtration using the vessel

From all the filtration experiments, a very clear filtrate was obtained. Figure (5-10) shows the photograph of pregnant liquor after filtration. The clarity of filtrate is very important because in some processes metal values can be obtained directly from the filtrate by precipitation without solvent extraction or ion exchange. Clarity of the filtrate illustrates how effective the

sintered metal is in separating liquid from the solids. After filtration, the filter medium was cleaned by back washing with water and air. The fact that all 18 experiments were carried out with a single sintered metal disk indicates that back flushing was successful. It has been shown in Figures (B-4) and (B-5) in Appendix B that most clogging of the sintered metal occurs on the surface. This implies that unblocking of sintered metal is still possible because only a few particles are deep within the pores.

5.4 Effect of roasting prior to leaching

Because of the low extraction of nickel from the unroasted ore, three experimental runs were carried out with roasted ore to find out whether nickel extraction will improve after roasting the ore under reducing conditions. The effect of roasting on both leaching and solid-liquid separation was determined. The roasting procedure is given in section 4.1.3 of Chapter 4. The experiments were carried using the optimum conditions obtained for unroasted ore given in Table (5-3). The same procedure of leaching and solid-liquid separation was used for the roasted saprolitic laterite ore.

5.4.1 Characterization of roasted ore

The surface area of the roasted ore was found to have decreased in comparison to the unroasted ore. The decrease in surface area indicates the possibility of sintering at the high temperatures of roasting (Chander and Sharmer, 1981). The major minerals present in the roasted as identified by XRD, are presented in Table (5-8). The XRD pattern of the roasted ore is given in Figure (5-11).

Table 5-8: Mineral phases present after reduction roasting of saprolitic laterite

Mineral Name	Chemical Formula
Forsterite ferrous	$Mg_{1.838}\,Fe._{156}\,Ni_{.006}\,Si\,O_4$
Quartz	$Si\,O_2$
Magnesioferrite	$Mg\,Fe_2\,+3\,O_4$

The XRD results show that when the ore is roasted under reducing conditions new phases are formed. When comparing the XRD pattern of roasted ore with the XRD pattern of raw ore in Figure (5-2), chlinochlore and lazardite break down to form Mg-olivine (forsterite).

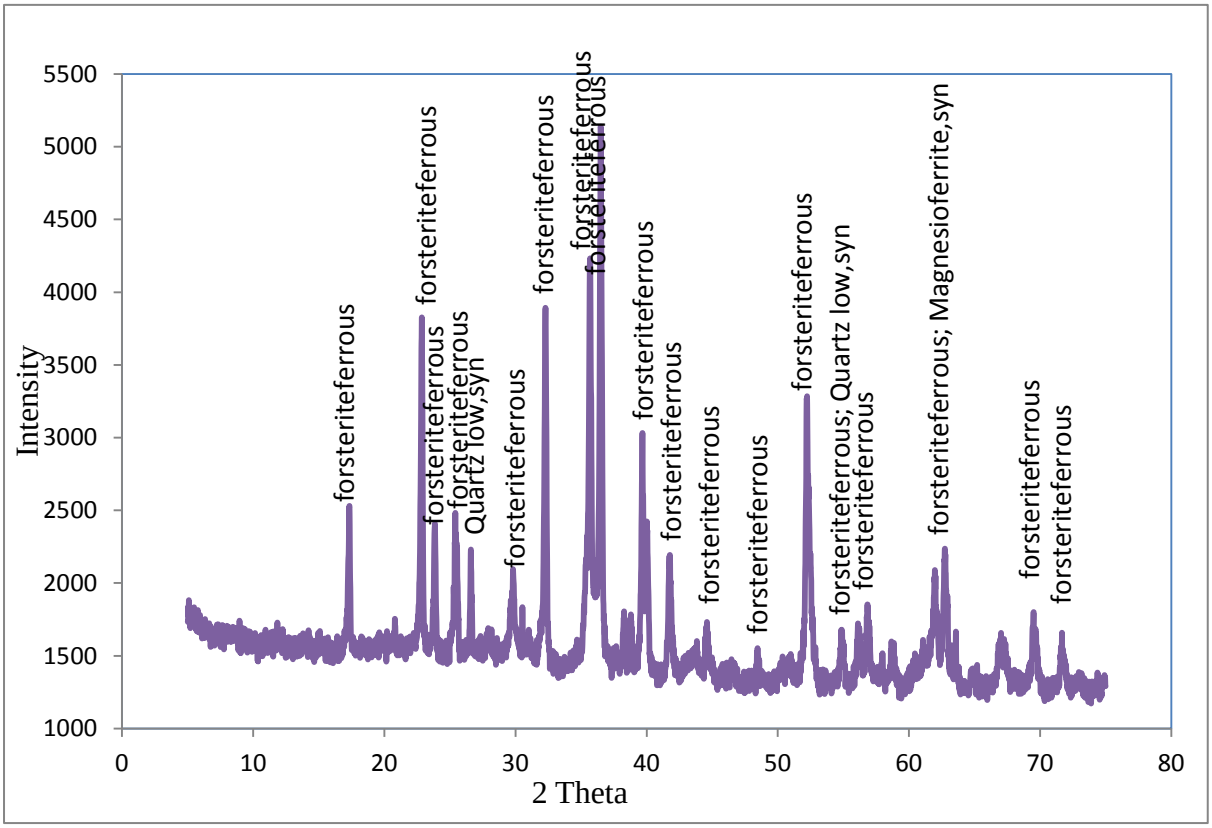

Figure 5-11: XRD pattern of roasted ore

5.4.2 **Leaching and solid-liquid separation**

The roasted ore was leached using optimum conditions determined for the unroasted ore. For the roasted ore, oxygen pressure was 5 bar instead of 2 bar, which was found to be optimum for the unroasted ore. This was chosen to ensure that the metalized nickel during reduction roasting would completely dissolve in the leaching solution.

Table 5-9: Leaching results for the roasted ore

Runs	T°C	[NH_3] (M)	[$(NH_4)_2CO_3$] (M)	O_2 (Bar)	% extraction
run1	100.00	3.00	2.00	5.00	19.43
run2	100.00	3.00	2.00	5.00	19.00
run3	100.00	3.00	2.00	5.00	19.32
average					19.25
standard deviation					0.184

The results for leaching roasted ore under conditions of 2 M $(NH_4)_2CO_3$, 3 M NH_3, 100 ^oC, and 5 bar O_2 are presented in Table (5-9). For three experimental runs under the same conditions, the average percentage extraction of nickel was 19.25%. No iron was found in the leach liquor after a leaching duration of 3 hours. The percentage extraction of nickel from the roasted ore improved slightly in comparison to the percentage extraction from the unroasted ore (refer to Table 5-1 and 5-4).

The reason for little improvement of nickel extraction could be due to formation of olivine $(Mg,FeNi)_2SiO_4$ during reduction roasting and inefficient roasting conditions (Li *et al.*, 2009). The ore should have been roasted at different conditions in order find the suitable conditions for the ore used in this study. The formation of forsterite in the roasted ore is evident from the XRD results given in Table (5-8). According to Valix and Cheung (2002), when saprolitic laterite is calcined and reduced at high temperatures, nickel is incorporated into magnesium silicate phase which recrystallizes into a forsterite phase making nickel inert to the leaching solution. For high silicate lateritic nickel ores, the extraction of nickel from the roasted ore has been reported to be poor (Valix and Cheung, 2002; Harris and peacey, 2009). Valix and Cheung (2002) reported values as low as 4%, 6%, and 8,7% when the ore was calcined at 500^{o}C, 600^{o}C, and 700^{o}C respectively. According to the literature survey by Harris and Peacey (2009), extraction of nickel from high silicate laterite can be improved by addition of elemental sulfur or pyrite during reduction roasting. Without addition of sulfur for saprolitic laterite, the extraction of nickel was only 28% in that study.

De Graff (1980) studied leaching behavior of reduced lateritic nickel of high silica content. From the study, he concluded that some part of the nickel within silicate lateritic ore after

roasting is inert to a solution of ammonia and ammonium carbonate. Nickel associated with recrystallized mineral phases such as olivine is best suited for pyrometallurgical processes.
For effective or improved nickel extraction, the optimum roasting conditions should be determined and finally optimum leaching conditions should be determined. According Li *et al*. (2009), roasting temperature plays an important role in determining mineral phases formed after roasting. A comprehensive study is required to find suitable roasting temperature for this particular ore because optimum roasting temperature differs depending on the origin of the ore. The optimum roasting conditions were not determined in this study because there was no roasting unit at Stellenbosch and therefore the ore had to be sent to Mintek. All of the ore that was available had to be sent at once because of distance and the availability of the roaster.

At the end of the of 3 hour leach period, the leach liquor below the filter medium was drained through V-9 and some of it was kept for analysis. The remaining mixture of solids and leaching solution above the filter medium was filtered under constant pressure of 5 bar. The amount of nickel extracted below and above the filter was combined. The results and calculation of amount nickel extracted are given in (Table C-1) in Appendix C. Table (5-10) shows results of filtration experiments. At the end of each filtration process, the sintered metal was back flushed with water and air to unblock the pores. From the filtration experiments, there is no indication of pore clogging since filtration rate is the same for all three experiments

The average filtration rate for the roasted was determined to be 2.60 ± 0.05 ml/min.cm^2. Filtration rate of the roasted ore improved in comparison to unroasted ore. However, clarity of the filtrate was poor. The clarity was poor due a lot particles passing through the filter medium. In order to improve clarity of the filtrate, particle size of the ore should be increased. Improvement in filtration rate after roasting suggests that roasting changes rheological properties and improves permeability of the ore. Li *et al*. (2010) suggested that during roasting removal of free and combined moisture and collapse of partial phase structure in laterite causes changes in mineralogical composition and increase the surface and porosity of the raw ore thus improving permeability of the ore. Figure (3-8 and 3-10) indicate that roasting reduces the viscosity of the ore. The results of particle size distribution of both unroasted and roasted ore presented in Figure (4-1 and 4-2) indicate that there is a slight

increase in particle size after the ore has been roasted. There is still fine particle in the ore which are less than 20µm and can still pass through the filter medium.

Table 5-10: Filtration experiments with roasted ore

Experiment no.	Volume (ml)	Time (min)	Filtration rate (ml/min.cm^2)
run1	1350	3.50	2.58
run2	1900	5.00	2.67
run3	1870	4.90	2.54
average			2.60
standard deviation			0.05
surface area of the filter medium	149.6cm^2		

5.5 **Kinetic study of unroasted saprolitic laterite**

In this section, the main objective is to study reaction kinetics for the leaching of unroasted saprolitic laterite. The main reasons for studying reaction kinetics is to prove some of the hypotheses made earlier in the introduction. These include, when leaching with ammonia and ammonium carbonate solution, operating at high temperatures improves reaction kinetics and the recovery of metals. For high temperature operation, a closed system vessel is required to prevent ammonia vaporizing into the atmosphere. In order to preserve ammonium ions the closed vessel should be pressurized to prevent decomposition of ammonium carbonate into water, carbon dioxide gas, and ammonia as shown in Equation (1-1).

In order to obtain the reaction regime controlling the leaching of nickel laterite ore within the vessel, reaction kinetics using the shrinking core model and activation energy studies were conducted. Because of intense agitation (320rpm) during leaching, external boundary layer diffusion was disregarded. It was assumed that, the particles have a spherical shape. If the low degree of nickel extraction is indeed affected by inert minerals in the ore, it is expected that diffusion through the ash layer would be the limiting factor. In this case, the ash layer would be would be inert minerals such as goethite, magnetite and quartz. However, for nickel dissolution kinetics two established shrinking core models were used in which the chemical

reaction and diffusion through the ash layer are used to determine the limiting factors. These models are explained in detail in Section4.4.4 of materials and methods.

5.5.1 **Effect of temperature**

The effect of temperature on the leaching of unroasted saprolitic laterite was investigated by changing the temperature while keeping other variables constant at optimum leaching conditions. The experiments were conducted at temperatures of 40, 60, 80, and 100^{o}C at pulp a density of 15%w/w solids, stirring speed of 320 rpm, 2M $(NH_4)_2CO_3$, 3M NH_3 and 4 bar oxygen pressure. The results are presented in Figure (5-12). Details of experimental conditions and calculations of the fraction extracted (x) are presented in Appendix C in Table (C-3).

The results indicate that in the first stages, the leaching rate was very rapid, and then reaction rate slows down. This behavior can be explained by leaching which is a two stage process. The rapid reaction rate in the first stage indicates leaching of free nickel and slow reaction rate after 15minutes indicates leaching of nickel associated with iron.

At low temperature, the degree of nickel extraction is relatively low. By comparing the slopes of the curves in Figure (5-12) in the first 15 minutes, it can be seen that reaction rate improves with an increase in temperature. When temperature increases both the degree of extraction and the reaction rate improves. According to Shimakage and Morioka (1971), at high temperatures, the solubility of oxygen in water increases. However, according to the ANOVA analysis in Table (5-2), the effect of oxygen is negative on the extraction of nickel. The increase in nickel extraction at high temperatures could due an increase in total pressure within the vessel. Refer to Table (C-1) in Appendix C for the values of total pressure for different experimental runs. High pressure within the vessel ensures that ammonium ions are always present with the vessel because decomposition of ammonium carbonate is prevented.

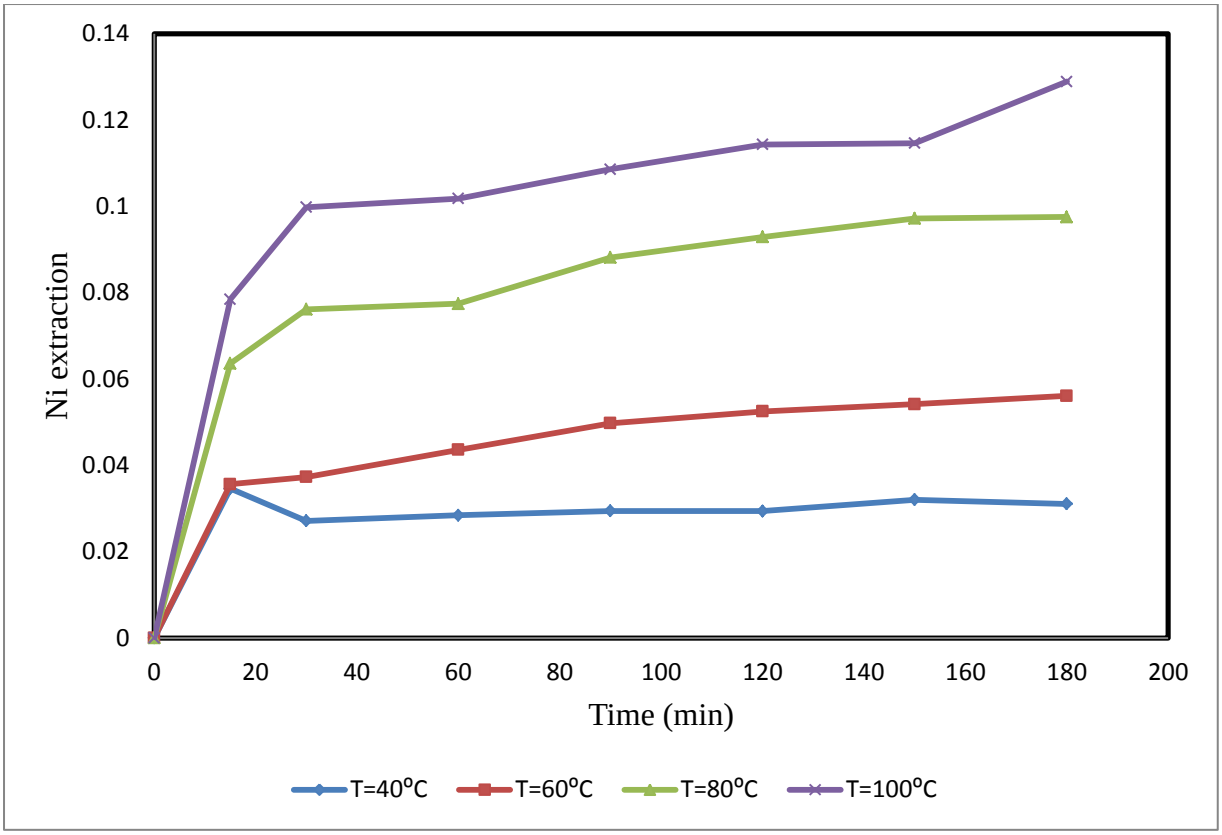

Figure 5-12: Effect of temperature on unroasted saprolitic laterite leaching

5.5.2 **Effect of ammonia concentration**

The effect of ammonia concentration on leaching unroasted saprolitic laterite was investigated by varying the ammonia concentration (0M, 1M, 2M and 3M), while keeping other variables constant at pre-determined optimum conditions (100°C, 2M $(NH_4)_2CO_3$ and 4 bar O_2 pressure). The results are presented in Figure (5-13) and the detailed experimental conditions are given in Appendix C in Table (C-4). The results indicate that in the absence of ammonia, nickel dissolves quickly for the first 15 minutes and then slows down for the entire leaching duration. However, there is some degree of nickel extraction in the absence of ammonia. The highest degree of nickel extraction is at 3M concentration of ammonia. Ammonia does not affect leaching rate but the degree of nickel extraction. This is evident from the slopes of the curves in the first of leaching for 1M, 2M, and 3M NH_3 for the first 15 minutes of the reaction.

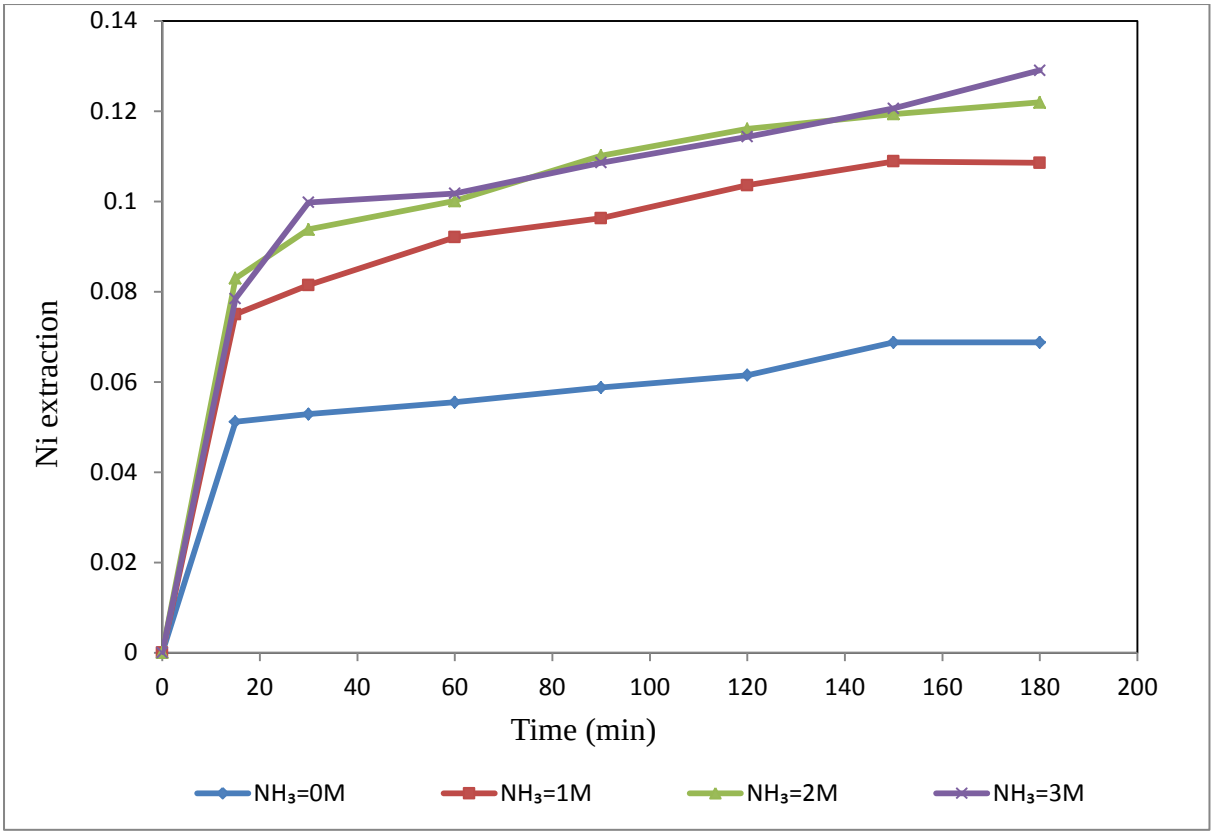

Figure 5-13: Effect of ammonia concentration on unroasted saprolitic laterite leaching

The results show that for high a degree of nickel extraction, ammonia concentration should be high. Similar results were obtained by Shimakage and Morioka (1971) for nickel powder in a solution containing NH_3 and $(NH_4)_2SO_4$. In the absence of ammonia, nickel dissolved in $(NH_4)_2SO_4$ forming a salt of $NiSO_4(NH_4)_2SO_4.6H_2O$ (Morioka and Shimakage, 1971). In this case the salt formed would probably be $NiCO_3(NH_4)_2CO_3.6H_2O$. Ammonia is essential for the formation of the metal ammonia complex. Furthermore, in the absence of ammonia the pH of the leaching solution drops to 8.7 (refer to experimental data in Appendix C) and at this pH, the nickel hexamine complex is not stable. For a high degree of metal extraction, NH_3 should be present in the leach solution to ensure that the pH of the solution is around the stable region for the nickel hexamine complex.

5.5.3 **Effect of ammonium carbonate concentration**

The effect of ammonium carbonate on leaching unroasted saprolitic laterite was investigated by varying ammonium carbonate concentration (0M, 1M, 2M, and 3M).The results are

presented in Figure (5-14) and detailed experimental conditions are presented in Table (C-5) in Appendix C.

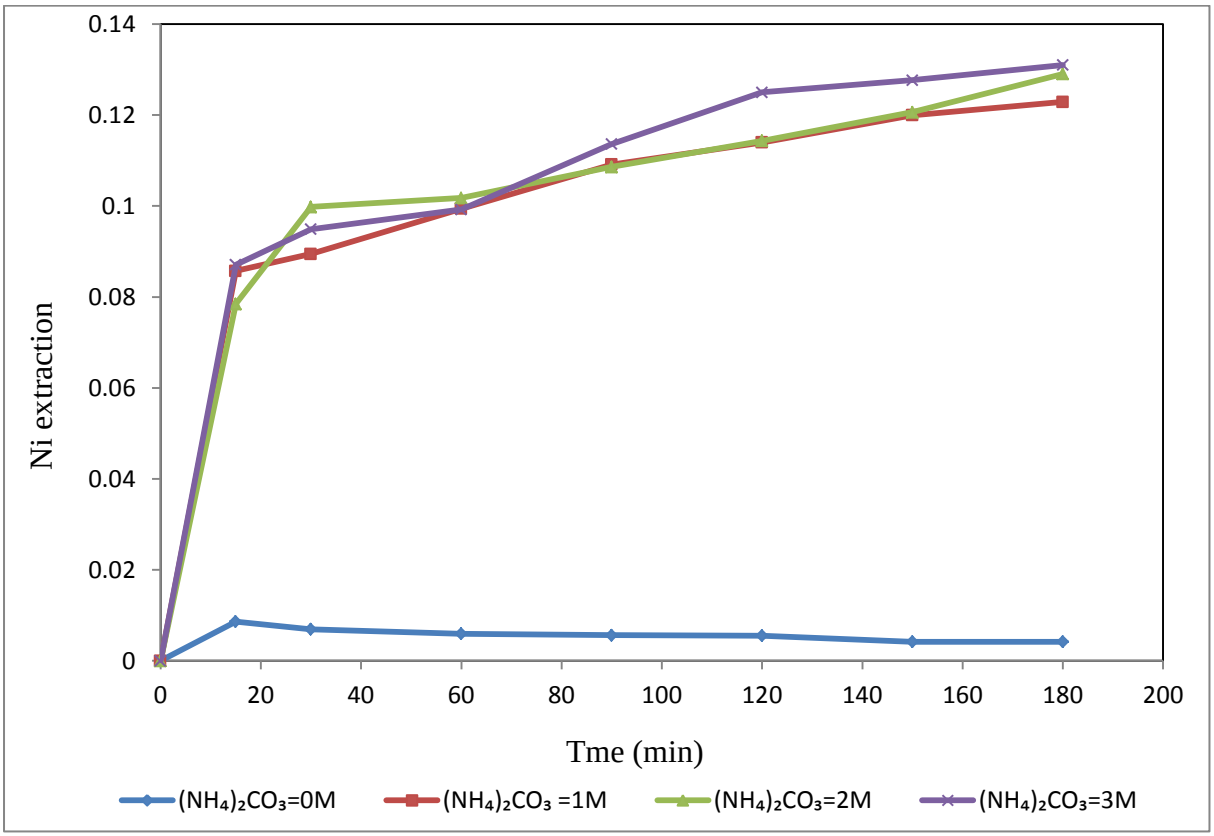

Figure 5-14: Effect of ammonium carbonate concentration on unroasted saprolitic laterite leaching

The results indicate that in the first stages, the leaching rate was very rapid, and then reaction rate slows down. At 2M and 3M concentration, the degree of nickel extraction is almost the same. The slopes of the curves at 1M, 2M, and 3M $(NH_4)_2CO_3$ are almost the same indicating that ammonium carbonate concentration does not affect the reaction rate but affects the degree of Ni extraction. In the absence of ammonium carbonate, the reaction rate is slow and the degree of Ni extraction is low. This is because OH^- ions produced by the dissolution of Ni in NH_3 solution cannot be removed by NH_4^+ ions (Morioka and Shimakage, 1971) (see reaction equation (2-12)). Hydrolysis of nickel ammonia complex occurs when OH^- ions concentration is high in the solution. The ammonia complex decomposes to form $NiCO_3.8Ni(OH)_2.8H_2O$. From Figure (5-14), it can be seen that nickel extraction decreases after 15 minutes. The main reason for this behavior could be due to the formation of

$NiCO_3.8Ni(OH)_2.8H_2O$ which is a yellowish precipitate (Morioka and Shimakage, 1971). This precipitate was noticed in the filtered leach liquor.

For a high degree of metal extraction, NH_4^+ ions should be present in the leaching solution. The NH_4^+ ions acts as a buffering agent in the leaching solution. From the experimental data given in Table (C-5) it can be seen that in the presence ammonium carbonate the pH of the solution does not drop or increase dramatically

5.5.4 **Effect of oxygen pressure**

The effect of oxygen was investigated by varying the O_2 pressure (0 bar, 2 bar, 4 bar and 5 bar) while keeping other variables constant. Experimental results are presented in Figure (5-15) and detailed experimental data is presented in Table (C-6) in Appendix C. The results indicate that oxygen pressure does not have a significant on the degree of nickel extraction. Most of the nickel in the unroasted ore exists as an oxide in the form of Ni^{2+}. For reduction-roasted ore, oxygen is required to convert Ni to Ni^{2+} for ammonia complex formation. In the case where the ore was not roasted, the need for oxygen is minimum. According to Morioka and Shimakage (1971), nickel is not extracted in the absence of oxygen but the results shown in Figure (5-15) show that at 0 bar nickel is extracted. This behaviour was expected due to the oxidized nature of the unroasted ore. However, when comparing the effect of oxygen in optimization reactions with the results shown in Figure (5-15), the effect of oxygen was significant and negative which is in total disagreement with results obtained from kinetic reactions. Replication of both experiments maybe necessary to confirm the discrepancy in the results.

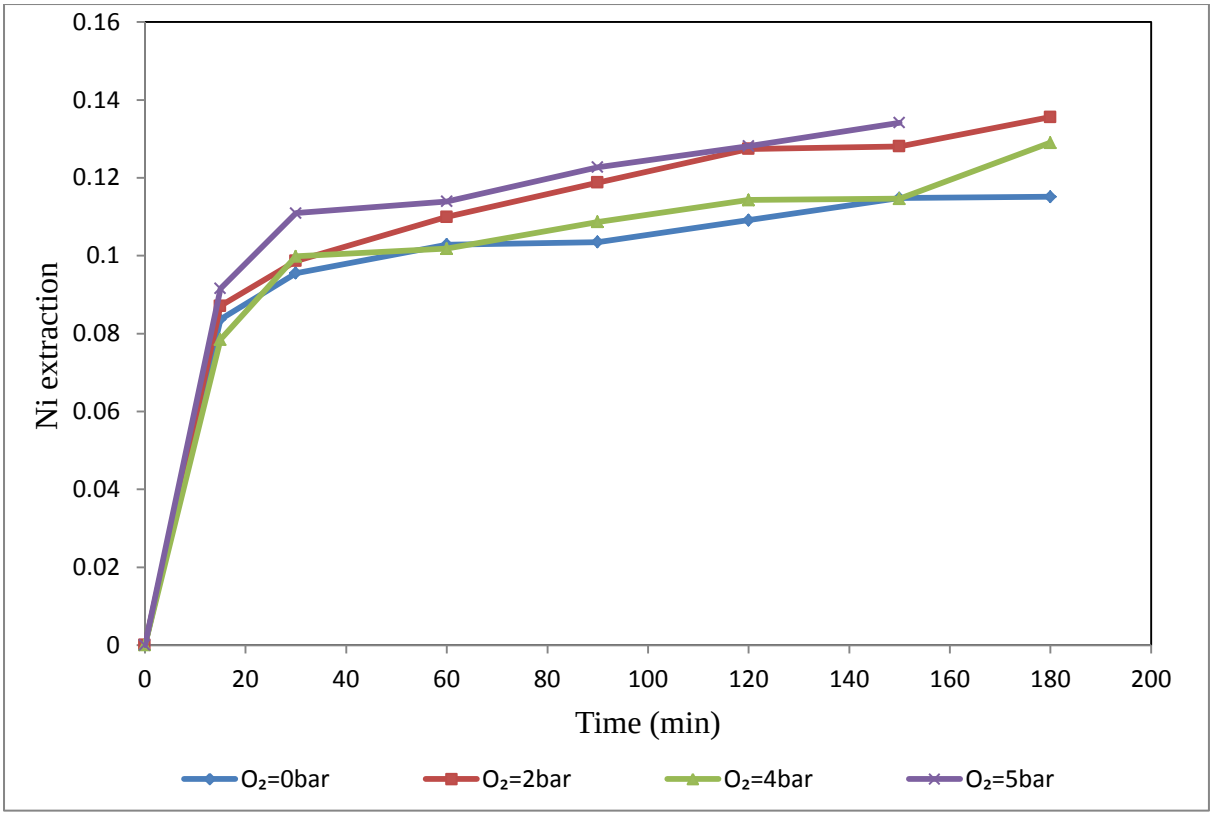

Figure 5-15: Effect of oxygen pressure on unroasted saprolitic laterite leaching

5.5.5 **Kinetic model for the unroasted ore**

The results discussed above were analyzed with different kinetic models to determine the leaching reaction mechanism of unroasted saprolitic laterite with ammonia and ammonium carbonate solution. An attempt was made to fit model equations with experimental data to give linear plots. The equations are also given is section 4.4.4 but are repeated here for clarity. The results and detailed experimental conditions are tabulated in Appendix C.

Surface reaction:

$1-(1-x)^{1/3}= k_s t$ Equation 4-9

Ash layer diffusion:

$1-3(1-x)^{2/3}+2(1-x)=k_d t$ Equation 4-11

Mixed model

$1-2(1-x)^{1/3}+(1-x)^{2/3}=kt$ Equation 5-1

Where k_s, k_d and k are apparent rate constants.

The mixed model has been applied by several authors ((Ekmekyapar *et al,* 2003; Bingol *et al,* 2005). Although not initially explained section 4.4.4, application of this model is briefly discussed in section 2.6.1 of literature review.

From the analysis of kinetics reaction data, about 60-80% of nickel is extracted within the first 15 minutes and the remainder over the next 3 hours. This indicates that leaching of nickel is a two stage process. The first stage indicates the possibility of reaction controlled mechanism because the reaction is rapid. In the first stage of leaching, the data was not fitted with shrinking core model because it is only two points from zero time to 15 minutes. Looking at Figures (5-16) to (5-18), the data was fitted with shrinking core model from 15 minutes to 180 minutes. This was done so that correlation coefficients for the second stage of leaching can be determined from regression analysis. The first stage could be indicating the leaching of free nickel within the ore. The second stage indicates ash layer diffusion because the reaction rate slows down. This could be indicating the leaching nickel which bound within the matrix of iron, silica and magnesium.

The results obtained kinetic reactions for second stage of leaching were analyzed using the shrinking core model; surface reaction control, ash layer diffusion control, and a combined model of the two. The results for the effect of temperature are presented graphically in Figure (5-16) to (5-18). Figure (5-16) indicate surface reaction control at different temperatures. Figure (5-17), indicate the ash layer diffusion control at different temperatures. Figure (5-18) indicate mixed model control at different temperatures. The rest of the results are summarized in Table (5-11). The table shows correlation coefficients for different models for the effect of temperature, ammonia concentration, ammonium carbonate concentration, and oxygen partial pressure. The graphical representation of the results for the effect of $[NH_3]$, $[(NH_4)_2CO_3]$ and O_2 are presented in the Appendix. The calculation for the data is presented in the Tables in Appendix C.

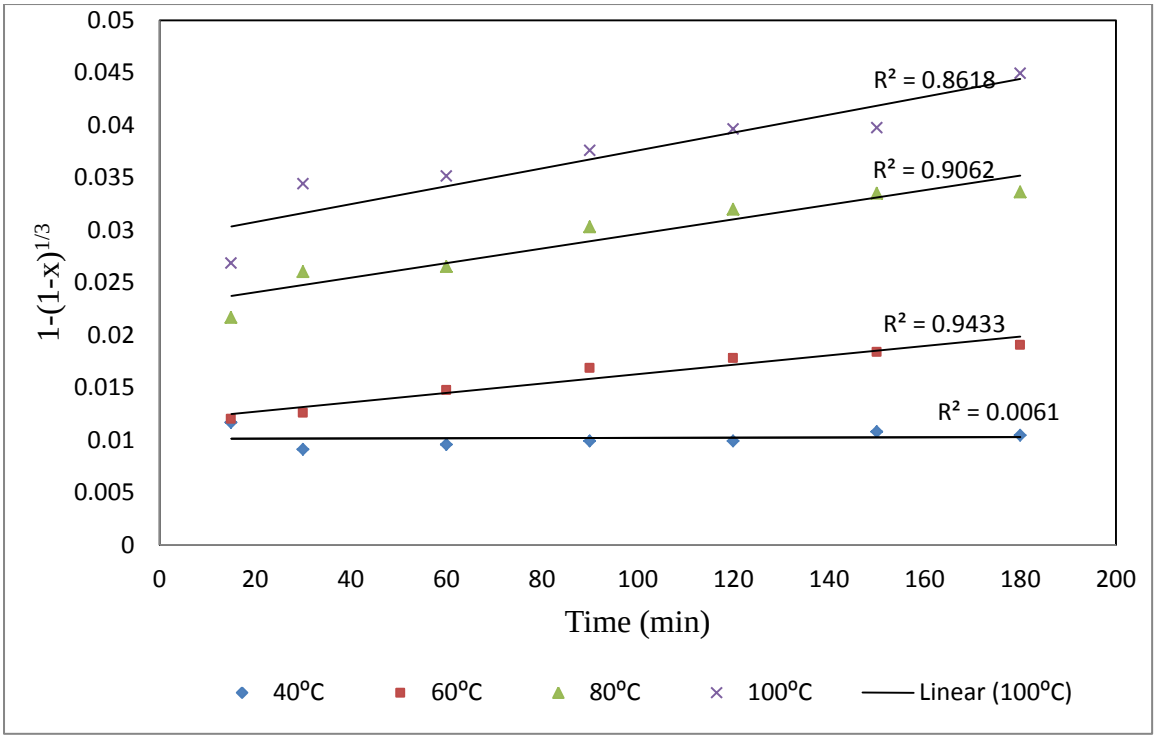

Figure 5-16: Plot of $1-(1-x)^{1/3}$ vs time for leaching nickel from unroasted saprolitic laterite at different temperatures

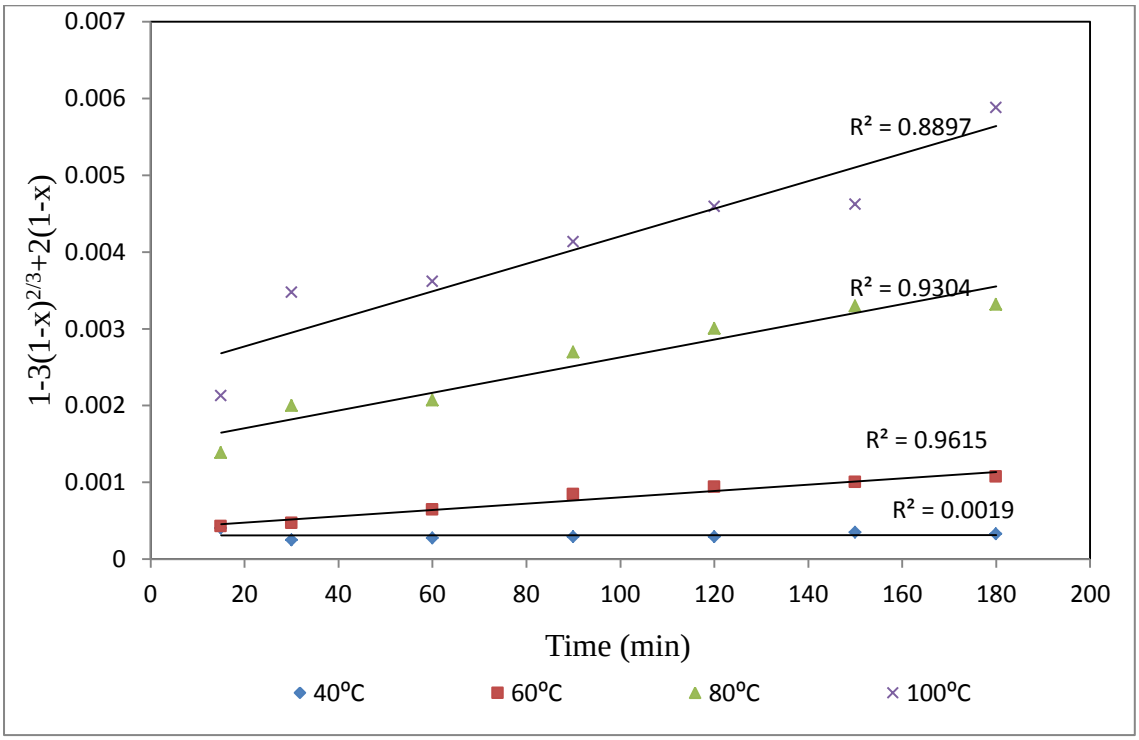

Figure 5-17: Plot of $1-3(1-x)^{2/3} + 2(1-x)$ vs time for leaching nickel from unroasted saprolitic laterite at different temperatures

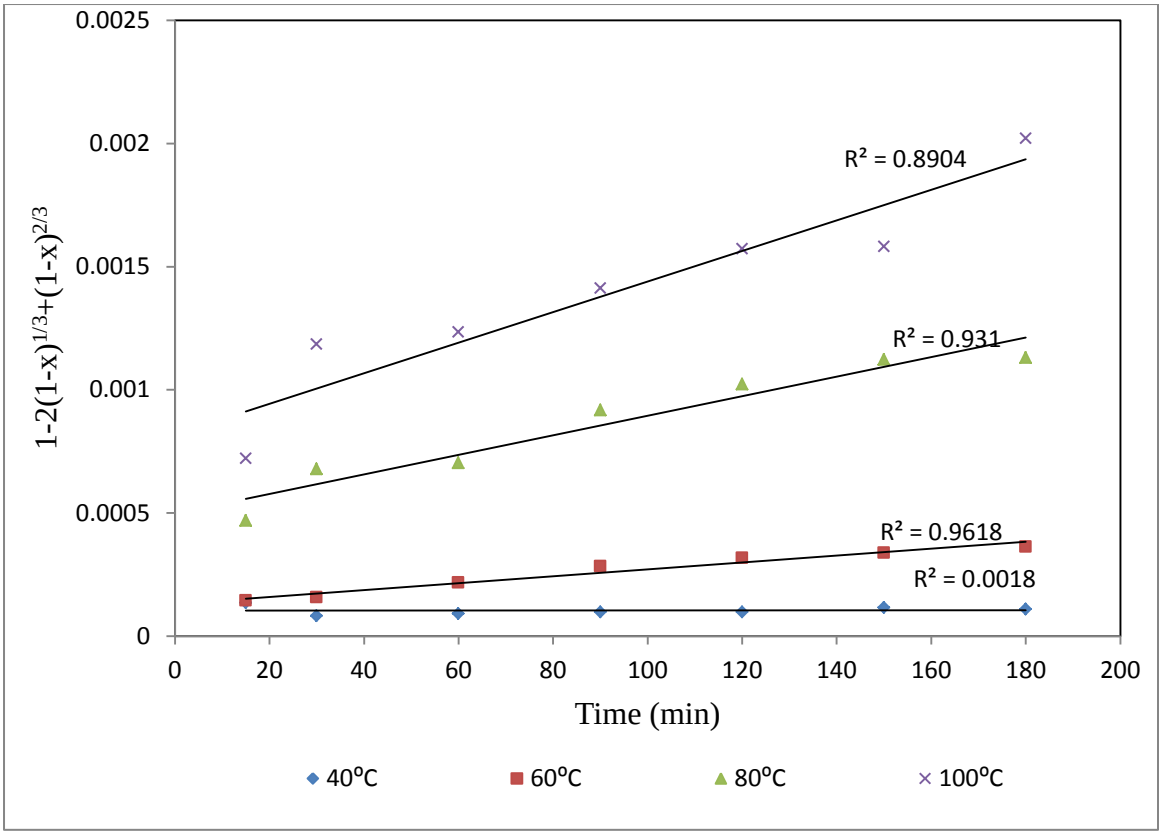

Figure 5-18: Plot of $1-2(1-x)^{1/3}+(1-x)^{2/3}$ vs time for leaching nickel from unroasted saprolitic laterite at different temperatures

Table 5-11: Correlation coefficients for different models various leaching conditions

		Model R^2 values		
		Surface reaction Control	Ash diffusion layer control	Mixed model
Temperature(^oC)	40	0.006	0.001	0.006
	60	0.94	0.96	0.96
	80	0.91	0.93	0.93
	100	0.86	0.89	0.89
$[NH_3]$ (M)	0	0.97	0.96	0.96
	1	0.94	0.95	0.95
	2	0.93	0.95	0.95
	3	0.90	0.93	0.93
$[(NH_4)_2CO_3]$ (M)	0	0.87	0.80	0.80
	1	0.97	0.98	0.98
	2	0.90	0.93	0.93
	3	0.95	0.97	0.97
O_2 pressure (Bar)	0	0.88	0.91	0.91
	2	0.86	0.90	0.90
	4	0.94	0.94	0.96
	5	0.90	0.90	0.93

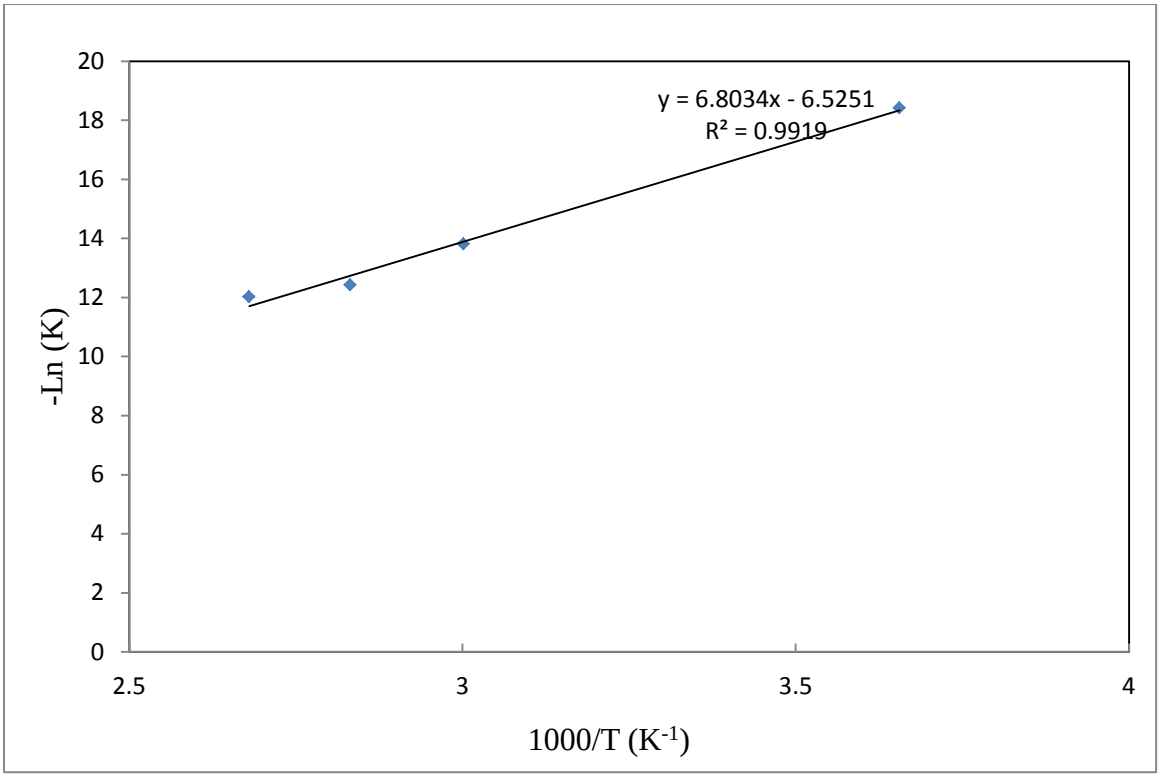

Figure 5-19: Arrhenius plot for nickel leaching from unroasted saprolitic laterite

From the analyzed data, the mixed model gave the best fit. This is evident from the relatively high correlation coefficient values for the mixed model. However, the correlation coefficient for ash layer diffusion is larger than for the surface reaction control. From the slopes of $1-2(1-x)^{1/3}+(1-x)^{2/3}$ vs t plots (Figure 5-18), the K values were obtained and the Arrhenius plot was constructed as shown in Figure (5-19). The slope of the Arrhenius plot gives Ea/R value. From the Ea/R value, the activation energy (Ea) was calculated as 56.6kJ/mol. The high activation energy indicates that the reaction is also reaction controlled. Detailed experimental data and calculations are given in Table (C-11) in Appendix C.

From the slopes of the straight lines in Figure (C-11) apparent rate constant (K) values were determined, -log(K) vs Log[NH_3] plot of Figure (5-20) was constructed to determine the order of dependency with respect to ammonia concentration. The empirical reaction order with respect to ammonia concentration was determined to be 0.31. Similarly, the shrinking core model mixed control fitted data relatively well at various ammonium carbonate concentrations. From the slopes of straight lines in Figure (C-14), experimental K values were determined and a plot of -logK vs log[$(NH_4)_2CO_3$] were constructed as shown in Figure (5-21). The reaction order with respect to ammonium carbonate concentration was

determined to be 0.26. This indicates that high dependency of the reaction on ammonia than ammonium carbonate as indicated in the optimization reaction.

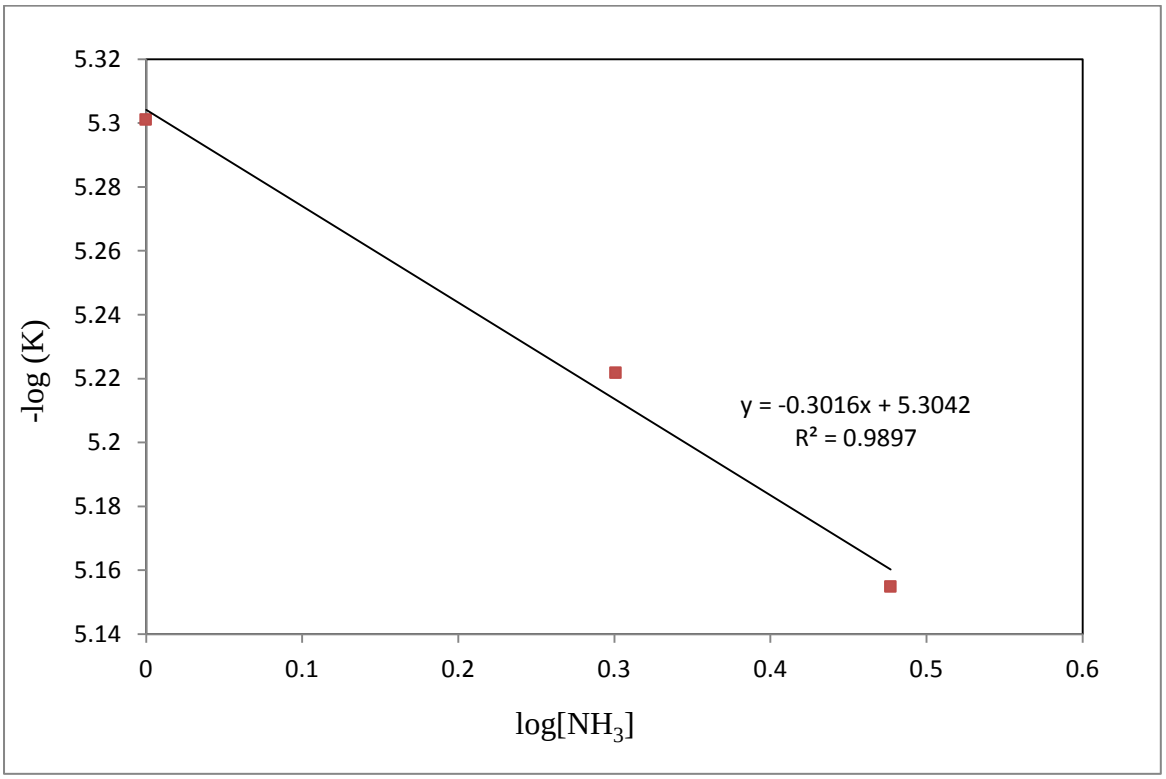

Figure 5-20: Plot -log K vs log [NH_3] for reaction order estimation

The analysis of the results from the kinetics leaching test of unroasted ore demonstrate that for high metal extraction and improved reaction kinetics using a ammonium carbonate solution, the temperature should be high. It is important to have ammonium ions in the leach solution even when the mixture of ammonia and ammonium carbonate is used. Lastly, the results indicate that in leaching unroasted saprolitic laterite ash layer diffusion is better in describing the reaction mechanism than the surface reaction control. However, a mixed model was found to be the most suitable model for describing the leaching mechanism due the high activation energy which also indicate surface reaction control. It is clear that the ash layer diffusion plays a major role in limiting the reaction in the second stage of leaching. The ash layer in this case is inert minerals in the unroasted saprolitic laterite. The low degree of nickel extraction is not due to limitations of the vessel but due to the inertness of the minerals hosting nickel within the ore.

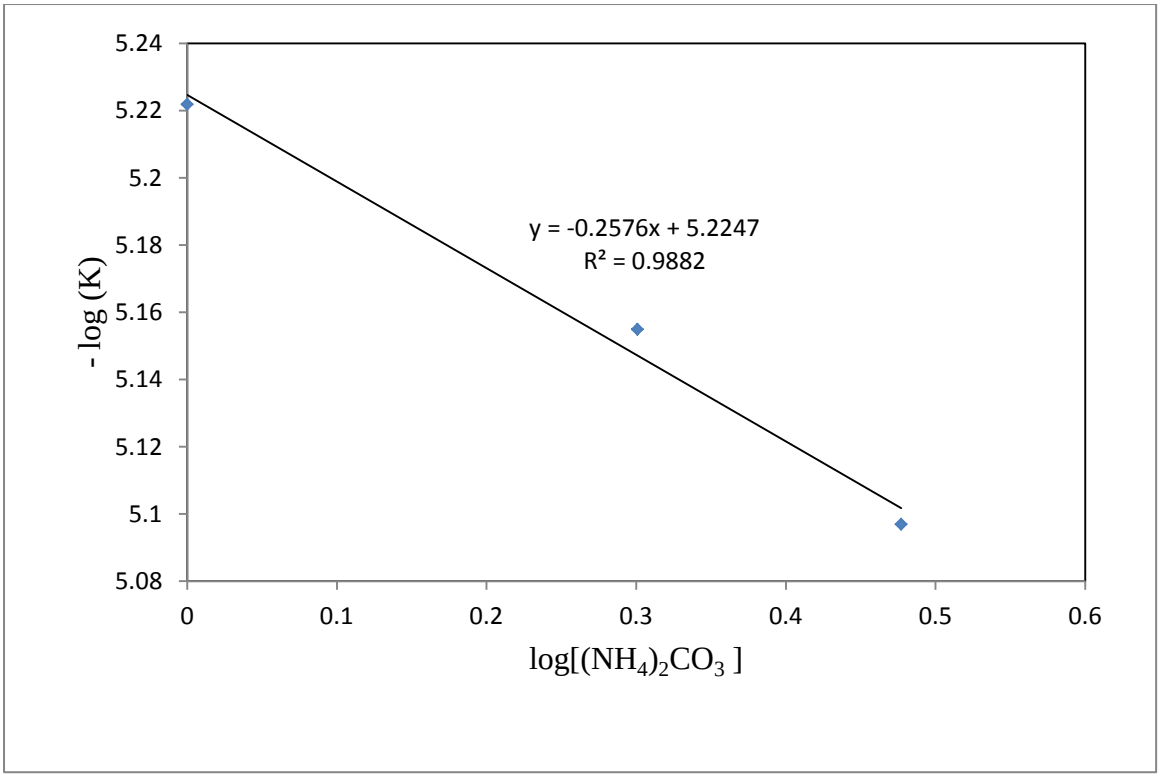

Figure 5-21: Plot of -log K vs log[$(NH_4)_2CO_3$] for reaction order estimation

5.6 **Kinetic study of roasted saprolitic laterite**

The kinetics of leaching saprolitic laterite was repeated with roasted ore because of the low extraction of nickel obtained for the unroasted ore. The same procedure used for analyzing the results of the unroasted ore was used with the roasted ore. For the roasted ore, iron is also leached under certain leaching conditions. The effect of temperature, [NH_3], [$(NH_4)_2CO_3$] and O_2 pressure with respect to time on the extraction nickel and iron is discussed in this section. The data obtained from leaching experiments at varying conditions was fitted with the shrinking core model to obtain a regime controlling the leaching of the roasted ore.

5.6.1 **Effect of temperature on roasted saprolitic laterite**

The effect of temperature on the leaching of roasted saprolitic laterite was investigated by changing the temperature while keeping the other variables constant at optimum leaching conditions. The experiments were conducted at temperatures of 40, 60, 80, and 100^oC at a

pulp density of 15%w/w solids, stirring speed of 320 rpm, 2M $(NH_4)_2CO_3$, 3M NH_3 and 5 bar oxygen pressure. The results are presented in Figure (5-31). Details of the experimental conditions and calculations of the fraction extracted (x) are presented in appendix C in Table (C-14).

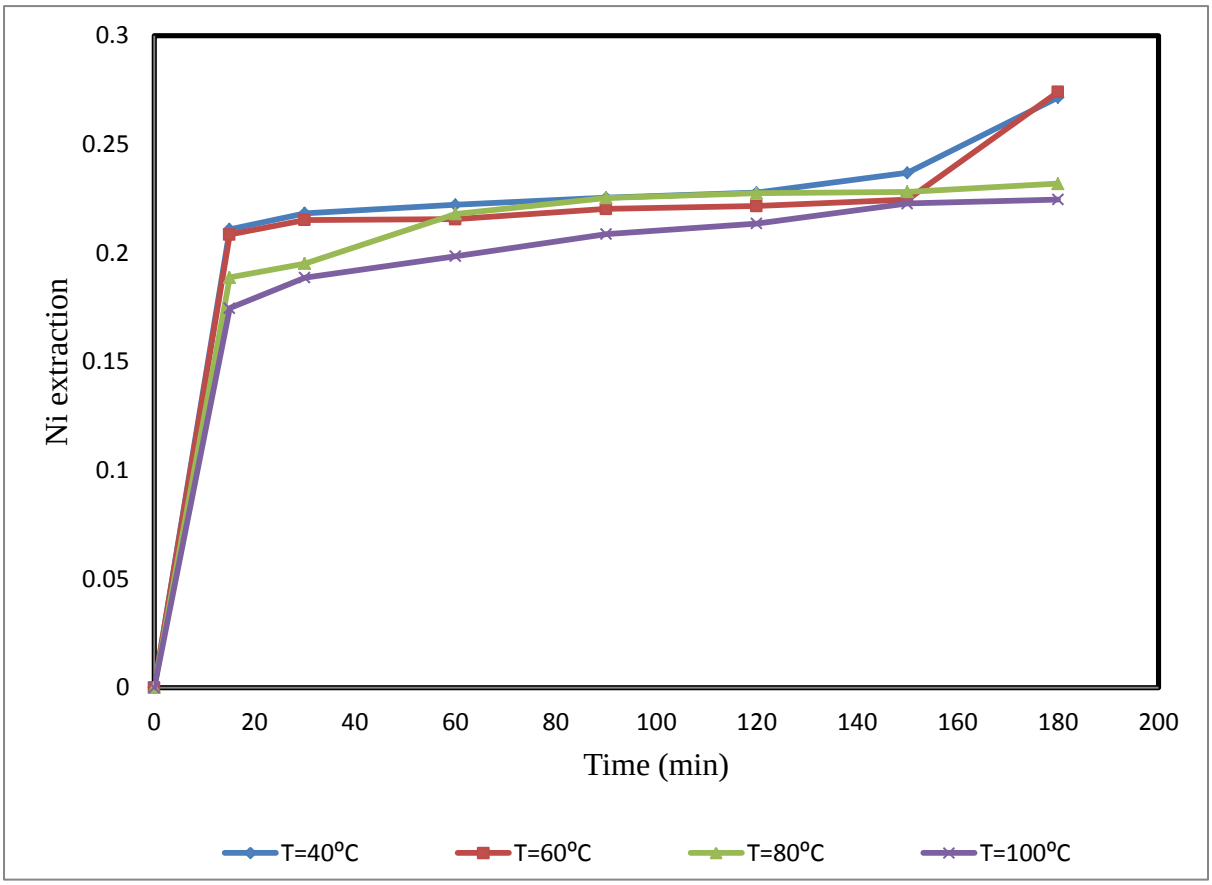

Figure 5-22: Effect of temperature on roasted saprolitic laterite leaching

In the roasted ore, the maximum extraction of nickel is obtained at 60°C. The percentage extraction of nickel at 60°C after a leaching duration of 3 hours is 28.7%. In the case of the unroasted ore, the maximum extraction of nickel occurs at 100°C. At 60°C both the degree of nickel extraction and leaching rate are relatively low for the unroasted ore, refer to Figure (5-12). The effect of temperature does not significantly affect leaching kinetics in the case of roasted ore. The slopes of nickel extraction with time at different concentrations are almost the same. Zuniga *et al*. (2010) studied the effect of temperature in the range of 50, 60, 70, and 80°C at atmospheric pressure and obtained different results. They found that the degree of nickel extraction and leaching kinetics improved with an increase in temperature. However, their experiments were carried out at atmospheric pressure. However, this does not apply in

the current study since the vessel was pressurized. Dutrizac and Monhemius (1986) postulated that if nickel was adsorbed when hydrated iron oxides begin to dehydrate, then nickel extraction would be poor. At high temperatures, dehydration kinetics are faster. The results found in this study show that there is more iron at low temperatures than at high temperatures. At 100 and 80^{o}C, it is found that in the first 15 minutes of leaching only small amount of iron is dissolved and at 40 and 60^{o}C iron is dissolved up to 30 minutes of leaching. The concentration of iron is highest at 40^{o}C, (see Figures (C-18 to C-21)) in Appendix C. All iron analyzed was in the form of a precipitate. The precipitate was dissolved in hydrochloric acid and analyzed for Fe using AAS.

5.6.2 **Effect of ammonia concentration on roasted saprolitic laterite**

The effect of ammonia concentration on leaching roasted saprolitic laterite was investigated by varying the ammonia concentration (0 M, 1 M, 2 M and 3 M), while keeping other variables constant at the pre-determined optimum conditions (100^{o}C, 2M $(NH_4)_2CO_3$ and 5 bar O_2 pressure). The results are presented in Figure (5-32) and the detailed experimental conditions are given in Appendix C in Table (C-15)

The trends in the effect of ammonia concentration on roasted ore are similar to ones of the unroasted ore. The only difference is in the degree of nickel extraction which is slightly higher for the roasted ore. The degree of nickel extraction in both is relatively low at 0 M [NH_3]. However just like with an unroasted ore, there is still a degree of nickel extraction in the absence of ammonia solution. Results on the comparison of nickel and iron extraction with ammonia concentration are presented in the Appendix in Figure (C-22 to C-25). Figure (C-22) shows that at 0M [NH_3] no Fe is found in the leach liquor. As ammonia concentration increases, Fe dissolution increases together with nickel. According Dutrizac and Monhemius (1986), when the ammonia concentration is at high levels, ferrous ions in solution increases. During leaching iron goes into solution as ferrous ammine complex. The ferrous ammine complex is then oxidized and the iron precipitate as hydrated iron oxide. The precipitate formed can adsorp nickel and reduce final recovery (refer to Equation (2-19) for the reaction which shows nickel adsorption to iron precipitate). This phenomenon was seen in the samples, which were analyzed. The samples contained a high amount of iron hydroxide

precipitate after filtration at high concentration of ammonia. This is also supported by Zuniga *et al*. (2010).

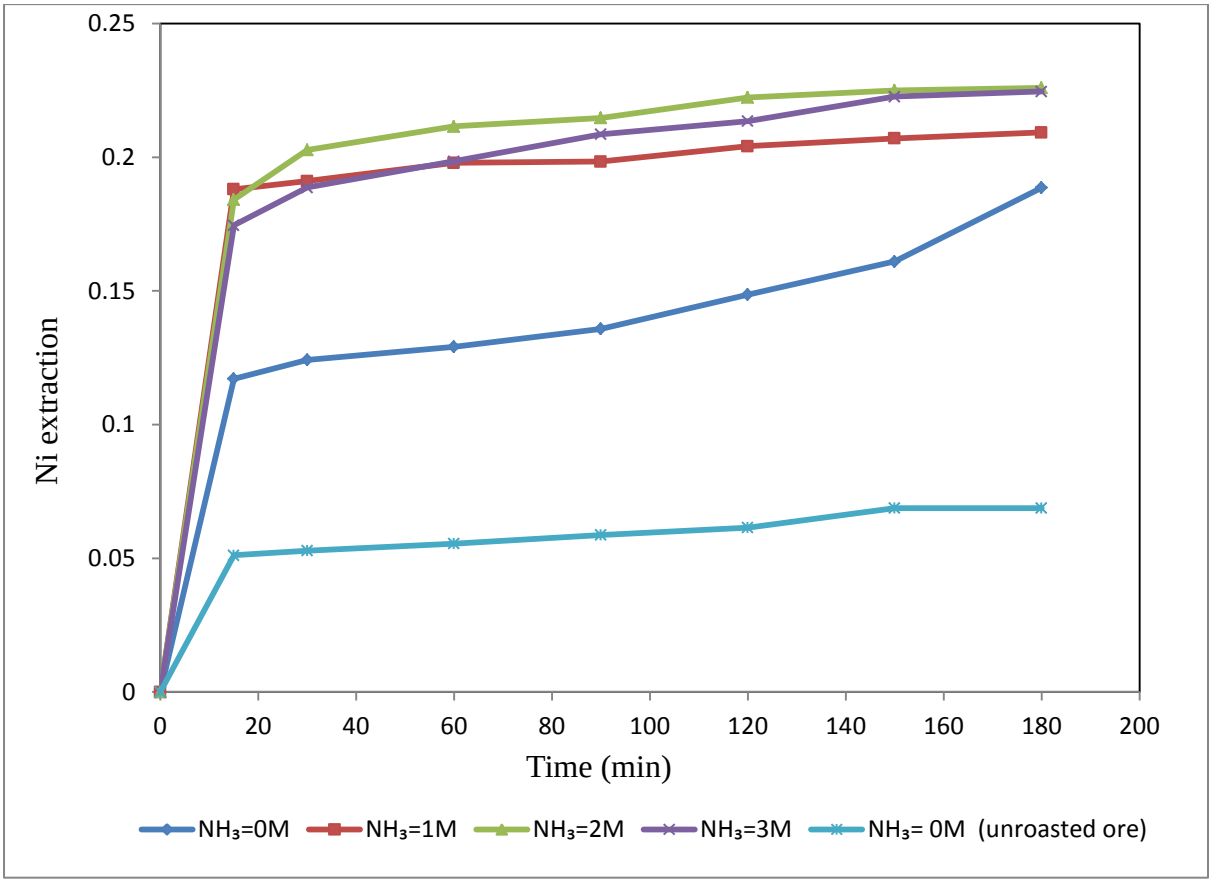

Figure 5-23: Effect of ammonia concentration on roasted saprolitic laterite

5.6.3 **Effect of ammonium carbonate on roasted saprolitic laterite leaching**

The effect of ammonium carbonate on leaching roasted saprolitic laterite was investigated by varying the ammonium carbonate concentration (0M, 1M, 2M, and 3M). The results are presented in Figure (5-23) and the detailed experimental conditions are presented in Table (C-16) in Appendix C.

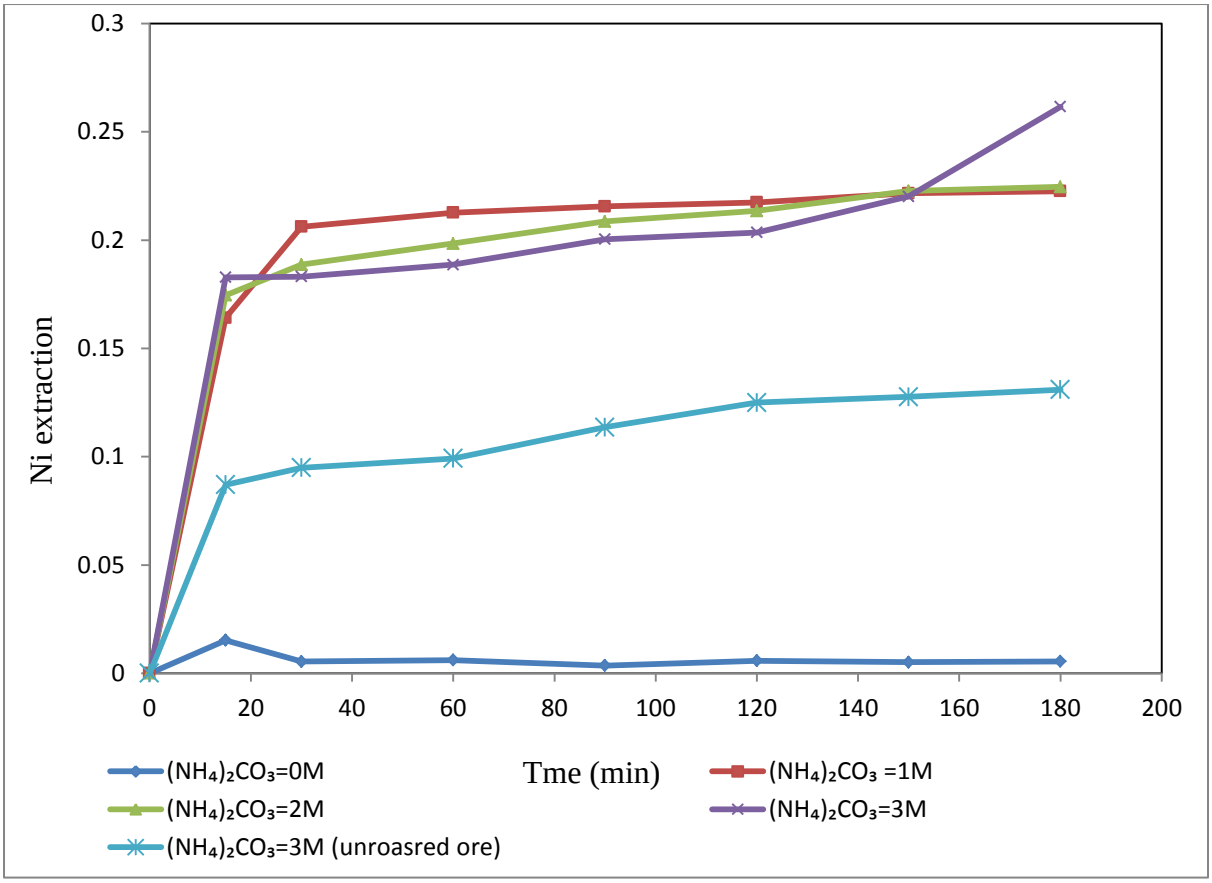

Figure 5-24: Effect of ammonium carbonate concentration on roasted saprolitic leaching

The effect of ammonium carbonate concentration on nickel extraction on the roasted ore shows similar trends with the unroasted ore. There is a slight improvement in nickel extraction for the roasted ore in comparison to the unroasted ore at 3M [$(NH_4)_2CO_3$]. At 0 M [$(NH_4)_2CO_3$] nickel extraction is very low. Ammonium carbonate has a significant effect on the pH of the leaching solution (see Table (C-16)) in the Appendix. At 0 M [$(NH_4)_2CO_3$] the pH of the leaching solution is around 11.5. As the concentration of ammonium carbonate increases, the pH of the leaching solution drops. Nickel extraction increases with increasing concentration of ammonium carbonate. Dutrizac and Monhemius (1986) infer that higher concentrations of ammonium ions in the solution result in less coprecipitation of Ni^{2+} with ferric hydroxide and this improves the recovery of nickel. Yun-chun *et al*. (2010) found that recovery of nickel improves significantly with the increase of ammonium carbonate. However, as recovery of nickel increased there was a slight increase in precipitation of iron hydroxide as can be seen in Figures (C-26 to C-29) in the Appendix C. The highest percentage extraction of nickel of 26.2% was obtained at 3M [$(NH_4)_2CO_3$] after leaching for 3 hours.

5.6.4 **Effect of oxygen pressure on roasted saprolitic laterite leaching**

The effect of oxygen on roasted saprolitic laterite was investigated by varying the O_2 pressure (0, 2, 4 and 5 bar) while keeping other variables constant. Experimental results are presented in Figure (5-34) and detailed experimental data is presented in Table (C-17) in Appendix C.

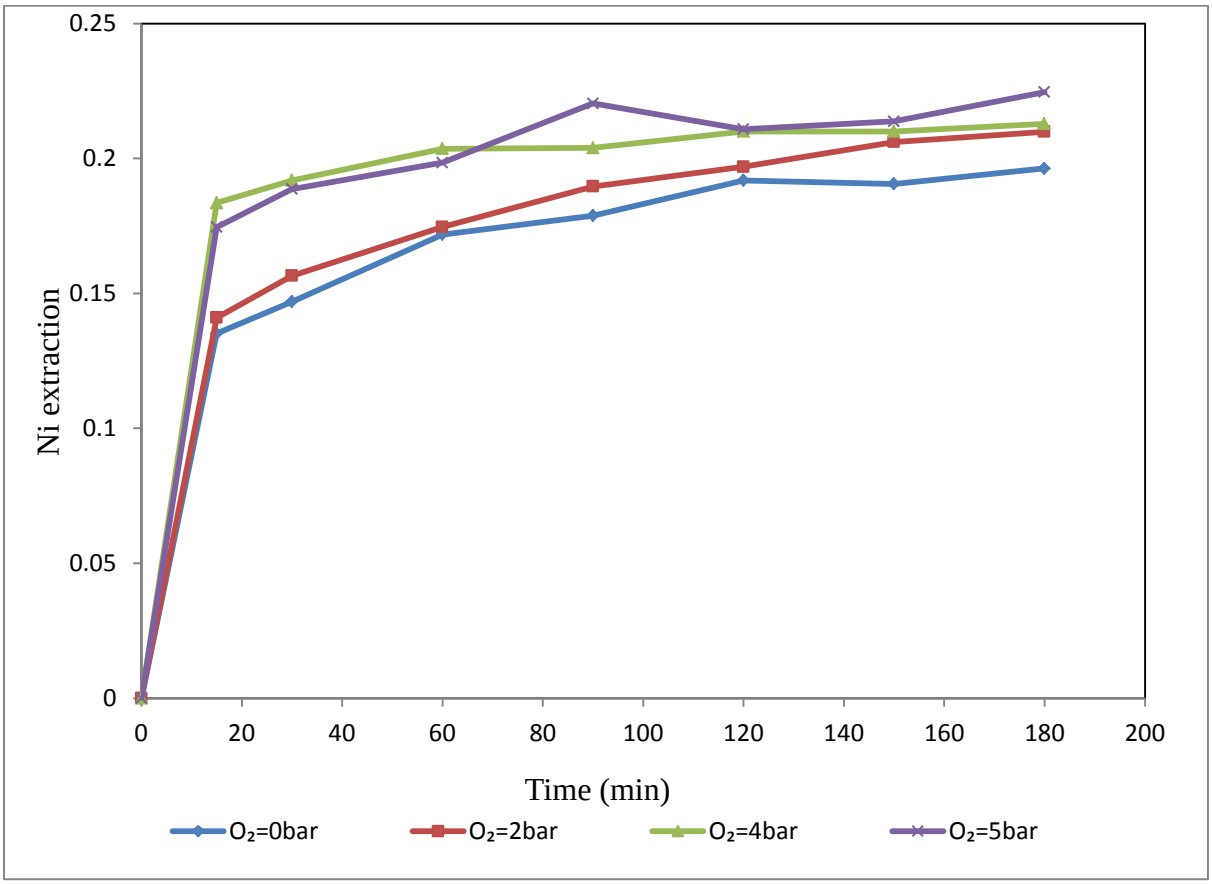

Figure 5-25: Effect of oxygen pressure on saprolitic laterite leaching

The rate of nickel extraction in the first 15 minutes of leaching is almost the same at varying oxygen pressure. However, the final extraction of nickel is high at an oxygen pressure of 5bar. The results differ from the ones obtained in optimization reactions. However, the trends of the results shown in Figure (5-15) are similar to the one shown in Figure (5-25). There is high nickel extraction at 0 bar. Here it would be expected that nickel was reduced to metallic state during reductive roasting and in order to dissolve, it should be first oxidized Ni^{2+}. The function of oxygen is to oxidize nickel to ionic form before it can form an ammonia complex (Gupta, 2003). It is not clear why in this case nickel extraction is high in the absence of

oxygen. In the case of an unroasted ore, the results can be explained by the fact that free nickel dissolved was already an oxide. The possible reason could be that there was air in the vessel which might have oxidized nickel but the vessel was purged nitrogen before leaching to remove air. Furthermore, the effect oxygen in the roasted ore is clearly visible in terms iron dissolution. The effect of oxygen pressure on iron is discussed in the next paragraph. The effect of oxygen pressure on nickel extraction needs to be studied thoroughly in order to understand why nickel dissolves in the absence of oxygen. Since the results are the almost for kinetic reactions of unroasted and roasted ore, the only experiments which might need to be replicated are optimization reactions.

The formation of iron hydroxide in the samples obtained after leaching was seen throughout the entire leaching duration when oxygen was not admitted into the vessel (see Figure (C-30) in Appendix C). When oxygen pressure was kept present in other samples, the precipitate disappeared after either 15 or 30 minutes depending on other leaching conditions. According to Dutrizac and Monhemius (1986), low oxidation rate favors formation of precipitate at high concentration of ferrous and increased adsorption of metals onto the precipitate. The use of high oxygen pressure increases nickel dissolution when other variables are kept at optimum conditions. The highest percentage extraction of nickel was 22.5% at 5 bar oxygen pressure.

Nickel extraction from the above experiments is still low despite the fact that the ore was roasted before leaching. There is a slight improvement in nickel extraction in comparison to the extraction from the unroasted ore. The main reason for low extraction of nickel is due to the formation of forsterite during reductive roasting of the ore. Forsterite has been shown to make nickel inert to the leaching solution (Valix and Cheung, 2002; (Harris and Peacey, 2009).

Nickel extraction is highest at mild temperatures. The increase in concentration of ammonia improves the extraction but a high concentration, the formation of iron hydroxide precipitate also occurs. Ammonium carbonate is essential for the dissolution of nickel. In the absence of ammonium carbonate nickel extraction is very low. Nickel extraction improves with an increase in ammonium carbonate concentration. Oxygen is essential in leaching roasted saprolitic laterite. The presence of oxygen in the leach solution minimizes steady state ferrous concentration and this minimizes chances of adsorption and improves recovery of nickel. Nickel extraction is highest at 60^{o}C, 2M $(NH_4)_2CO_3$, 3M NH_3 and 5 bar O_2 pressure. The degree of nickel extraction did not increase substantially after roasting. It was observed that

the ore used contained significant amounts of silica. Some nickel is associated with recrystallized silicate minerals and perhaps the type of ore used in this study is more suitable for pyrometalluygical processing than hydrometallurgical.

5.6.5 **Kinetic models for the roasted ore**

The experimental leaching data for the roasted ore was analyzed in the same manner as that of the unroasted ore, for determining the reaction mechanism. The procedure for analyzing experimental data for unroasted ore is given in Section 5.5.5. The percentage extraction of nickel for the roasted ore as function of time at different ammonia concentrations, temperatures, ammonium carbonate concentrations, and oxygen pressures were first determined. The results for the percentage of extraction of nickel are presented in Tables (C-18 to C-21) in Appendix C. Looking at Figures (5-22) to (5-25) the reactions are rapid in the first 15 minutes of leaching and slow throughout the remaining time. This indicates that leaching of roasted ore with ammonia and ammonium carbonate solution is a two stage leaching process. The data for second stage of leaching was then fitted to the shrinking core models; surface reaction, ash layer diffusion control and the mixed model.

An attempt to fit the experimental data for second stage of leaching with either of these models failed to give linear plots under present experimental conditions. This is evident from the low values obtained for the correlation coefficients. Furthermore, no single model fitted the data well for different experimental conditions. For the effect of temperature from these models, the surface reaction control model fitted the data well at 60 ^{o}C and 40 ^{o}C and the mixed model fitted the data well at 100 ^{o}C and 80 ^{o}C. For the effect of ammonia concentration, the mixed model fits the data well at 1 M and 2 M and the ash layer diffusion model at 3 M. For the effect of ammonium carbonate concentration, the surface reaction model fit the data well for 0 M and 1 M and the mixed model at 2 M and 3 M. For the effect of oxygen pressure, the mixed model fit the data well. Only the results for effect of temperature on the models explained above are presented in this section. The rest are presented in Figures (C-25 to C-33) in Appendix C.

The reason for the models not fitting experimental data well could be due to sampling time interval which was too far apart. In the first 30 minutes, the sample was obtained after 15 minutes. After the leaching duration of 30 minutes, the sample was obtained after 30 minutes.

The recommendation here could be that these experiments should be repeated with shorter sampling periods (for examples in the first 15 min when reaction rate is much faster, sample should be obtained after every 5 minutes). These experiments could not be repeated due to small amount of ore which was left after performing all experiments.

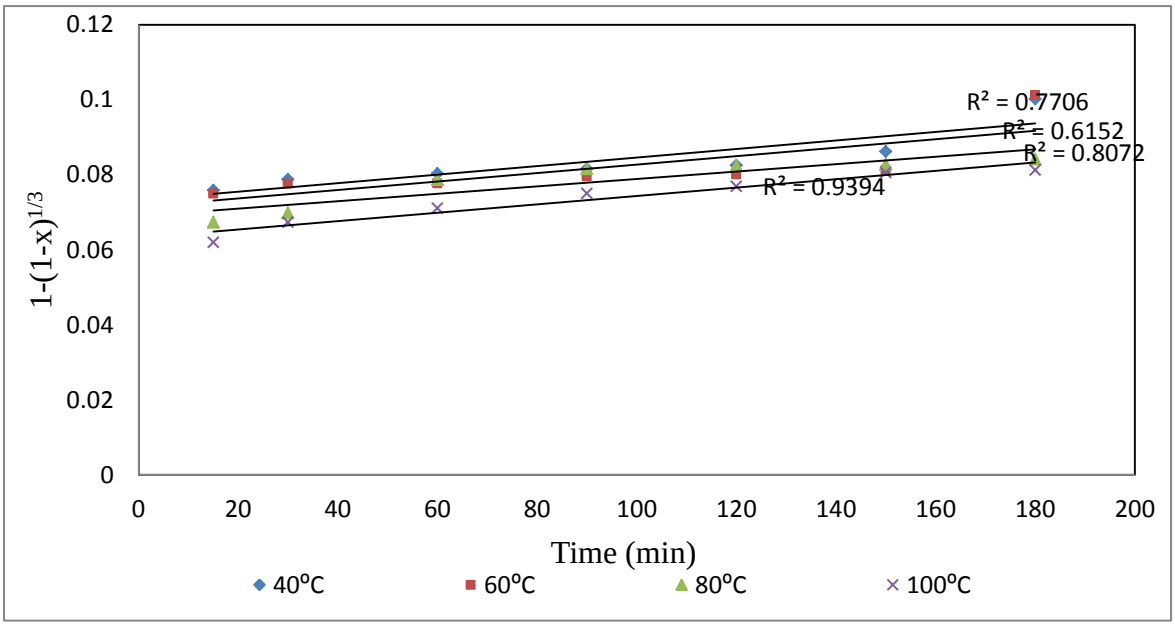

Figure 5-26: Plot of $1-(1-x)^{1/3}$ vs time for leaching nickel from roasted saprolitic laterite at different temperatures

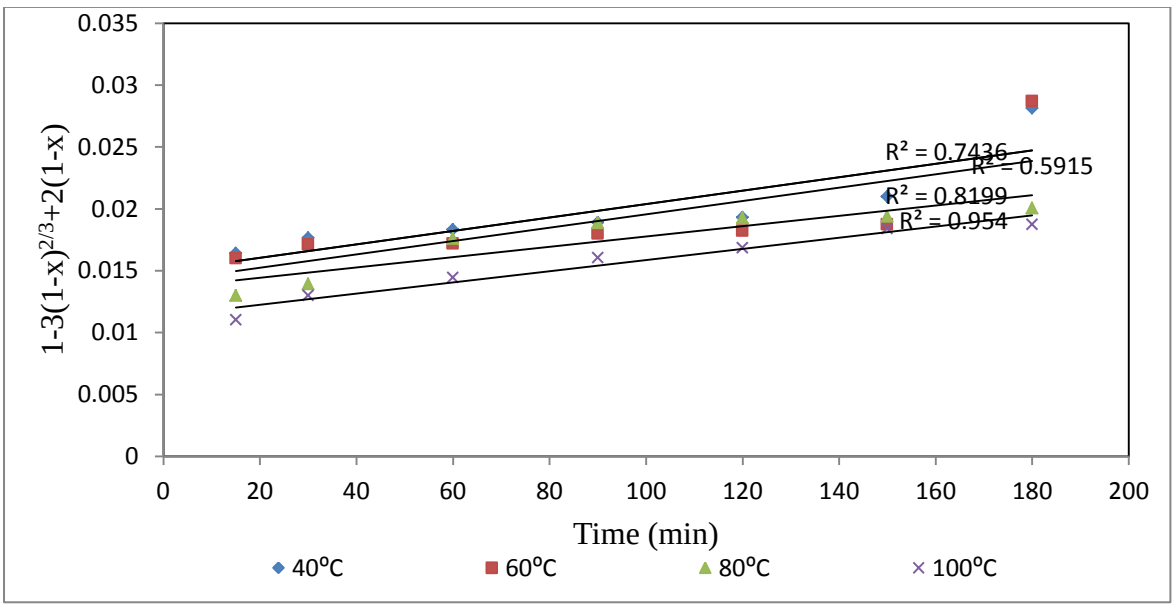

Figure 5-27: Plot of $1-3(1-x)^{2/3}+2(1-x)$ vs time for leaching nickel from roasted saprolitic laterite at different temperatures

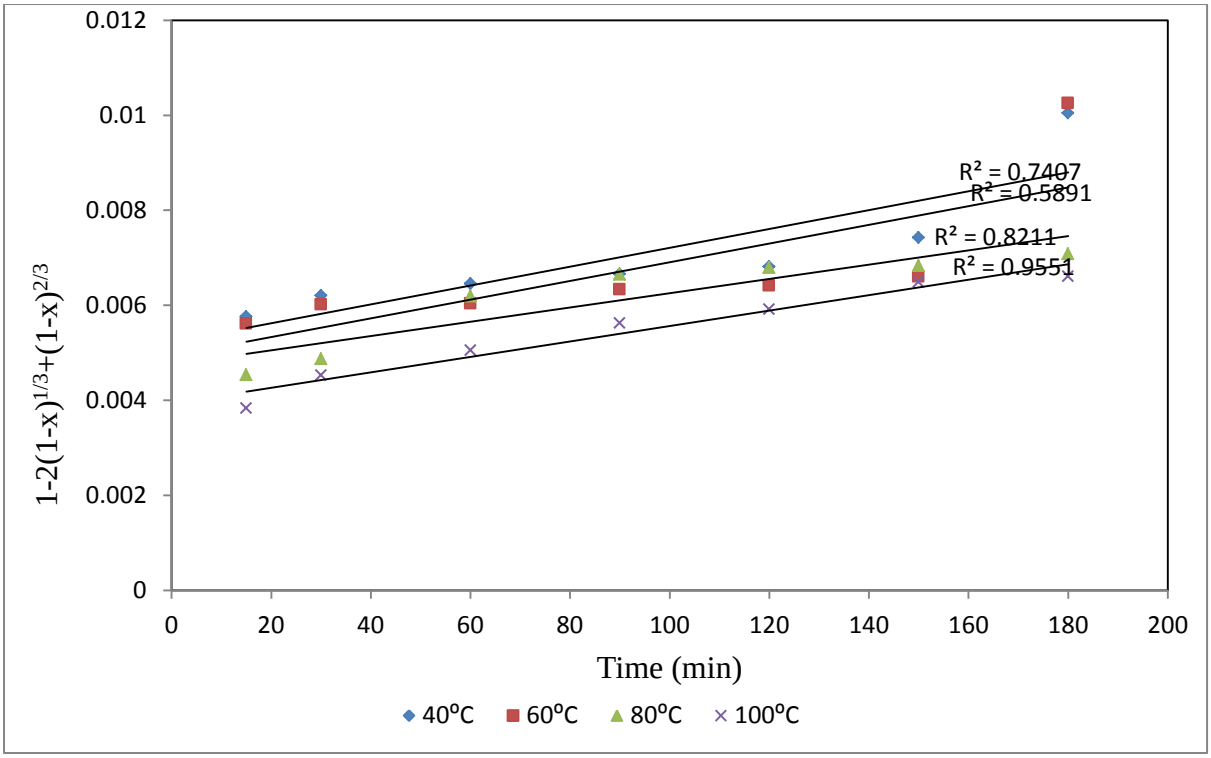

Figure 5-28: Plot of 1-2(1-x)1/3+(1-x)2/3 vs time for leaching nickel from roasted saprolitic laterite at different temperatures

6 Conclusions and recommendations

6.1 Optimization reactions

Leaching experiments were designed using a four-factor central composite design. All four factors (temperature, ammonia concentration, ammonium carbonate concentration, and oxygen pressure) had a significant effect on the percentage extraction of nickel. Ammonia had the most significant effect on the percentage extraction of nickel. The maximum extraction of nickel from unroasted ore was 11.9 % at 100 ^{o}C, 4 M NH_3, 2 M $(NH_4)_2CO_3$ and 2 bar O_2 pressure. Optimum leaching conditions were found to be 100 ^{o}C 3M NH_3, 2 M $(NH_4)_2CO_3$ and 2 bar O_2 pressure. The predicted response at these conditions was 12% nickel extraction.

Using the optimum conditions, the effect of time was investigated by increasing leaching duration to 6 hours and 12 hours. The effect of time had a slight improvement on the percentage extraction of nickel. After 12 hours of leaching, the percentage extraction of nickel was 15.1%. Using optimum conditions and leaching duration of 12 hours, the chemistry and mineralogy of the ore before and after leaching was studied. Only nickel was extracted from the ore. Co, Mg, Si, and Fe were not leached from the ore. Nickel was found to be mostly associated with iron in the ore. The results indicate that the relatively low degree of extraction of nickel in unroasted saprolitic laterite is due to inert minerals in the ore.

6.2 Solid-liquid separation

At the end of each leaching experiment in the 18 experimental runs designed for leaching the unroasted ore, the pregnant liquor was separated from solids by differential filtration over the filter medium under pressure.

Pressure did not affect the filtration rate. The average filtration rate was determined to be 0.29 ml/min.cm^2± 0.07. The low filtration rate was associated with quick pore clogging of the sintered metal.

Rheological studies of the ore showed non-Newtonian behavior. Viscosity studies indicated that the slurry exhibited shear-thickening properties. The properties of the ore and clay content in the ore reduce water permeability. The filter medium was successfully unblocked by back flushing with water and air after each leaching experiment.

A very clear filtrate was obtained in all cases during filtration.

6.3 Effect of roasting prior to leaching

Because of the low degree of nickel extraction from an unroasted ore, some experimental runs were carried out with roasted ore in order to improve nickel extraction from the ore. After roasting the ore, XRD analyses revealed that new mineral phases were formed.

From three experimental runs carried out using optimum leaching conditions obtained for the unroasted ore, there was a slight improvement in the degree of nickel extraction. The average percentage extraction from the three experimental runs was 19.25 ±0.18 % at 100 ^{o}C, 3 M NH_3, 2 M $(NH_4)_2CO_3$ and 5 bar O_2 pressure. The low degree of nickel extraction was due to formation of olivine or forsterite during reduction roasting.

Roasting improved the filtration rate. An average filtration rate of 2.60± 0.05(L/min.cm^2) was obtained when filtration was carried at 5 bar pressure. The differential clarity of the filtrate was poor due to change in mineralogical and structural change of the ore.

6.4 Kinetic study on the unroasted ore

Dissolution kinetics of unroasted saprolitic laterite ore was investigated with respect to the effect of temperature, ammonia, ammonium carbonate, and oxygen pressure. It was found that an increase in the temperature increases both the degree of nickel extraction and the reaction kinetics. An increase in both ammonia and ammonium carbonate increased the degree of nickel extraction but did not improve the reaction kinetics. Extraction of nickel in the absence of ammonium carbonate was very low. The effect of oxygen on the degree of nickel extraction and leaching kinetics was insignificant. Leaching of unroasted saprolitic laterite with a solution of ammonia and ammonium carbonate was found to be a two stage

leaching process. The first stage represents leaching of fee nickel in the ore. The second stage represents leaching of nickel associated with Fe, Mg and Si.

The leaching kinetics of unroasted saprolitic laterite for the second stage were characterized using a shrinking core model for changing single spherical particle size with the nickel dissolution data. The nickel dissolution was characterized using the equation describing a reaction controlled by a mixed (combined) model (ash layer diffusion and surface reaction control). An activation energy of 56.5kJ/mol was determined. The reaction order with respect to [NH_3] and [$(NH_4)_2CO_3$] was determined to be 0.3 and 0.26, respectively. The extraction of nickel is considered as two stage leaching mechanism. The first stage represent where the reaction is fast represents the extraction of free nickel which is surface reaction control. The second stage where the reaction is slow represents extraction of nickel associated with iron, magnesium and silicon which is ash layer diffusion control.

Ash layer diffusion control indicates that the relatively low degree of nickel extraction is mainly due to inert minerals hosting nickel in the ore. The inert minerals represent the ash layer.

6.5 **Kinetic study on the roasted ore**

Dissolution kinetics for the roasted saprolitic laterite was investigated with respect to temperature, ammonia concentration, ammonium carbonate concentration and oxygen pressure. For the roasted ore, temperature did not have a significant effect on the leaching rate in the first stage of leaching. The degree of nickel extraction was high at low temperatures. An increase in ammonia and ammonium carbonate concentration increased the degree of nickel extraction but did not improve the leaching rate. In the absence of ammonium carbonate nickel extraction was very low. This indicates the need for a closed vessel for preventing the loss of ammonium ions. The degree of nickel extraction improved with an increase in oxygen pressure. Presence of oxygen minimized iron hydroxides precipitation in the leach liquor. For the roasted ore, the highest percentage extraction of nickel was 28.2 % at 100 ^oC, 3 M NH_3, 2 M $(NH_4)_2CO_3$, and 5 bar O_2 pressure.

The effect of oxygen pressure for optimization and kinetic reactions for unroasted and roasted ore is different. Kinetic reactions for roasted and unroasted ore show similar trends. It is

suggested that optimization should be replicated. However, it is not clear why nickel extraction is high in the absence of oxygen for kinetic reactions for unroasted and roasted ore. A separate study of the effect of oxygen on leaching nickel laterite in a solution of ammonia and ammonium carbonate is required is required to understand why nickel is dissolves in the absence of oxygen.

Leaching of roasted saprolitic laterite was found to be a two stage leaching process. The shrinking core models for the roasted ore did not fit the experimental data very well under experimental conditions investigated here.

6.6 **Recommendations**

According to the findings of this study, when leaching with ammonium carbonate solution at temperatures above 60 ^{o}C, a closed vessel system is required. However, to prove this some experiments with an open vessel should be conducted to compare the results with closed vessel.

Filtration of unroasted saprolitic laterite seemed to be difficult probably due to the fine nature of the ore. For proper solid-liquid separation after leaching, ore particles should be larger with an average particle diameter of 75µm. The ore should be roasted for proper filtration. However, some modification may still be necessary for the original design of the vessel to work properly.

- The diameter of filter medium-2 should be larger in order to increase filtration surface area on the circulation port.
- The pump delivery pressure on P-3 should be interlocked with the pump drive so that the pump automatically stops when the pressure reaches 10 bar in order to avoid damaging the pump.
- The pressure relieve valve should be automated to avoid pressure build up in the vessel which can damage filter medium.
- Filtration should be a two-stage process. The leaching and filtration vessel will become the first stage of filtration. In this stage, pore size of filter should be slightly larger (40µm) to allow some fine particles pass through but not enough to block the pipes during circulation. In the first stage, oxygen should be directly splurged into the

leach solution rather on top of the leaching vessel to ensure proper mass transfer between the gaseous phase and liquid phase. Once leaching and filtration in the first stage is complete, the leach liquor should be transferred to the second vessel with a filter medium of smaller pore size (20µm). This set up is demonstrated in the Figure below.

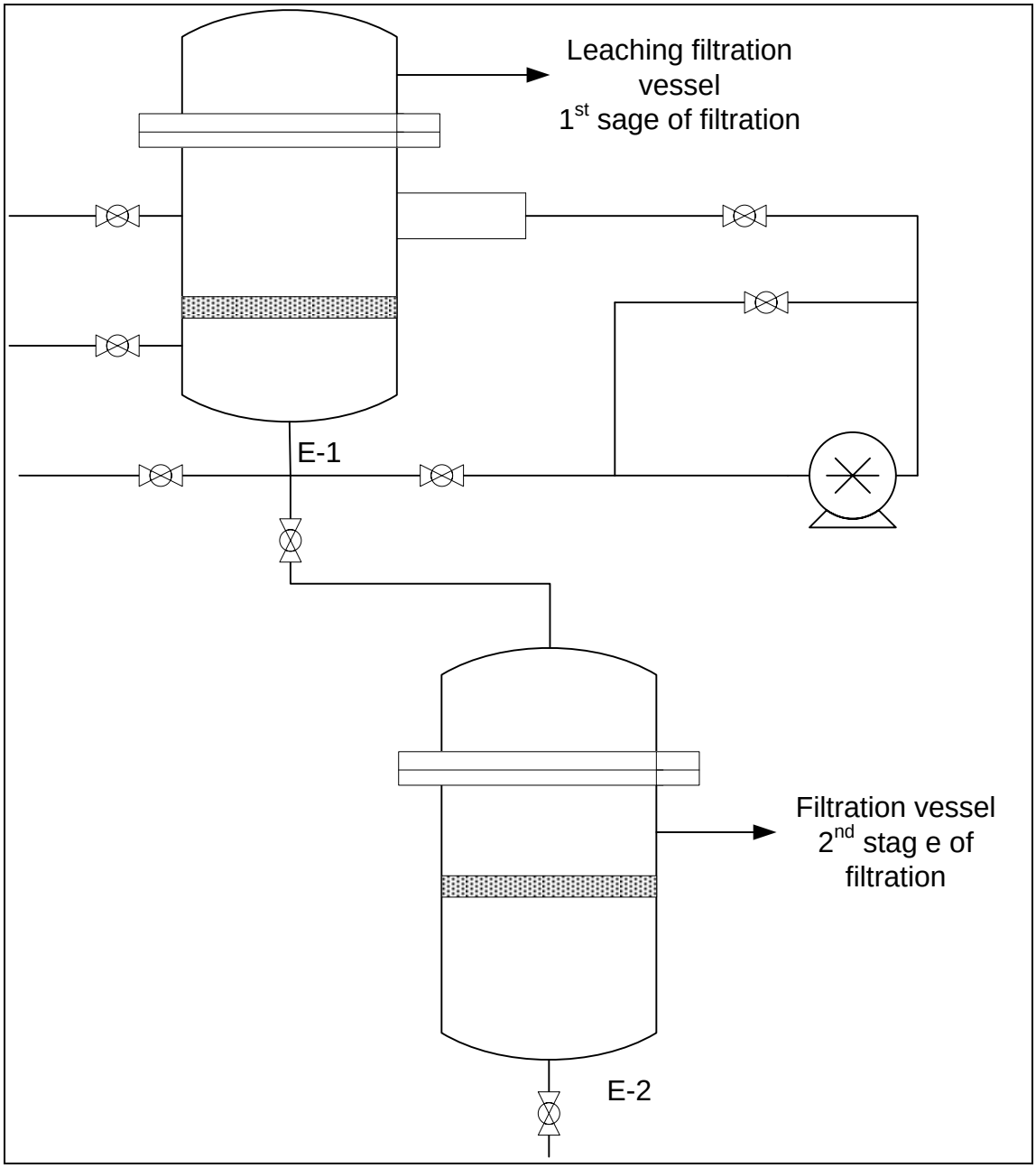

Figure 6-1: Pressure leaching vessel with two-stage filtration

After roasting the degree of nickel, extraction did not improve substantially. Reductive roasting should be carefully controlled, optimum roasting conditions which will give the maximum yield should first be determined.

7 References

Aarslan-Alaton, I., Tureli, G. and Olmez-Hanci, O., 2009. Treatment of azo dye production wastewater streams using Photon-Fenton -like oxidation process: Optimization by response Surface methodology. Journal of Photochemistry and Photobiology: Chemistry, 202: 142-153.

Agrawal, A., Kumar, V., Pandey, B.D. and Sahu, K.K., 2006. A comprehensive review on the hydro metallurgical process for the production of nickel and copper powders by hydrogen reduction. Materials Research Bulletin, 41: 879-892.

Anand, S. and Das, R.P., 1994. Precipitation of iron oxide from ammonia ammonium sulfate solutions. Hydrometallurgy, 38: 161-173.

Ashok, D.D., Osborne, R.C. and Bacon, G.W., 2004. The past and future of nickel laterites. In: Osborne (Editor), International Convention Trade show and Investors Exchange. Inco Limited, Canada, pp. 1-200.

Baghalha, M., 1998. The pressure acid leaching of laterites at 250^{o}C: A solution chemical model and its application. Metal and Materials Transaction B, 98: 945-952.

Bare (Patent), C.B., 1960. A new method of treating laterite ore, United States of America, 2,928,732.

BASF, 2008. "BASF chemical company", Retrieved on 8 March 2009, http://www.corperate.basf.com/en.

Bell, L.S., Welch, G.D. and Bennet, P.G., 1995. Development of ammoniacal lixiviants for the in-situ leaching of chalcopyrite. Hydrometallurgy, 39: 11-23.

Bhat, K.L., 1987. Recovery of zinc from leach residues-problems and developments. Indian Institute of Metals, India.

Bhattacharya, I.N., Panda, D. and Bandopadhyay, P., 1998. Rheological behavior of nickel laterite suspension. International Journal of Mineral Processing, 53: 251-263.

Bhuntumkomol, K., Han, K.N. and Lawson, F., 1982. The leaching behavior of nickel laterite in acid and ammoniacal solutions. Hydrometallurgy, 35: 147-263.

Bingol, D., Canbazoglu, M. and Aydogan, S., 2005. Dissolution kinetics of malachite in ammonia/ammonium carbonate leaching. Hydrometallurgy, 76: 147-160.

Buckett (Patent), G.F., 1998. The process for nickel and cobalt extraction from laterite ores. United States of America, WO9836102.

Chander, S. and Sharmer, V.N., 1981. Reduction roasting/ammonia leaching of nickelferrous laterites. Hydrometallurgy, 7: 315-327.

Christine, M.A. and Montgomery, D.C., 2008. Response surface design evaluation and comparison. Journal of Statistical Planning and Inference, 30: 1-8.

Ciminelli, V.S., Osseo-Asare, K, 1987. Kinetics of pyrite oxidation by oxygen in sodium carbonate solution. Industrial Chemical Engineering Research, 26: 824-830.

Coulson, J.M. and Richardson, J.F., 1983. Chemical Engineering, 6. Pergamon Press, Oxford.

Curlook, W., 2002. Improvement to acid pressure leaching of nickel laterite ore, International Laterite Nickel Symposium, Australia, pp. 325-355.

Dillion, C., 1992. Materials selection for chemical process industries. McGraw-Hill, United States of America.

Dreisinger, D.B., 1990. Hydrometallurgy. John Willey and Sons, Canada.

Dutrizac, J.E. and Monhemius, A.J., 1986. Iron control in hydrometallurgy. In: E. Horwood (Editor), 1st International Symposium on Iron Control in Hydrometallurgy. John Wiley and Sons, Toronto.

Duyvesteyn (Patent), W.P., Liu, H. and Davis, D.M., 2001. Heap leaching of nickel containing ores, United States of America, US 6,312,500B1.

Ekmekyapar, A., Oya, R. and Kunkul, A., 2003. Dissolution kinetics of an oxidized copper ore in ammonium chloride solution. Chemical, Biochemical Engineering, 17: 261-266.

Erasmus, M.P., 2011. Development of a pressurized leach and filtration vessel for use with ammonium carbonate solution, Stellenbosch University, Cape Town, 189 pp.

Fogler, H., 2007. Elements of chemical reaction engineering. Pearson Education Inc United State of America.

Forward (Patent), F., 1948. Ammonium carbonate leaching of nickel sulfide, United States of America, 2,576,314.

Forward, F.A. and Halpern, J., 1953. Studies in the carbonate leaching of uranium ores. The Canadian Mining and Metallurgy Bulletin(46): 634-648.

Francis, B.R., 2004. Process for nickel and cobalt extraction from laterite ores, United States of America, WO 2004/067787.

GKN, 2009. "Sintered Metals", Retrieved on 29 March 2009, from http//:www.gkn-filter.com.

Gladstone, S., 1958. Source book on atomic energy. D.Van Nostrando.Inc, Princeton.

Globe, 2005. "Globe program", Retrieved on 23 October 2009. Globe, from http//:www.soil.gsf.nasa.gov.

Gogate, R.P., Beenacker, A.C.M.A. and Pandit, B.A., 2000. Multiple impeller system with a special emphasis on bioreactors; A critical review. Biochemical Engineering Journal, 6: 109-144.

Goldwyer, N., 2007. Modified leaching process of uranium, Mining Weekly, 17, 55

Graff, J.E., 1980. The Treatment of Laterite Nickel Ores-A Further Study on the Caron Process and Other Possible Improvements: Part II Leaching Studies. Hydrometallurgy (5): 255-271.

Gupta, C.K., 2003. Chemical Metallurgy. Wiley-VCH, India.

Harris, C.T. and J.C, P., 2009. Thermal upgrading of nickelferrous laterites-A United states Patents Review. In: J. Liu. (Editor), Pyrometallurgy of Nickel and Cobalt Proceedings of the 48th Annual Conference of Metallurgists of CIM. METSOC, Canada, pp. 51-75.

Harvey, G.T., 2006. The hydrometallurgical extraction of zinc by ammonium carbonate: A review of the Schnabel process. Mineral and Extractive Metallurgy, 27: 231-279.

Houyuan, L., J. G, 2004. Atmospheric leaching of laterite with iron precipitation as goethite, International Laterite Nickel Symposium -2004, Charlotte, NC, USA, pp. 347-355.

Im(Patent), S.J. and Johnson, J.D., 1975. Nickel extraction process, United States of America, 3,953,200.

Javad, M.E., 2005. Determination of optimum conditions for the leaching of non-sulfide zinc ore (High SiO_2). Industrial Engineering Chemistry, 32: 8952-8956.

Klein, B. and Hallborn, D.J., 2002. Modifying the rheology of nickel laterite suspension. Mineral Engineering, 15: 745-749.

Kukura, M.E., 1979. Development of UOP process for oxide silicate ore of nickel and cobalt, International Laterite Symposium of Mining Engineering -1979, Industrial Engineering Chemistry Journal. India, pp. 527-552.

Langston, B.G., Macdonald, R.D. and Stephen, F.M., 1957. Pressure leaching of uranium. Mining Engineering, 5: 989-993.

Li, J., Li, L., Hu, Q., Wang, Z., Zhou, Y., Zheng, J., Liu, L. and Li, L., 2009. Effect of pre-roasting on leaching of laterite. Hydrometallurgy, 99: 84-88.

Lou, W., Feng, Q., Ou, L., Zhang, G. and Lu, Y., 2009. Fast dissolution of nickel from a lazardite-rich saprolitic by sulfuric acid at atmospheric pressure. Hydrometallurgy, 96: 171-175.

Madigan, C., Leong, Y.K, Ong, B.C.,2009. Surface and rheological properties of as received colloidal goethite (α-FeOOH) suspension: pH and polyethylenimine effects. International Journal of Mineral Processing, 93. 41-47

Marczenko, Z., 1976. Spetrophotometric determination of elements. John Wiley and Sons, New York.

Masuda, H., Higashitani, K. and Yoshida, H., 2006. Powder Technology. Taylor and Francis Group, United States of America.

Matson (Patent), R.F., 1971. Nickel laterite processing, New York, 3,714,326.

Mcketta, J.J., 1996. Encyclopedia of chemical processing and design. CRC Press, New York.

Meng, X. and Han, K.N., 1994. The principles and application of ammonia leaching of metals-A Review. Mineral and Extractive Metallurgy, 16: 23-61.

Mizokuchi, T., Nakamura, J. and Ishii, H., 1978. Oxygen pressurized leaching of metallic nickel in ammoniacal ammonium carbonate solution. Journal of Chemical Society, 6: 23-61.

Morioka, S. and Shimakage, K., 1971. Fundamental studies on the ammoniacal pressure leaching of metallic nickel powder. Institution of Mining and Metallurgy Section C, 80: 228-234.

Moskalyk, R.R. and Afantazi, A.M., 2002. Nickel laterite processing and electrowinning practice. Mineral Engineering, 15: 593-605.

Nagata, S. (1975). Mixing principles and application. London, John Wiley and Sons.

Nikoloski, A.N., Nicol, M.J. and Fittock, J.E., 2004. A Fundamental study of the leaching reactions involved in the Caron Process. International Laterite Nickel Symposium. Charlotte, NC. TMS, Warrendale, pp. 369-398.

Papangelakis, V.G., 1998. Pressure acid leaching of laterites at 523K: A solutions Model and its application. Metal and Materials Transaction B, 34: 945-951.

Perry, R., 2007. Perry's Chemical Engineer's Handbook. McGraw-Hill, New York.

Renaldo, M.M., 2007. Fundamentals of transfer and kinetics. Mettler-Toledo AutoChem Inc, Switzerland, pp. 1-14.

Rousseau, R.W., 1987. Hand Book of Separation Technology. John Wiley and Sons, Canada.

Seaborg, G.T., 1949. The Transuranium Elements. McGraw-Hill Book Co, New York.

Sedzimir, J. and Bujanska, M., 1978. Kinetics of leaching copper in copper (II)-ammonium sulfate solutions as determined by rotating disc. Hydrometallurgy, 3: 233-248.

Shurtz, R.W., 1984. Hydrometallurgical application of titanium, Industrial Application Titanium and Zirconium. ASTM STP 830, Webster, pp. 29-47.

Siemens (Patent), E.R. and Good, C.P., 1976. Process for recovery of non-ferrous metals from oxide ores and concentrates, United States of America, 3,929,468.

Sohn, H.Y. and Wardsworth, M. E., 1979. Rate process of extractive metallurgy. Plenum Press, New York.

Spink (Patent), 1986. Recovery of base metals values from base metal and iron bearing sulfide material, United States of America, 0192459.

Stapp (Patent), P.R., 1983. Uranium value leaching with ammonium carbonate and/or bicarbonate plus nitrate oxidant and optionally oxidation-catalytic metal compounds, United States of America, 4,405,567.

Suarez (Patent), J.C. and Villanueva, G.A., 2003. Hydrometallurgical process for the recovery of nickel and cobalt by ammoniacal leaching, United states of America, US 6,524,367 B1.

Tolley (Patent), W.K. and Rademaker, P.D., 1982. Enhanced hydrometallurgical recovery of cobalt and nickel from laterites, United States of America, 4,312,841.

Valix, M. and Cheung, W.H., 2002. Study of phase transformation of laterite ore at high temperature. Minerals Engineering, 15: 607-612.

Vosahlova (Patent), E.A. and Weir, D.R., 1972. Method for leaching reduced laterite ores, United States of America, 3,644,114.

Webb, 2002. A primer on particle sizing by static laser light scattering, Introduction to the latest ANS/ISO standard for laser particle size analysis. Micrometrics Instrument Corp, United Kingdom.

WIKIPEDIA, 2009. "Uranium", Retrieved on 6 April 2009, from http//:www.en.wikipedia.org/wiki.

WIKIPEDIA, 2010. "BET theory", Retrieved on 15 March 2010, from http://www.en.wikipedia.org/wiki/BET_theory.

Wood, D.R., 2007. Rule of Thumb in Engineering Practice. John Wiley and Sons, New York.

Xia, G.X. and Hu, Z.W., 1980. Studies on the kinetics of copper dissolution in aqueous ammoniacal solution. Acta Metallurgical Sinica, 6: 442-453.

Yu-Chun, Z., Wen ning, M., Yan, L. and Qian, X., 2010. A green process for recovering nickel from nickelferrous laterite ores. Transaction of Nonferrous Metals Society of China, 20: 65-70.

Zubryckyj (Patent), N., Mackiw, V. and Weir, D.R., 1972. Method of recovering substantially pure nickel from ammoniacal ammonium carbonate leach solutions, United States of America, 3,640,706.

Zuniga, M., Parada, F. and Asselin, E., 2010. Leaching of limonitic laterite in ammoniacal solutions with metallic iron. Hydrometallurgy, 104: 260-267.

A Appendix A

Figure A- 1: Pressurized filtration vessel

A- 1: Design matrix and response for pressure filtration (PDE project)

	pore size of medium µm	pressure (bars)	clarity	filtration rate (ml/ min.cm^2)
1	20.00	0.50	very clear	1.1
2	20.00	1.50	very clear	1.99
3	80.00	0.50	not clear	2.42
4	80.00	1.50	not clear	4.3
5	20.00	1.00	very clear	1.62
6	80.00	1.00	not clear	3.25
7	60.00	0.50	clear	1.83
8	60.00	1.50	not clear	2.75
9 (C)	60.00	1.00	not clear	2.14
10 (C)	60.00	1.00	not clear	2.3

A- 2: Optimization for clarity of filtrate and filtration rate

Level of pore size of medium um	Level of pressure (bars)	Predicted clarity	Predicted filtration rate (ml/ min.cm^2)
20.00000	1.00	Very clear	1.364

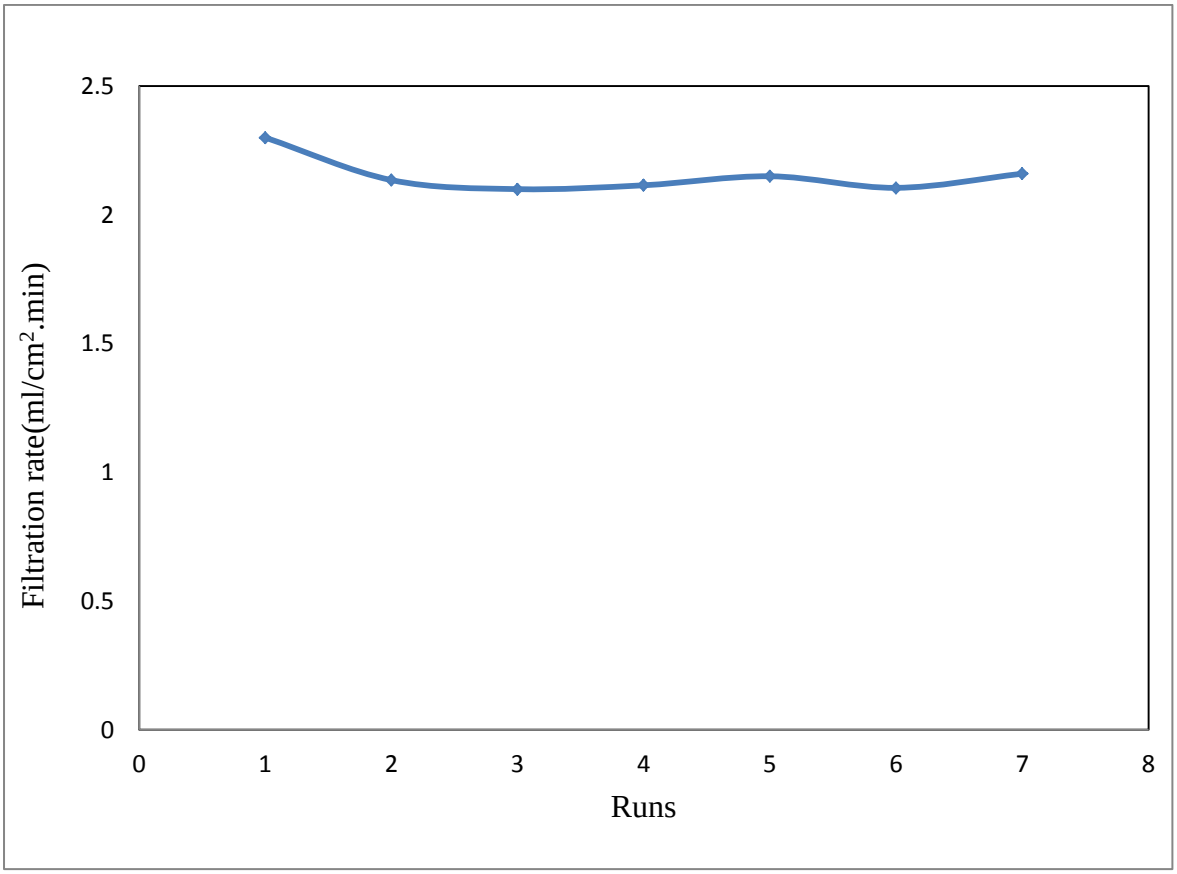

Figure A- 2: Filtration rate profile (back washing after each run)

B Appendix B

B.1 Stirrer design

B.1.1 Calculating pulley size on the vessel shaft (driven pulley) required to deliver maximum speed of 320 rpm

Table B- 1: Data for pulley size calculations

Motor with gearbox maximum speed (S)	1380.00	rpm
speed ratio	10.15	
Diameter of primary pulley (D)	200.00	mm
Speed of the primary pulley of diameter (S).	135.96	rpm
required speed	320.00	rpm

The pulley diameter was calculated using the following equations

From the relationship of centrifugal forces

F1=F2

$$S \times D = s \times d$$ Equation B- 1

Driven pulley diameter

$$d = \frac{D \times S}{s}$$ Equation B- 2

Where

d= diameter of driven pulley

D= diameter of driving Pulley (primary pulley)

s = speed of driven pulley

S= speed of primary pulley.

The pulley Diameter was found to be 85 mm.

B.1.2 Determination of agitator critical speed

Table B- 2: Calculation for critical agitator speed

Critical speed of agitation		
K	191.00	
D	0.15	m
ρ_d	2.48	g/cm^3
ρ_l	1.00	g/cm^3
d_p	0.02	mm
μ	0.89	Cp
V_p	7.26	ml
Vp'	18.00	ml
N_f	120.13	rpm

The data given in Table B-2 was instead into Equation 3-2 which is shown again below.

$$N_f = KD_i^{-2/3} d_p^{1/3} \left(\frac{\rho_d - \rho_l}{\rho_l}\right)\left(\frac{\mu}{\rho_l}\right)^{-1/9}\left(\frac{V_p'}{V_p}\right)^{-0.7}$$

The viscosity of water was given as 0.89 cP which is viscosity of water at 25^{o}C and density was assumed to be density of water at 25^{o}C. Vp and Vp' were calculated from the data which was used in the calculation of particle density and bulk density given in Table B-11.

B.2 Pump calibration

Table B- 3: Pump calibration data

rdy	time S	V Ml	rate ml/s	ml/min	L/min	L/h
15.00	44.00	5000.00	113.64	6818.18	6.82	409.09
20.00	38.00	5000.00	131.58	7894.74	7.89	473.68
25.00	30.00	5000.00	166.67	10000.00	10.00	600.00
30.00	24.00	5000.00	208.33	12500.00	12.50	750.00
35.00	21.00	5000.00	238.10	14285.71	14.29	857.14
40.00	18.00	5000.00	277.78	16666.67	16.67	1000.00
45.00	15.00	5000.00	333.33	20000.00	20.00	1200.00
50.00	12.00	5000.00	416.67	25000.00	25.00	1500.00
55.00	11.00	5000.00	454.55	27272.73	27.27	1636.36

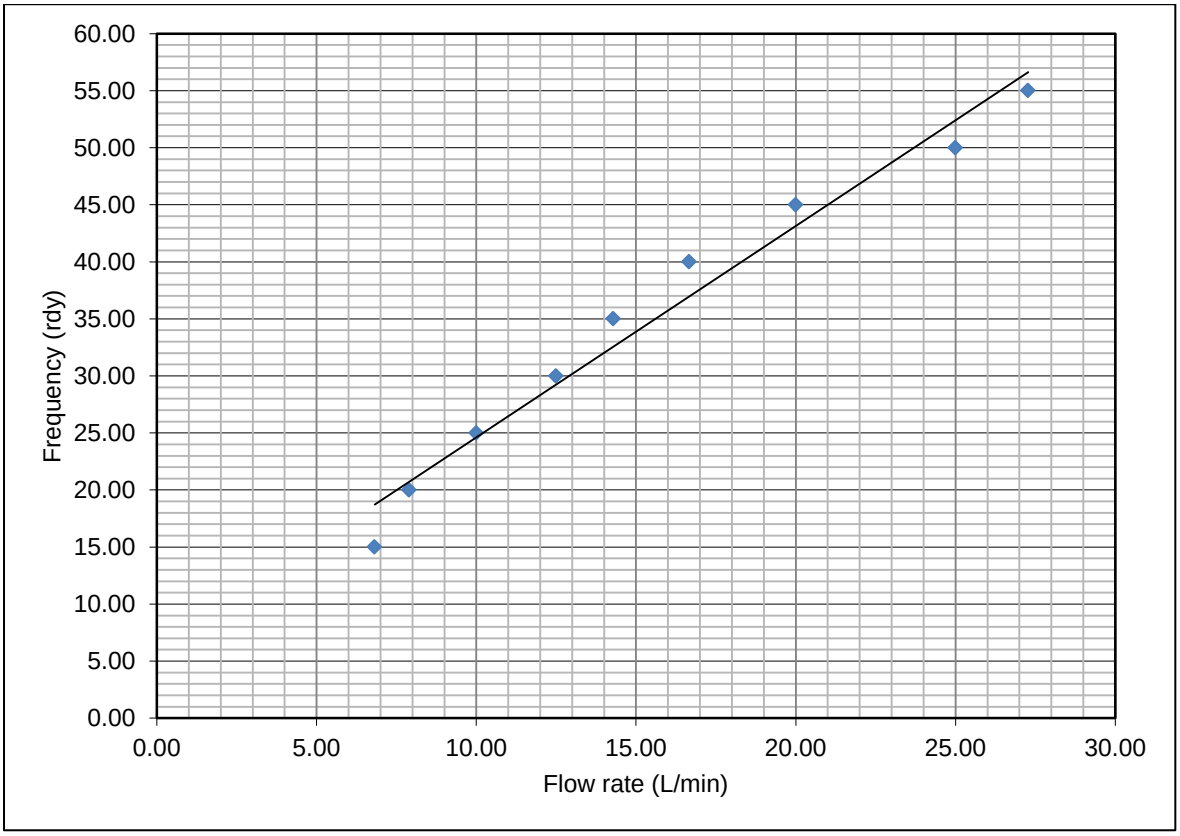

Figure B- 1: Pump calibration curve

B.3 Determining flow rate required to circulate leaching solution throughout the vessel.

Table B- 4: Permeability data for water through a 20µm stainless steel Filter medium regenerated from (GKN, 2009)

Pressure drop (psi)	Flow rate ($m^3/m^2.h$)	Pressure drop Pa
0	0	0.00
0.076	4	523.94
0.148	8.5	1,020.31
0.219	13	1,509.79
0.295	17	2,033.73
0.367	21	2,530.10
0.438	25	3,019.57
0.5	29	3,447.00

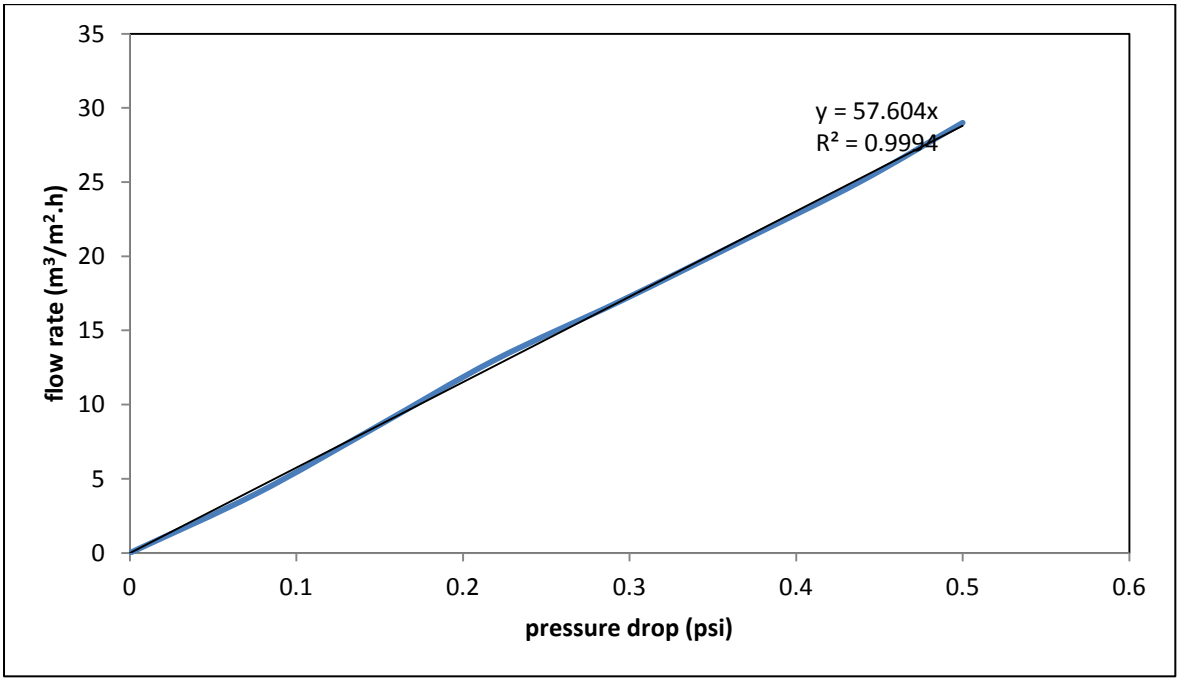

Figure B- 2: Flow rate across a 20µm stainless filter medium

From the equation of determining average flow diameter, porosity of the sintered metal can be determined.

$$d_{LE} = \sqrt{\frac{32 \times H \times V \times \eta}{A \times \Delta P \times \varepsilon}}$$ Equation B- 3

Rearranging

$$\varepsilon = \frac{32 \times H \times V \times \eta}{A \times (d_{LE})^2}$$ Equation B- 4

Table B- 5: Determination filter medium porosity

d_{LE}= average pore diameter (m).	0.000023
η= dynamic viscosity (Pa.s)	0.001
H= filter thickness (m)	0.003
V= flow rate (m^3/s)	
ΔP= pressure drop (Pa)	
A= filter surface (m^2)	5.54E-03
ε= porosity	

The value V/ΔP.A was determined from the slope of the line given in the figure above. Which is equal to 57.6 m^3/h.m^2.psi which is equal to 2.32E-06 m^3/s.m^2.Pa. By substituting these values into the equation, porosity equals 0.42.

Fluid flow through the sintered metal medium

$$\frac{(-\Delta P)}{H} = 150 \times \frac{\mu U(1-\varepsilon)^2}{x^2\varepsilon^3} + 1.75 \times \frac{\rho_f U^2(1-\varepsilon)}{x\varepsilon^3}$$ Equation B- 5

Rearranging the equation to determine superficial velocity

$$\frac{(-\Delta P)}{H} x^3\varepsilon^6 = 150\mu U(1-\varepsilon)^2 x\varepsilon^3 + 1.75\rho_f U^2(1-\varepsilon)x^2\varepsilon^3$$ Equation B- 6

Where x is average pore diameter, μ viscosity of water U is the superficial velocity, H is the filter medium thickness, and ρ_f is the density of fluid.

Let X = U

a=$1.75\rho_f(1-\varepsilon)x^2\varepsilon^3$

b=$150\mu(1-\varepsilon)^2 x\varepsilon^3$

$$Y = \frac{(-\Delta P)x^3\varepsilon^6}{H}$$ Equation B- 7

Using equation

$Y = aX^2 + bX$

By substituting the values in a, and b, X can be solved using the above quadratic equation.

Table B- 6: Determination of superficial velocity using Ergun equation

ρf	1000	kg/m^3
x	2.00E-05	m
ε	0.42	
μ	0.001	Pa.s
(-ΔP)	5000	Pa
H	0.003	m
a	3.01E-08	
b	7.48E-08	
Y	7.32E-11	

Solving the quadratic equation and using positive square roots give superficial velocity of 9.78E-4 m/s. Actual flow rate Ua equal U/ε which is 0.002329 m/s. this can be converted to flow rate across the filter medium according the following relationship

$$Ua = \frac{Q}{A}$$ Equation B- 8

B.3.1 Filter medium 1

Table B- 7: Flow rate across filter medium-1

A	πr^2	
r=	0.07	m
A	1.50E-02	m^2
Q	3.48E-05	m^3/s
	2.09	L/min

Table B- 8: Flow rate across filter medium-1 at different pressure drop

(-ΔP) Pa	U	Ua	flow rate m^3/s	flow rate L/min
5,000.00	9.78E-04	2.33E-03	3.48E-05	2.09E+00
10,000.00	1.95E-03	4.64E-03	6.94E-05	4.17E+00
50,000.00	9.75E-03	2.32E-02	3.47E-04	2.08E+01
100,000.00	1.94E-02	4.62E-02	6.91E-04	4.15E+01

B.3.2 Filter medium 2

Table B- 9: Flow rate across filter medium-2

A	πr^2	
r=	0.02	m
A	1.26E-03	m^2
Q	2.45E-06	m^3/s
	0.15	L/min

Table B- 10: Flow rate across filter medium-2 at different pressure drop

(-ΔP) Pa	U	Ua	flow rate m^3/s	flow rate L/min
5,000.00	9.78E-04	2.33E-03	4.66E-05	2.79E+00
10,000.00	1.00E+00	2.38E+00	4.77E-02	2.86E+03
50,000.00	2.00E+00	4.76E+00	9.53E-02	5.72E+03
100,000.00	3.00E+00	7.15E+00	1.43E-01	8.57E+03

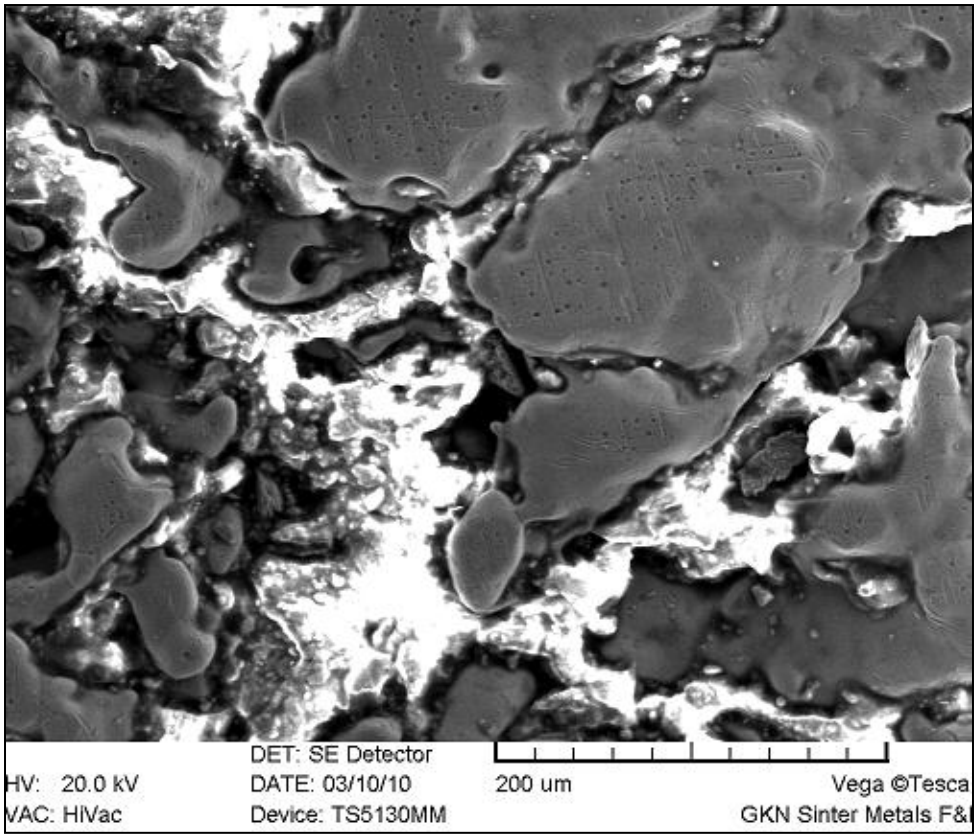

Figure B- 3: SEM image filter medium indicating pore clogging (dark grey areas show ore particles on the disk)

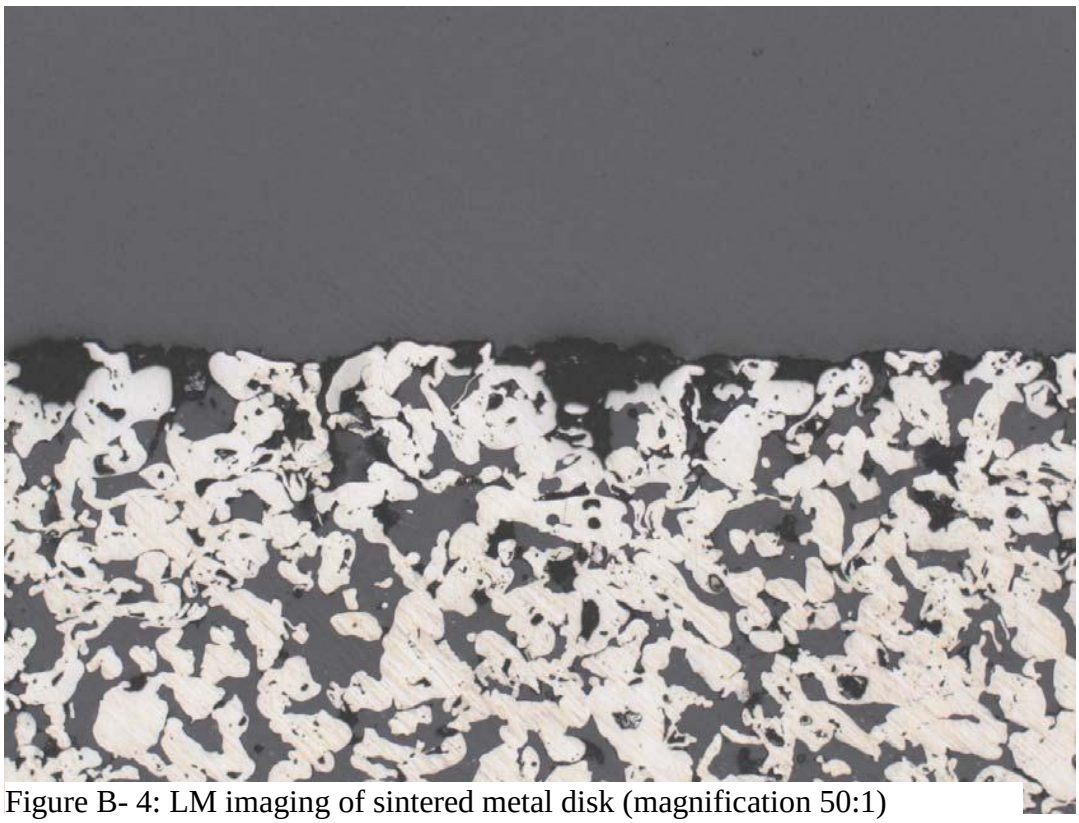

Figure B- 4: LM imaging of sintered metal disk (magnification 50:1)

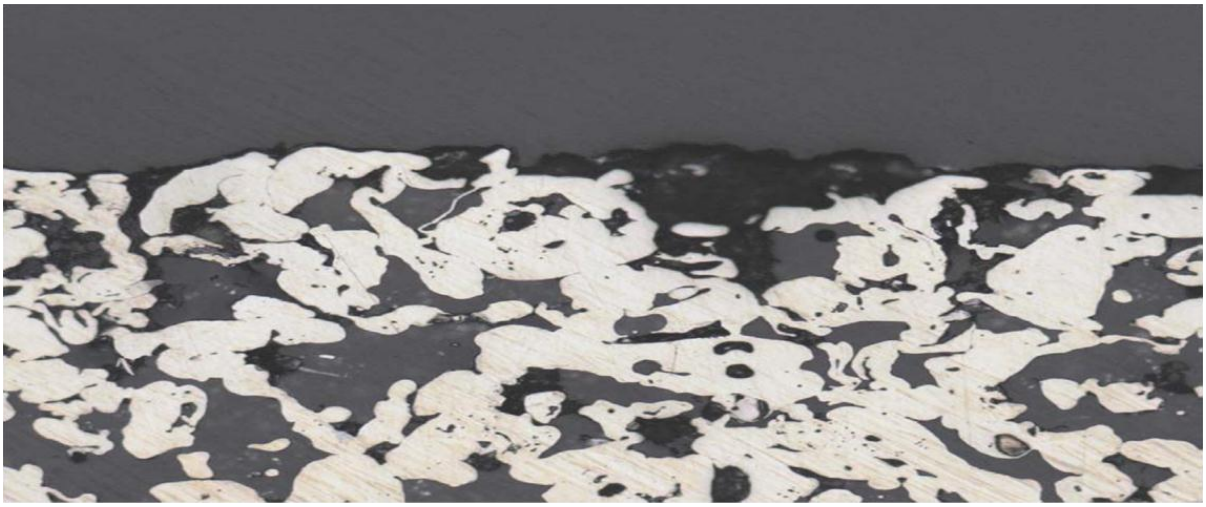

Figure B- 5: LM imaging of sintered metal disk (magnification 100:1)

B.4 Physical properties of the ore

B.4.1 Particle density

Table B- 11: Data for determining particle density

A mass of sample + empty flask (g)	79.60
B Mass of empty flask (g)	54.60
C Mass of soil (A-B) (g)	25.00
D Mass of water + soil + flask (g)	169.90
E Mass of water (D-A) (g)	90.30
F water temperature (oC)	15.50
G Density of water (g/ml) ~ 1.0	1.00
H volume of water (ml) E/G	90.30
I volume of sample ml (100ml-H)	9.70
J sample particle density (g/ml)	2.58
K Mass of small bottle (g)	9.60
L Volume of small Bottle	18.00
M mass of small bottle + sample (g)	23.90
N mass sample inside bottle (M-K) (g)	14.30
Specific surface area m^2/g	76.61

$$\rho_b = \frac{\rho_1(m_s - m_o)}{(m_1 - m_o) - (m_{sl} - m_s)}$$ Equation B- 9

Where ρ_d is particle density, ρ_1 is density of water, m_s is mass of solids, m_o is mass of empty flask, m_l is mass of liquid in 100 ml flask, and m_{sl} is mass of solids and water.

B.4.2 Specific surface area

$$\frac{1}{v\left[\left(P/P_o\right)-1\right]} = \frac{C-1}{V_m C}\left(\frac{P}{P_o}\right) + \frac{1}{V_m C}$$ Equation B-1

P and P_o are the equilibrium and saturation pressure of adsorbate at the temperature of adsorption, v is the adsorbed quantity (units of volume), and V_m is the monolayer adsorbed gas quantity. C is the BET constant, which is expressed by

$$c = e^{\left(\frac{E_1 - E_L}{RT}\right)}$$ Equation B-2

E_1 is the heat of adsorption for the first layer and E_L is that for the second and higher layers and is equal to the heat of liquefaction (Wikipedia, 2010).

B.4.3 Rheological properties of the ore

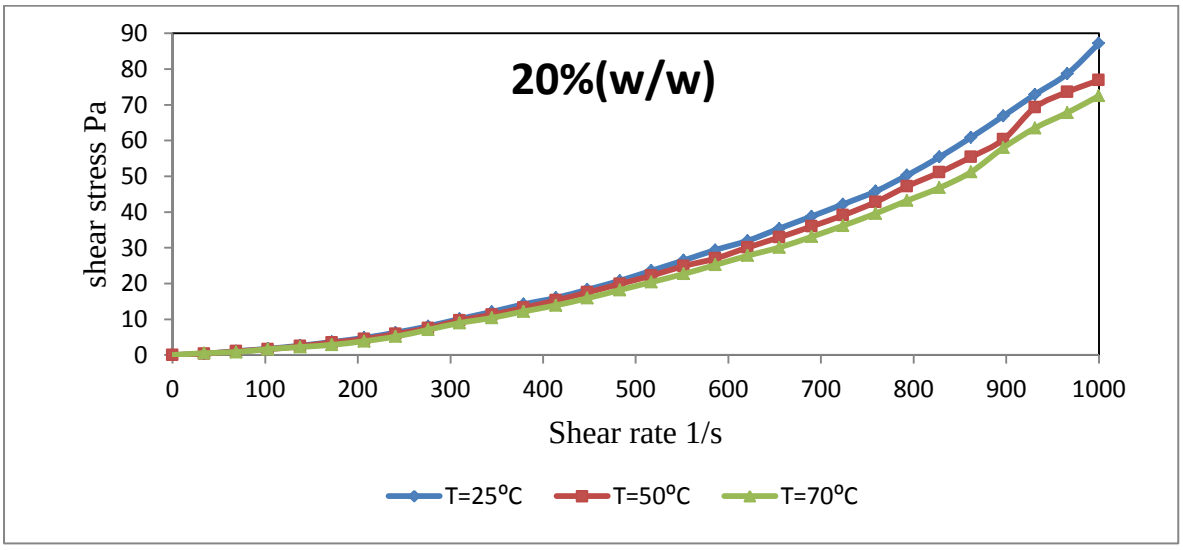

Figure B- 6: Shear stress vs shear stress at different temperatures (20% w/w solids)

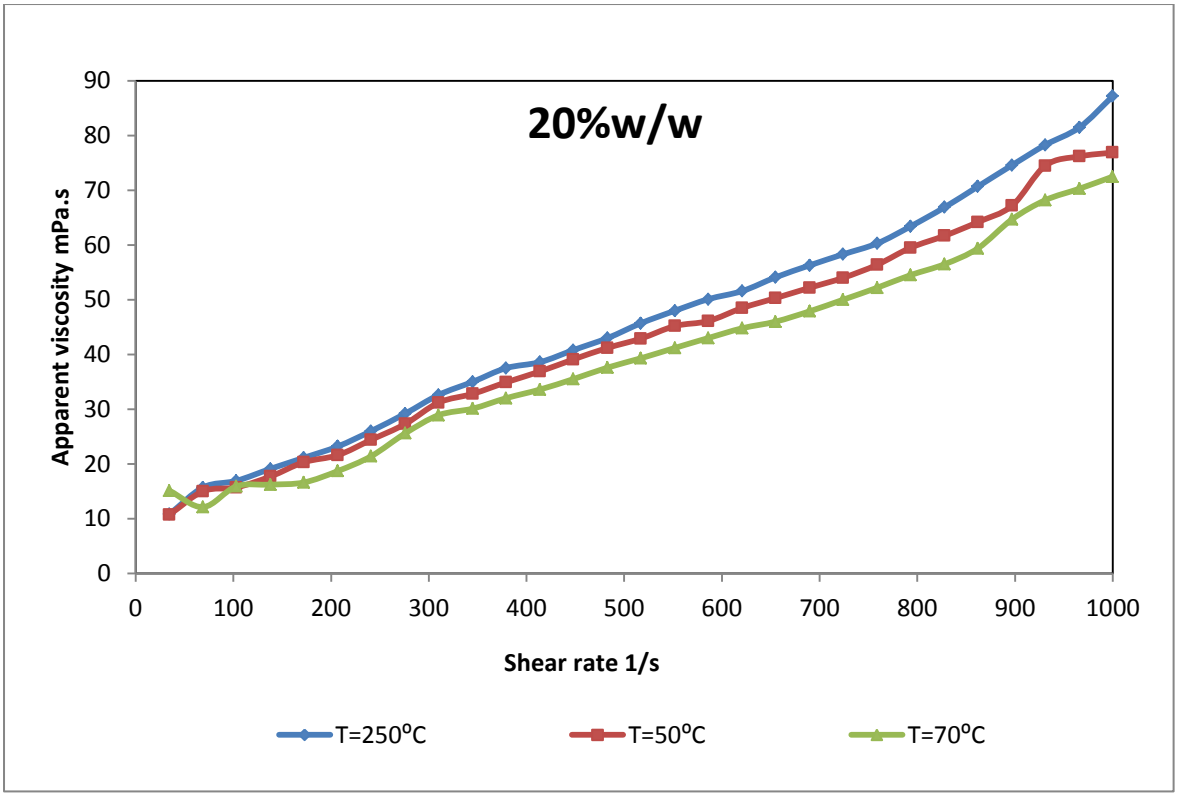

Figure B- 7: Apparent viscosity vs shear rate at different temperatures (20% w/w solids)

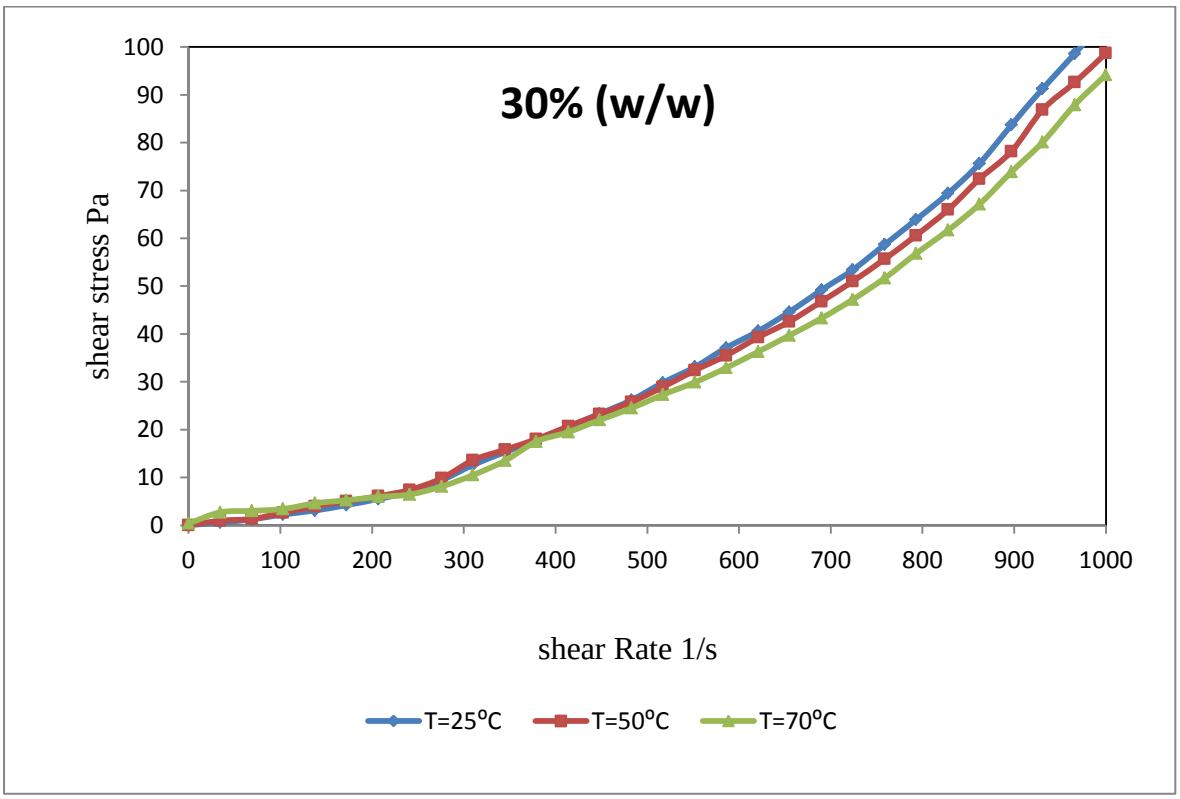

Figure B- 8: Shear stress vs shear stress at different temperatures (30% w/w solids)

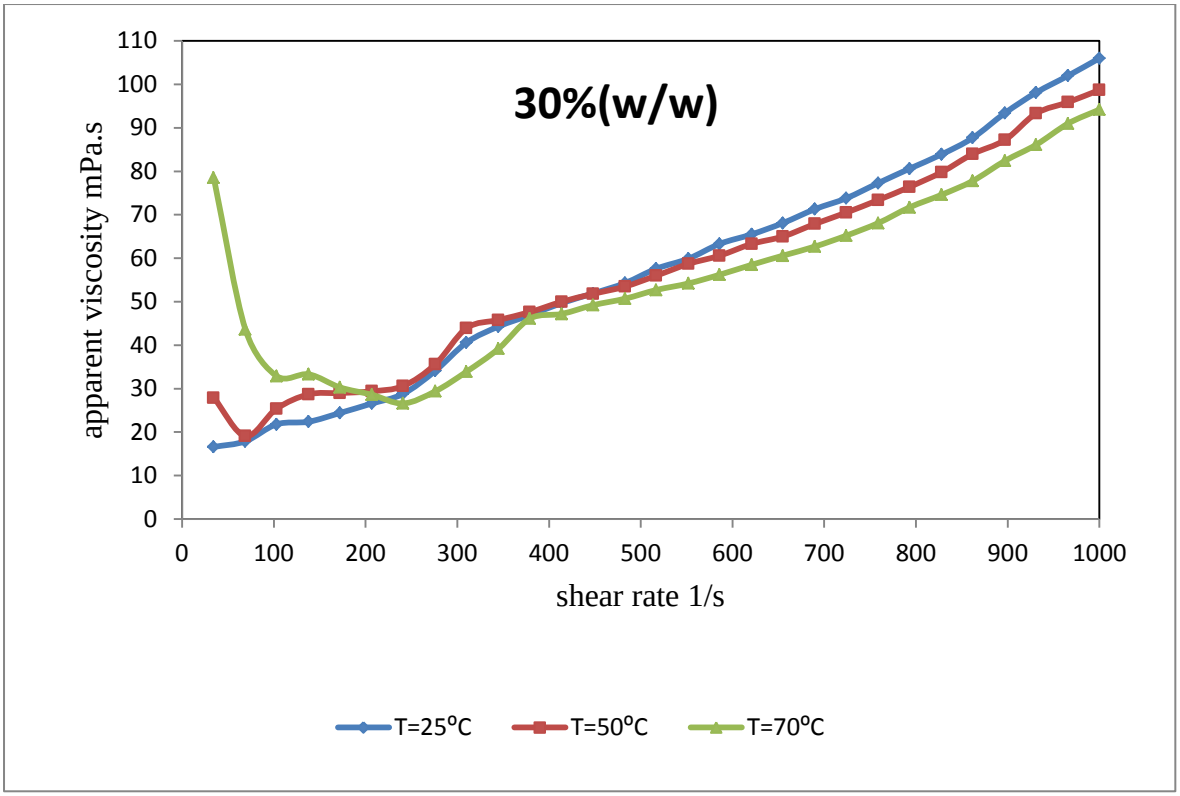

Figure B- 9: Apparent viscosity vs shear rate at different temperatures (30% w/w solids)

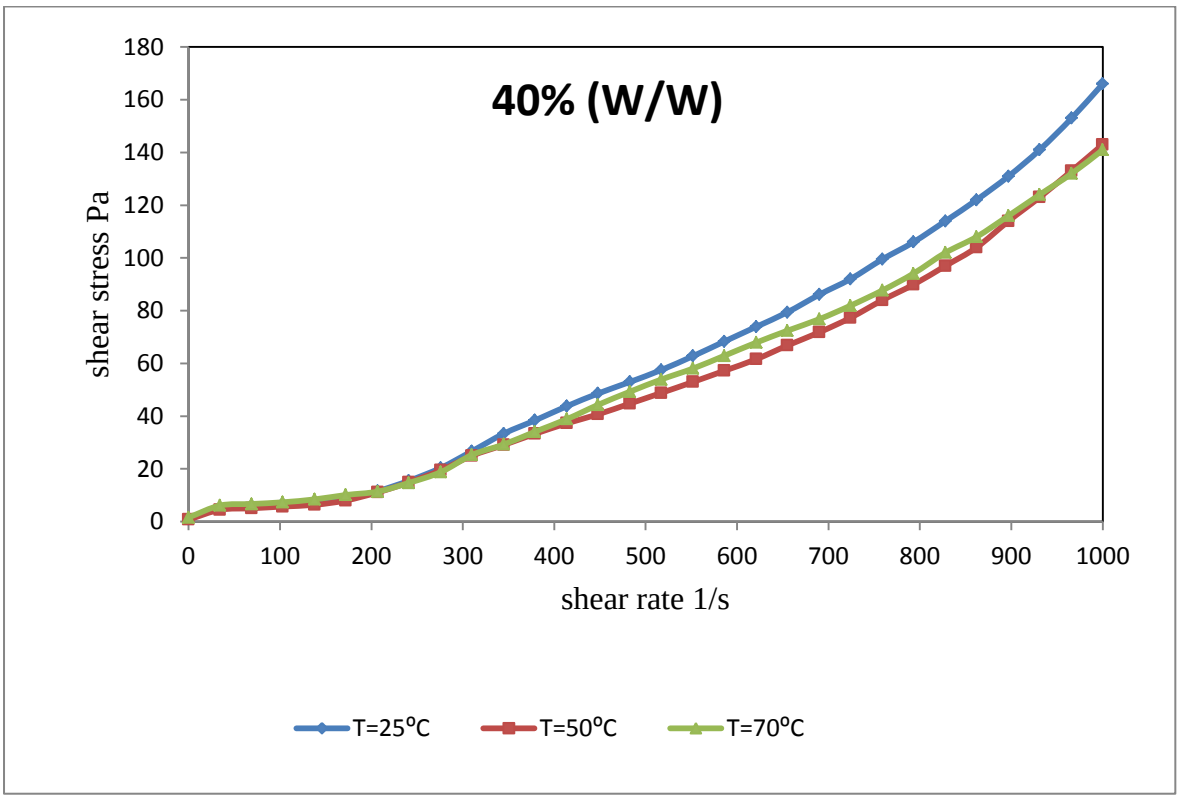

Figure B- 10: Shear stress vs shear stress at different temperatures (40% w/w solids)

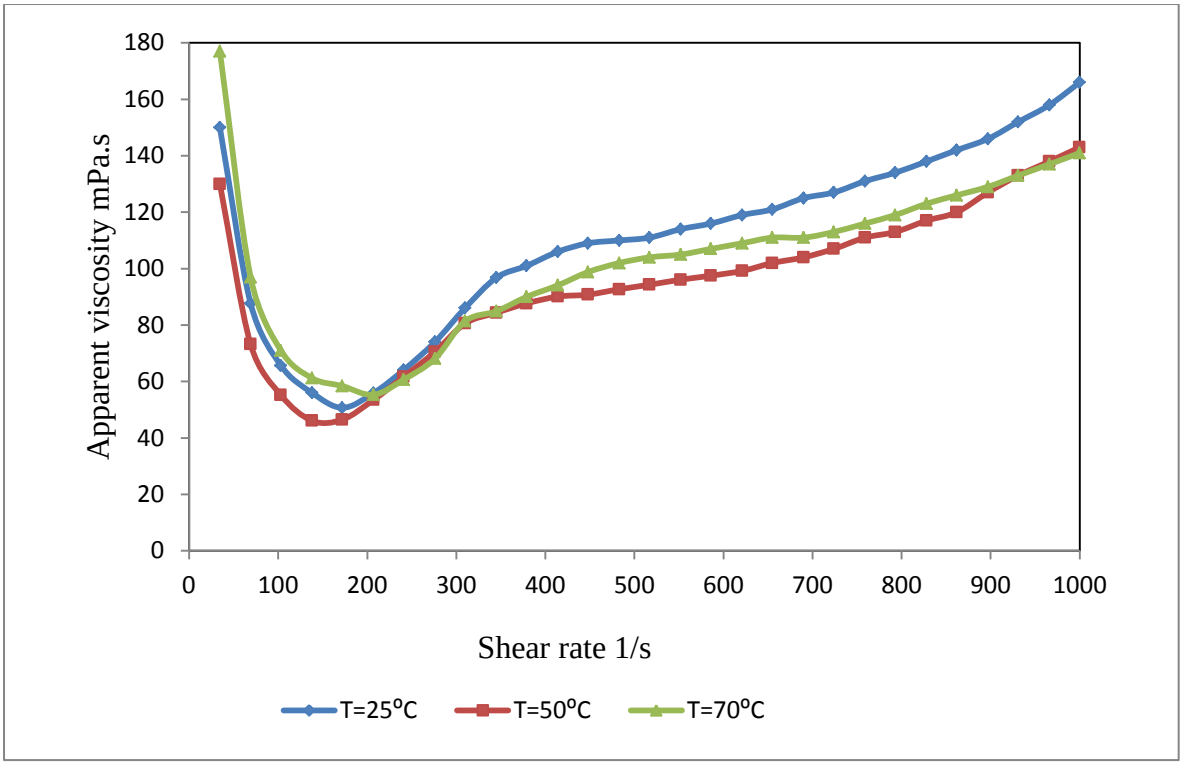

Figure B- 11: Apparent viscosity vs shear rate at different temperatures (40% w/w solids)

B.5 Preparation of leaching solution

B.5.1 Amount solids for making a pulp of 15%(w/w) density

The amount of reagents required to prepare the leaching solution, the amount of solids and water required for making a pulp of 15%w/w density were determined using the following equations;

$$\rho_p = \frac{m_s}{m_s + m_l} \qquad \text{Equation B- 10}$$

Where m_s the mass of solids, ρ_p is the pulp density and m_l is mass of liquid solution.
Mass of solids can also be expressed in terms of particle density and porosity.

$$m_s = (1 - \varepsilon)\rho_d AH \qquad \text{Equation B- 11}$$

Where ε is the porosity of solids, ρ_d is the particle density of solids, A is the cross sectional area occupied by solids and H is the height of solids. AH is also the volume (Vs) occupied by solids.

$$m_l = \rho_f V_L \qquad \text{Equation B- 12}$$

$$V_T = V_s + V_L \qquad \text{Equation B- 13}$$

Where ρ_f is the fluid density (assuming density of water), V_T is the total volume of the solution and V_L is the fluid volume. Combining the above equations and solving simultaneously the following equation is derived.

$$V_s = \frac{V_T \rho_p \rho_f}{(1-\varepsilon)\rho_d - (1-\varepsilon)\rho_p \rho_d + \rho_p \rho_f} \qquad \text{Equation B- 14}$$

Table B- 12: Amount of solids required to make the required pulp density.

Total volume required VT (cm^3)	3500
Pulp density	0.15
Combining the equations and solving simultaneously	
Vs (cm^3)	256.66
VL (cm^3)	3243.30
ms (g)	572.35

B.5.2 Amount of Reagents

To prepare a solution of required ammonia concentration, percent concentration was first converted to morality concentration using the following equations;

$$C_M = \frac{n_{NH3}}{V_{solution}} \qquad \text{Equation B- 15}$$

Where C_m is the concentration of NH_3 of in the solution in molarity, n_{NH3} is number of moles of NH_3 and $V_{solution}$ is the volume of the solution. Moles of NH_3 can be determined from the relationship of mass and number of moles

$$n_{NH3} = \frac{m_{NH3}}{m_M} \qquad \text{Equation B- 16}$$

Where mNH_3 is mass of ammonia in the solution and m_M is molar mass of NH_3

To convert to moles, the relationship of mass of NH_3 with percentage concentration was used.

$$C_{\%(w/w)} = \frac{m_{NH3}.100\%}{m_{solution}}$$ Equation B- 17

$C_{\%(w/w)}$ is NH_3 concentration in weight percent and $m_{solution}$ is mass of the solution. Rearranging the above equation becomes

$$m_{NH3} = \frac{C_{\%(w/w)}}{100\%}.m_{solution}$$ Equation B- 18

Combining equation (3-15) and (3-16) and rearranging, moles of ammonia can be determined.

$$n_{NH3} = \frac{C_{\%(w/w)}}{m_M 100\%}.m_{solution}$$ Equation B- 19

The next step was to convert volume of solution to mass of solution using density of solution.

$$V_{solution} = \frac{m_{solution}}{1000.\rho_{solution}}$$ Equation B- 20

($\rho_{solution}$) is the density of ammonium hydroxide solution. Combining all the equations above Concentration of NH_3 in molarity can be determined as follows

$$C_M = \frac{n_{NH3}}{V_{solution}} = \frac{\frac{C_{\%(w/w)}}{m_M 100\%}.m_{solution}}{\frac{m_{solution}}{1000.\rho_{solution}}} = \frac{10C_{\%(w/w)}.\rho_{solution}}{m_M}$$ Equation B- 21

C_MWhere n_{NH3} is number of moles of NH_3 and $V_{solution}$ is the volume of the solution, m_M is molar mass of NH_3, $C_{\%(w/w)}$ is NH_3 concentration in weight percent, $m_{solution}$ is mass of the solution and ($\rho_{solution}$) is the density of ammonium hydroxide solution.

Table B- 13: Determining amount of reagents

C% (w/w) NH_3	28.00
Molar mass (g)	17.00
Density(g/cm^3)	0.90
Ammonia concentration in molarity (M)	14.82
Required concentration (M)	Stock solution (L)
2	0.44
4	0.88
Required concentration (M)	$(NH_4)_2CO_3$ (g)
0.50	155.83
1.00	311.65
2.00	623.30

Table B- 14: Full elemental analysis by ICP

constituent	**Al**	**Ba**	**Ca**	**Co**	**K**	**Na**	**Cr**	**Cu**	**Fe**	**Mg**	**Mn**	**Ni**	**P**	**Pb**	**Si**	**Ti**	**V**	**Zn**
Content (wt%)	0.58	< 0.05	< 0.05	< 0.05	0.01	0.05	1.01	< 0.05	9.08	17.5	0.13	1.76	< 0.05	< 0.05	16.6	< 0.05	< 0.05	< 0.05

Table B- 15: Chemical analysis of raw (CAF)

Major elements													
Constituents	Al_2O_3	CaO	Fe_2O_3	K_2O	MgO	MnO	Na_2O	P_2O_5	SiO_2	TiO_2	LOI	H_2O-	Sum
Content (Wt%)	0.75	0.013	16.73	BD	29.50	0.18	0.009	0.011	35.62	0.020	12.73	1.22	96.77
Minor elements													
Constituents	V	Cr	Co	Ni	Cu	Zn	Ga	Rb	Sr	Y	Zr	Nb	Ba
Content (ppm)	2	6035	226	22552	47	168	2	2	6	3	15	3	15

C Appendix C

C.1 Optimization reactions

Table C- 1: Experimental conditions and experimental results for optimization leaching experiments

			Solution pH	Solution pH	Ni content ppm	Ni content ppm	amount extracted		volume (ml)	volume (ml)	Ni extracted (g)	Ni extracted (g)		
	vapor at T (bar)	total P (bar)	below	above	below	above	initial mass of solids g	amount of nickel g	below	above	below	above	total nickel	% extracted
7	0.75	5.75	11	11.09	146	114.5	573.23	10.089	720	2480	0.11	0.28	0.39	3.86
15	1.8	3.8	10.38	10.43	199.2	189	572.17	10.07	750	2450	0.15	0.46	0.61	6.08
4	1	6	10.69	10.82	127.9	123.9	572	10.067	840	2360	0.11	0.29	0.40	3.97
12	1.2	4.2	10.35	10.78	197	191.2	572.04	10.068	700	2500	0.14	0.48	0.62	6.12
5	4	9	9.16	9.2	30.1	31.1	527.6	9.29	700	2500	0.02	0.081	0.10	1.06
10	4	7	9.9	10.39	327.2	288.6	572.5	10.076	635	2565	0.21	0.74	0.95	9.41
9	1.3	4.3	10.15	10.86	325.1	166.5	572.78	10.081	560	2640	0.18	0.44	0.62	6.17
13	2.3	5.3	10.5	10.98	280.6	227.8	572.01	10.067	360	2840	0.10	0.65	0.75	7.43
3	5	10	9.31	9.4	203.9	193	573.14	10.087	720	2480	0.15	0.480	0.63	6.20
18	2.1	5.1	10.48	10.8	296.3	203.1	572.5	10.076	310	2890	0.093	0.59	0.68	6.74
11	2.7	5.7	9.04	9.21	66.3	78.7	572.7	10.080	470	2730	0.030	0.21	0.25	2.44
8	1.5	3.5	8.92	9.19	27	35.6	572.5	10.076	640	2560	0.021	0.092	0.11	1.08
6	4	6	9.04	9.18	175.7	112	572.56	10.077	400	2800	0.073	0.31	0.38	3.81
1	4	7	11.24	11.53	400	368	572.08	10.069	640	2560	0.260	0.94	1.20	11.90
2	2	5.2	10.3	10.2	341	278.1	570	10.032	100	3100	0.034	0.86	0.90	8.93
14	2	5	10.31	10.41	215	226	572.55	10.077	65	3135	0.01	0.71	0.72	7.17
16	2	7	10.5	10.76	230.1	195	572.56	10.077	125	3075	0.032	0.60	0.63	6.24
17 (C)	2	5	10.68	10.75	306.7	210.4	572	10.067	50	3150	0.024	0.66	0.68	6.74

Table C- 2: ANOVA table for Ni extraction (linear effects and two-way interactions)

ANOVA; Var.:% extracted Ni; R-sqr=.7904

	Sum of squares	Degrees of Freedom	Mean squares	F	p
(1)Temperature ^{o}C(L)	1.87	1.00	1.87	0.47	0.51
(2)Ammonia concentration M(L)	1.61	1.00	1.61	0.40	0.55
(3)ammonium carbonate concentration M(L)	9.036	1.00	9.036	2.25	0.18
(4)Oxygen pressure bar(L)	2.44	1.00	2.44	0.61	0.46
1L by 2L	0.097	1.00	0.097	0.024	0.88
1L by 3L	3.99	1.00	3.99	1.00	0.35
1L by 4L	1.032	1.00	1.03	0.26	0.63
2L by 3L	3.37	1.00	3.37	0.84	0.39
2L by 4L	0.80	1.00	0.80	0.20	0.67
3L by 4L	0.018	1.00	0.018	0.004	0.95
Error	28.10	7.00	4.014		
Total SS	134.054	17.00			

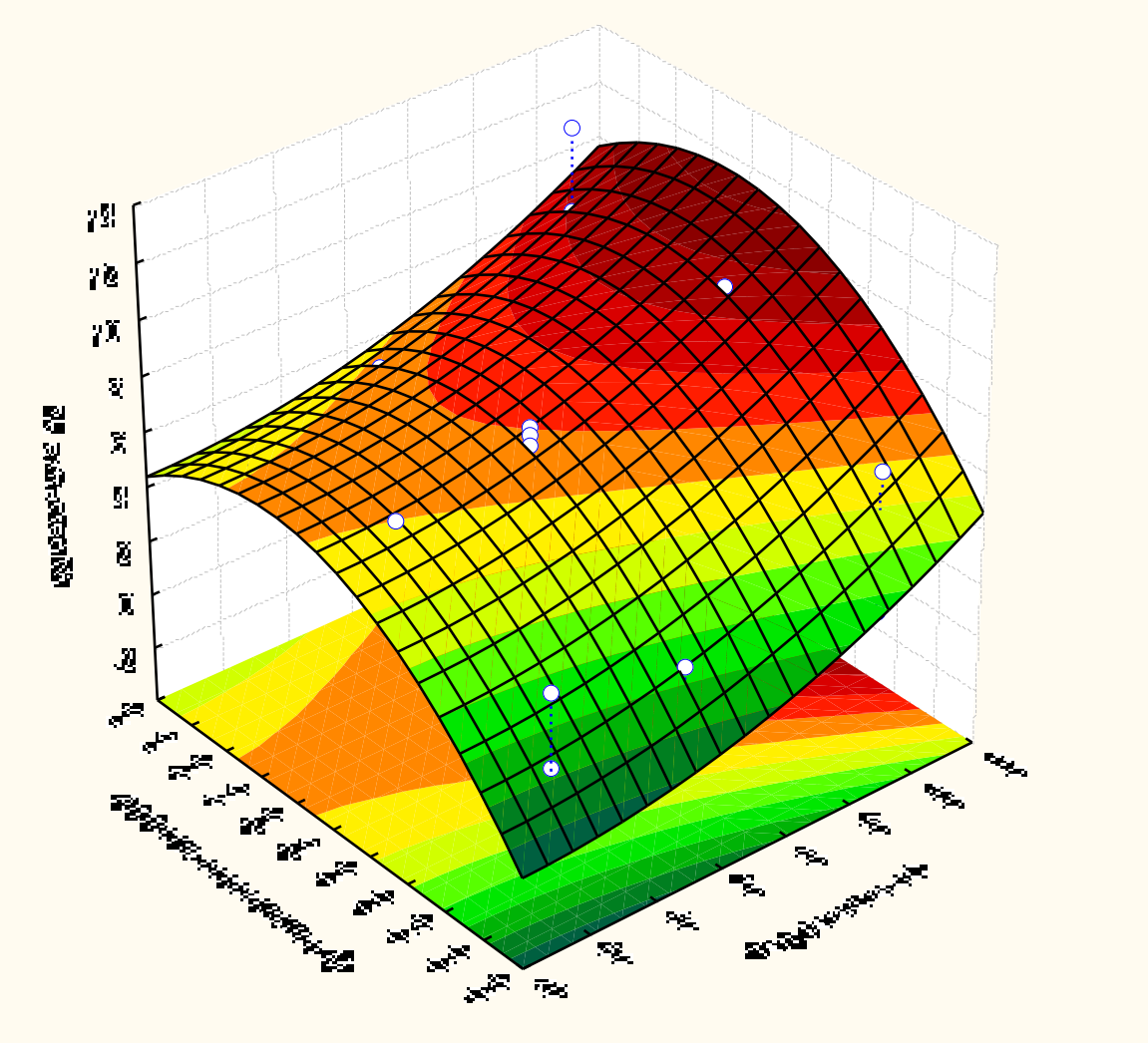

Figure C- 1: Variation of % Ni extraction with [NH3] and temperature

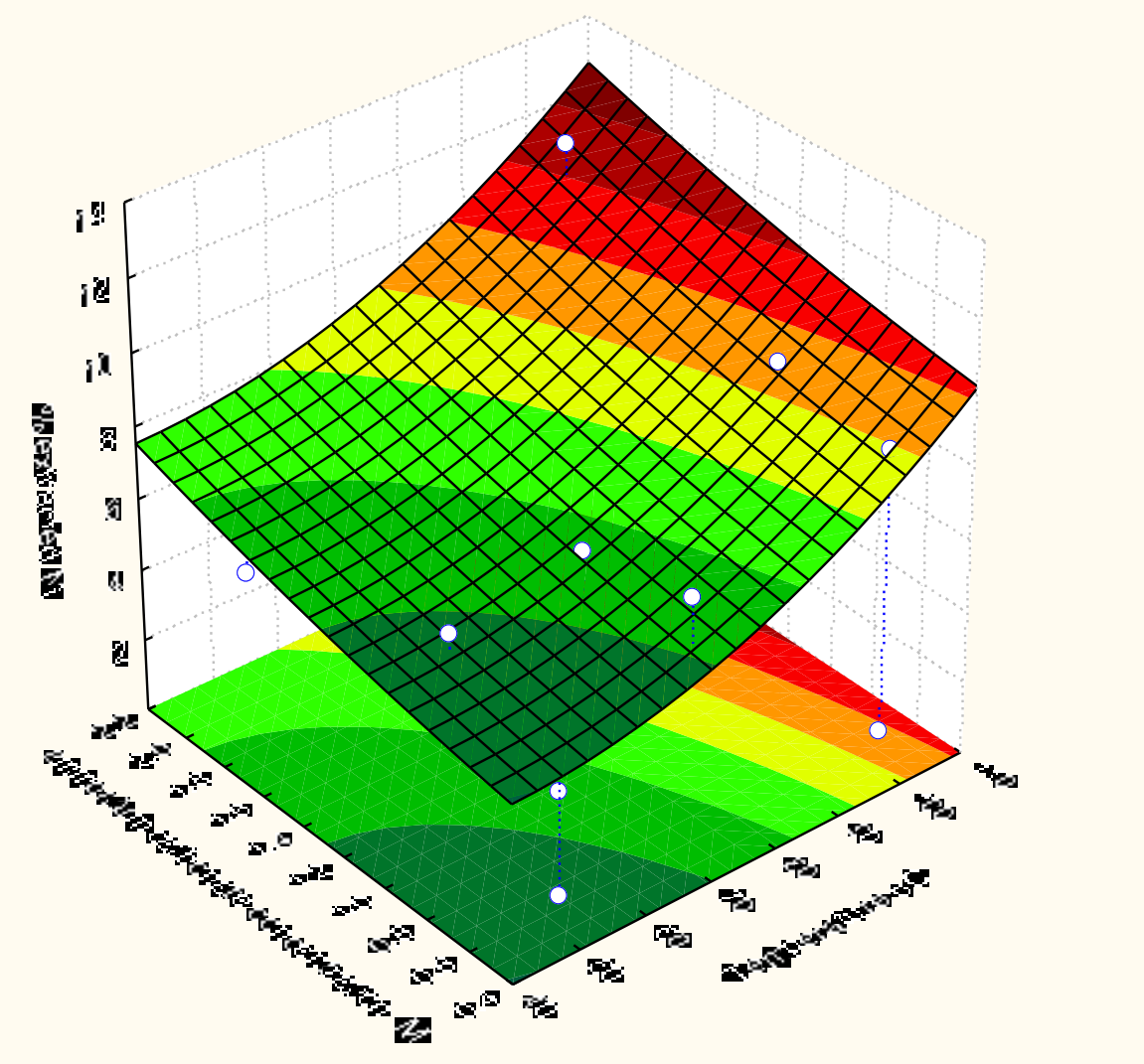

Figure C- 2: Variation of %Ni extraction with $[(NH_4)_2CO_3]$ with temperature

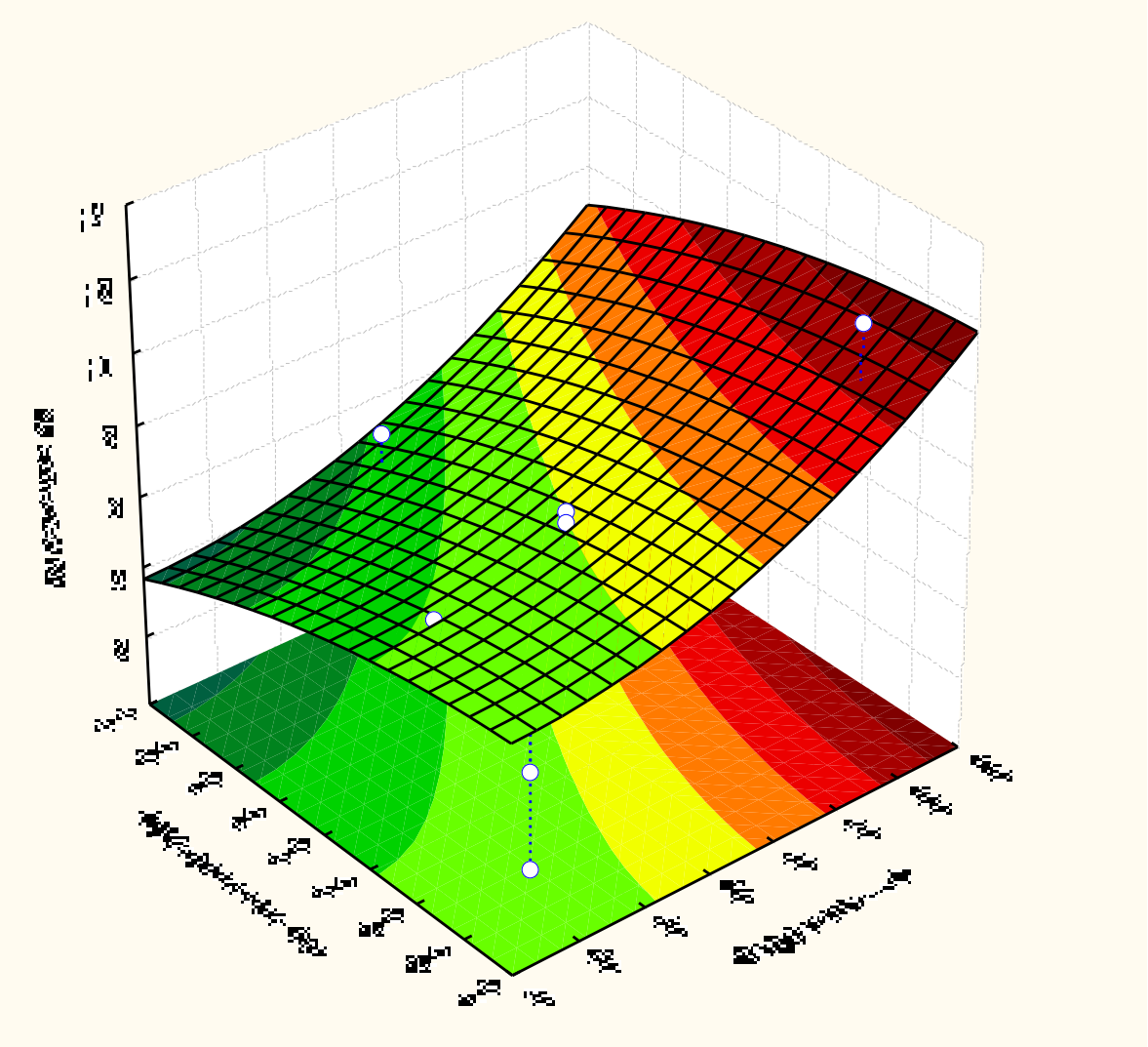

Figure C- 3: Variation of % Ni extraction with O_2 pressure and temperature

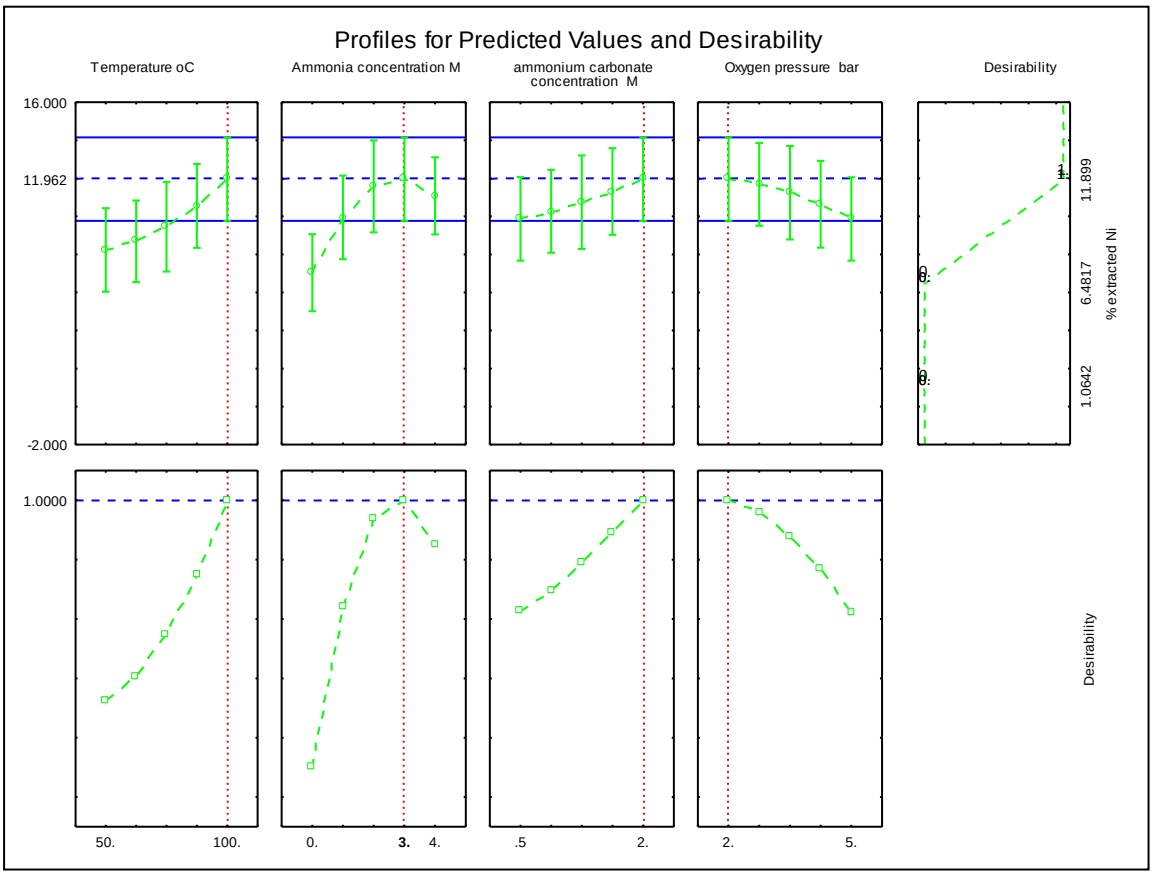

Figure C- 4: Profiles of predicted response and desirability

C.2 Chemical and mineralogical analysis of the ore

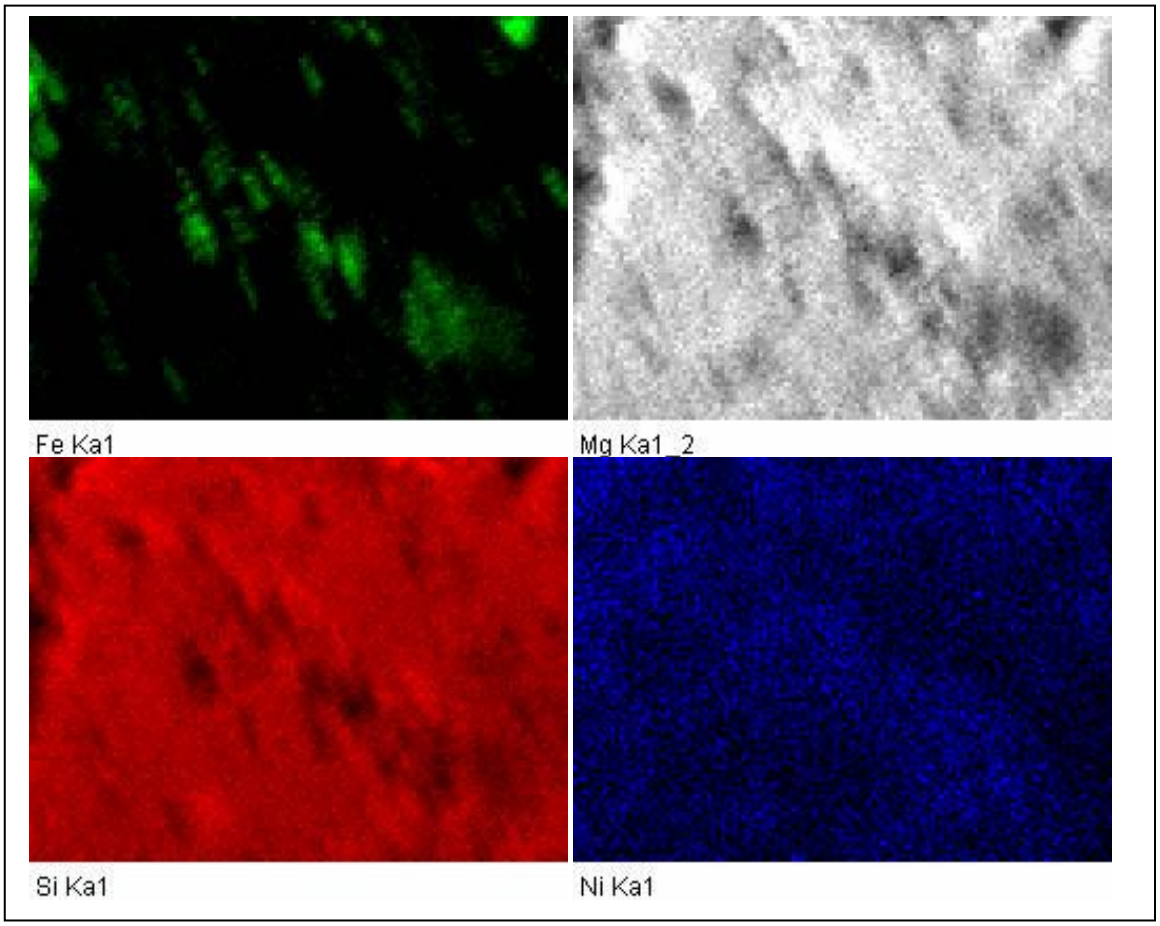

Figure C- 5: Distribution of Si, Mg, Fe, and Ni in raw Saprolitic laterite (Bright green=Fe, Red Si, Grey=Mg and Bright blue=Ni)

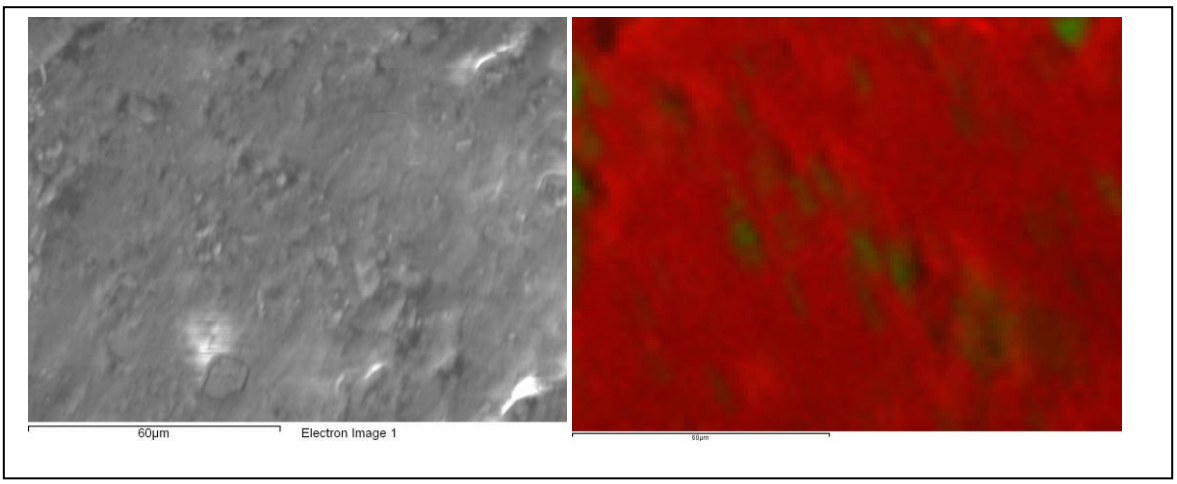

Figure C- 6: SEM image of raw ore and Mixed map of Ni,Si Fe and Mg

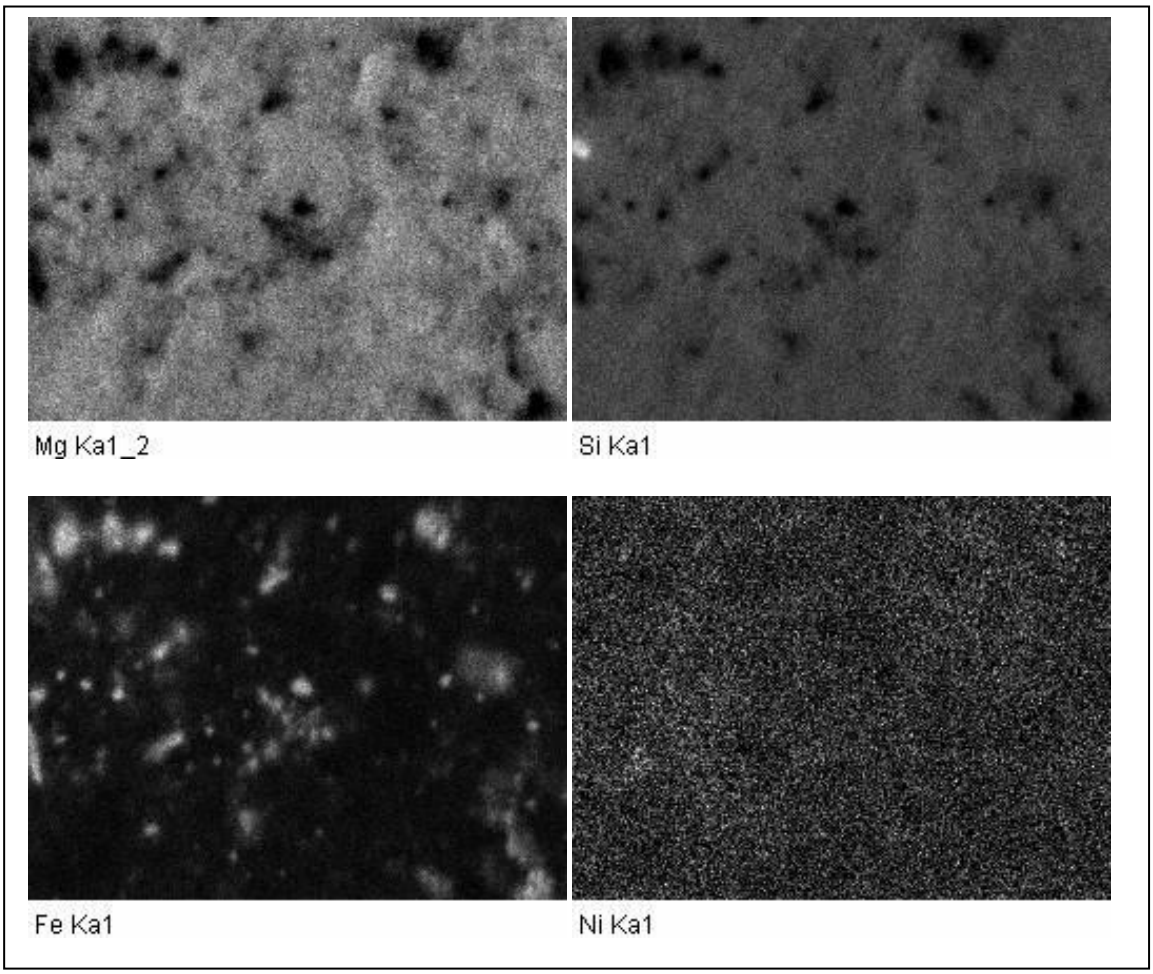

Figure C- 7: Distribution of Si, Mg, Fe, and Ni in leached Saprolitic laterite

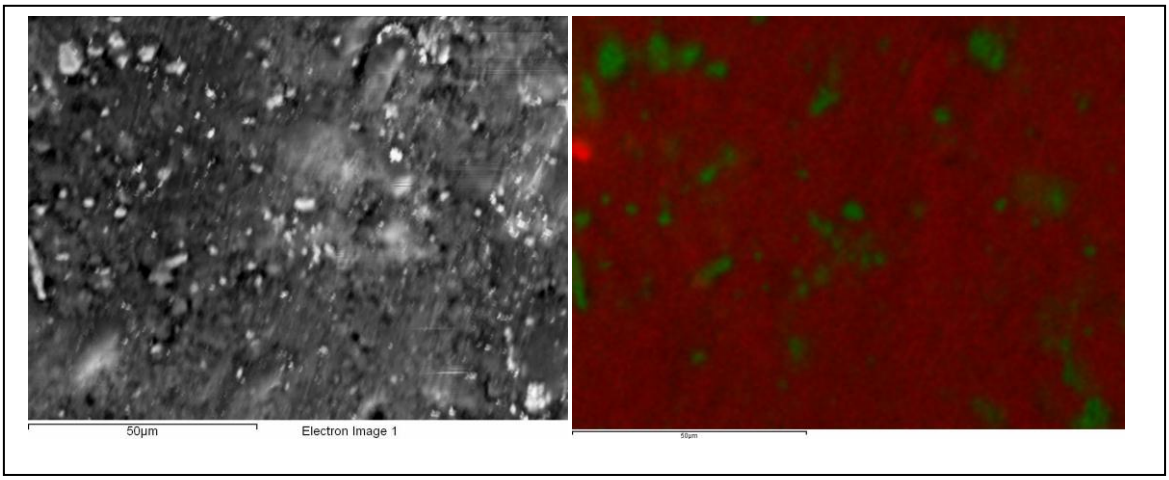

Figure C- 8: SEM image of leached ore and Mixed map of Ni, Si, Fe and Mg

C.3 Kinetic reactions for the unroasted ore

Table C- 3: Effect of temperature of Ni extraction for the unroasted saprolitic laterite

time	Effect of Temperature 2M $(NH_4)_2CO_3$, 3M NH_3, and O_2 pressure 4 bar															
	40°C				60°C				80°C				100°C			
	V (L)	Ni (ppm)	pH	Ni extraction	V (L)	Ni (ppm)	pH	Ni extraction	V (L)	Ni (ppm)	pH	Ni extraction	V (L)	Ni (ppm)	pH	Ni extraction
0	0	0			0	0			0	0			0	0		
15	0.042	100	10.01	0.035	0.045	103	9.98	0.036	0.045	184	9.88	0.064	0.045	227	10.04	0.078
30	0.045	78	9.96	0.027	0.045	108	9.96	0.037	0.045	221	9.86	0.076	0.045	290	9.98	0.100
60	0.045	82	9.95	0.028	0.045	127	9.94	0.044	0.045	225	9.86	0.077	0.045	296	9.96	0.102
90	0.045	85	9.95	0.029	0.045	146	9.94	0.050	0.045	258	9.86	0.088	0.045	317	9.96	0.109
120	0.045	85	9.95	0.029	0.045	152	9.94	0.052	0.045	269	9.86	0.093	0.045	331	9.96	0.114
150	0.045	93	9.95	0.032	0.045	157	9.94	0.054	0.045	282	9.86	0.097	0.045	332	9.96	0.115
180	0.045	90	9.95	0.031	0.045	163	9.94	0.056	0.045	283	9.86	0.098	0.045	376	9.96	0.129

Table C- 4: Effect ammonia concentration on Ni extraction for the unroasted saprolitic laterite

time	Effect of Ammonia Concentration 2M $(NH_4)_2CO_3$, T=100^oC and 4 bar O_2 pressure															
	0M				1M				2M				3M			
	V (L)	Ni (ppm)	pH	Ni extraction	V (L)	Ni (ppm)	pH	Ni extraction	V (L)	Ni (ppm)	pH	Ni extraction	V (L)	Ni (ppm)	pH	Ni extraction
0	0	0		0	0	0		0	0	0		0	0	0		0
15	0.045	148	9	0.051	0.045	217	9.62	0.075	0.045	240	9.76	0.083	0.045	227	10.04	0.078
30	0.045	153	9	0.053	0.045	236	9.6	0.081	0.045	272	9.74	0.094	0.045	290	9.98	0.100
60	0.045	161	8.75	0.055	0.045	268	9.61	0.092	0.045	291	9.74	0.100	0.045	296	9.96	0.102
90	0.045	171	8.73	0.059	0.045	281	9.61	0.096	0.045	322	9.73	0.110	0.045	317	9.96	0.109
120	0.045	178	8.73	0.061	0.045	300	9.61	0.104	0.045	336	9.73	0.116	0.045	331	9.96	0.114
150	0.045	200	8.73	0.069	0.045	316	9.61	0.109	0.045	346	9.73	0.119	0.045	332	9.96	0.115
180	0.045	200	8.73	0.069	0.045	315	9.61	0.109	0.045	354	9.73	0.122	0.045	376	9.96	0.129

Table C- 5: Effect of ammonium carbonate concentration on Ni extraction for the unroasted saprolitic laterite

time	Effect of Ammonium carbonate 3M NH_3, T=100^oC and 4 bar O_2 pressure															
	0M				1M				2M				3M			
	V (L)	Ni (ppm)	pH	Ni extraction	V (L)	Ni (ppm)	pH	Ni extraction	V (L)	Ni (ppm)	pH	Ni extraction	V (L)	Ni (ppm)	pH	Ni extraction
0	0	0		0	0	0	10.19	0	0	0		0	0	0		0
15	0.045	25	11.48	0.009	0.045	248	10.18	0.086	0.045	227	10.04	0.078	0.045	252	9.82	0.087
30	0.045	20	11.4	0.007	0.045	259	10.19	0.089	0.045	290	9.98	0.100	0.038	275	9.82	0.095
60	0.045	17	11.38	0.006	0.045	289	10.18	0.099	0.045	296	9.96	0.102	0.035	288	9.83	0.099
90	0.045	16	11.4	0.006	0.045	319	10.18	0.109	0.045	317	9.96	0.109	0.03	315	9.83	0.114
120	0.045	16	11.38	0.006	0.045	330	10.18	0.114	0.045	331	9.96	0.114	0.03	345	9.82	0.125
150	0.045	12	11.35	0.004	0.045	348	10.18	0.120	0.045	332	9.96	0.115	0.031	345	9.82	0.136
180	0.045	12	11.34	0.004	0.045	357	10.18	0.123	0.045	376	9.96	0.129	0.04	380	9.82	0.131

Table C- 6: Effect of Oxygen pressure on Ni extraction for the unroasted saprolitic laterite

time	Effect of Oxygen pressure (bar) 3M NH_3, 2M $(NH_4)_2CO_3$) and T=100^oC															
	0 bar				2 bar				4 bar				5 bar			
	V (L)	Ni (ppm)	pH	Ni extraction	V (L)	Ni (ppm)	pH	Ni extraction	V (L)	Ni (ppm)	pH	Ni extraction	V (L)	Ni (ppm)	pH	Ni extraction
0	0	0			0	0		0	0	0			0	0		0
15	0.04	242	9.99	0.084	0.04	252	9.97	0.087	0.04	227	9.99	0.078	0.04	265	10.04	0.092
30	0.04	277	9.96	0.096	0.04	286	9.95	0.099	0.04	290	9.97	0.100	0.04	322	9.98	0.111
60	0.04	299	9.96	0.103	0.04	320	9.95	0.110	0.04	296	9.97	0.102	0.04	331	9.96	0.114
90	0.04	301	9.96	0.104	0.04	347	9.96	0.119	0.04	317	9.96	0.109	0.04	358	9.96	0.123
120	0.04	316	9.96	0.109	0.04	369	9.95	0.127	0.04	331	9.96	0.114	0.04	371	9.96	0.128
150	0.04	333	9.96	0.115	0.04	371	9.95	0.128	0.04	332	9.96	0.115	0.04	389	9.96	0.134
180	0.04	334	9.96	0.115	0.04	394	9.95	0.136	0.04	376	9.96	0.129	0.04	400	9.96	0.138

Table C- 7: Effect of temperature on shrinking core models for the unroasted ore

time (min)	Effect of Temperature (2M $(NH_4)_2CO_3$), 3M NH_3, and O_2 pressure 4 bar									
	40°C					60°C				
	Ni (ppm)	X	$1-(1-x)^{1/3}$	$1-3(1-x)^{2/3}+2*(1-x)$	$1-2(1-x)^{1/3}+(1-x)^{2/3}$	Ni (ppm)	X	$1-(1-x)^{1/3}$	$1-3(1-x)^{2/3}+2*(1-x)$	$1-2(1-x)^{1/3}+(1-x)^{2/3}$
0	0.000		0.000	0.000	0.000	0.000	0.000	0.000	0.000	0.000
15	120.000	0.035	0.012	0.000	0.000	103.000	0.036	0.012	0.000	0.000
30	78.000	0.027	0.009	0.000	0.000	108.000	0.037	0.013	0.000	0.000
60	82.000	0.028	0.010	0.000	0.000	127.000	0.044	0.015	0.001	0.000
90	85.000	0.029	0.010	0.000	0.000	146.000	0.050	0.017	0.001	0.000
120	85.000	0.029	0.010	0.000	0.000	152.000	0.052	0.018	0.001	0.000
150	90.000	0.032	0.011	0.000	0.000	157.000	0.054	0.018	0.001	0.000
180	93.000	0.031	0.010	0.000	0.000	163.000	0.056	0.019	0.001	0.000

	80°C					100°C				
Ni (ppm)	X	$1-(1-x)^{1/3}$	$1-3(1-x)^{2/3}+2(1-x)$	$1-2(1-x)^{1/3}+(1-x)^{2/3}$		Ni (ppm)	X	$1-(1-x)^{1/3}$	$1-3(1-x)^{2/3}+2*(1-x)$	$1-2(1-x)^{1/3}+(1-x)^{2/3}$
0.000	0.000	0.000	0.000	0.000		0.000	0.000	0.000	0.000	0.000
184.000	0.064	0.022	0.001	0.000		227.000	0.078	0.027	0.002	0.001
221.000	0.076	0.026	0.002	0.001		290.000	0.100	0.034	0.003	0.001
225.000	0.077	0.027	0.002	0.001		296.000	0.102	0.035	0.004	0.001
258.000	0.088	0.030	0.003	0.001		317.000	0.109	0.038	0.004	0.001
269.000	0.093	0.032	0.003	0.001		331.000	0.114	0.040	0.005	0.002
282.000	0.097	0.034	0.003	0.001		332.000	0.115	0.040	0.005	0.002
283.000	0.098	0.034	0.003	0.001		376.000	0.129	0.045	0.006	0.002

Table C- 8: Effect of ammonia concentration on shrinking core models for the unroasted ore

t(min)	Effect of Ammonia Concentration (2M $(NH_4)_2CO_3$), T=100°C and 4 bar O_2 pressure									
	0M					1M				
	Ni (ppm)	X	$1-(1-x)^{1/3}$	$1-3(1-x)^{2/3}+2(1-x)$	$1-2(1-x)^{1/3}+(1-x)^{2/3}$	Ni (ppm)	X	$1-(1-x)^{1/3}$	$1-3(1-x)^{2/3}+2*(1-x)$	$1-2(1-x)^{1/3}+(1-x)^{2/3}$
0	0.000	0.000	0.000	0.000	0.000	0.000	0.000	0.000	0.000	0.000
15	148.000	0.051	0.017	0.001	0.000	217.000	0.075	0.026	0.002	0.001
30	153.000	0.053	0.018	0.001	0.000	236.000	0.081	0.028	0.002	0.001
60	161.000	0.055	0.019	0.001	0.000	268.000	0.092	0.032	0.003	0.001
90	171.000	0.059	0.020	0.001	0.000	281.000	0.096	0.033	0.003	0.001
120	178.000	0.061	0.021	0.001	0.000	300.000	0.104	0.036	0.004	0.001
150	200.000	0.069	0.023	0.002	0.001	316.000	0.109	0.038	0.004	0.001
180	200.000	0.069	0.023	0.002	0.001	315.000	0.109	0.038	0.004	0.001

2M					3M				
Ni (ppm)	X	$1-(1-x)^{1/3}$	$1-3(1-x)^{2/3}+2(1-x)$	1-2(1-x)^(1/3)+(1-x)^(2/3	Ni (ppm)	X	$1-(1-x)^{1/3}$	$1-3(1-x)^{2/3}+2*(1-x)$	$1-2(1-x)^{1/3}+(1-x)^{2/3}$
0.000	0.000	0.000	0.000	0.000	0.000	0.000	0.000	0.000	0.000
240.000	0.083	0.028	0.002	0.001	227.000	0.078	0.027	0.002	0.001
272.000	0.094	0.032	0.003	0.001	290.000	0.100	0.034	0.003	0.001
291.000	0.100	0.035	0.003	0.001	296.000	0.102	0.035	0.004	0.001
322.000	0.110	0.038	0.004	0.001	317.000	0.109	0.038	0.004	0.001
336.000	0.116	0.040	0.005	0.002	331.000	0.114	0.040	0.005	0.002
346.000	0.119	0.041	0.005	0.002	350.000	0.121	0.042	0.005	0.002
354.000	0.122	0.042	0.005	0.002	376.000	0.129	0.045	0.006	0.002

Table C- 9: Effect ammonium carbonate concentration on shrinking core models for the unroasted ore

time (min)	Effect of Ammonium carbonate (3M NH^3), T=100^oC and 4 bar O_2 pressure									
	1M					2M				
	Ni (ppm)	X	$1-(1-x)^{1/3}$	$1-3(1-x)^{2/3}+2(1-x)$	$1-2(1-x)^{1/3}+(1-x)^{2/3}$	Ni (ppm)	X	$1-(1-x)^{1/3}$	$1-3(1-x)^{2/3}+2*(1-x)$	$1-2(1-x)^{1/3}+(1-x)^{2/3}$
0	0.000	0.000	0.000	0.000	0.000	0.000	0.000	0.000	0.000	0.000
15	25.000	0.009	0.003	0.000	0.000	248.000	0.086	0.029	0.003	0.001
30	20.000	0.007	0.002	0.000	0.000	259.000	0.089	0.031	0.003	0.001
60	17.000	0.006	0.002	0.000	0.000	289.000	0.099	0.034	0.003	0.001
90	16.000	0.006	0.002	0.000	0.000	319.000	0.109	0.038	0.004	0.001
120	16.000	0.006	0.002	0.000	0.000	330.000	0.114	0.040	0.005	0.002
150	12.000	0.004	0.001	0.000	0.000	348.000	0.120	0.042	0.005	0.002
180	12.000	0.004	0.001	0.000	0.000	357.000	0.123	0.043	0.005	0.002

3M					4M				
Ni (ppm)	X	$1-(1-x)^{1/3}$	$1-3(1-x)^{2/3}+2(1-x)$	$1-2(1-x)^{1/3}+(1-x)^{2/3}$	Ni (ppm)	X	$1-(1-x)^{1/3}$	$1-3(1-x)^{2/3}+2*(1-x)$	$1-2(1-x)^{1/3}+(1-x)^{2/3}$
0.000	0.000	0.000	0.000	0.000	0.000	0.000	0.000	0.000	0.000
227.000	0.078	0.027	0.002	0.001	252.000	0.087	0.030	0.003	0.001
290.000	0.100	0.034	0.003	0.001	275.000	0.095	0.033	0.003	0.001
296.000	0.102	0.035	0.004	0.001	288.000	0.099	0.034	0.003	0.001
317.000	0.109	0.038	0.004	0.001	315.000	0.114	0.039	0.005	0.002
331.000	0.114	0.040	0.005	0.002	320.000	0.125	0.044	0.006	0.002
350.000	0.121	0.042	0.005	0.002	370.000	0.128	0.045	0.006	0.002
376.000	0.129	0.045	0.006	0.002	380.000	0.131	0.046	0.006	0.002

Table C- 10: Effect of oxygen pressure on shrinking core models for the unroasted ore

time (min)	Effect of Oxygen pressure (bar) (3M NH_3, 2M $(NH_4)_2CO_3$) and T=100^oC									
	0 bar					2bar				
	Ni (ppm)	X	$1-(1-x)^{1/3}$	$1-3(1-x)^{2/3}+2*(1-x)$	$1-2(1-x)^{1/3}+(1-x)^{2/3}$	Ni (ppm)	X	$1-(1-x)^{1/3}$	$1-3(1-x)^{2/3}+2*(1-x)$	$1-2(1-x)^{1/3}+(1-x)^{2/3}$
0	0.000		0.000	0.000	0.000	0.000	0.000	0.000	0.000	0.000
15	242.000	0.084	0.029	0.002	0.001	252.000	0.087	0.030	0.003	0.001
30	277.000	0.096	0.033	0.003	0.001	286.000	0.099	0.034	0.003	0.001
60	299.000	0.103	0.036	0.004	0.001	320.000	0.110	0.038	0.004	0.001
90	301.000	0.104	0.036	0.004	0.001	347.000	0.119	0.041	0.005	0.002
120	316.000	0.109	0.038	0.004	0.001	369.000	0.127	0.044	0.006	0.002
150	333.000	0.115	0.040	0.005	0.002	371.000	0.128	0.045	0.006	0.002
180	334.000	0.115	0.040	0.005	0.002	394.000	0.136	0.047	0.007	0.002

4bar					5bar				
Ni (ppm)	X	$1-(1-x)^{1/3}$	$1-3(1-x)^{2/3}+2*(1-x)$	$1-2(1-x)^{1/3}+(1-x)^{2/3}$	Ni (ppm)	X	$1-(1-x)^{1/3}$	$1-3(1-x)^{2/3}+2*(1-x)$	$1-2(1-x)^{1/3}+(1-x)^{2/3}$
0.000		0.000	0.000	0.000	0.000	0.000	0.000	0.000	0.000
227.000	0.078	0.027	0.002	0.001	265.000	0.092	0.032	0.003	0.001
290.000	0.100	0.034	0.003	0.001	322.000	0.111	0.038	0.004	0.001
296.000	0.102	0.035	0.004	0.001	331.000	0.114	0.040	0.005	0.002
317.000	0.109	0.038	0.004	0.001	358.000	0.123	0.043	0.005	0.002
331.000	0.114	0.040	0.005	0.002	371.000	0.128	0.045	0.006	0.002
332.000	0.115	0.040	0.005	0.002	389.000	0.134	0.047	0.006	0.002
376.000	0.129	0.045	0.006	0.002	400.000	0.138	0.048	0.007	0.002

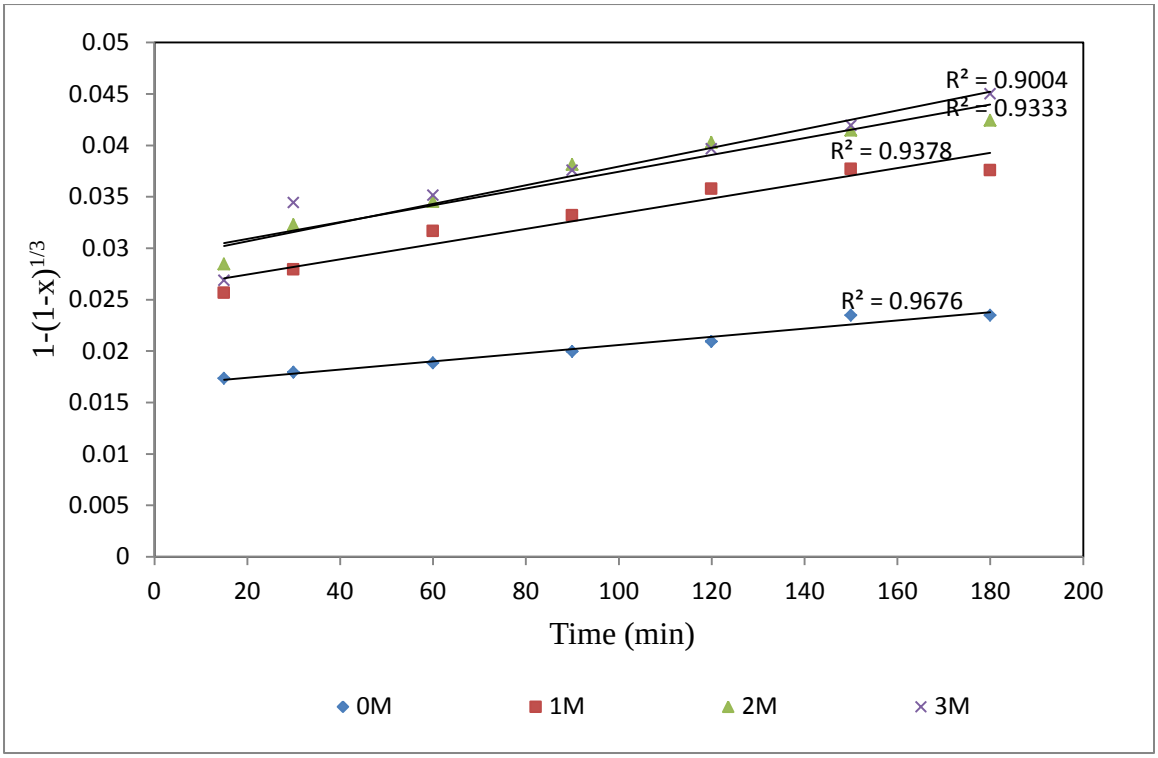

Figure C- 9: Plot of $1-(1-x)^{1/3}$ vs time for leaching nickel from unroasted saprolitic laterite at different $[NH_3]$

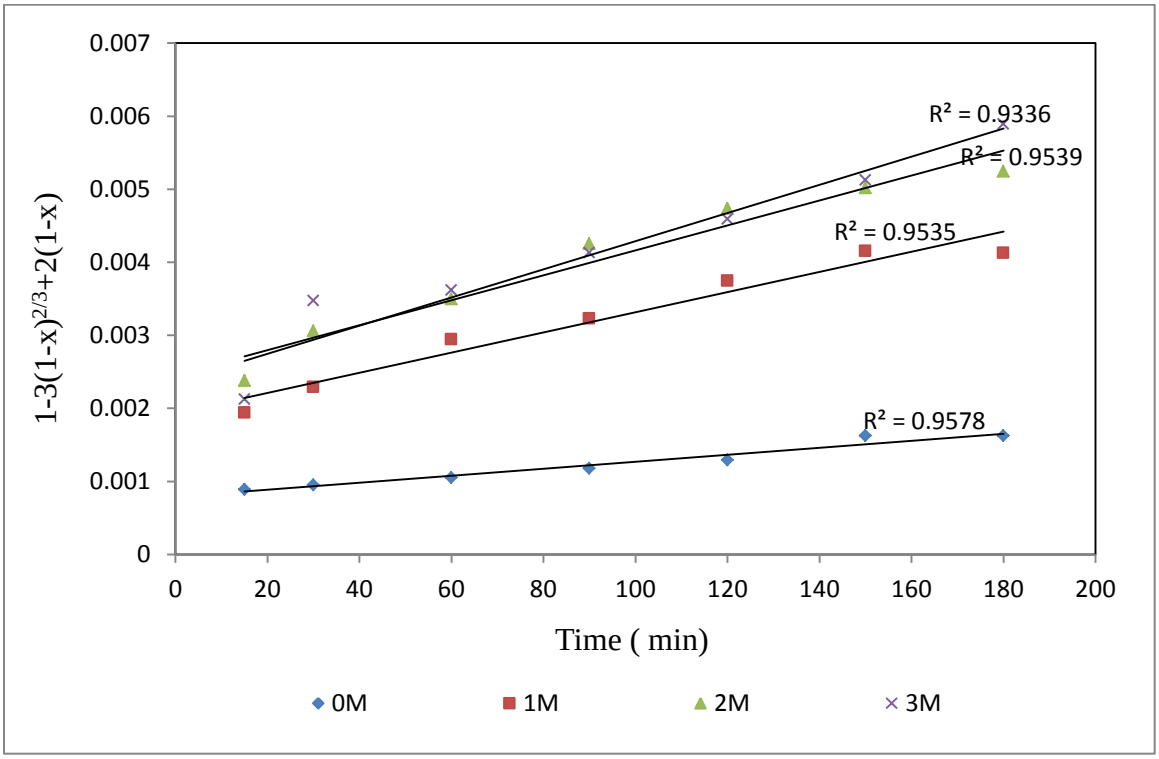

Figure C- 10: Plot of $1-3(1-x)^{2/3}+2(1-x)$ vs time for leaching nickel from unroasted saprolitic laterite at different at $[NH_3]$

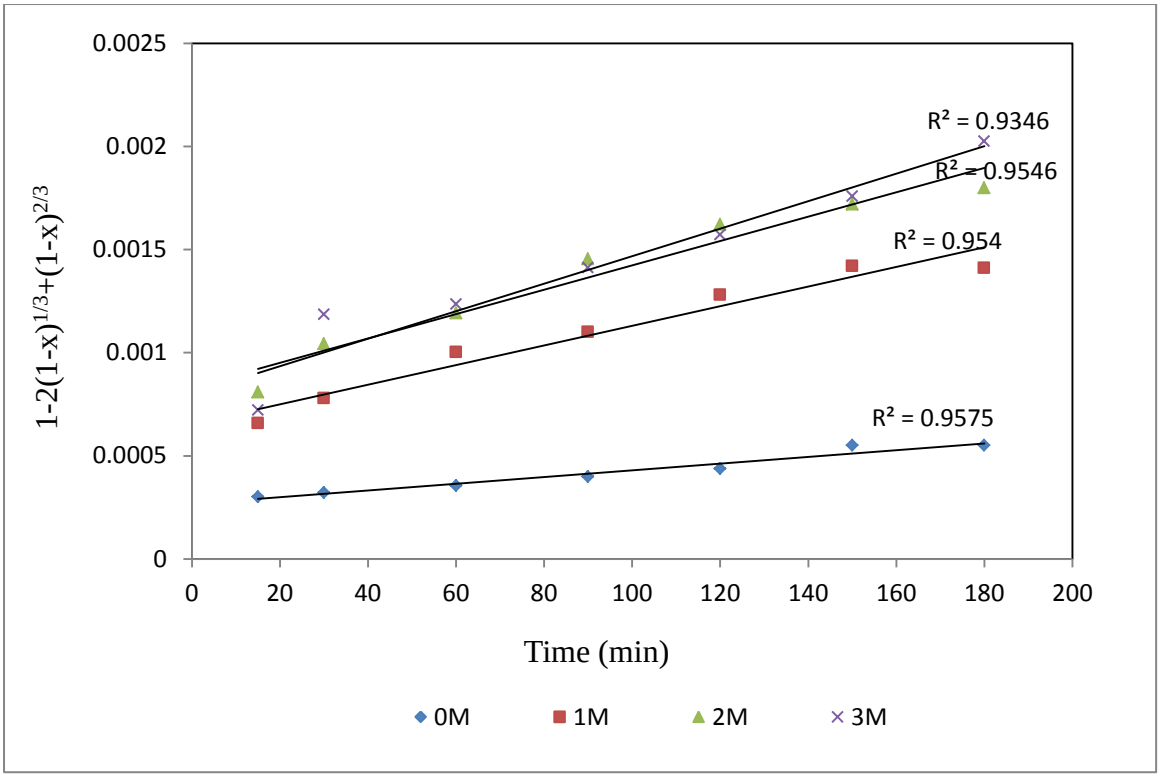

Figure C- 11: Plot of $1-2(1-x)^{1/3}+(1-x)^{2/3}$ vs time for leaching nickel from unroasted saprolitic laterite at different $[NH_3]$

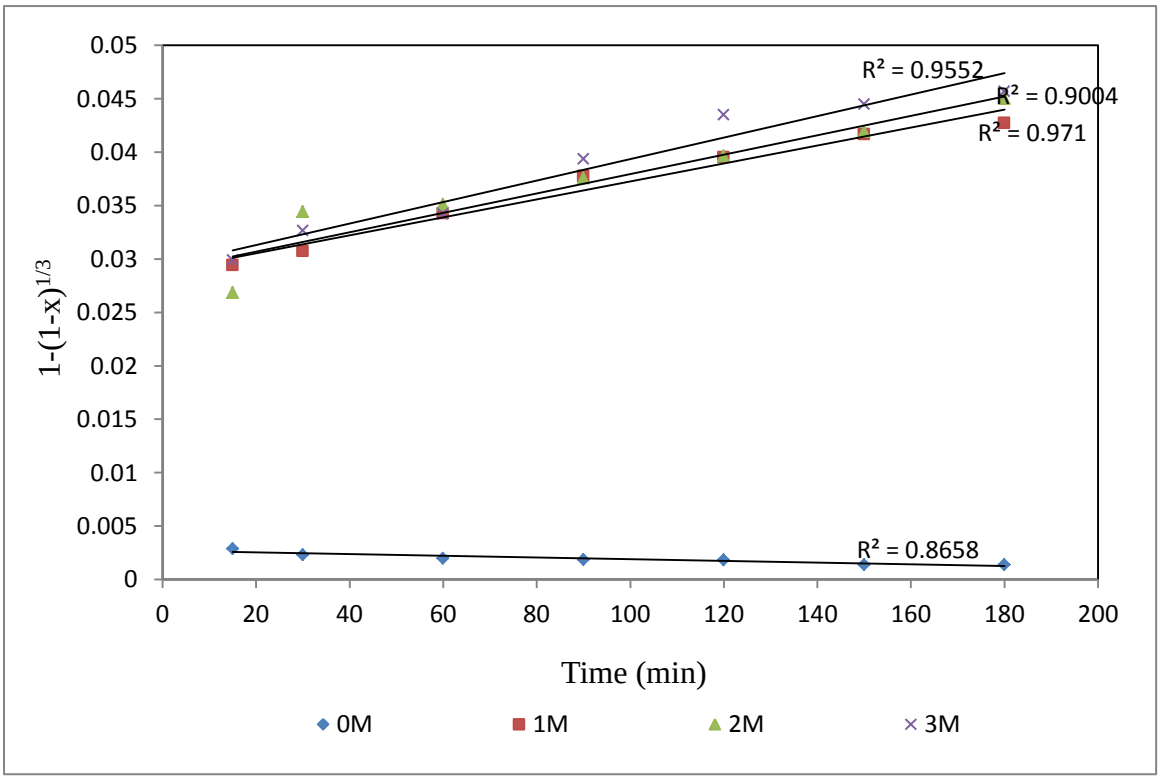

Figure C- 12: Plot of $1-(1-x)^{1/3}$ vs time for leaching nickel from unroasted saprolitic laterite at different $[(NH_4)_2CO_3]$

APPENDICES

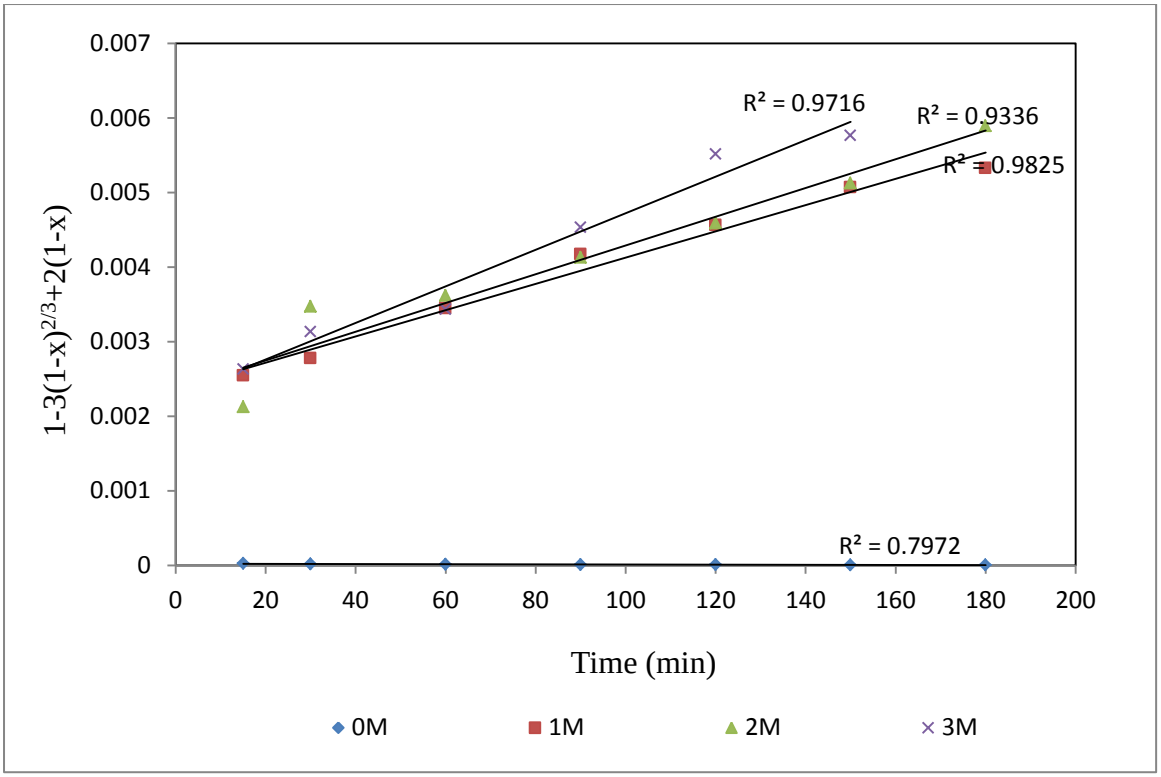

Figure C- 13: Plot of $1-3(1-x)^{2/3}+2(1-x)$ vs time for leaching nickel from unroasted saprolitic laterite at different $[(NH_4)_2CO_3]$

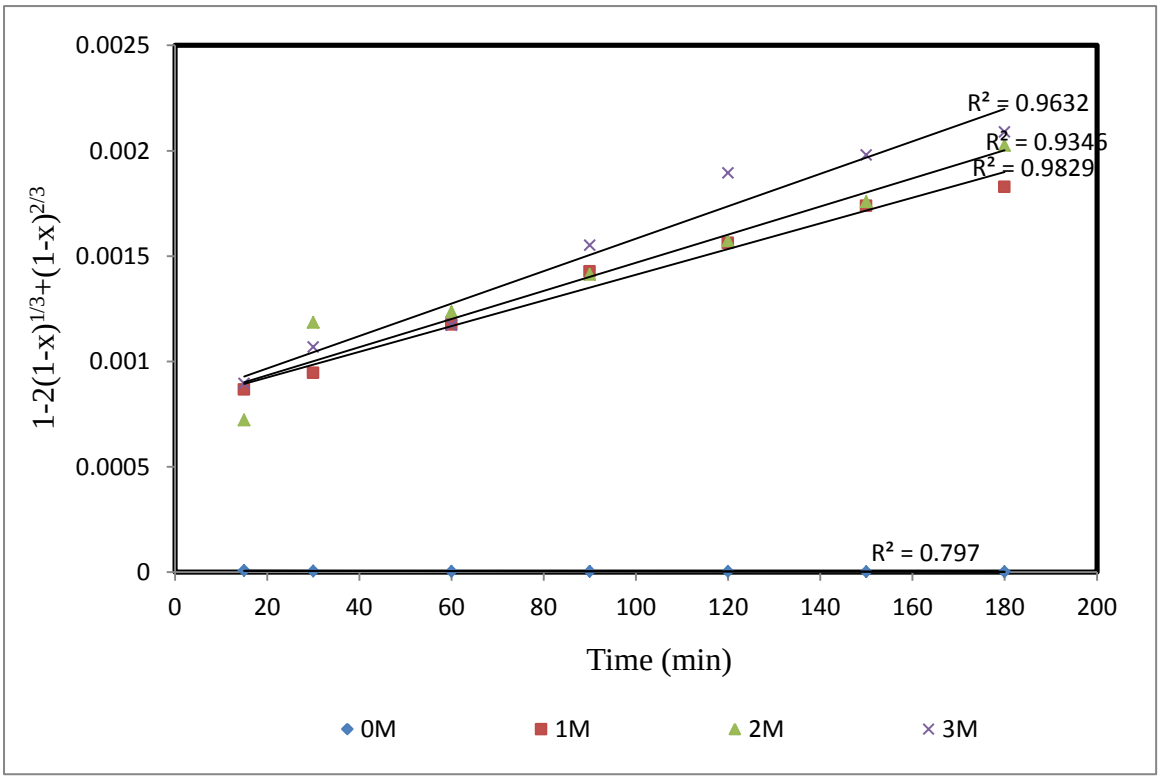

Figure C- 14: Plot of $1-2(1-x)^{1/3}+(1-x)^{2/3}$ vs time for leaching nickel from unroasted saprolitic laterite at different $[(NH_4)_2CO_3]$

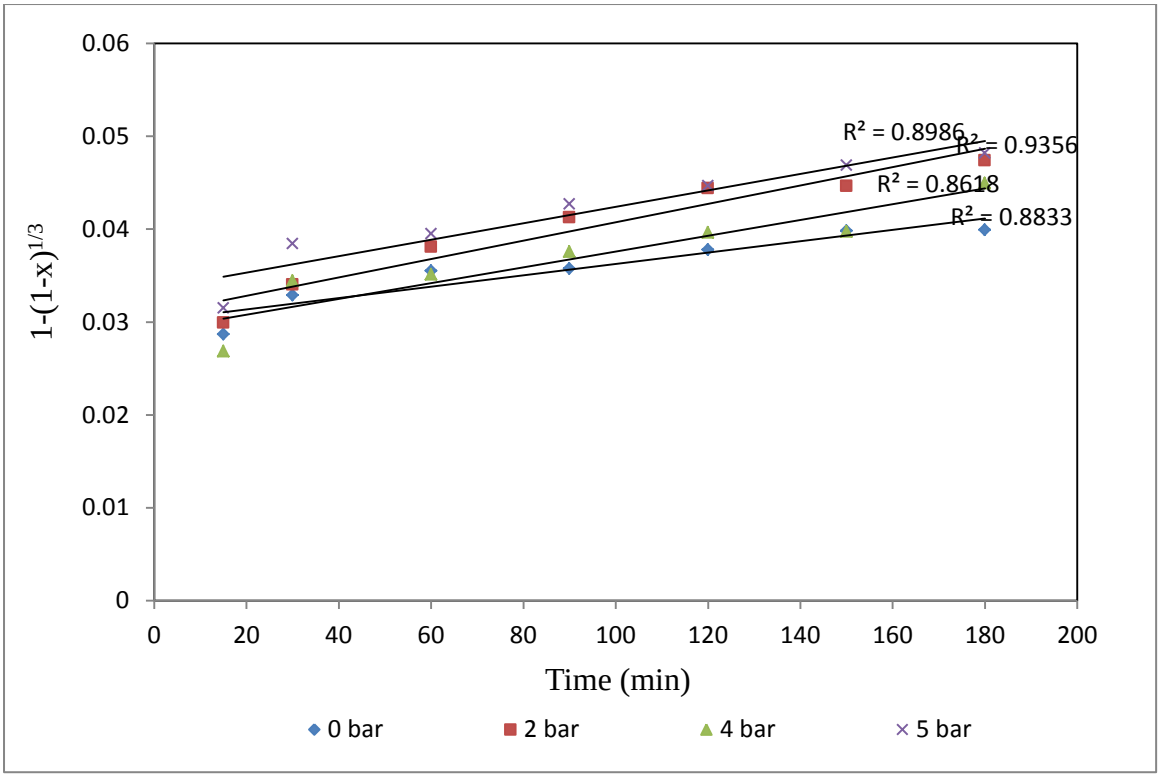

Figure C- 15: Plot of $1-(1-x)^{1/3}$ vs time for leaching nickel from unroasted saprolitic laterite at different O_2 pressure

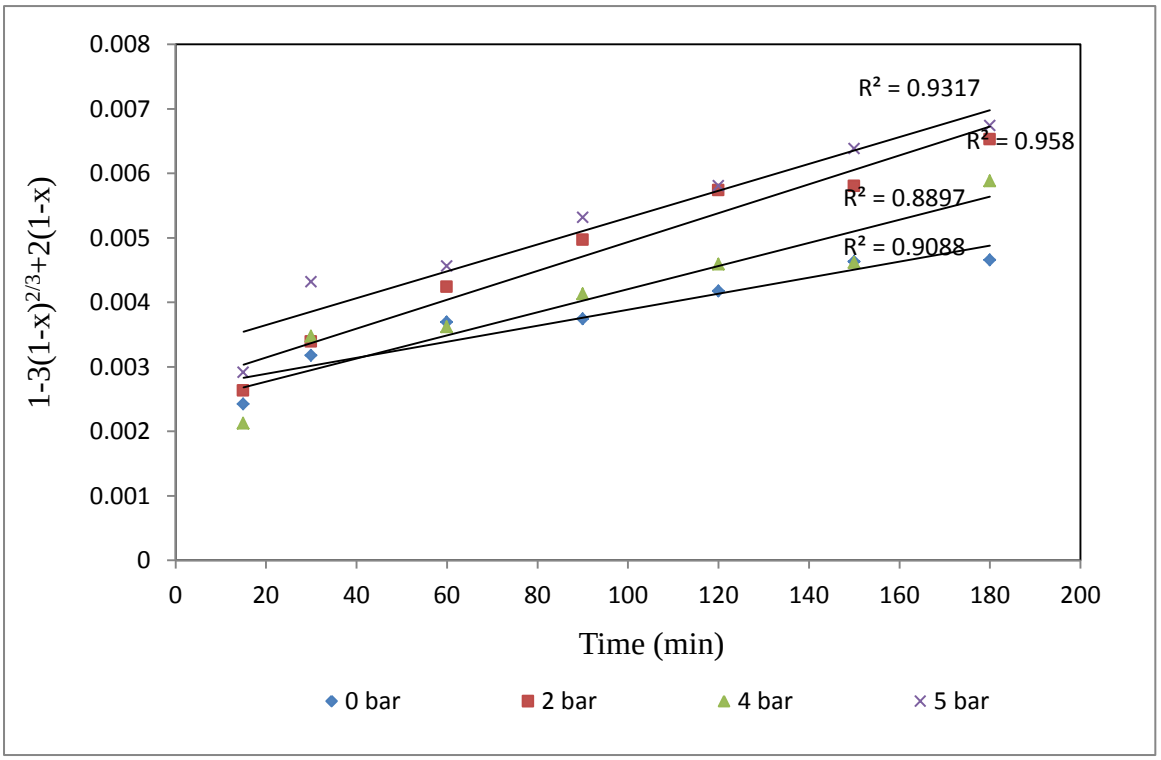

Figure C- 16: Plot of $1-3(1-x)^{2/3}+2(1-x)$ vs time for leaching nickel from unroasted saprolitic laterite at different O_2 pressure

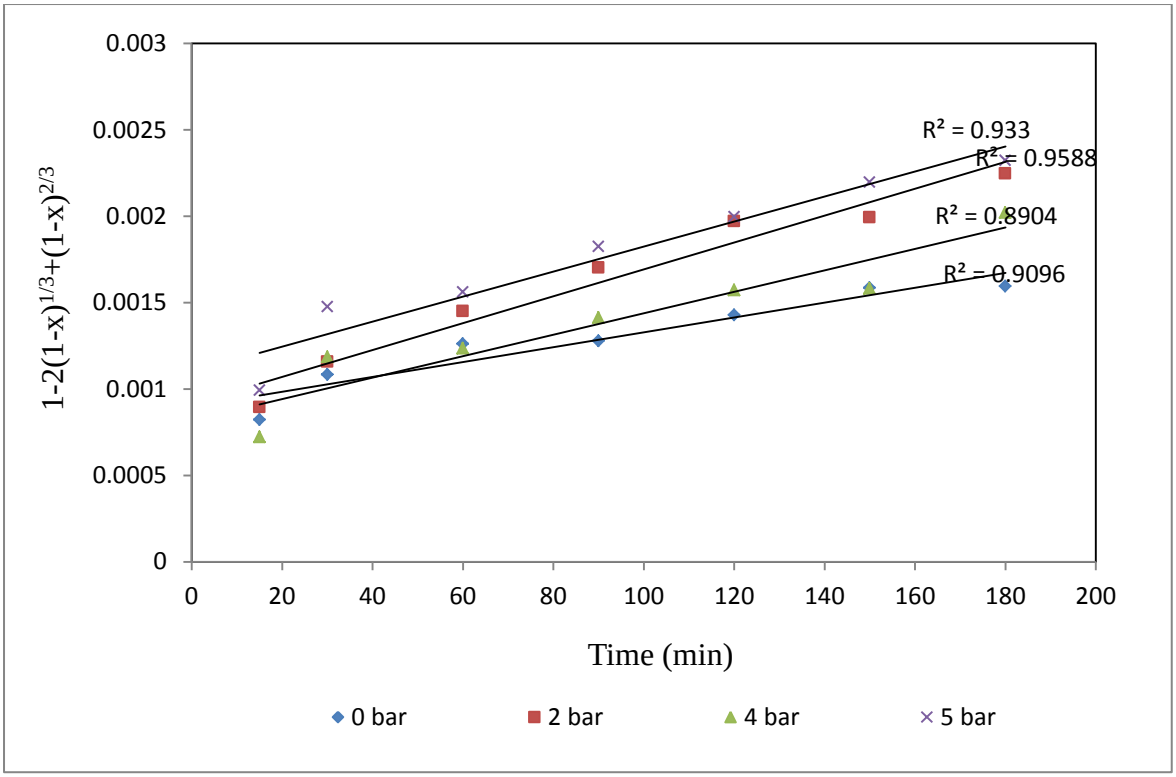

Figure C- 17: Plot of $1-2(1-x)^{1/3}+(1-x)^{2/3}$ vs time for leaching nickel from unroasted saprolitic laterite at different O_2 pressures

Table C- 11: Activation energy determination

K	T°C	T K	1/T	1000/T K^{-1}	-ln k	slope	Ea KJ/mol
6.00E-06	100	373.15	0.0027	2.68	12.024	6.80	56.56
4.00E-06	80	353.15	0.0028	2.83	12.43		
1.00E-06	60	333.15	0.0030	3.0016	13.82		
1.00E-08	40	273.55	0.0037	3.66	18.42		

Table C- 12: Determination of reaction order with respect to $[NH_3]$

K(min)	C_{NH3}	-log K	Log C	α
7.00E-06	3	5.15	0.477121	0.301
6.00E-06	2	5.22	0.30103	
5.00E-06	1	5.30	0	
2.00E-06	0	5.70		

Table C- 13: Determination of reaction order with respect to $[(NH_4)_2CO_3]$

K(min)	$C_{(NH4)2CO3}$	-log K	log C	β

8.00E-06	3	5.097	0.477121	0.257
7.00E-06	2	5.15	0.30103	
6.00E-06	1	5.22	0	
4.00E-06	0	5.40		

C.4 Kinetic reaction for the roasted ore

Table C- 14: Effect of temperature of Ni extraction for the roasted saprolitic laterite

time (min)	Effect of Temperature (2M $(NH_4)_2CO_3$), 3M NH_3, and O_2 pressure 5bar											
	40°C						60°C					
	V (L)	Fe (ppm)	Co (ppm)	Ni (ppm)	pH	% Ni extraction	V (L)	Fe (ppm)	Co (ppm)	Ni (ppm)	pH	% Ni extraction
0	0	0	BD	0		0	0	0	BD	0		0
15	0.06	2800	BD	610	10.19	0.211	0.058	800	BD	603	10.14	0.208
30	0.058	740	BD	632	11.18	0.218	0.06	460	BD	623	10.14	0.215
60	0.058	0	BD	644	10.1	0.222	0.062	0	BD	624	10.16	0.215
90	0.058	0	BD	654	10.12	0.225	0.06	0	BD	639	10.14	0.220
120	0.058	0	BD	659	10.08	0.228	0.056	0	BD	641	10.17	0.222
150	0.058	0	BD	687	10.08	0.237	0.06	0	BD	650	10.16	0.224
180	0.056	0	BD	796	10.05	0.272	0.062	0	BD	806	10.17	0.274

80°C						100°C					
V (L)	Fe (ppm)	Co (ppm)	Ni (ppm)	pH	% Ni extraction	V (L)	Fe (ppm)	Co (ppm)	Ni (ppm)	pH	% Ni extraction
0	0	BD	0		0	0	0	BD	0		0
0.06	240	BD	546	10.11	0.189	0.06	180	BD	505	10.19	0.175
0.06	14	BD	565	10.11	0.195	0.058	6	BD	547	10.18	0.189
0.056	0	BD	621	10.17	0.218	0.058	0	BD	577	10.1	0.198
0.056	0	BD	635	10.16	0.225	0.058	0	BD	609	10.12	0.209
0.062	0	BD	658	10.14	0.227	0.058	0	BD	618	10.08	0.214
0.058	0	BD	660	10.14	0.228	0.058	0	BD	646	10.08	0.223
0.056	0	BD	673	10.13	0.232	0.056	0	BD	652	10.05	0.225

Table C- 15: Effect of ammonia concentration on Ni extraction for the roasted saprolitic laterite

time (min)	Effect Ammonia Concentration (2M $(NH_4)_2CO_3$), T=100^oC and 5 bar O_2 pressure											
	0M						1M					
	V (L)	Fe (ppm)	Co (ppm)	Ni (ppm)	pH	% Ni extraction	V (L)	Fe (ppm)	Co (ppm)	Ni (ppm)	pH	% Ni extraction
0	0	0	BD	0		0	0	0	BD	0		0
15	0.058	0	BD	339	8.97	0.117	0.058	150	BD	544	9.84	0.188
30	0.058	0	BD	360	8.99	0.124	0.06	0	BD	553	9.86	0.191
60	0.066	0	BD	375	8.97	0.129	0.6	0	BD	574	9.9	0.198
90	0.064	0	BD	396	8.97	0.136	0.062	0	BD	576	9.88	0.198
120	0.056	0	BD	431	9.04	0.149	0.06	0	BD	591	9.86	0.204
150	0.062	0	BD	469	8.95	0.161	0.06	0	BD	600	9.92	0.207
180	0.066	0	BD	556	8.91	0.189	0.06	0	BD	607	9.95	0.209

2M						3M					
V (L)	Fe (ppm)	Co (ppm)	Ni (ppm)	pH	% Ni extraction	V (L)	Fe (ppm)	Co (ppm)	Ni (ppm)	pH	% Ni extraction
0	0	BD	0		0	0	0	BD	0		0
0.058	180	BD	533	9.76	0.184	0.06	720	BD	505	10.19	0.175
0.058	6	BD	588	9.74	0.203	0.058	100	BD	547	10.18	0.189
0.058	0	BD	615	9.74	0.212	0.058	0	BD	577	10.1	0.198
0.058	0	BD	625	9.73	0.215	0.058	0	BD	609	10.12	0.209
0.06	0	BD	644	9.73	0.222	0.058	0	BD	618	10.08	0.214
0.06	0	BD	652	9.73	0.225	0.058	0	BD	646	10.08	0.223
0.064	0	BD	655	9.73	0.226	0.056	0	BD	652	10.05	0.225

Table C- 16: Effect of Ammonium carbonate concentration on Ni extraction for the roasted saprolitic laterite

time (min)	Effect of Ammonium carbonate (3M NH_3), T=100^oC and 5bar O_2 pressure											
	0M						1M					
	V (L)	Fe (ppm)	Co (ppm)	Ni (ppm)	pH	% Ni extraction	V (L)	Fe (ppm)	Co (ppm)	Ni (ppm)	pH	% Ni extraction
0	0	0	BD	0		0	0	0	BD	0	0	0
15	0.056	21	BD	44	11.52	0.015	0.06	25	BD	475	10.44	0.16
30	0.062	2	BD	15	11.56	0.005	0.062	2	BD	600	10.39	0.21
60	0.062	0	BD	17	11.59	0.006	0.064	0	BD	620	10.47	0.21
90	0.062	0	BD	9	11.51	0.004	0.064	0	BD	629	10.45	0.22
120	0.056	0	BD	17	11.57	0.006	0.066	0	BD	629	10.41	0.22
150	0.058	0	BD	15	11.5	0.005	0.064	0	BD	642	10.43	0.22
180	0.05	0	BD	16	11.54	0.005	0.066	0	BD	645	10.55	0.22

2M						3M					
V (L)	Fe (ppm)	Co (ppm)	Ni (ppm)	pH	% Ni extraction	V (L)	Fe (ppm)	Co (ppm)	Ni (ppm)	pH	% Ni extraction
0	0	BD	0		0	0	0	BD	0		0
0.06	100	BD	505	10.19	0.18	0.062	180	BD	529	9.95	0.18
0.058	2	BD	547	10.18	0.19	0.062	6	BD	530	10.1	0.18
0.058	0	BD	577	10.1	0.20	0.058	0	BD	547	10.08	0.19
0.058	0	BD	609	10.12	0.21	0.062	0	BD	584	10.07	0.20
0.058	0	BD	618	10.08	0.21	0.062	0	BD	589	10.08	0.20
0.058	0	BD	646	10.08	0.22	0.062	0	BD	640	10.07	0.22
0.056	0	BD	652	10.05	0.23	0.062	0	BD	771	10.08	0.26

Table C- 17: Effect of oxygen pressure on Ni extraction for the roasted saprolitic laterite

time (min)	Effect of Oxygen pressure (bar) (3M NH_3, 2M $(NH_4)_2CO_3$) and T=100^oC											
	0 bar							2 bar				
	V (L)	Fe (ppm)	Co (ppm)	Ni (ppm)	pH	% Ni extraction		V (L)	Fe (ppm)	Co (ppm)	Ni (ppm)	pH	% Ni extraction
0	0	0	BD	0		0		0	0	BD	0		0
15	0.06	1860	BD	391	10.17	0.14		0.054	440	BD	408	10.13	0.14
30	0.052	1300	BD	426	10.18	0.15		0.054	100	BD	454	10.12	0.16
60	0.06	2560	BD	502	10.2	0.17		0.054	0	BD	509	10	0.18
90	0.06	2600	BD	524	10.2	0.18		0.054	0	BD	556	10	0.19
120	0.056	2000	BD	556	10.2	0.19		0.054	0	BD	570	10.13	0.20
150	0.056	3040	BD	552	10.19	0.19		0.06	0	BD	598	10.1	0.21
180	0.052	2760	BD	570	10.18	0.20		0.06	0	BD	610	10.11	0.21

4 bar						5 bar					
V (L)	Fe (ppm)	Co (ppm)	Ni (ppm)	pH	% Ni extraction	V (L)	Fe (ppm)	Co (ppm)	Ni (ppm)	pH	% Ni extraction
0	0	BD	0		0	0	0	BD	0		0
0.07	580	BD	531	10.08	0.18	0.06	180	BD	505	10.19	0.18
0.058	17	BD	556	10.07	0.19	0.058	6	BD	547	10.18	0.19
0.062	0	BD	592	10.03	0.20	0.058	0	BD	577	10.1	0.20
0.062	0	BD	593	10.07	0.20	0.058	0	BD	609	10.12	0.22
0.064	0	BD	608	10.03	0.21	0.058	0	BD	618	10.08	0.21
0.06	0	BD	608	10.03	0.21	0.058	0	BD	646	10.08	0.21
0.062	0	BD	617	10.04	0.21	0.056	0	BD	652	10.05	0.23

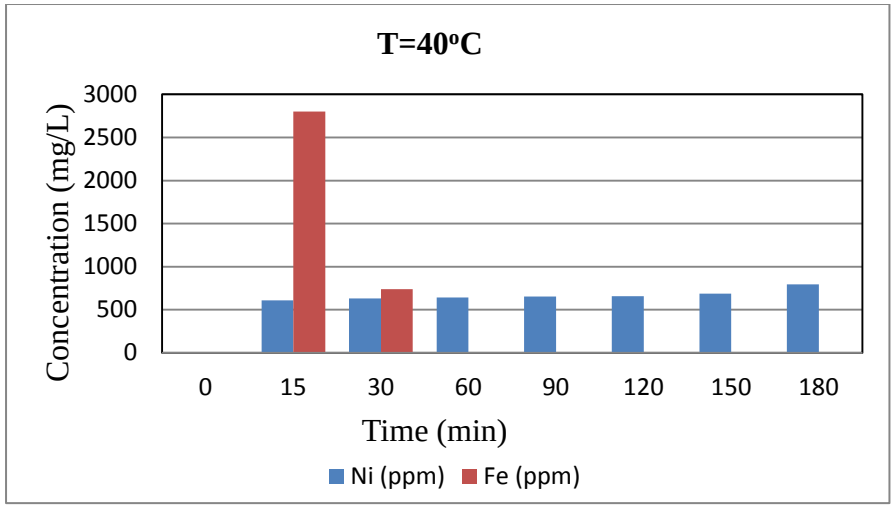

Figure C- 18: Comparison of Fe and Ni extraction at 40°C

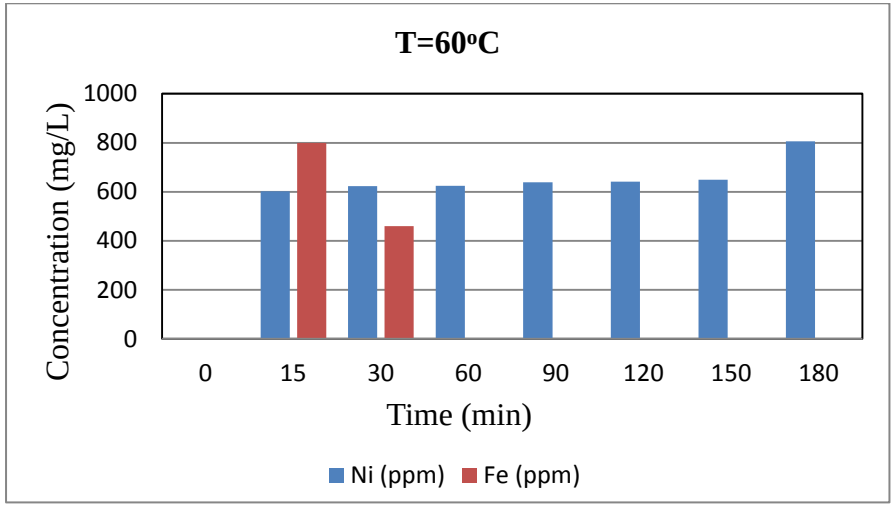

Figure C- 19: Comparison of Fe and Ni extraction at 60°C

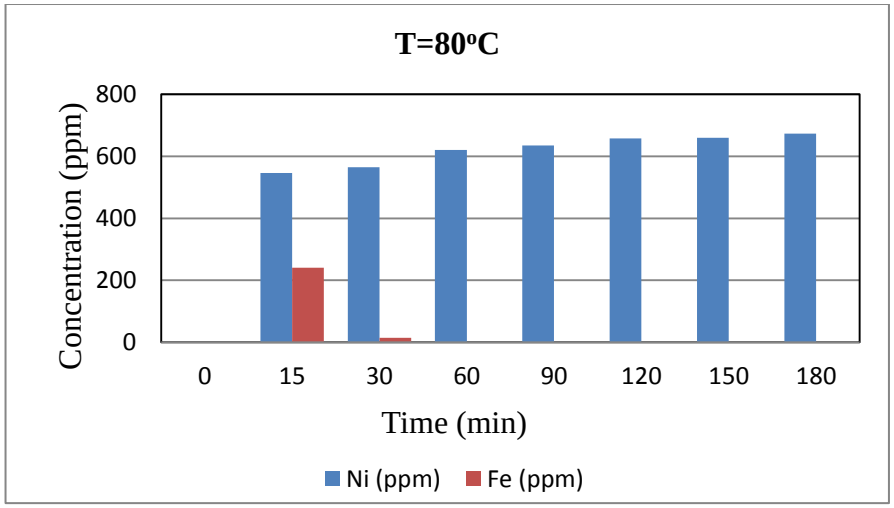

Figure C- 20: Comparison of Ni and Fe Extraction at 80°C

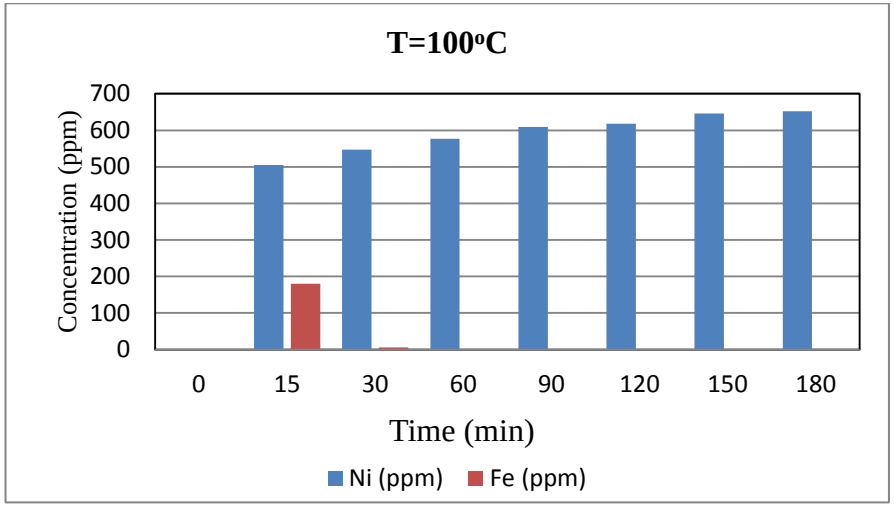

Figure C- 21: Comparison Ni and Fe extraction at 100°C

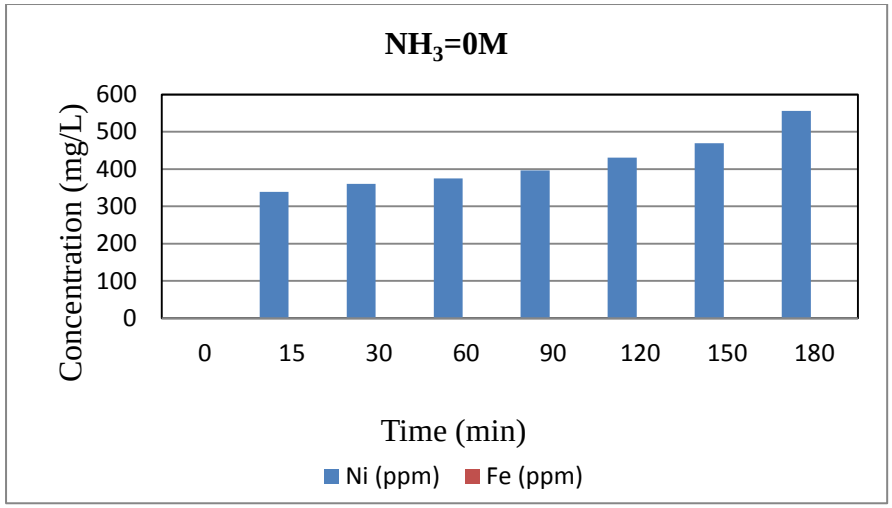

Figure C- 22: Comparison of Ni and Fe extraction at 0M [NH_3]

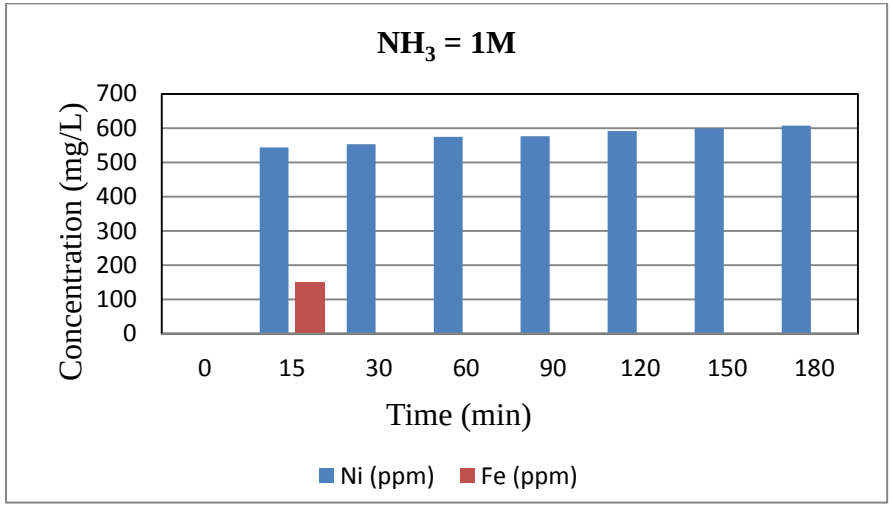

Figure C- 23: Comparison of Ni and Fe extraction at 1M [NH_3]

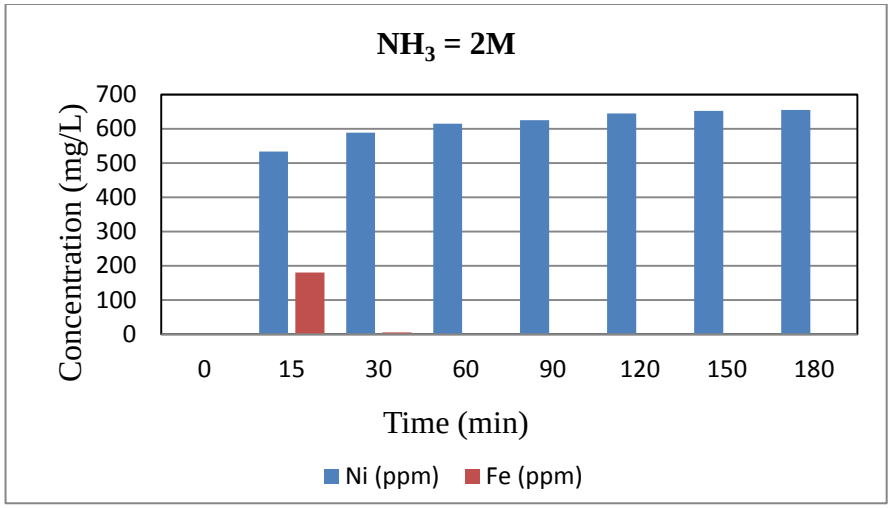

Figure C- 24: Comparison of Ni and Fe extraction at 2M [NH_3]

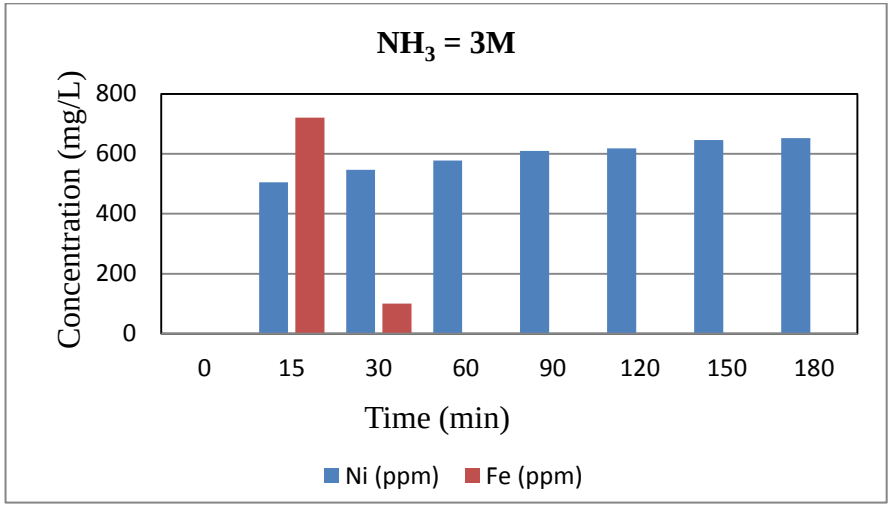

Figure C- 25: Comparison of Ni and Fe extraction at 3M [NH_3]

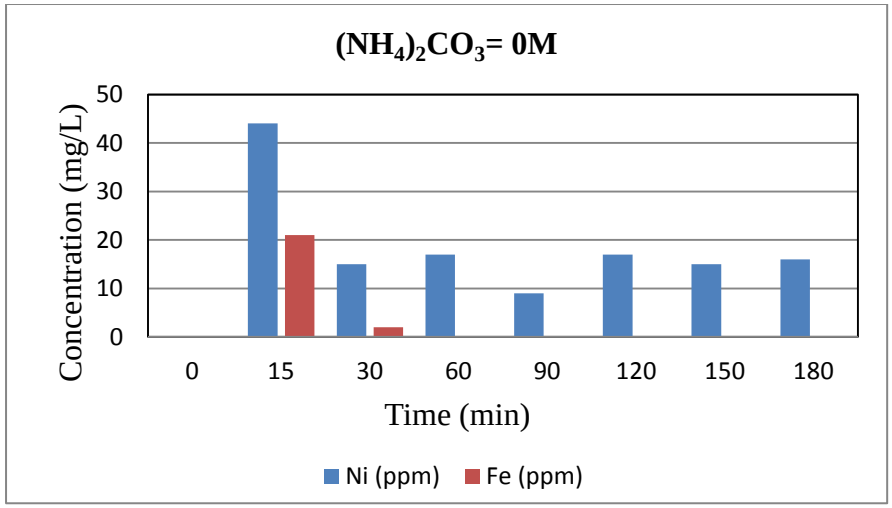

Figure C- 26: Comparison of Ni and Fe extraction at 0M [$(NH_4)_2CO_3$]

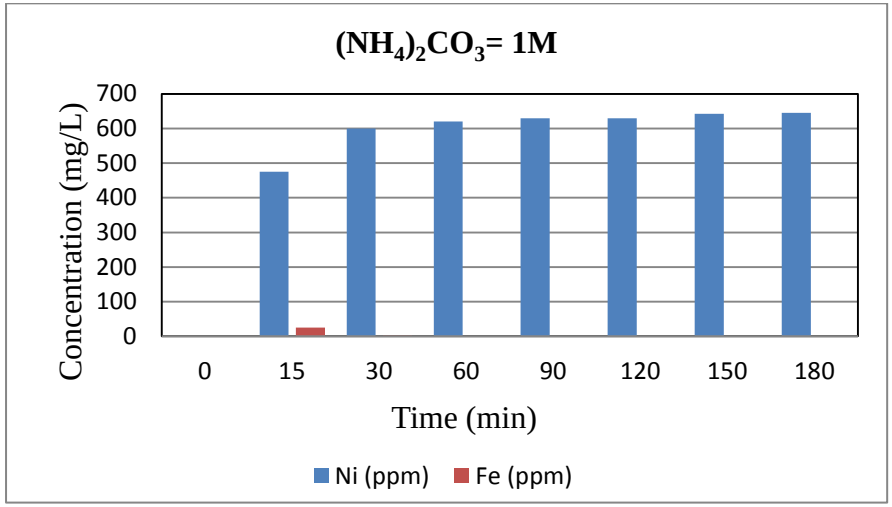

Figure C- 27: Comparison of Ni and Fe extraction at 1M [$(NH_4)_2CO_3$]

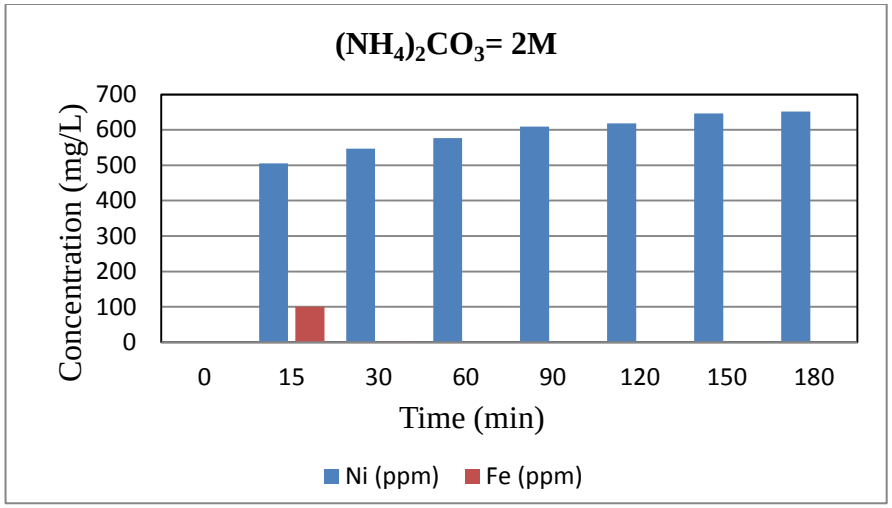

Figure C- 28: Comparison of Ni and Fe extraction at 2M [$(NH_4)_2CO_3$]

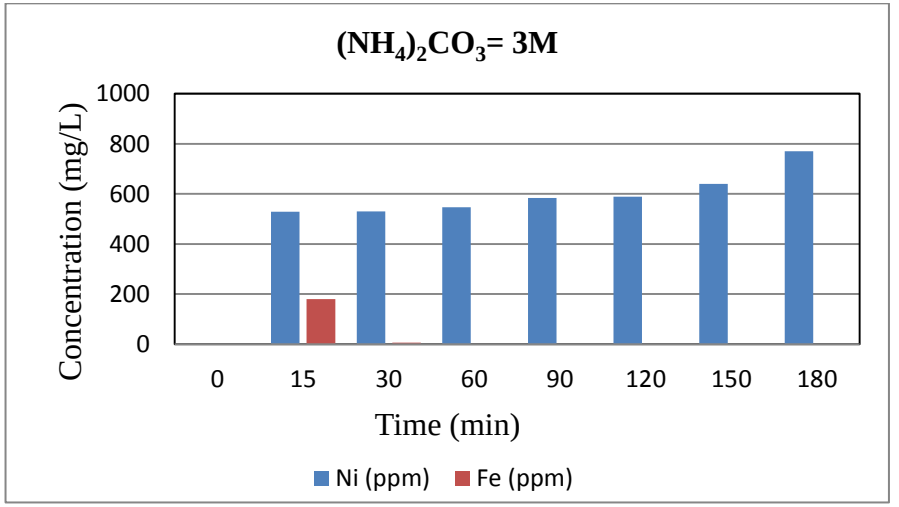

Figure C- 29: Comparison of Ni and Fe extraction at3M [$(NH_4)_2CO_3$]

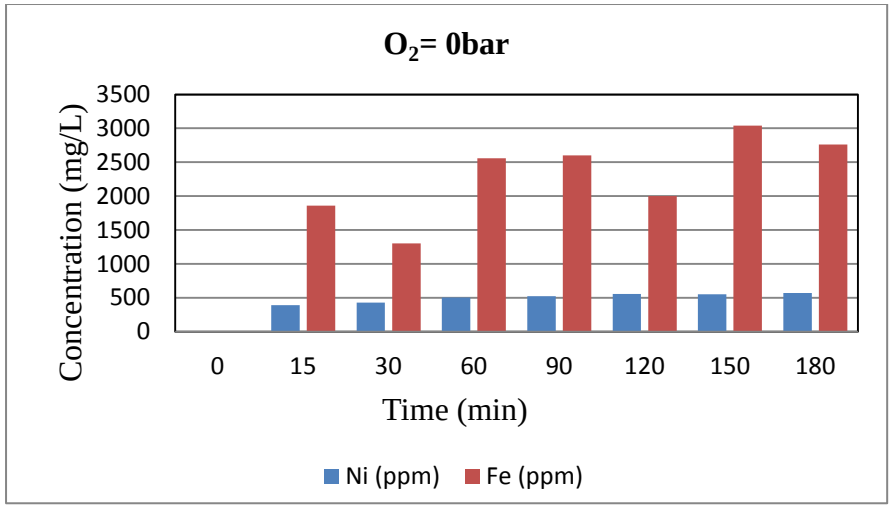

Figure C- 30: Comparison of Ni and Fe extraction at 0bar O_2

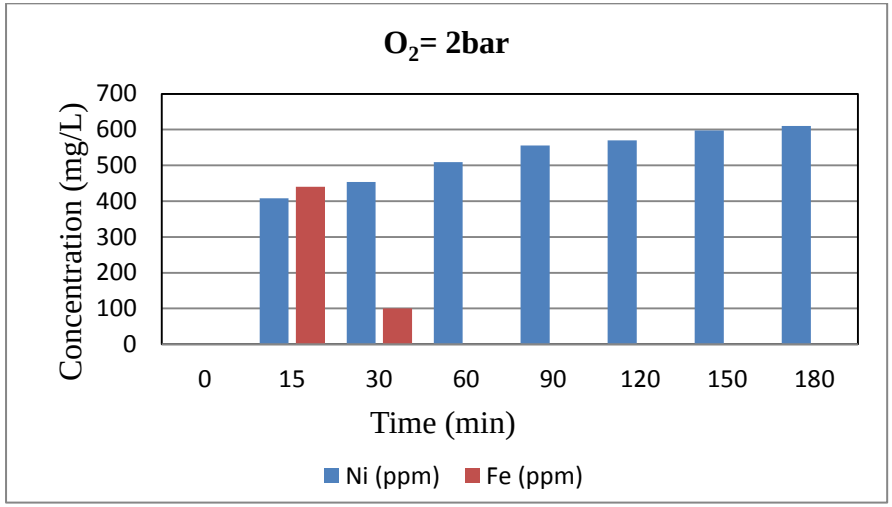

Figure C- 31: Comparison of Ni and Fe extraction at 2bar O_2

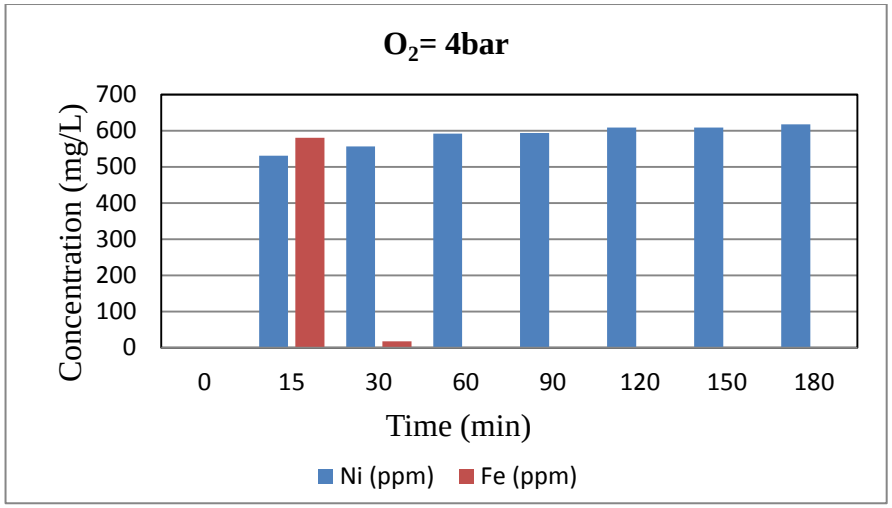

Figure C- 32: Comparison of Ni and Fe extraction at4bar O_2

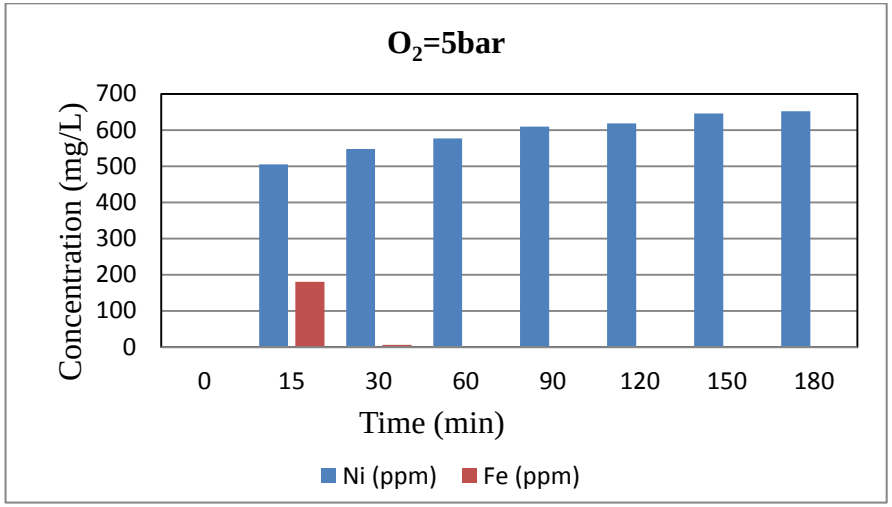

Figure C- 33: Comparison of Ni and Fe extraction at 5bar O_2

Table C- 18: Effect of temperature on shrinking core models for the roasted ore

time (min)	Effect of temperature 2M $(NH_4)_2CO_3$), 3M NH_3 and 4 bar O_2 pressure									
	40°C					60°C				
	Ni (ppm)	X	$1-(1-x)^{1/3}$	$1-3(1-x)^{2/3}+2(1-x)$	$1-2(1-x)^{1/3}+(1-x)^{2/3}$	Ni (ppm)	X	$1-(1-x)^{1/3}$	$1-3(1-x)^{2/3}+2(1-x)$	$1-2(1-x)^{1/3}+(1-x)^{2/3}$
0.000	0.000	0.000	0.000	0.000	0.000	0.000	0.000	0.000	0.000	0.000
15.000	610.000	0.211	0.076	0.016	0.006	603.000	0.208	0.075	0.016	0.006
30.000	632.000	0.218	0.079	0.018	0.006	623.000	0.215	0.078	0.017	0.006
60.000	644.000	0.222	0.080	0.018	0.006	624.000	0.215	0.078	0.017	0.006
90.000	654.000	0.225	0.082	0.019	0.007	639.000	0.220	0.080	0.018	0.006
120.000	659.000	0.228	0.083	0.019	0.007	641.000	0.222	0.080	0.018	0.006
150.000	687.000	0.237	0.086	0.021	0.007	650.000	0.224	0.081	0.019	0.007
180.000	796.000	0.272	0.100	0.028	0.010	806.000	0.274	0.101	0.029	0.010
	80°C					100°C				
Ni (ppm)	X	$1-(1-x)^{1/3}$	$1-3(1-x)^{2/3}+2(1-x)$	1-2(1-x)1/3+$(1-x)^{2/3}$		Ni (ppm)	x	$1-(1-x)^{1/3}$	$1-3(1-x)^{2/3}+2(1-x)$	$1-2(1-x)^{1/3}+(1-x)^{2/3}$
0.000	0.000	0.000	0.000	0.000		0.000	0.000	0.000	0.000	0.000
546.000	0.189	0.067	0.013	0.005		505.000	0.175	0.062	0.011	0.004
565.000	0.195	0.070	0.014	0.005		547.000	0.189	0.067	0.013	0.005
621.000	0.218	0.079	0.018	0.006		577.000	0.198	0.071	0.014	0.005
635.000	0.225	0.082	0.019	0.007		609.000	0.209	0.075	0.016	0.006
658.000	0.227	0.082	0.019	0.007		618.000	0.214	0.077	0.017	0.006
660.000	0.228	0.083	0.019	0.007		646.000	0.223	0.081	0.018	0.006
673.000	0.232	0.084	0.020	0.007		652.000	0.225	0.081	0.019	0.007

Table C- 19: Effect of ammonia concentration on shrinking core models for the roasted ore

time(min)	Effect Ammonia Concentration (2M $(NH_4)_2CO_3$), T=100^oC and 5 bar O_2 pressure									
	0M					1M				
	Ni (ppm)	X	$1-(1-x)^{1/3}$	$1-3(1-x)^{2/3}+2(1-x)$	$1-2(1-x)^{1/3}+(1-x)^{2/3}$	Ni (ppm)	X	$1-(1-x)^{1/3}$	$1-3(1-x)^{2/3}+2(1-x)$	$1-2(1-x)^{1/3}+(1-x)^{2/3}$
0.000	0.000	0.000	0.000	0.000	0.000	0.000	0.000	0.000	0.000	0.000
15.000	44.000	0.015	0.005	0.000	0.000	475.000	0.164	0.058	0.010	0.003
30.000	15.000	0.005	0.002	0.000	0.000	600.000	0.206	0.074	0.016	0.005
60.000	17.000	0.006	0.002	0.000	0.000	620.000	0.213	0.077	0.017	0.006
90.000	9.000	0.004	0.001	0.000	0.000	629.000	0.216	0.078	0.017	0.006
120.000	17.000	0.006	0.002	0.000	0.000	629.000	0.217	0.078	0.018	0.006
150.000	15.000	0.005	0.002	0.000	0.000	642.000	0.222	0.080	0.018	0.006
180.000	16.000	0.005	0.002	0.000	0.000	645.000	0.223	0.081	0.018	0.006

2M					3M				
Ni (ppm)	X	$1-(1-x)^{1/3}$	$1-3(1-x)^{2/3}+2(1-x)$	$1-2(1-x)^{1/3}+(1-x)^{2/3}$	Ni (ppm)	X	$1-(1-x)^{1/3}$	$1-3(1-x)^{2/3}+2(1-x)$	$1-2(1-x)^{1/3}+(1-x)^{2/3}$
0.000	0.000	0.000	0.000	0.000	0.000	0.000	0.000	0.000	0.000
505.000	0.175	0.062	0.011	0.004	529.000	0.183	0.065	0.012	0.004
547.000	0.189	0.067	0.013	0.005	530.000	0.183	0.065	0.012	0.004
577.000	0.198	0.071	0.014	0.005	547.000	0.189	0.067	0.013	0.005
609.000	0.209	0.075	0.016	0.006	584.000	0.200	0.072	0.015	0.005
618.000	0.214	0.077	0.017	0.006	589.000	0.204	0.073	0.015	0.005
646.000	0.223	0.081	0.018	0.006	640.000	0.220	0.080	0.018	0.006
652.000	0.225	0.081	0.019	0.007	771.000	0.262	0.096	0.026	0.009

Table C- 20: Effect ammonium carbonate on shrinking core model for the roasted ore

time (min)	Effect of Ammonium carbonate (3M NH_3), T=100^oC and 5 bar O2 pressure									
	0M					1M				
	Ni (ppm)	X	$1-(1-x)^{1/3}$	$1-3(1-x)^{2/3}+2(1-x)$	$1-2(1-x)^{1/3}+(1-x)^{2/3}$	Ni (ppm)	X	$1-(1-x)^{1/3}$	$1-3(1-x)^{2/3}+2(1-x)$	$1-2(1-x)^{1/3}+(1-x)^{2/3}$
0.000	0.000	0.000	0.000	0.000	0.000	0.000	0.000	0.000	0.000	0.000
15.000	44.000	0.015	0.005	0.000	0.000	0.049	0.007	0.002	0.135	0.047
30.000	15.000	0.005	0.002	0.000	0.000	0.055	0.009	0.003	0.147	0.052
60.000	17.000	0.006	0.002	0.000	0.000	0.062	0.011	0.004	0.172	0.061
90.000	9.000	0.004	0.001	0.000	0.000	0.068	0.013	0.005	0.179	0.064
120.000	17.000	0.006	0.002	0.000	0.000	0.070	0.014	0.005	0.192	0.069
150.000	15.000	0.005	0.002	0.000	0.000	0.074	0.016	0.005	0.191	0.068
180.000	16.000	0.005	0.002	0.000	0.000	0.076	0.016	0.006	0.196	0.070

2M					3M				
Ni (ppm)	X	$1-(1-x)^{1/3}$	$1-3(1-x)^{2/3}+2(1-x)$	$1-2(1-x)^{1/3}+(1-x)^{2/3}$	Ni (ppm)	X	$1-(1-x)^{1/3}$	$1-3(1-x)^{2/3}+2(1-x)$	$1-2(1-x)^{1/3}+(1-x)^{2/3}$
0.000	0.000	0.000	0.000	0.000	0.000	0.000	0.000	0.000	0.000
505.000	0.175	0.062	0.011	0.004	529.000	0.183	0.065	0.012	0.004
547.000	0.189	0.067	0.013	0.005	530.000	0.183	0.065	0.012	0.004
577.000	0.198	0.071	0.014	0.005	547.000	0.189	0.067	0.013	0.005
609.000	0.209	0.075	0.016	0.006	584.000	0.200	0.072	0.015	0.005
618.000	0.214	0.077	0.017	0.006	589.000	0.204	0.073	0.015	0.005
646.000	0.223	0.081	0.018	0.006	640.000	0.220	0.080	0.018	0.006
652.000	0.225	0.081	0.019	0.007	771.000	0.262	0.096	0.026	0.009

Table C- 21: Effect of oxygen pressure on shrinking core model for the roasted ore

time (min)	Effect of Oxygen pressure (bar) (3M NH_3, 2M $(NH_4)_2CO_3$) and T=100^oC									
	0 bar					2bar				
	Ni (ppm)	X	$1-(1-x)^{1/3}$	$1-3(1-x)^{2/3}+2(1-x)$	$1-2(1-x)^{1/3}+(1-x)^{2/3}$	Ni (ppm)	X	$1-(1-x)^{1/3}$	$1-3(1-x)^{2/3}+2(1-x)$	$1-2(1-x)^{1/3}+(1-x)^{2/3}$
0.000	0.000	0.000	0.000	0.000	0.000	0.000	0.000	0.000	0.000	0.000
15.000	391.000	0.135	0.047	0.006	0.002	408.000	0.141	0.049	0.007	0.002
30.000	426.000	0.147	0.052	0.008	0.003	454.000	0.157	0.055	0.009	0.003
60.000	502.000	0.172	0.061	0.011	0.004	509.000	0.175	0.062	0.011	0.004
90.000	524.000	0.179	0.064	0.012	0.004	556.000	0.190	0.068	0.013	0.005
120.000	556.000	0.192	0.069	0.013	0.005	570.000	0.197	0.070	0.014	0.005
150.000	552.000	0.191	0.068	0.013	0.005	598.000	0.206	0.074	0.016	0.005
180.000	570.000	0.196	0.070	0.014	0.005	610.000	0.210	0.076	0.016	0.006
4bar						5bar				
Ni (ppm)	X	$1-(1-x)^{1/3}$	$1-3(1-x)^{2/3}+2(1-x)$	$1-2(1-x)^{1/3}+(1-x)^{2/3}$		Ni (ppm)	X	$1-(1-x)^{1/3}$	$1-3(1-x)^{2/3}+2(1-x)$	$1-2(1-x)^{1/3}+(1-x)^{2/3}$
0.000	0.000	0.000	0.000	0.000		0.000	0.000	0.000	0.000	0.000
531.000	0.184	0.065	0.012	0.004		505.000	0.175	0.062	0.011	0.004
556.000	0.192	0.069	0.013	0.005		547.000	0.189	0.067	0.013	0.005
592.000	0.204	0.073	0.015	0.005		577.000	0.198	0.071	0.014	0.005
593.000	0.204	0.073	0.015	0.005		609.000	0.220	0.080	0.018	0.006
608.000	0.210	0.076	0.016	0.006		618.000	0.211	0.076	0.016	0.006
608.000	0.210	0.076	0.016	0.006		646.000	0.214	0.077	0.017	0.006
617.000	0.213	0.077	0.017	0.006		652.000	0.225	0.081	0.019	0.007

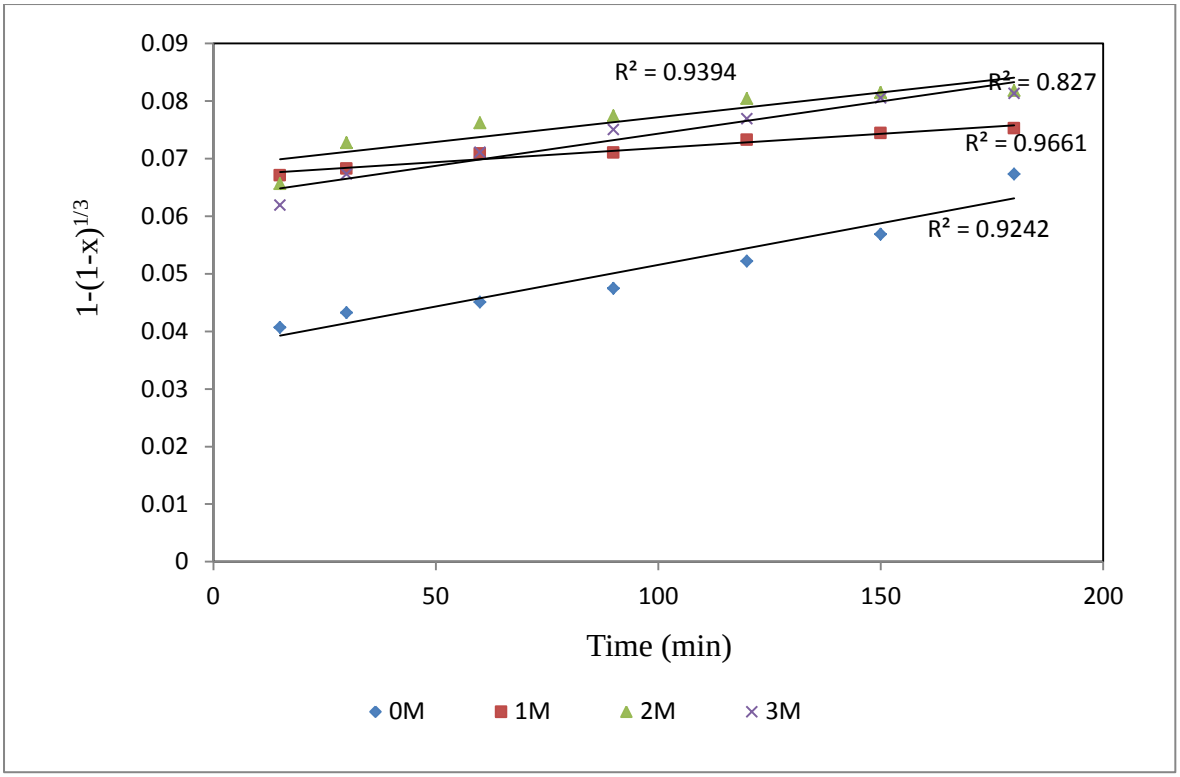

Figure C- 34: Plot of $1-(1-x)^{1/3}$ vs time for leaching nickel from roasted saprolitic laterite at different [NH_3]

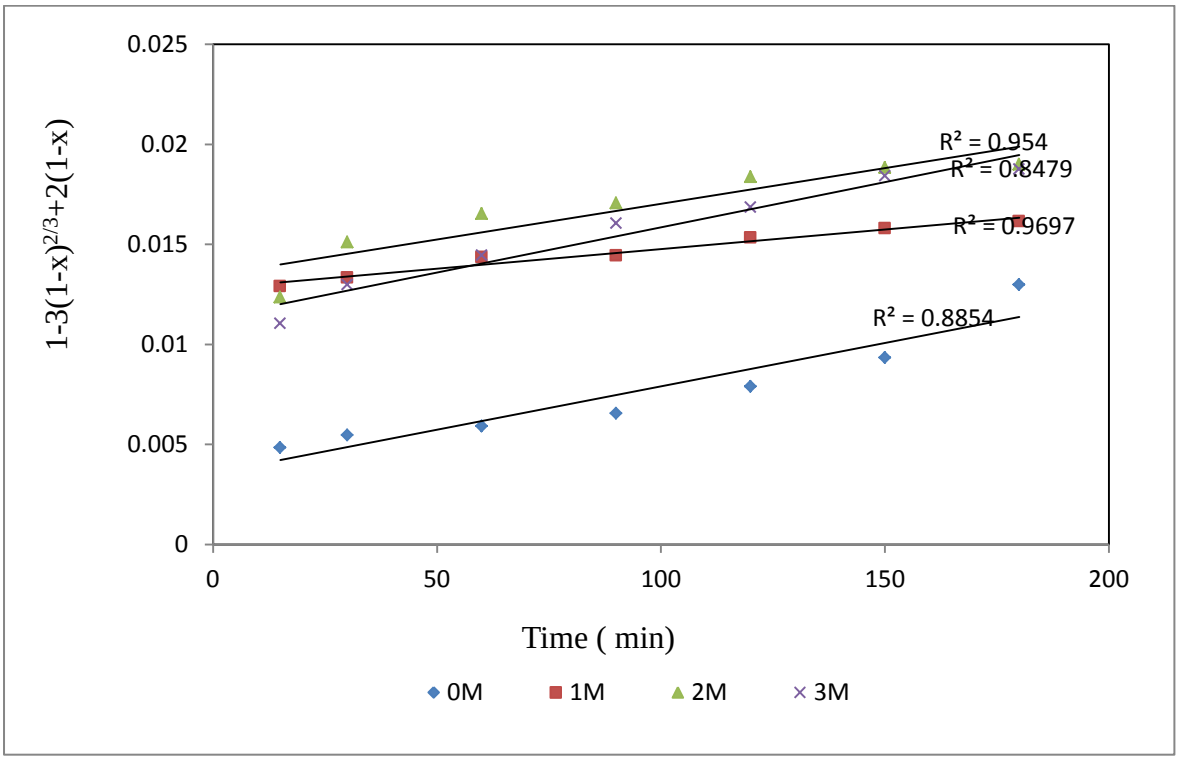

Figure C- 35: Plot of $1-3(1-x)^{2/3}+2(1-x)$ vs time for leaching nickel from roasted saprolitic laterite at different [NH_3]

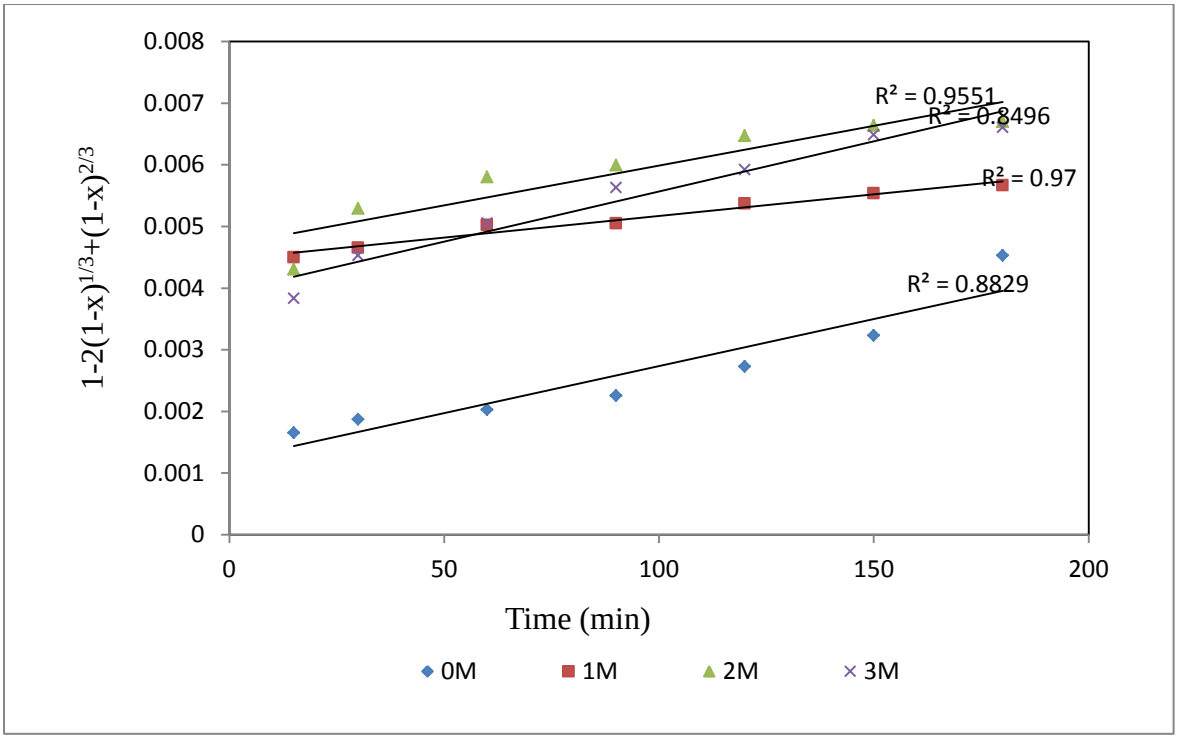

Figure C- 36: Plot of $1-2(1-x)^{1/3}+(1-x)^{2/3}$ vs time for leaching nickel from roasted saprolitic laterite at different $[NH_3]$

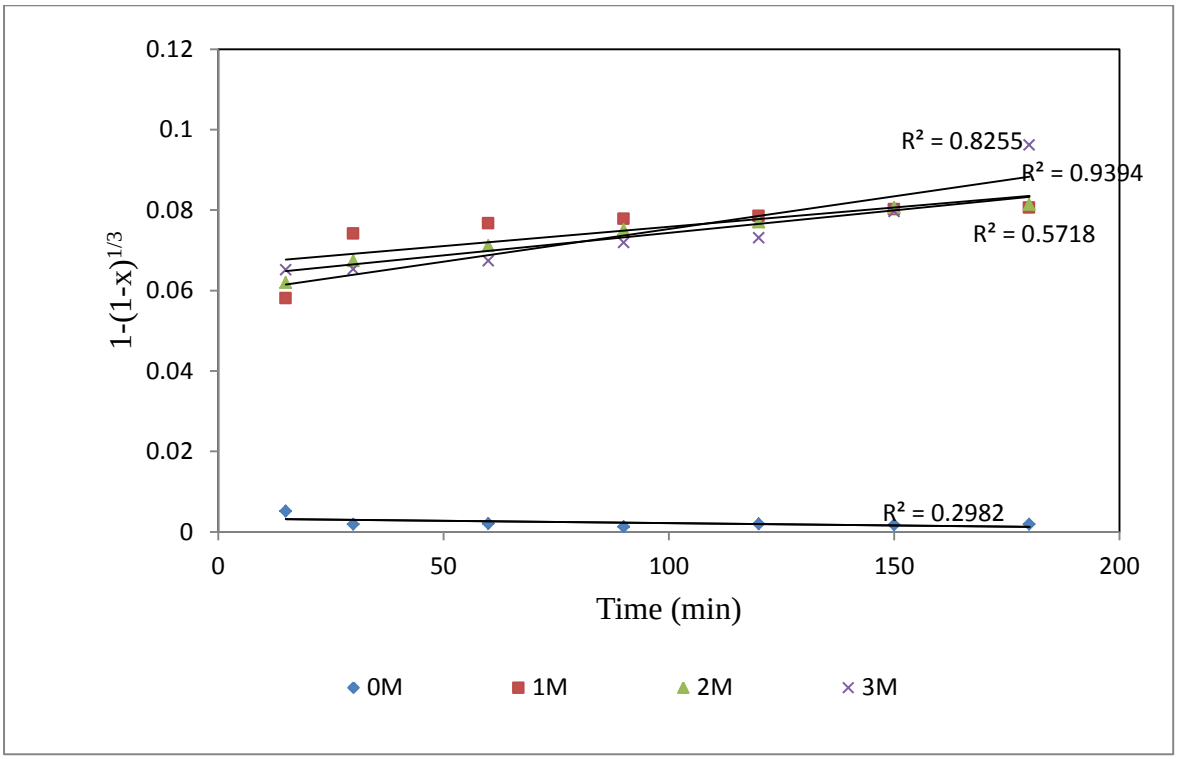

Figure C- 37: Plot of $1-(1-x)^{1/3}$ vs time for leaching nickel from roasted saprolitic laterite at different $[(NH_4)_2CO_3]$

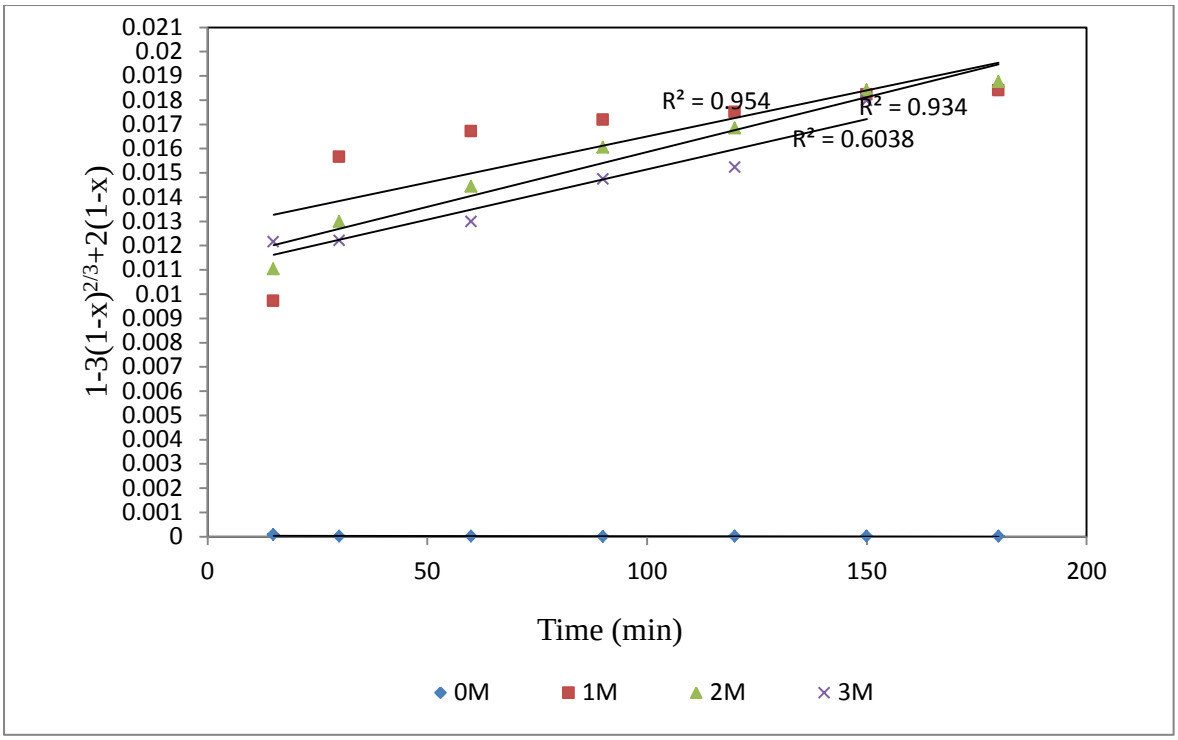

Figure C- 38: Plot of $1-3(1-x)^{2/3}+2(1-x)$ vs time for leaching nickel from roasted saprolitic laterite at different $[(NH_4)_2CO_3]$

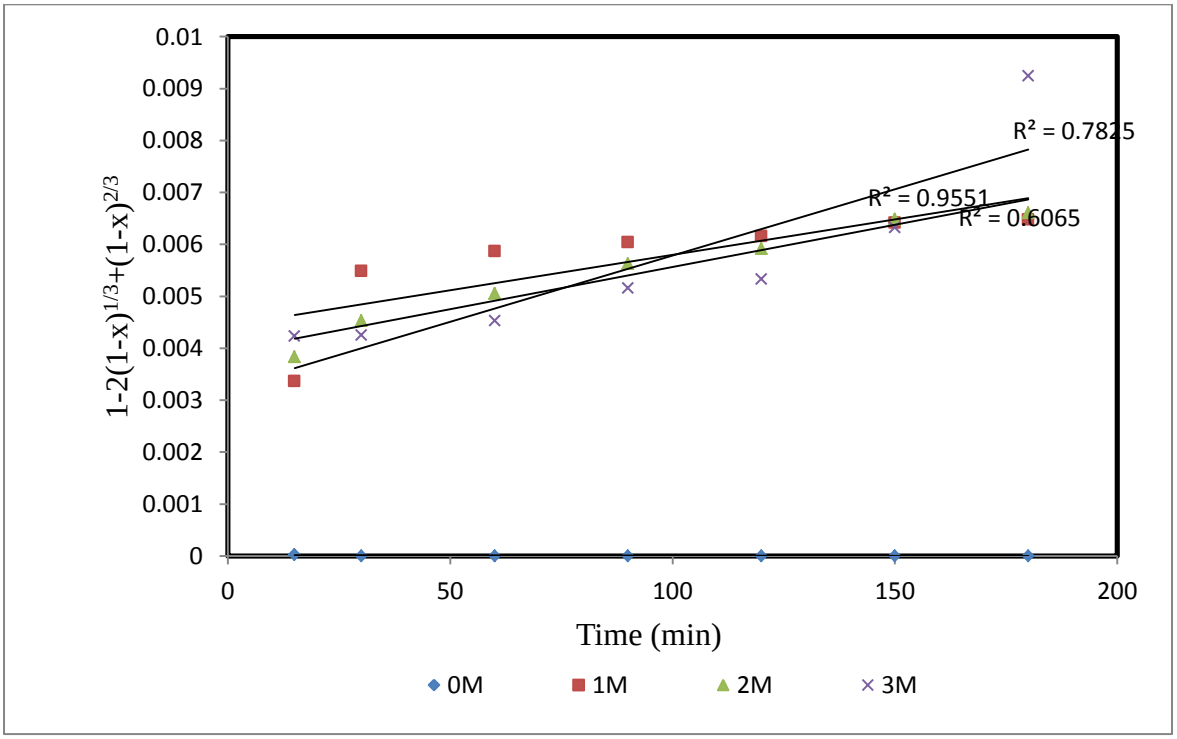

Figure C- 39: Plot of $1-2(1-x)^{1/3}+(1-x)^{2/3}$ vs time for leaching nickel from roasted saprolitic laterite at different $[(NH_4)_2CO_3]$

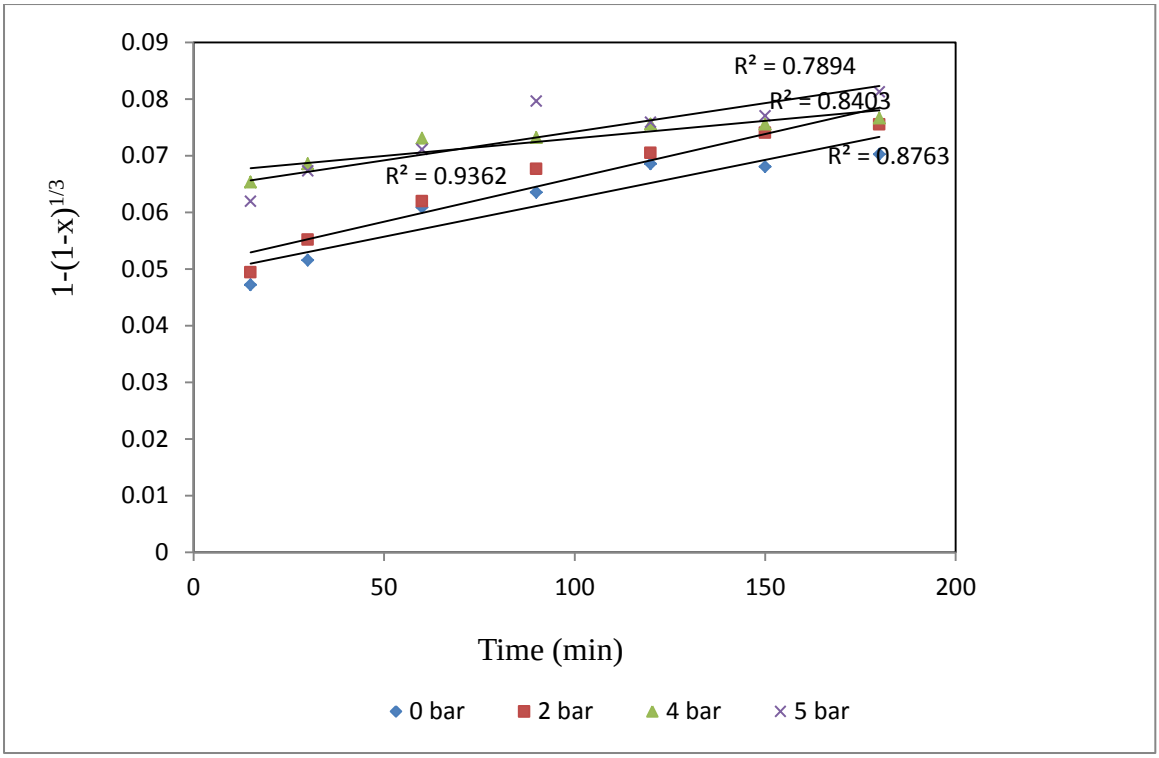

Figure C- 40: Plot of $1-(1-x)^{1/3}$ vs time for leaching nickel from roasted saprolitic laterite at different O_2 pressure

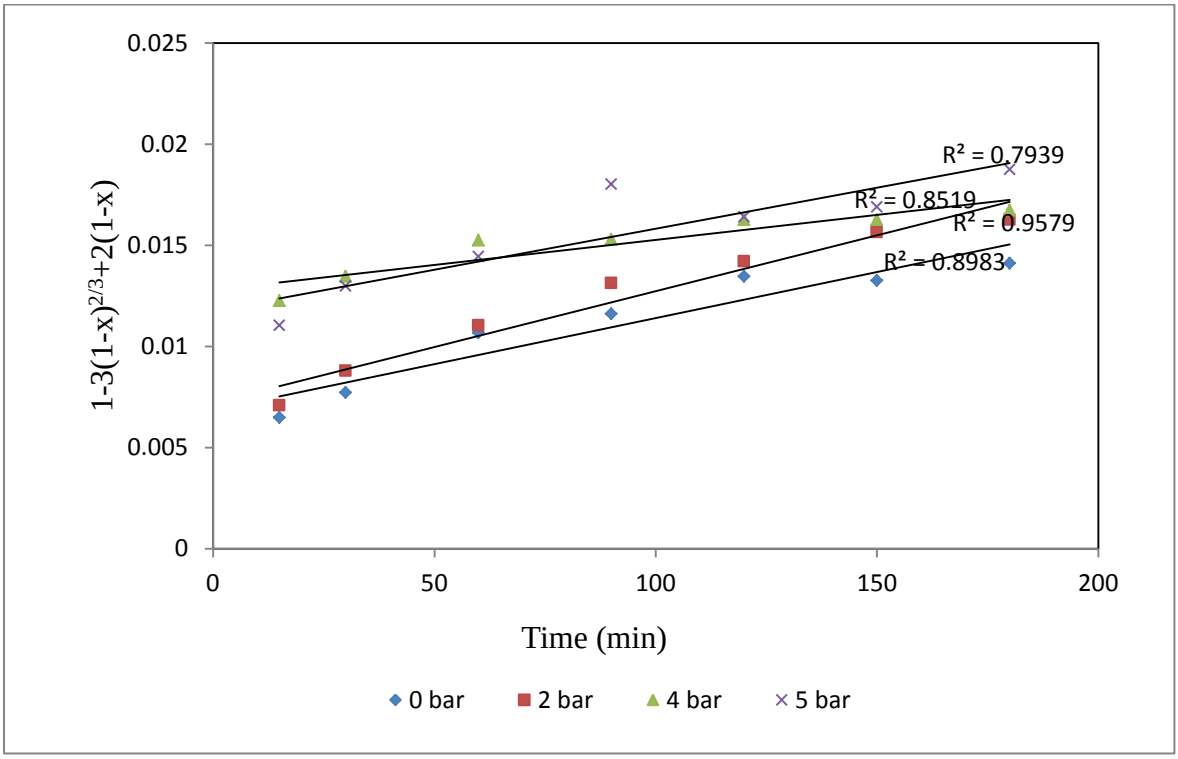

Figure C- 41: Plot of $1-3(1-x)^{2/3}+2(1-x)$ vs time for leaching nickel from roasted saprolitic laterite at different O_2 pressure

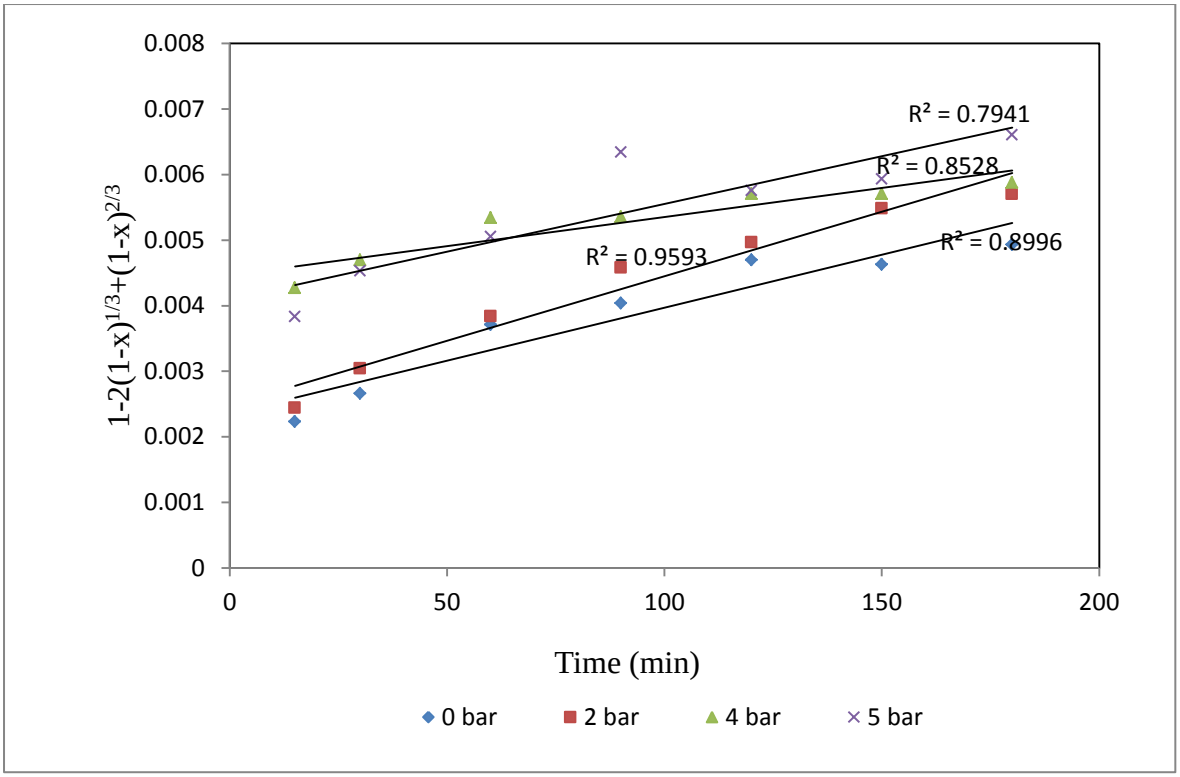

Figure C- 42: Plot of $1-2(1-x)^{1/3}+(1-x)^{2/3}$ vs time for leaching nickel from roasted saprolitic laterite at different O_2 pressure